

# **Integrating Satellite and Ancillary Data to Predict Site Quality**

by

**Yushan Long**

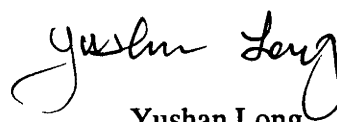
Thesis submitted for the degree of  
Doctor of Philosophy of the Australian National University

August 1994



## Statement of Originality

I hereby declare that this submission is my own work and that, to the best of my knowledge and belief, it contains no material previously published or written by another person nor material which to a substantial extent has been accepted for the award of any other degree or diploma of a university or other institute of higher learning, except where due acknowledgment is made in the text of the thesis.

  
Yushan Long

## Acknowledgments

This study was financially supported by the Australian Development Assistance Bureau.

I owe a great deal to many people who have helped and encouraged me in the preparation of this thesis. Before all others, I am particularly indebted to my supervisor, Dr Brian J. Turner (Reader, Department of Forestry, School of Resource and Environmental Management (SREM), The Australian National University (ANU)) for his continued encouragement and guidance, especially in the preparation of the manuscript. He has patiently supervised this research, from a proposal to the final draft, in not only the structure of the thesis, but the presentation in English and editing and proof-reading. The thesis would have been impossible without his continued help, patience, support, criticism, encouragement and guidance.

I would like to thank the members of my advisory committee Dr Ross Florence and Dr John Field (Department of Forestry, SREM, ANU) who attended regular committee meetings, made comments and suggestions during the studies. I owe special thanks to Dr R. Florence for his help and supervision during my diploma study, and for directing me to this project, which has since changed my academic life.

The Department of Forestry provided satellite data and facilities for data processing and a study environment. The forestry section of the Australian Capital Territory (ACT) Administration provided detailed forest compartment records, maps and aerial-photos.

The members of the Forestry Department were friendly and very helpful. My special thanks are due to Mr E.W.A. Cziesso, Mrs J. Lejins, and Mr P. Beutel for their assistance in field investigations. I am indebted to Dr A. Gibson for her help in English editing. I express my thanks to those who helped me in many ways during this study.

My greatest thanks goes to my wife, Yuhua Li, for her patience, encouragement, support and cheerfulness. Throughout the project, she has worked very hard to support the family, and looking after our child, especially when we faced financial difficulties.

Finally, I express my sincere gratitude to my parents for their encouragement, support and sacrifice.

## Abstract

A forest site is an area of land considered to be representative of the topography, vegetation, soils and other biotic and abiotic features associated with tree growth. Forest site quality refers to the timber-growing capacity of a forest site for a given tree species over a period of time. It is traditionally measured by site index defined by the height-age relations of a specific tree species. In this study, the capability of satellite data for estimating forest site quality was investigated. The study was concerned with the methodology and precision of integrating satellite imagery from different growing seasons and remote sensors with ground-collected and computer-generated biogeographical data for a localised site and forest study. The study area, centred at 35°15' S and 149°22' E, was located in the northeast corner of the Australian Capital Territory, covering an area of about 3000 hectare of radiata pine (*Pinus radiata* D. Don) plantation stands. The ancillary biogeographical variables were nine stand variables (stand age, top height, mean diameter, volume, basal area, density, canopy depth, understory coverage, and canopy cover), six site quality indices (site index, the mean annual increments in height, basal area, diameter, volume, and canopy depth), four topographic variables (elevation, aspect, slope, topographic positions), and two edaphic variables (soil depth of horizons A and B and gravel content). Satellite data comprised Landsat Thematic Mapper (TM) and SPOT images recorded in two growing seasons. Statistical tests, correlation, principal component analysis, canonical correlation analysis, regression modelling and classification techniques were used for data analysis.

The sensitivity and the relationships of satellite data to stand ages and growth processes were tested. An important implication is that the changes in spectral reflectance patterns were, in timing, close to the changes in stand growth processes. The age range found to be most spectrally sensitive and related to the variations of stands is between 5 to 25 years in the visible, middle-infrared (MIR) and thermal-infrared (TIR) bands. For the near-infrared (NIR) band, it can be extended to about 30 to 35 years.

The study examined the relationships between spectral data and stand variables. In general, except for the understory variable, all stand variables were statistically significantly correlated with spectral variables, but the degree of significance of correlation coefficients

was band dependent. NIR bands showed higher correlations with stand age, top height and canopy closure, while MIR bands were more highly correlated with basal area and volume than other bands. These correlations may be used to accurately estimate the mean or median of the given forest stand (type), but a high degree of predicability on small, site-specific areas probably can not be expected on a single pixel basis.

The relationships between spectral data and several site quality indices were tested. All site quality indices (except for the mean annual increment in volume) were found strongly correlated with the NIR bands. The best correlations were obtained from the mean annual increment in height and site index based on the "height-age" relationship. The mean annual increment in volume showed poor correlations with the NIR bands, but was significantly correlated with all other bands, the MIR bands in particular. The correlations were significantly improved with principal component transformation and/or band combinations (such as vegetation indices).

Various spectral bands and their combinations were regressed against site quality (site index and mean annual increment in height) to develop prediction models. All regression models derived were strongly significant ( $p < 0.001$ ). Using the NIR bands alone, the simple linear regression models could explain about 65-70% of the total variances. The stepwise regression analysis showed that the best band combinations were the green and the NIR bands for SPOT data and the NIR and the two MIR bands for TM data ( $r^2 = 0.78$ ). With topographic variables (elevation, aspect, slope and topographic positions), the best model could explain about 89% of the total variance of site quality, an increase of about 10% over the models without site variables. The estimated site quality showed an agreement of 89% ( $r^2$ ) with the observed site quality.

Several site quality class maps based on site index and mean annual increment in height were produced using the model-derived site quality values. The overall plot-based mapping accuracy for the four site quality classes considered was 68%. The study results suggest that the site quality for radiata pine plantations may be predicted with reasonable accuracy at compartment-based level. This can be done by means of geographic information systems using satellite and biogeographical data.

# Table of Contents

<b>Statement of Originality</b> .....	I
<b>Acknowledgments</b> .....	II
<b>Abstract</b> .....	III
<b>Table of Contents</b> .....	V
<b>Symbols, Abbreviations and Acronyms</b> .....	X
<b>List of Tables</b> .....	XIII
<b>List of Figures</b> .....	XVI

## Chapter 1

### General Introduction

<b>1.1 Need to Estimate Site Quality</b> .....	1
<b>1.2 A Brief Discussion on Site and Site Quality Concepts</b> .....	3
1.2.1 Introduction .....	3
1.2.2 Site .....	4
1.2.3 Site Quality .....	6
1.2.4 Summary .....	7
<b>1.3 Possibility of Estimating stand variables and Site Quality Using Remote Sensing: Research Hypothesis</b> .....	8
<b>1.4 Objectives of the Study</b> .....	10
<b>1.5 Thesis Outline</b> .....	10

## Chapter 2

### Literature Review on Evaluation of Forest Site Quality and Applications of Remote Sensing

<b>2.1 Introduction</b> .....	12
<b>2.2 Historical Development of Forest Site Quality Evaluation</b> .....	13
2.2.1 Unwritten Records .....	13
2.2.2 Early Documents .....	14
2.2.3 Pioneer Studies .....	16
2.2.4 Development of Last Five Decades .....	20
2.2.5 Summary Implications .....	22
<b>2.3 Main Approaches for Evaluating Forest Site Quality: an Brief Overview</b> .....	24
<b>2.4 Forestry Applications of Remote Sensing</b> .....	26
2.4.1 Introduction .....	26
2.4.2 Definition of Remote Sensing .....	26
2.4.3 The Development of Remote Sensing in Forestry: an Overview .....	28
2.4.4 Remote Sensing of Vegetation: an Overview .....	32
2.4.4.1 Visible Region (0.4 - 0.7 $\mu\text{m}$ ) .....	32
2.4.4.2 Near-Infrared Region (about 0.7 – 1.3 $\mu\text{m}$ ) .....	33
2.4.4.3 Middle-Infrared Region (1.3 – 2.5 $\mu\text{m}$ ) .....	34
2.4.4.4 Thermal-Infrared Region (about 3 – 20 $\mu\text{m}$ ) .....	34
2.4.4.5 Microwave Region (about 30 $\mu\text{m}$ - 1 m) .....	35
2.4.4.6 Some General Features of Reflectance of Forest Canopies .....	36
2.4.4.7 Three Basic Characteristics of Forest Cover .....	37
2.4.5 Applications of Satellite Data to Forests .....	38
2.4.5.1 Introduction .....	38

2.4.5.2	Some General Features of Forestry Applications .....	38
2.4.5.3	Mapping of Forest (Site) Types .....	41
2.4.5.4	Forest Inventory .....	51
2.4.5.5	Evaluation of Stand Variables .....	55
2.4.5.6	Estimation of Site Productivity .....	59
2.4.5.7	Detection of Forest Change .....	61
2.4.5.7.1	<i>Introduction</i> .....	61
2.4.5.7.2	<i>Deforestation</i> .....	62
2.4.5.7.3	<i>Forest Damage</i> .....	63
2.4.5.7.4	<i>Change Dynamics</i> .....	64
2.4.5.7.5	<i>Seasonal or Interannual Change</i> .....	65
2.4.5.7.6	<i>Land Quality and Degradation Changes</i> .....	65
2.4.5.8	Conclusion .....	66
2.5	Summary and Conclusion .....	68

### Chapter 3

## Description of Study Site

3.1	Introduction .....	69
3.2	Location of the Study Area .....	70
3.3	Site Characteristics .....	70
3.3.1	Geology .....	70
3.3.2	Soils .....	71
3.3.3	Climate .....	73
3.3.4	Topography .....	73
3.3.5	Vegetation .....	75
3.3.6	Land Capacity Classes .....	75
3.4	Silvicultural Conditions .....	76
3.4.1	Establishment of Kowen Forest .....	76
3.4.2	Site Preparation .....	76
3.4.3	Planting and Tending Techniques .....	77
3.5	Previous Work on Studies of Site Quality at Kowen: a Brief Overview .....	77

### Chapter 4

## Data Sources

4.1	Introduction .....	79
4.2	Site and Stand Variables .....	80
4.2.1	Selection of Sample Points .....	80
4.2.2	Measurement of Stand Variables .....	81
4.2.3	The Measures of Site Quality for Radiata Pine.....	82
4.2.4	Selection and Field Measurements of Site Variables .....	85
4.2.4.1	Soil Variables .....	85
4.2.4.2	Topographic Variables.....	87
4.3	Satellite Data .....	88
4.4	Generation of Digital Ground Truth and Digital Terrain Models .....	91
4.4.1	Needs for Digitising .....	91
4.4.2	Digitisation of Compartment Maps .....	92
4.4.3	Generation of Digital Terrain Model .....	92
4.4.3.1	Hardware and Software Used .....	93
4.4.3.2	Data Sources for Digitising .....	94
4.4.3.3	Digitising Procedures .....	94
4.4.3.4	Interpolation .....	95

4.4.3.5	Calculation of Slope and Aspect .....	96
4.5	Data Combinations .....	97
4.6	Spectral Data of Sample Points .....	97

### Chapter 5

## Relationships Between Spectral Characteristics of SPOT And TM Data And Age of a Coniferous Forest

5.1	Introduction .....	100
5.2	Methodology .....	102
5.2.1	Data Generation .....	102
5.2.1.1	Stand Age .....	102
5.2.1.2	Satellite Data .....	102
5.2.2	Data Analysis .....	103
5.2.2.1	Basic Statistics .....	103
5.2.2.2	Data Combinations and Transformations .....	103
5.2.2.3	The Computations of Vegetation Indices .....	105
5.2.2.4	Difference Tests .....	106
5.2.2.5	Scatter Plots .....	106
5.2.2.6	Principal Component Analysis .....	106
5.2.2.7	Correlation Analysis .....	108
5.2.2.8	Cluster Analysis .....	108
5.3	Results .....	109
5.3.1	Data Characteristics .....	109
5.3.2	Comparison of Spectral Data .....	110
5.3.3	Changes of Spectral Values with Stand Age .....	111
5.3.4	Principal Component Analysis .....	115
5.3.5	Correlations .....	120
5.3.5.1	Inter-correlations Within and Between Images .....	120
5.3.5.2	Correlations between Raw Spectral Values and Stand Ages .....	120
5.3.5.3	Correlations Between Principal Component Images and Stand Age .....	122
5.3.5.4	Non-linear Correlation .....	124
5.3.5.5	Correlation between Vegetation Indices and Stand Ages .....	125
5.3.6	Clustering and Grouping of Mean Spectral Values of Stands .....	126
5.4	Discussion .....	129
5.4.1	Variations of Spectral Values .....	129
5.4.2	Changes of Spectral Values with Stand Age .....	130
5.4.3	Correlation Analysis .....	132
5.4.4	Principal Component Transformation .....	135
5.4.5	The Sensitivity and Separability of Spectral Reflectance of Stands .....	136
5.5	Summary and Conclusion .....	137

### Chapter 6

## A Correlation, Principal Component and Canonical Correlation Analysis of Stand Variables Versus SPOT and TM Data

6.1	Introduction .....	139
6.2	Data Collection .....	140
6.3	Data analysis Techniques .....	141
6.3.1	Correlation Analysis .....	141
6.3.2	Principal Component Transformation .....	141



6.3.3	Canonical Correlation Analysis .....	142
6.3.3.1	Introduction .....	142
6.3.3.2	Some Basic Computational Procedures .....	143
<b>6.4</b>	<b>Results</b> .....	<b>147</b>
6.4.1	Data Characteristics .....	147
6.4.2	Inter-correlations between The Stand Variables .....	149
6.4.3	Correlations between Stand and Site Variables .....	149
6.4.4	Correlations between Stand Variables and Raw Spectral Values .....	150
6.4.5	Correlations between Stand Variables and "Between-Image" Band Combinations ....	151
6.4.6	Correlations between Stand Variables and Principal Component Images .....	152
6.4.7	Correlations between Stand Variables and "Within-Image" Band Combinations .....	155
6.4.8	Canonical Correlations .....	156
6.4.8.1	Canonical Correlations between Stand Variables and SPOT Data .....	157
6.4.8.2	Canonical Correlations Between Stand Variables and TM Data .....	159
6.4.8.3	Canonical Correlations Between Stand and Site Variables .....	162
<b>6.6</b>	<b>Discussion</b> .....	<b>165</b>
6.5.1	Sensitivity of SPOT and TM Data in Stands .....	165
6.5.2	The Capability of SPOT and TM Data to Estimate Variables .....	165
6.5.3	Comparison of SPOT and TM Data .....	165
6.5.4	Selection of Predictable Stand Variables .....	166
6.5.5	Principal Component Images .....	167
6.5.6	Canonical Variables .....	168
<b>6.6</b>	<b>Summary and Conclusion</b> .....	<b>168</b>

## Chapter 7

# Estimating Forest Site Quality Using Satellite and Biogeographical Data

<b>7.1</b>	<b>Introduction</b> .....	<b>170</b>
<b>7.2</b>	<b>Methodology</b> .....	<b>171</b>
7.2.1	Data Sources .....	171
7.2.1.1	Site Variables .....	171
7.2.1.2	Satellite Data .....	172
7.2.1.3	Measure of Site Quality .....	172
7.2.2	Data Analysis .....	173
7.2.2.1	Correlation Analysis .....	173
7.2.2.2	Canonical Correlation Analysis .....	173
7.2.2.3	Principal Component Transformations .....	173
7.2.2.4	Regression Modelling .....	174
7.2.2.5	Site Quality Classification and mapping .....	176
<b>7.3</b>	<b>Results and Discussion</b> .....	<b>177</b>
7.3.1	Correlations .....	177
7.3.1.1	Correlations between Site Quality and Stand Variables .....	177
7.3.1.2	Correlations between Site Quality and Raw Spectral Data .....	178
7.3.1.3	Correlations between Site Quality and Principal Component Images .....	179
7.3.1.4	Correlations between Site Quality and Difference and Mean Images .....	180
7.3.1.5	Correlations between Site Quality and Vegetation Indices .....	181
7.3.1.6	Correlations between Site Quality and Site Variables .....	183
7.3.2	Canonical Correlations .....	183
7.3.2.1	Canonical Correlations between SPOT Image and Site Quality .....	184
7.3.2.2	Canonical Correlations between TM Images and Site Quality .....	185

7.3.2.3	Comparisons of the Multi-temporal and Multi-sensor Image .....	187
7.3.2.4	Canonical Correlations between Site Quality and Site Variables .....	188
7.3.3	Estimation of Site Quality .....	190
7.3.3.1	Introduction .....	190
7.3.3.2	Scatter Plots .....	191
7.3.3.3	Simple Regression .....	191
7.3.3.4	Multiple Regression with Spectral Variables .....	197
7.3.3.5	Regression Modelling with Spectral and Site variables .....	198
7.3.3.6	Regression Modelling with Multi-temporal and Multi-Sensor Data and Site Variables .....	200
7.3.4	Site Quality Mapping and Assessment of Accuracy .....	201
7.3.5	Selection of Variables for Site Quality Estimation .....	207
7.6	Summary and Conclusion .....	208

## Chapter 8

# Summary and Conclusion

	.....	210
References	.....	214
Appendix A	.....	246
Appendix B	.....	247
Appendix C	.....	248
Appendix D	.....	249
Appendix E	.....	250
Appendix F	.....	251
Appendix G	.....	252

## Symbols, Acronyms and Abbreviations

<i>2TM</i>	<i>Landsat TM images recorded on 9 February, 1988</i>
<i>4TM</i>	<i>Landsat TM images recorded on 21 April, 1988.</i>
<i>AB</i>	<i>Depth of A and B soil horizons</i>
<i>ACT</i>	<i>Australian Capital Territory</i>
<i>AET</i>	<i>Actual EvapoTranspiration</i>
<i>AHVRR</i>	<i>Advanced Very High Resolution Radiometer</i>
<i>ALT</i>	<i>Altitude</i>
<i>ANPP</i>	<i>Above-ground Net Primary Production</i>
<i>ASP</i>	<i>Aspect</i>
<i>ATM</i>	<i>Airborne Thematic Mapper (i.e. TMS)</i>
<i>AVI</i>	<i>Agricultural Vegetation index</i>
<i>AVIRIS</i>	<i>Airborne Visible/Infrared Imaging Spectrometer</i>
<i>BC</i>	<i>Before Christ</i>
<i>B/W</i>	<i>Black-and-White</i>
<i>BA</i>	<i>Basal Area</i>
<i>BAOB</i>	<i>Basal Area Over Bark</i>
<i>BI</i>	<i>Basal Index</i>
<i>CAM</i>	<i>Computer Aided Mapping</i>
<i>CASI</i>	<i>Compact Airborne Spectrographic Imager</i>
<i>CC</i>	<i>Canopy Cover</i>
<i>CCA</i>	<i>Canonical Correlation Analysis</i>
<i>CCT</i>	<i>Computer Compatible Tape</i>
<i>CD</i>	<i>Canopy Depth</i>
<i>CI</i>	<i>Canopy Index</i>
<i>CIR</i>	<i>Colour infrared</i>
<i>CSIRO</i>	<i>Commonwealth Scientific and Industrial Research Organisation</i>
<i>CV</i>	<i>Coefficient of Variation</i>
<i>D<sub>p</sub> ..., D<sub>7</sub></i>	<i>Difference of 2TM and 4TM Data</i>
<i>DBH</i>	<i>Diameter at Breast Height</i>
<i>DBHOB</i>	<i>Diameter at Breast Height Over Bark</i>
<i>DEM</i>	<i>Digital Elevation Models (see DTM)</i>
<i>DF</i>	<i>Degree of Freedom</i>
<i>DI</i>	<i>Diameter Index</i>
<i>DTM</i>	<i>Digital Terrain Models (see DEM)</i>
<i>FAO</i>	<i>Food and Agriculture Organisation</i>
<i>EMR</i>	<i>Electromagnetic Radiation</i>
<i>EMS</i>	<i>Electromagnetic Spectrum</i>
<i>ERIM</i>	<i>Environmental Research Institute of Michigan</i>
<i>ESSA</i>	<i>Environmental Science Service Administration</i>
<i>F</i>	<i>F Statistic</i>
<i>GC</i>	<i>Gravel Content</i>
<i>GI</i>	<i>Green Index, Growth Index</i>
<i>GIS</i>	<i>Geographic Information Systems</i>
<i>GVI</i>	<i>Global Vegetation Index</i>
<i>HCMR</i>	<i>Heat Capacity Mapping Radiometer</i>
<i>HI</i>	<i>Height Index (mean annual increment in height)</i>
<i>HIRIS</i>	<i>High Resolution Imaging Spectrometer</i>

<i>HRV</i>	<i>Higher Resolution Video</i>
<i>ICSU</i>	<i>International Council of Scientific Unions</i>
<i>IEEE</i>	<i>Institute of Electrical and Electronics Engineers</i>
<i>ILRI</i>	<i>Institute for Land Reclamation and Improvement</i>
<i>ISSS</i>	<i>International Society of Soil Science</i>
<i>IUFRO</i>	<i>International Union of Forestry Research Organisations</i>
<i>LAI</i>	<i>Leaf Area Index</i>
<i>LU</i>	<i>Land Unit</i>
<i>LUT</i>	<i>Land Utilisation Type</i>
$\lambda_i$	<i>Eigenvalues</i>
<i>m</i>	<i>Mean vector</i>
$M_p, \dots, M_7$	<i>Mean of 2TM and 4TM Data</i>
<i>MAE</i>	<i>Mean Absolute Error</i>
<i>MAI</i>	<i>Mean Annual Increment</i>
<i>MD</i>	<i>Mean Diameter</i>
<i>MERIS</i>	<i>Medium Resolution Imaging Spectrometer</i>
<i>MIR</i>	<i>Middle Infrared (Mid-Infrared)</i>
<i>MLC</i>	<i>Maximum Likelihood Classification</i>
<i>MSS</i>	<i>Multiple Spectral Scanner</i>
<i>NDVI</i>	<i>Normal Difference Vegetation Index</i>
<i>NIR</i>	<i>Near-Infrared</i>
<i>NASA</i>	<i>National Aeronautics and Space Administration</i>
<i>NFI</i>	<i>National Forest Inventory</i>
<i>NOAA</i>	<i>National Oceanic and Atmospheric Administration</i>
<i>NPP</i>	<i>Net Primary Productivity</i>
<i>NSW</i>	<i>New South Wales (Australia)</i>
<i>PC</i>	<i>Principal Component</i>
<i>PCA</i>	<i>Principal Components Analysis</i>
<i>PCT</i>	<i>Principal Components Transformation</i>
<i>PPMC</i>	<i>Pearson Product Moment Correlation</i>
<i>PS</i>	<i>Panchromatic Band of SPOT HRV Data</i>
<i>PSN</i>	<i>( Net ) Photosynthesis</i>
<i>r</i>	<i>Correlation Coefficients</i>
$r^2$	<i>Squared Correlation Coefficients (r-squared)</i>
$r_a^2$	<i>Adjusted Squared Correlation Coefficients</i>
$r_{op}^2$	<i>Correlations between observed and model-predicted data</i>
<i>RADAR</i>	<i>Radio Detection And Ranging</i>
<i>RMSE</i>	<i>Root Mean Squared Error</i>
<i>RVI</i>	<i>Relative Vegetation Index</i>
$S^2$	<i>Variance (or Variance-Covariance matrix)</i>
<i>SAF</i>	<i>Society of America Foresters</i>
<i>SAR</i>	<i>Synthetic Aperture Radar)</i>
<i>SAS</i>	<i>Statistical Analysis System</i>
<i>SD</i>	<i>Standard Deviation</i>
<i>SE</i>	<i>Standard Error</i>
<i>SI</i>	<i>Site Index</i>
<i>SLAR</i>	<i>Side (or sideways)-Looking Airborne Radar</i>
<i>SLP</i>	<i>slope</i>
<i>SN</i>	<i>Stem Number per Hectare</i>
<i>SPOT</i>	<i>Système Probatoire d'Observation de la Terre</i>
<i>SQ</i>	<i>Site Quality</i>

<i>SSSA</i>	<i>Soil Science Society of America</i>
<i>STH</i>	<i>Stand Top Height</i>
<i>t</i>	<i>t statistic</i>
<i>TH</i>	<i>Top height</i>
<i>TIR</i>	<i>Thermal Infrared</i>
<i>TIROS</i>	<i>Television Infrared Observation Satellite</i>
<i>TM</i>	<i>Thematic Mapper</i>
<i>TMS</i>	<i>Thematic Mapper Simulator</i>
<i>TP</i>	<i>Topographic Position (slope position)</i>
<i>TRAN</i>	<i>Transpiration</i>
<i>u, v</i>	<i>Canonical variables</i>
<i>UC</i>	<i>Understory cover</i>
<i>UNESCO</i>	<i>United Nations Educational, Scientific and Cultural Organisation</i>
<i>USDA</i>	<i>United States Department of Agriculture</i>
<i>USGS</i>	<i>United States Geological Survey</i>
<i>VI</i>	<i>Volume Index</i>
<i>VOL</i>	<i>Volume</i>
<i>x, y</i>	<i>variable names</i>
<i>XS</i>	<i>SPOT Multispectral Bands</i>
$\chi^2$	<i>Chi-squared Statistic</i>

## The List of Tables

Table 2.1 Remote sensing timeline. Some of the important dates in civilian remote sensing programs.	31
Table 2.2 Classification scheme for forest inventories (FAO 1982).	39
Table 2.3 Forestry information requirement and possible forestry applications of remote sensing.	40
Table 3.1 Mean and median monthly and annual rainfall (mm), raindays (no.), humidity (%) and temperature (°C).	74
Table 3.2 Site classes of radiata pine defined by top height (TP) at 20 years of age (Gray 1945), site index (SI) and mean annual increment (MAI) of volume (Gunn <i>et al.</i> 1969; and Lewis <i>et al.</i> 1976).	78
Table 4.1 The category division levels of qualitative site variables (aspect and topographic positions) over the study area. The division levels are used for '0-1' coding and quantitative analysis in Chapter 7.	87
Table 4.2 The basic statistics of imagery data over the whole study area. The total pixel number is 216000 (576 x 375). SD - Standard deviation, CV - coefficients of variation (%).	91
Table 4.3 The digitised stands at different age levels. Pixel size is 20 x 20 meters (0.04 ha).	93
Table 5.1 General statistics of the radiata pine stands selected to calculate spectral values aged from 3 to 42 years.	104
Table 5.2 The data characteristics of SPOT and Landsat TM imagery data of the radiata pine plantation stands aged from 3 to 42 years. The total pixels on radiata pine plantation stands were 60869.	109
Table 5.3 Summary of the mean ( $M_1$ to $M_7$ ) and difference images ( $D_1$ to $D_7$ ) of the two TM data sets over the radiata pine plantation stands ranging aged from 3 to 42 years. $n = 36$ .	110
Table 5.4 Difference significance test on mean reflectance ( $t$ -test) and equal variances test ( $F$ -test) of the three data sets recorded by SPOT and Landsat TM on three dates.	111
Table 5.5 Results of PCA for SPOT XS data.	116
Table 5.6 Results of PCA for the February-9 TM data.	116
Table 5.7 Results of PCA for the April-21 TM data.	116
Table 5.8 Results of PCA for the difference image of the two TM data sets.	117
Table 5.9 Results of PCA for the mean image of the two TM data sets.	117
Table 5.10 Results of PCA for the three data sets together (18 channels).	118
Table 5.11 Correlations within and between the three data sets.	121
Table 5.12 Correlations between stand ages and the raw spectral values and the combined TM data. The correlation coefficients were computed with the values from stands aged from 3 to 42 and 5 to 30 years respectively.	122
Table 5.13 Correlations between the first two principal components and stand ages (3 - 42).	123
Table 5.14 Regression models relating spectral values to stand age. The models listed in the table were defined in Section 5.2.2.7.	125
Table 5.15 Relationships between vegetation indices and stand age. The regression was computed using equation: $VI = a + b \cdot \log(\text{age}) + c \cdot \log^2(\text{age})$ , $n = 36$ .	126
Table 5.16 Growth patterns of radiata pine plantation stands (from Jacobs 1937).	132

Table 6.1 Summary of the forest stand variables of 60 0.01-hectare sample plots.	148
Table 6.2 Summary of the site variables of 60 0.01-hectare sample plots	149
Table 6.3 The basic statistics of spectral values of the 60 sample points on 3 x 3 pixel windows	149
Table 6.4 Correlations between stand variables.	150
Table 6.5 Correlations between stand variables and site variables	151
Table 6.6 Correlations between raw imagery data and stand variables. 2TM and 4TM represents the February-9 TM and the April-21 TM images respectively.	151
Table 6.7 Correlations between the difference ( $D_1, \dots, D_7$ ) and mean ( $M_1, \dots, M_7$ ) imagery data and stand variables	153
Table 6.8 Results of PCA using SPOT XS data and correlation analysis between the stand variables and the principal component image.	154
Table 6.9 Results of PCA using the February-9 TM data and correlation analysis between the stand variables and the principal component image.	154
Table 6.10 Results of PCA using the April-21 TM data and correlation analysis between the stand variables and the principal component image.	155
Table 6.11 Results of PCA using the TM data for two dates (14 channels) and correlation analysis between the stand variables and the principal component image.	155
Table 6.12 Correlations between stand variables and the "within-image" band combinations of SPOT image. XS3/1 and XS3-1 represent the ratio and differences of bands XS3 and XS1.	155
Table 6.13 Correlations between stand variables and the "within-image" band combinations of the February-9 TM image. TM4-2, TM4/5, TM4/2 and TM4-1 denotes the differences and/or ratios of the corresponding band numbers.	155
Table 6.14 Correlations between stand variables and "within-image" band combinations of the April-21 TM image. For band combinations see Table 6.13.	156
Table 6.15a Results of CCA between stand variables and the SPOT data.	157
Table 6.15b Standardised canonical coefficients and correlations between the original variables and the canonical variables of opposite sets of variables.	157
Table 6.15c Canonical redundancy analysis between stand variables and the SPOT data.	158
Table 6.16a Results of CCA between stand variables and the February-9 TM data.	160
Table 6.16b Standardised canonical coefficients and correlations between the original variables and the canonical variables of opposite sets of variables.	160
Table 6.16c Canonical redundancy analysis for February-9 TM data and stand variables.	161
Table 6.17a Results of CCA between stand variables and the April-21 TM data.	161
Table 6.17b Standardised canonical coefficients and correlations between the original variables and the canonical variables of opposite sets of variables.	161
Table 6.17c Canonical redundancy analysis for the April-21 TM data and stand variables.	162
Table 6.18a Results of CCA between stand and site variables.	163
Table 6.18b Standardised canonical coefficients and correlations between the original variables and the canonical variables of opposite sets of variables.	163
Table 6.18c Canonical redundancy analysis for site and stand variables.	163

Table 7.1 The coding of the qualitative site variables (topographic position and aspect) for qualitative analysis (the definition of the variable attributes is given in Table 4.1). $n$ - sample number.	176
Table 7.2 Correlations between SQ indices.	177
Table 7.3 Correlations between SQ indices and stand variables.	178
Table 7.4 Correlations between SQ indices and raw band data	178
Table 7.5 Correlations between SQ indices and principal component images.	180
Table 7.6 Correlations between SQ indices and difference ( $D_1$ to $D_7$ ) and mean ( $M_1$ to $M_7$ ) images	181
Table 7.7 Correlations between SQ indices and "within-image" band combinations ( <i>i.e.</i> vegetation index).	182
Table 7.8 Correlations between SQ indices and site variables.	183
Table 7.9a Results of CCA between SQ indices and SPOT data.	184
Table 7.9b Standardised canonical coefficients and correlations between the original variables and the canonical variables of opposite sets of variables.	184
Table 7.10a The results of CCA between SQ indices and the February-9 TM image.	186
Table 7.10b Standardised canonical coefficients and correlations between the original variables and the canonical variables of opposite sets of variables.	186
Table 7.11a Results of CCA between SQ indices and the April-21 TM image.	186
Table 7.11b Standardised canonical coefficients and correlations between the original variables and the canonical variables of opposite sets of variables.	186
Table 7.12a Results of CCA between site quality and all three data sets together (XS+PS+2TM+4TM).	187
Table 7.12b Standardised canonical coefficients and correlations between the original variables and the canonical variables of opposite sets of variables.	188
Table 7.13a Results of CCA between SQ indices and site variables.	189
Table 7.13b Standardised canonical coefficients and correlations between the original variables and the canonical variables of opposite sets of variables..	189
Table 7.14 The basic statistics of SQ indices HI (m/yr) and SI (m).	191
Table 7.15 Evaluation of simple regression model performance for predicting radiata pine plantation site quality (HI and SI) using single band data. $n = 60$ .	196
Table 7.16 Results of simple regression analysis between SQ indices and "between-image" combinations. The model parameters are the same as in Table 7.15.	197
Table 7.17 Results of multiple and stepwise regression analyses between SQ indices (HI and SI) and the original band data. The significance level ( $p$ ) selected for entering variables in stepwise regression was 0.15.	198
Table 7.18 Results of multiple regression analyses by integrating spectral bands with topographic variables ( <i>i.e.</i> ALT, SLP, ASP and TP defined in Chapter 4).	199
Table 7.19 Performance of several best regression models ( <i>a-h</i> ) relating SQ indices (HI and SI) to the multi-temporal and multi-sensor data and site variables.	200
Table 7.20 Site quality classes of the radiata pine plantation sites.	202
Table 7.21 Error matrix for actual and model-derived (Model-h) SQ classes.	207



## The List of Figures

Figure 2.1 Approaches for estimating site quality and relationships among them.	24
Figure 2.2 Spectral reflectance curves of typical green vegetation, soil and water. Also shown are the system parameters of the four most common digital satellite remote sensing systems: SPOT, TM, MSS, and AVHRR.	33
Figure 3.1 Location of the study area.	71
Figure 3.2 Radiata pine plantation stands over the study area (adapted from AUSMAP CSU 89/011, Edition 4, AUSLIG 1989)	72
Figure 4.1 The frequency of spectral values over the study area (576 x 375 pixels).	89
Figure 4.2 Radiata pine plantations in the study area. The map was produced with SPOT panchromatic band and the February-9 TM bands 4 and 5. The pine plantations are dark green in colour surrounded by compartment boundaries.	90
Figure 4.3 The digitised 5-year age class map of the radiata pine plantation stands in the study area. The areas and percentages of each age level are summarised in Table 4.3 (see Section 4.4.2).	90
Figure 4.4 The terrain and geomorphological map of the study area. The map was generated from digital terrain model (DTM).	98
Figure 4.5 The elevation (m) of the radiata pine plantation area.	98
Figure 4.6 Slope ( ° ) of the radiata pine plantation area.	99
Figure 4.7 Aspect over the radiata pine plantation stand area. It is displayed in eight directions, each 45° clockwise from north.	99
Figure 5.1 Proportions of the radiata pine plantation stands at the different age levels (a) and 5-year age classes (b).	104
Figure 5.2 Relationships between spectral band data and stand age .	112
Figure 5.3 Relationships between the difference and mean spectral values of the two TM data sets for two dates and stand age.	113
Figure 5.4 Relationships between 5-year age classes and mean spectral values: the January-24 SPOT data (a); the February-9 TM data (b); the April-21 TM data (c); and (d) is the comparison of the three similar bands, the green, red and NIR, of the three data sets.	114
Figure 5.5 Relationships between stand age and the three vegetation indices: AVI (a); RVI (b); and NDVI (c).	115
Figure 5.6 Plots of PC2 against PC1 calculated from the images of the January-24 SPOT data (a), the February-9 TM (b) and the April-21 TM (c). The characters from a to z and several other symbols represent the stand age from 3 to 42 (see Table 5.1)	119
Figure 5.7 Relationships between stand age and the first two PCs of the January-24 SPOT data (a); the February-9 TM data (b); the April-21 TM data (c); and the three data sets together (d).	124
Figure 5.8 Clustering dendrograms showing the resemblance between the spectral bands of the three single date images (a) - (c) and showing the relationships among the three images and corresponding spectral bands (d).	127

Figure 5.9 Clustering dendrograms of the mean spectral values of stands aged from 3 to 42. The number at the right of each diagram is the stand age in years. The figures show the classifications of the mean spectral values of the stands computed from the February-9 TM data (a), the April-21 TM data (b), the January-24 SPOT data (c), and the three data sets together (i.e. SPOT+2TM+4TM: 18 channels) (d).	128
Figure 5.10 Curves of changes in spectral values in the red and NIR bands with increasing stand age.	134
Figure 5.11 Band data ranges of the three data sets over the radiata pine stands aged from 5 to 42 years.	136
Figure 7.1 Relationships between SQ indices (SI (m) and HI (m/yr)) and the SPOT band data.	192
Figure 7.2 Relationships between SQ indices (SI (m) and HI (m/yr)) and the February-9 TM band data.	193
Figure 7.3 Relationships between SQ indices (SI (m) and HI (m/yr)) and the April-21 TM band data.	194
Figure 7.4 Relationships between AVIs and SQ indices (SI (m) and HI (m/yr)).	195
Figure 7.5 Relationships between PC2 (greenness) and SQ indices (SI (m) and HI (m/yr)).	195
Figure 7.6 Relationships between observed and model-estimated SQ indices (SI (m) and HI (m/yr)). Models a to Model-h were defined in table 7.19.	201
Figure 7.7 Distribution of site quality of the radiata pine plantation sites in the study area: Mean annual increment in height (HI) (b) and site index (SI) (a).	202
Figure 7.8 Site quality classes based on HI (m/yr) estimated from model-a (see Tables 7.19 and 7.20 for details)..	203
Figure 7.9 Site quality classes based on HI (m/yr) estimated from model-b (see Tables 7.19 and 7.20 for details)..	203
Figure 7.10 Site quality classes based on HI (m/yr) estimated from model-c (see Tables 7-19 and 7.20 for details)..	204
Figure 7.11 Site quality classes based on HI (m/yr) estimated from model-d (see Tables 7-19 and 7.20 for details)..	204
Figure 7.12 Site quality classes based on SI (m) estimated from model-e (see Tables 7-19 and 7.20 for details)..	205
Figure 7.13 Site quality classes based on SI (m) estimated from model-f (see Tables 7-19 and 7.20 for details)..	205
Figure 7.14 Site quality classes based on SI (m) estimated from model-g (see Tables 7-19 and 7.20 for details)..	206
Figure 7.15 Site quality classes based on SI (m) estimated from model-h (see Tables 7-19 and 7.20 for details)..	206

## **General Introduction**

### **1.1 NEED TO ESTIMATE SITE QUALITY**

Future forest growth depends on maintaining forest site productivity. There must be increasing intensity of forest management on the shrinking land base available for forestry. Together with effects of world-wide environmental pollution, this will alter the nature of the environments in which future forest crops are grown. More critically, demand for wood will continue to increase because of the shrinking land base, increasing world population and greater use of wood for energy and fuel. This is particularly true in most developing countries. Forest scientists and managers all over the world will face increasing difficulties in planning and managing forest resources for future use on decreasing and degrading forest land to meet the challenge of growing wood demand. To decide how best to balance the many demands on the resources for best utilisation for future generations, forest managers must know where the forest resources occur, and what the quantity and quality of forest sites and their productivity potential are. As the foundation of modern silviculture and management planning, accurate and rapid prediction and evaluation of the quantity and quality of forest sites and their productivity become more critical for economic planning and decision-making, since the quantity and quality of forest resources not only decide the forest products and economic development, but also affect the balance of environmental ecology.

Reliable information about site quality is required principally for operational management, forest planning, silvicultural design, research and industry planning. It is a prerequisite for the most efficient utilisation of a forest site. There have been many cases where planted trees have failed due to lack of consideration of site quality. In Australia, for instance, introduced pine has failed on eucalypt forest sites with low phosphorus status soils (Florence 1981). Therefore, in countries where forestry is highly developed, modern silviculture is characterised by the strong emphasis placed on the site conditions. In Germany, for example, the forester speaks of the "Iron Law of the Site" (Wittich 1960). This means that, notwithstanding the fact that improper measures can ruin the best forest sites, there are certain factors deriving from the very nature of the site that determine development of the forest and reactions to forestry treatments. As stated by Daniel *et al.* (1979): "No silvicultural decision can be made without reference to site quality and other site conditions." To most forest managers, an accurate and timely knowledge of the quality, value, or suitability of forest sites becomes essential for deciding their usage and management planning.

The wide recognition of importance of site assessment leads to intensive and extensive studies on forest sites. Various different methods and modelling techniques for site classification and evaluation have been developed according to particular geographic and economic conditions and the historical background in different countries (see Chapter 2). Many site factors and indicators have been suggested for use as measures of site quality (Jones 1969; Lewis *et al.* 1976; Hägglund 1981; and Clutter *et al.* 1983), but no consistently applicable index of quality has been standardised. Forest managers and researchers have generally used total (or dominant) height at a designated age (called site index) as a measure of forest site quality (or productivity). Such indices, however, are applicable only to single species for a limited geographical area. Most of the established methods for site information collection involve very time-consuming and very expensive direct field measurements of a large number of temporary or permanent sample plots and trees. To date, forest scientists have been seeking ways of accurately estimating site quality using modern technologies in site information collection and analysis. These include the applications of modern remote sensing, geographic information systems (GIS) and other computer-aided spatial analysis, mapping and modelling techniques (see Chapter 2).

Remote sensing techniques clearly offer an alternative for forest growth and productivity estimation and especially for up-dating purposes. This is because the spectral values of individual pixels of digital remotely-sensed imagery and the values of corresponding

forest stand structure characteristics are often correlated clearly with each other. The usability and capability of remotely-sensed imagery increases with the increase of the correlation. In particular, remote sensing provides an opportunity to view, assess and estimate forest resources in inaccessible areas at any season of the year, and very valuable information can be acquired at low cost.

In spite of its great potential, satellite remote sensing has found few direct applications in forest management. In principle, remote sensing can be expected to offer information on tree species, size, productivity and yield, and their variations, within a forest stand. However, in addition to the difficulties of establishing robust predictive relationships for these factors, practical applications are severely limited by logistic constraints: the spatial and radiometric resolution and sensitivity of the imagery (relative to the scales of variation that are important); the frequency and timing of the measurements (relative to the time scale of growth); and the cost of the data (relative to the benefit to be gained from it). This is why forest managers have generally been reluctant users of satellite remote sensing to date, despite the fact that numerous demonstrations have shown the possibility of using satellite remotely-sensed data for forest management purposes. Due to uncertain and variable results from imagery data quality, species and stand conditions, they have a strong preference for gathering detailed information using statistical sampling methods and relying heavily on the measurement of individual trees within discrete forest stands. Moreover, forestry organisations usually employ experienced aerial photo-interpreters rather than digital satellite imagery interpreters. Any decision on the use of satellite remote sensing to replace or supplement aerial photography and field sampling is therefore subjected to rigorous comparison of cost advantages and precision of stand measurements. This suggests that there is a need for further study to determine the capability of remotely-sensed imagery to detect, either directly, or indirectly by calculation, subtle changes of forest structure and site quality and the information required for modern site quality assessment.

## **1.2 A BRIEF DISCUSSION ON SITE AND SITE QUALITY CONCEPTS**

### **1.2.1 Introduction**

The concepts of *site*, *site quality* and *site classification* have traditionally been central to forest management, but as forestry terms they can be ambiguous and confusing. In some respects they are discredited and archaic terms, and their continued use and abuse can be

seen as a ‘hang-up’ of an inherently conservative profession. They are nonetheless entrenched terms, which are used with reservation, where necessary, in this work but alternative terminology is also introduced. This section aims to review the concepts of *site* and *site quality* found in the literature. Some synonyms for these concepts are also introduced.

### 1.2.2 Site

In the *Shorter Oxford English Dictionary* (Williams *et al.* 1964), the word *site* is defined as “the place or position occupied by some specific thing.” This definition is not very meaningful in forestry. The earliest concept of forest *site* might be that of *locality*, i.e. a different locality indicates a different *site quality* (see below), which was later shortened to *site* (Fernow 1905). In *Forest Terminology* (SAF 1960), the term *locality* was seen as the synonym of *site*. According to Jiang (1990), as early as the latter part of last century, *site* had been used as a formal forestry term in German by Ramann (1893) in his book *Forstliche Bodenkunde und Standortlehre* (Forest Soil Science and Site Theory). For about a century, there have been various interpretations of the concept of *site*, consequently, many different definitions. In forestry, *site* is used to represent the sum total of environmental effects upon the quantity of wood grown by forest trees on any particular area (Minor 1954). The first official definition was given by the Society of American Foresters (SAF) in 1919: “an area considered as to its physical factors with reference to forest producing power; the combination of climatic and soil conditions of an area” (Frothingham 1921). Similar definitions were given later by many researchers (e.g Chapman *et al.* 1921; SAF 1960; and Davis 1966). In 1971, SAF redefined *site* as “an area considered in terms of its environment, particularly as this determines the type and quality of vegetation the area can carry.” (SAF 1971). In Australia, Speight and McDonald (1984) also defined *site* as “a small area of land considered to be representative of the landform, vegetation, land surface and other land features associated with the soil classification.” In Canada, it was defined as “an area homogeneous in all environmental conditions significant for the development of forest communities” (Green *et al.* 1984). This definition put emphasis on the climatic, physiographic and edaphic properties used for *site diagnosis* purposes. In Finland, Cajander (1926 and 1949), the founder of forest typology, suggested that *site type* (also called *forest type*) could be defined by composition of the undergrowth and used to indicate environment and its potential for growth of canopy trees. In these definitions, the term *site* is used in a dual

sense. The SAF's definition shows first that the term *site* carries a connotation of geographic and spatial location and second that the meaning of the word involves the totality of environmental conditions (i.e. biotic, edaphic, and climatic) existing at a particular location. This distinction may seem overly academic since a location cannot exist without an associated environment, and no environment can exist without being located at some particular place.

However, the site can also be understood in a wider sense, as the complex of the environment in which a given vegetal community lives and grows and of the plant community itself. Site embraces the atmosphere, soil and the underlying geology, the hydrology, and the plants on, above and below a particular place. In ecology, the term has two meanings: (i) an area described or defined by its biotic, climatic, and soil conditions as related to its capacity to produce vegetation; (ii) an area sufficiently uniform in biotic, climatic, and soil conditions to produce a particular climax vegetation. In much of the plant ecology literature and, to some extent, in that of forestry, the term site has been used as a synonym of *ecosystem* (or *ecotope*), *biogenoconis*, and *total site*, referring only to the physiographic or land features (Hills and Pierpoint 1960, and Burger 1976). Tansley (1935), the founder of ecosystem theory, considered the site of a plant or of a vegetal community to be "the sum of the effective conditions under which the plant or plant community lives" (Phillipis 1960). This definition has been seen as the simplest and clearest of all and has been widely accepted. The SAF also interpreted site as synonymous with ecosystem. After Tansley put forward the concept of ecosystem, many site specialists considered site as ecosystem or *elementary ecological unit*, an *ecotope* (Rowe 1953; Phillipis 1960). In North America, ecosystem principles were introduced into forest site classification and evaluation by Hills (1952b; 1953; and 1959), and Hill and Pierpoint (1960). The concept of total site and/or *forest productivity system* was developed and later simply called *forest productivity* or total site (Hills and Pierpoint 1960; Hills 1961). Gessel (1967) also called forest productivity site or yield.

From the literature, many concepts of forest site have been developed for the purpose of describing the relationships between forests and their environmental conditions. The concepts similar to forest site include site type and/or forest type (Frothingham 1914; Cajander 1926; Forristall and Gessel 1955; Ray 1956), locality (Fernow 1905), total site (Hills 1952a; Rowe 1953), *habitat* or *habitat type* (Yapp 1922; Daubermire 1952; Hanley 1976; Pfister 1976; Pfister and Arno 1980; Spurr and Barnes 1980; Verbyla and Fisher 1989), ecosystem (Klinka *et al.* 1980; Bailey 1981; Daubenmire 1984; Barnes *et al.* 1982; Barnes 1984; and Pfister 1984), elementary ecological unit or ecotope (Phillipis 1960),

*land type* (Hills 1961), biogeocenosis (Suchachev 1960; Suchachev and Dylis 1964; and Burger 1976), *land unit* (LU) (Beek and Laban 1981) and *land utilisation type* (LUT) (Beek 1972; and Andel *et al.* 1981; and Gelens 1984). To a great extent, these definitions seem to share the same ideas, but with different emphasis on particular site attributes and/or combinations of site attributes in different physiographical backgrounds. From the viewpoint of forest management, the site concept tends to be relatively 'simple', while from the viewpoint of ecology it tends to be complex and may not be very applicable to everyday practical work. Attempts have been made to find a simple and accurate unit of measurement to define site, but there has been no agreement on which are the most significant and most reliable factors. Most of the current site classification systems and evaluation standards are based on climate, soil, ground vegetation, forest stands, or multi-factors with one of them as a major feature. In the minds of most foresters, a forest site is every part of the forest environment that is relatively uniform in physiography and soil, and has the same biotic potential, usually expressed by a specific pattern of indicator plant species. Within a given regional climate, sites are recognised on the basis of significant differences in topography (slope position, gradient and aspect), soil parent materials, and/or morphological properties of the soil (e.g. the kind and arrangement of organic and mineral soil horizons, their colour, texture, structure, consistency, thickness, and coarse fragment content).

### 1.2.3 Site Quality

In forestry, the productivity of a forest site is largely defined in terms of *site quality*, which is measured by the maximum timber crop the site can produce in a given time. Coile (1952) defined site quality as the productive capacity (or actual production) of an area of land for a tree species or mixture of species. Clutter *et al.* (1983) also defined site quality as "the timber productivity potential of a site for a particular species or forest type." The words *good* and *poor* are frequently-used modifiers of site quality and simply imply a high productive potential as opposed to a low potential. Daniel *et al.* (1979) defined site quality in a more comprehensive way: "Site quality is the sum of many environmental factors: soil depth, soil texture, profile characteristics, mineral composition, steepness of slope, aspect, microclimate, species, and others. These factors, in turn, are functions of geologic history, physiography, macroclimate, and successional development."

Since site quality is measured by the maximum timber yield produced within a given period, it can vary with the tree species and time element chosen. Although the site is



relatively constant, in the short term, regardless of species selection, site quality has meaning only with respect to the one or more species selected for a given location. Therefore, site quality remains a relative concept, and cannot be defined in an absolute sense, as a particular area may be a good site for one species and a bad site for another (Meyer 1953). For instance, a given site might have an excellent site quality for radiata pine but a very poor site quality for white ash.

Site quality is, in a general sense, a use-oriented concept, mainly for the purpose of site classification, evaluation and site management (silviculture), and with economic yield emphasised. Therefore, many concepts involved in economic yield have been developed to define site quality, such as *site productivity* (Smithers 1959; Ralston 1964; and Spurr and Burnes 1980), *site class* (Suchachev 1960), *land quality* (McCormack 1967; Löffler 1981; Lundgren 1981; Nelson 1981; and Gelens 1984), *land suitability* (FAO 1984; Lewis *et al.* 1976; Nelson 1981; and Plochmann 1981), and *land (site) capability* (McCormack 1967; Gunn *et al.* 1969a; Lacate and Romaine 1978), and *soil fertility* or *soil productivity* (Baker 1982). The development of forest site studies will be discussed in more detail in the next chapter.

#### 1.2.4 Summary

Logically, site quality concepts can be grouped as class concepts, relational concepts, or quantitative concepts. The class concept enables certain groupings to be made, for instance, forest site - non-forest site; good-medium-poor site. The relational concept allows comparisons rating from "different" to "better than." The quantitative treatment of forest site quality calls for numerical modelling.

As noted above, the site concept is designated by the term 'site'. By itself, it is ambiguous. Attempts to reduce ambiguity have involved addition of words to the term, such as *site quality* and *site productivity*. *Quality* seems in general less useful than *productivity* as the former usually connotes some sort of nonmetric measure of forest producing power. *Productivity* connotes both the relation between sites and forest vegetation on them or ecosystems and metric measurement. However, site quality is a widely-accepted concept in forestry, while productivity is usually used in ecology by ecologists. For this reason, site quality will be used to designate the concept of the forest-producing-power of a site in this thesis.

### 1.3 POSSIBILITY OF ESTIMATING STAND VARIABLES AND SITE QUALITY USING REMOTE SENSING: RESEARCH HYPOTHESIS

The success of monitoring and estimating forest resources by remote sensing depends on its capability to determine forest tree species, growth rate, size, and various stand variations from canopy reflectance measurements. In other words, it depends on the capability of remotely-sensed data to detect the subtle variations existing in forest stand growth processes. Current satellite remote sensing technology can be used for a number of ecologically meaningful analyses at various scales. In forestry applications, satellite remotely-sensed data have demonstrated some sensitivity to the canopy and stand structure parameters. For detecting changes in forest canopy, many investigations have been undertaken to relate spectral reflectance values in the different spectral regions (bands) to canopy closure (Butera 1986; Peterson *et al.* 1986; and Sader 1987), leaf area index<sup>1</sup> (LAI) (Curran and Milton 1983; Curran and Williamson 1987; Spanner *et al.* 1990), and biomass (Franklin 1986; Hardisky *et al.* 1984; Sader *et al.* 1989; Lee and Hoffer 1990; Hope *et al.* 1993). Spectral data have also been used by many researchers to detect variations in forest dendrometric variables, including basal area (Brockhaus and Khorram 1992), stand age (Danson 1987; Turner *et al.* 1987), volume (Jaakkola and Saukkola 1978 and 1979; Kazmierczak 1991; and Ardö 1991 and 1992), density of trees (Franklin 1986; Strahler *et al.* 1988; Woodcock *et al.* 1990; Cohen and Spies 1992; Joffre and Lacaze 1993), and diameter and height (Danson 1987). With repetitive acquisition of imagery, studies have shown that seasonal and/or inter-annual changes of vegetation can be detected and predicted using multi-temporal satellite data (Choudhury and Tucker 1987; Running and Nemani 1988; Spanner *et al.* 1990; Curran *et al.* 1992; ). There has been limited success in the detection of variation in site, such as site classification (Fox *et al.* 1985; Lovén 1986; Walsh 1987; Pu and Miller 1991; Poso *et al.* 1987; Tompro 1992), mapping (Getter and Tom 1977; Tom and Miller 1978 and 1980; and Häme 1984), and forest ecosystem productivity estimates (Cook *et al.* 1989; Vanclay and Preston 1990). Studies have also shown that the variation of spectral reflectance can be seen as a function of chemical constituents such as chlorophyll a and b (Khorram *et al.* 1987; Wessman *et al.* 1988; Wessman 1990; Curran *et al.* 1991; Ritchie *et al.* 1990; Chappelle *et al.* 1992; Myneni *et al.* 1992; Oliso *et al.* 1992).

The applications mentioned above have shown the possibility of measuring and estimating forest stands and their site quality from satellite remotely-sensed imagery.

---

<sup>1</sup> LAI — total area of leaves per unit area of ground.

However, accurate classification, assessment and estimation of forest site quality in a local area has been hindered by the considerable species and site variability and relatively coarse spatial, spectral, and radiometric resolution. Furthermore, the results reported are inconsistent and are generally data dependent. In some cases the near-infrared (NIR) band was found to be most important (Franklin 1986; Danson 1987), while in others the middle infrared (MIR) (Band 5 and 7) or thermal infrared (TIR) (Band 6) were reported to be best correlated with stand variables (Butera 1986; Peng 1987; and Brockhaus and Khorram 1992) (see Chapter 2 for details).

Applications of environmental remote sensing are generally based upon an implicit assumption that the spectral information from remote sensors can detect the variations of different objects of interest due to differences of optical properties (emittance, reflectance and absorption). These variations have usually been attributed to the internal changes of research targets over time, space, and spectrum (see Section 2.4.4). Studies have demonstrated that high resolution (including temporal, spatial, spectral, and radiometric resolutions) imagery has high internal variability within relatively homogenous land-cover types (Maxwell 1976; and Cushnie 1987). This high internal variability led to the development of the following research hypotheses:

- Internal variability in a remotely sensed image of a forest will be due to variation in stand structural properties;
- Remotely sensed imagery of high resolution (such as SPOT, TM, and lower altitude air-borne imagery) can detect subtle changes due to forest stand growth and site quality levels;
- Changes in the behaviour of spectral reflectance over time are related to the growth changes in stands, and therefore the *height-age* relation used for site evaluation can be paralleled by a *reflectance-age* relation;
- Stand variables and site quality can be seen as the functions of band spectral reflectances or band combinations as well as other site and stand variables, and by using these functional relationships, a model can be developed to predict the desired information on the basis of the satellite data.
- The accuracy and precision of estimation of site quality estimation can be improved by integrating remotely sensed imagery with ground ancillary data.

- Based on the above hypothesis, direct modelling and prediction of the growth of stands and site productivity are possible using remotely sensed data and ancillary data;
- Site quality can be classified and mapped using remotely sensed imagery and ancillary data.

## **1.4 OBJECTIVES OF STUDY**

The major objective of this study was to determine whether remotely-sensed imagery, either directly, or indirectly by modelling, can give meaningful site quality information, and to develop ways of using satellite remotely-sensed imagery and ancillary data to estimate forest growth and site quality at a local scale. The ancillary data used must be ecologically meaningful and able to be generated by computers, and used directly for the purposes of forest management in a GIS. More specific objectives included:

- testing the relationships between stand variables and spectral reflectance;
- determining the capability of remotely sensed imagery to detect variations in coniferous forest stands;
- testing the sensitivity and separability of remotely-sensed imagery to the characteristics of forest stands at different age levels and different site quality levels;
- determining the optimal combination of site and spectral variables for estimating forest stand variables and site quality.
- Comparing the differences between TM and SPOT data for predicting forest site quality;
- comparing the differences of spectral data acquired from different growing seasons.

## **1.5 THESIS OUTLINE**

This chapter has outlined the need for and possibility of estimating forest growth and site quality. It has also reviewed the conceptual development of site and site quality. Questions concerning the research assumptions and objectives were also raised in this chapter.

Chapter 2 is a review of the literature relating to forest site quality evaluation, remote sensing and its applications to forestry. The Chapter first reviews the historical development of the technologies of forest site quality evaluation and classifications and the principal approaches of site quality evaluation. It then reviews the applications of remote sensing technologies in forestry by giving an overview of the development of forestry remote sensing and a discussion of the spectral characteristics of forest canopies. The focus is on the following uses of satellite imagery: (1) mapping of forest (site) types; (2) forest inventories; (3) evaluation of stand variables; (4) assessment of forest (or site) productivity; and (5) detection of forest changes.

The physical and silvicultural characteristics of the study area are described in detail in Chapter 3. Chapter 4 presents the methods and procedures used for digitising and generating the digital ground truth data and the digital terrain model (DTM). The procedures for field sampling and measurement of stand and site variables are also described in Chapter 4 which also presents the image pre-processing procedures and the compilation of stand and site quality measures at each of the sampling points.

Chapter 5 investigates the relationships between stand age and satellite data. The main objective was to evaluate the sensitivity of spectral values to the plantation stands at different age levels. The study was conducted using correlation, principal component, regression and classification techniques.

Chapter 6 focuses on the relationships between stand variables and spectral data. The capability of the spectral data to estimate stand variables is evaluated by calculating the correlation coefficients between stand variables and raw band data and their various combinations. Correlation, principal component, and canonical correlation analysis techniques are used to determine the information content of each spectral band and optimal spectral bands and stand variables.

In Chapter 7 the relationships between site quality expressed as site index and/or mean annual increment and spectral band data and their various combinations and transformations are investigated. The aim was to develop models to estimate site quality with satellite and biogeographical data. The study was undertaken by using regression modelling techniques, including single, multiple and stepwise regression analysis.

Chapter 8 gives a summary of the methodology and procedures developed as well as conclusions on the results obtained. It also offers suggestions for future directions in localised forest site studies using satellite data.

# Literature Review on Evaluation of Forest Site Quality and Applications of Remote Sensing

## 2.1 INTRODUCTION

Observation and study of forests and their sites has a very long history. Particularly since early this century, with the development of forest ecology and soil science and other relevant disciplines, research into forest-site relationships has been receiving considerable attention from scientists working in a variety of disciplines. Numerous studies on specific aspects of site factors in relation to forest yields have been reported, utilising various methods, approaches and modelling techniques of forest-site relationships. These methods have been applied in site evaluation and classification for forest silvicultural management and planning. Since the 1950s, discussions and/or reviews on the topics of "site evaluation" and/or "site classification" have been published regularly, including those of Coile (1952 and 1960), Heiberg (1956), Gaertner (1964), Ralston (1964), Page (1970), Carmean (1975), Daniel *et al.* (1979), Daubenmire (1976), Damman (1979), Spurr and Barnes (1980), Bailey (1981), Zonneveld (1981), Hägglund (1981), Barnes *et al.* (1982), Kilian (1984), Lavery (1986), Grey (1989b), and Meads and Roberts (1992).

With the advent of computers and the space age, the techniques of computer-aided spatial data analysis, modelling, data capture and satellite-based information collection have been introduced into forest studies, causing a revolution in forest site classification and evaluation. In particular, since the launching of the first earth-observing civilian Landsat

satellite in 1972, satellite remote sensing has been used for gathering synoptic information on forests. In the early years, satellite remotely-sensed imagery was used mostly by geographers to create maps of forests or forest types. These early efforts almost entirely depended upon satellite-collected digital spectral data with no integration of ground-based information such as topography. With the improvements in remote sensing technologies (e.g. spatial, spectral, radiometric and temporal resolution) and data analysis techniques, the use of satellite imagery has evolved from merely detecting forest phenomena to identifying and monitoring forest resources and currently to estimating and predicting forest ecosystem parameters. Accuracy and precision have also improved with the development of new data analysis techniques and through the integration of ancillary ground data sources.

In this chapter the development of site quality evaluation and the applications of remote sensing technology in forestry are reviewed. The discussion is organised in two major parts. The first part (Section 2.2 and 2.3) overviews the historical development of site evaluation with regard to the applications of major site quality evaluation techniques and approaches rather than the evaluation of them. The second part (Sections 2.4 and 2.5) reviews the development and applications of remote sensing to forestry, with an emphasis on the application aspects of digital remote sensing data in forest inventory. A brief discussion on the spectral properties of forest canopy is given in order to understand the reflectance mechanism of forest vegetation.

## **2.2 HISTORICAL DEVELOPMENT OF FOREST SITE QUALITY EVALUATION**

### **2.2.1 Unwritten Records**

Since time immemorial, people's daily needs for forests have stimulated interest in the understanding and observation of the relationships between forests and their environmental conditions. In primitive societies individuals, to survive, needed to have definite knowledge of their environments, i.e. "the force of nature and of plants and animals around him" (Odum 1959). The earliest observations of the relationships between site and forest vegetation were made by the primitive forest dwellers. For many centuries American Indians and Mongolian tribes in Eurasia have had a remarkably clear concept of the adaptation and productivity of various soil types (Wilde 1958). The dependence of these people upon woodland crops led to an intimate understanding of the factors affecting the distribution of a variety of forest vegetation types and the quality of the

wood. These understandings of forest-site relationships were recorded in a variety of forms such as symbols or stories, transmitted from generation to generation, and finally the results were accumulated as a multitude of collective experiences.

According to Wilde (1958), ancient American Indians could recognise certain types of soils as substrates of their medicinal plants and searched for different plants in different forest environments. In Southern China, ancient Chinese knew how to plant different trees in different site conditions. For example, they put the Chinese fir (*Cunninghamia lanceolata*) seeds on the mountains and pine seeds on the hilltops. As the local people said “hat (pine trees) on uphill and skirt (firs or deciduous) on downhill.” or “Chinese fir not cross half way up the hills”. This common knowledge has been transmitted for thousands of years and still can be heard nowadays in the Chinese fir productive regions.

*Kalevala*, the national epic of the Finns, has been seen as the oldest unwritten testament to the profound insight of the people of the wilderness. This document was transmitted by wandering bards and storytellers for nearly three thousand years, until it was recorded by philologists in the nineteenth century in a volume of many hundred pages. In one part of the *Kalevala*, there is a description of the hero, Pellerwoinen, broadcasting seed of forest trees on different sites. As was described by Wilde (1958): “In the words of a modern ecologist, they spread the spruce seed on the mountains and the pine on the hilltops; in the swamps he sows the birches, on the quaking marshes alder, and the basswood in the valleys; in the moist earth sows the willows, mountain ash in virgin places, on the banks of streams the hawthorn, junipers on knolls and highlands. ...” This implied a notion of “the right tree in right place” (Minckler 1941), as we call forest site quality today.

### 2.2.2 Early Documents

The classification of lands into more fertile and less fertile is as old as agriculture itself and antedates all written history (Roth 1916). There are many descriptions of forests and their growth environments left by philosophers of earlier civilisation. 《诗经》(*Book of Songs*), the earliest collection of poems and songs in China’s history (between 2100 - 1600 BC), described the differences of tree growth at different locations, such as “mulberry grows on hills and poplar trees on low and wet places” (Tang 1990). 《管子》(*Guanzi*) and 《周礼》(*Zhou Li*) (800—300 BC) gave systematical descriptions of the relationships between tree growth and environment and these two books have been used as a guide to tree planting and crop cultivation in practice. Theophrastus (370 BC — 285 BC), a student of the famous philosophers Aristotle and Plato, described in his nine books of the *Enquiry into Plants* the relationships between plants and environments



(Oschman 1961). He described the differences between the plant world of the Mediterranean area, the semi-deserts of Libya, the south asiatic tropics of India, the pontic forests, steppes, and mangroves of the Persian Gulf, and the floodplain vegetation of the Nile (Bakuzis 1974). In *The History of Plants*, Theophrastus repeatedly attempted to classify a variety of natural phenomena and to explain the typical differences among plant species. This might be the earliest instance of using plants to indicate site type and quality. The modern division of plants into trees, bushes, shrubs, and herbs is attributable to Theophrastus (Makkonen 1968).

According to Bukazis (1974), Theophrastus definitely forecast the natural associations of plants in particular places. He discussed the influence of habitat on tree growth, for instance, by remarking that the forest grows better on northern slopes than on southern slopes, by writing of trees that grow on exposed, sunny slopes, of those that flourish only on northern exposures, and also of those limited to the more frigid summits. It could be the first purposeful attempt in human history to describe the differences between plants on different sites. Theophrastus is therefore regarded as a forest ecologist in history (Allee *et al.* 1949).

Marcus Portius Cato (234 - 139 BC) has been seen as the first to write on site fertility classification (Heisdijk 1975). He described, in the book *De re rustica* (On Agriculture), nine classes of soil according to the vegetation, beginning with vine-yard land and ending with vineyard forest land (a mixture of vineyard and forest serving both wine and timber production) and pasture-forest land (Makkonen 1968). It is the first known classification of fertility of the ground encountered in the literature. Cato's methods of land classification and evaluation influenced many successive generations.

Terntius Varro (116-27 BC) further developed Cato's land classification evaluation and first suggested a landuse terminology. For example, he implemented the "tripart classification" of varying characteristics, i.e. "a classification which could be most appropriately described by the words *much*, *average*, and *little*." He also suggested that ground can be divided into three classes: especially stony, average stony and virtually free of stones (Makkonen 1968). Even today this land evaluation is still serviceable in many cases.

Lucretius (96 - 55 BC) in his volume, *On the Nature of Things*, reasoned the process of plant succession and the victory of forest vegetation over its eternal adversary-grass (Taylor 1972). The influence of soil and climate on the distribution of woody plants was outlined by Vigil in his 'Georgics', written during the first century B. C.: "Nor indeed can

all soils bear things. By riversides willows grow, and alders in thick swamps, barren mountain-ashes on rocky hills; on the seashore myrtle thickets flourish best; and the god of the vine loves open slopes as yew trees do the freezing north ... So diverse are the native lands of trees.”

It should be mentioned that many ancient writers describe the relationships between forest and environment. For example, Pliny (23 - 79 A. D.), in his “Natural History”, described ecosystem classification of vegetation (Allee *et al.* 1949). He also associated soils which supported elder, wild plum, thimbleberry, and oak with good wheat land (Kelley 1922; and Sampson 1939). Lucius Iunius Moderatus (first century A. D.) divided the terrain into three groups: the plain, hilly terrain, and mountainous terrain; he said that to each group belong six possibilities of ground quality, namely, rich or lean, porous or compact, damp or dry. He observed also that different combinations of these cause exceedingly great variation in the quality of the ground (Makkonen 1968). Boethius in about 500 AD intuitively foretold the importance of soil nutrients in the growth of trees (Wilde 1958).

After the fall of the Roman Empire, for more than a thousand years there were few signs of the contemplation of the nature of the universe. Even in the course of the seventeenth and eighteenth centuries only a few works were published on the subject of forest lands and forestry. As described by some researchers (Allee *et al.* 1949; Wilde 1958; and Bakuzis 1974) the studies of “the plant-environment relation had to wait for the development of other foundation sciences such as geography, geology, climatology, etc”.

### **2.2.3 Pioneer Studies**

After the 17th and 18th century AD it became necessary in Europe to supplement the dwindling supply of timber from natural stands by the establishment of plantations. On the one hand, recognition of the obvious variation in wood productivity and quality associated with habitat variances made it imperative to strive for means of evaluating the potential of the environment as a guide in locating such plantations (Daubermire 1976). On the other hand, the advances in other disciplines (such as geology, soil science, plant physiology, biology, etc.) made it possible to evaluate forest site productivity systematically and scientifically.

Carl Von Linné (1707-1778) pointed out that floristic differences between sites depended upon elevation, climate, and soil (Bakuzis 1974). In his “Flora Lapponica”, Linnaeus (1737) commented on the dependence of vegetation upon habitat factors—climate, soil, and elevation (Udvandy 1969). In Russia, Nartov (1765) divided all types of habitat according to topography and soil-and-ground conditions in Russia, and distinguished

three groups: dry terrain, bogged terrain, and marshland (cited in Renczov and Pogrebnyak 1965). At first, wholly subjective appraisals were based on the appearance of the trees, as illustrated by G. L. Hartig's site quality classification of 1795 (Cajander 1949; and Udvandy 1969).

Modern purposeful and systematic observations of forest sites and their productivity began in the late eighteenth and early 19th centuries, particularly in relation to the forest management practices developing at that time in Europe. Especially after the 18th century, site productivity evaluation from tree appearance and/or location began to be replaced by the practice of measuring trees and other site factors and arranging the data in tables or graphs showing the range in average tree height or volume at different times in the life history of the stands (Daubermire 1976). The first growth curves (tree height and volume over age) for individual trees were developed by Spaeth in 1797 and Seutter in 1799 (Spurr 1952). According to Cajander (1926) and Spurr (1952), Huber first used site index in Germany as early as 1824. At the same time, he and Hundeshagen introduced the concept of *normal yield tables*. Many German and other central-European yield tables are based on site index curves in which cubic volume per hectare is plotted over age. German foresters also developed three methods of preparing site index charts: (1) index method, (2) strip method, and (3) directing-curve method. These methods were discussed in English by Spurr (1952), Jones (1969) and Hägglund (1981). The use of site index spread to Scandinavia and the United States early this century (Jones 1969). The height-age relationship and the concept of site index were discussed in a series of articles in the United States (Roth 1916 and 1918; Spring 1917; Watson 1917; and especially Frothingham 1918), and compared with the volume-age relationship, vegetation types, and site factors as possible alternative indices (Frothingham 1918 and 1921).

In 1840, the principles of soil science and ecology were introduced into silviculture by Grebe, a German forester. In his doctoral thesis "On Conditions Essential for Sound Growth of Our Trees," by stressing "The iron law of the locality", Grebe emphasised the importance of site factors including topography, geology, type of soil, and climate in forest management practice. This idea of site quality has been widely accepted all over the world and has been used for classification and evaluation of forest site quality till today. Grebe's work is therefore considered to be a cornerstone of forest soil science (Daubermire 1976) and soil-based site studies have been one of the main directions in site quality evaluation since his time, as was summarised by Wittich (1960).

In 1860, Pfeil, a German authority on forest management, published a book with an extensive chapter entitled "Science of Forest Habitat." This work was widely introduced into silviculture and strongly affected a number of text books on silviculture, particularly the "Diagnosis of Forest Stands" by Gayer (1876) (cited in Wilde 1946 and 1958). In about 1860, Cooper (1859) and Hilgard (1860) began ecological site study in America (cited in Wilde 1958). Their work may be considered as the basis of later ecological forest (site) classification (total site), and Cooper and Hilgard are therefore seen as the forerunners of the ecological school.

Since the seventeenth century, European foresters have gauged the quality of the site for the production of forest crops from plant forms. For example, *Oxalis* in Prussia had been looked upon for generations as an indicator of site quality (cited in Korstian 1917). According to Korstian (1917), Heyer in his *Bodenkunde*, published in 1856, emphasised the significance of indigenous plants as indicators of site quality. Ramann of Germany, in 1893, in his book 'Bodenkunde' also devoted a number of pages to *Bodenbestimmende Pflanzen*, which may be liberally translated as "soil-determining plants or indicators" (see Korstian 1917). The notion of indicator plants was developed later into the plant indicator approach to classifying and evaluating site quality (Sampson 1939). Rowe (1956) outlined a specific methodology for using groups of undergrowth species as indicators of moistness of site in the southern boreal forest of Manitoba and Saskatchewan. The indicator plant approach was stressed and used until recently for site assessment (Gagnon and MacArthur 1959; Daubermire 1966; Hodgkins 1968; Damman 1979; Randuska 1982; and Ferguson *et al.* 1989).

Considering the influences of treatment and density of stand on volume and the difficulties encountered in evaluating site, Schwappach (1908) first suggested using stand height to measure site quality (cited in Roth 1916). He recommended that "the starting point is the study and determination of height curves of the main stand; the height is the factor least affected by treatment." Using the height-age relationship, he replaced the site classes by volume by height-age classes. The methods and principles of the height-age relation were discussed in the early review by Watson (1917) and Frothingham (1918). It was developed later into site index approach.

According to Spurr and Barnes (1980), the multifactor site assessment approach evolved from the pioneering work of another German scientist, G. A. Krauss who, beginning in about 1926 in Tharandt, initiated a team approach to study complex site relationships. The method consists of a synthesis of important site factors at regional and local ecosystem

levels. The site classification system developed in the Baden-Württemberg region of Germany combines site classification, productivity evaluation and site mapping and it has been used widely in guiding silvicultural activities. The method, later called the Baden-Württemberg model (Spurr and Barnes 1980), became the main example of site classification and evaluation for many countries, Canada and United States in particular. Indeed, the ecosystem approach used in Northern America is a further development of the Baden-Württemberg model.

Since early this century, site research has been widely and intensively carried out in Russia, Finland, Germany, United States, and Canada, with many methods of site evaluation and many classification systems being proposed. Because of the varied possibilities for classifying sites, many schools have developed, each distinctive in its response to the site factors of different areas but interrelated through the sharing of ideas. These schools which have significantly influenced site quality evaluation are: the Finland school by Cajander (1909; 1926; and 1949), Cajander and Ilvessalo (1921), the Russian school by Morozov (1904) and later by Suchachev (1928 and 1944) (cited in Frey 1980), and the ecosystematical school by Tansley (1935). For example, the theory of forest (site) types created by Morozov (1904) and Suchachev (1913) of Russia and Cajander and Ilvessalo (1906-1909) of Finland was established during this period (cited in Frey 1980). According to Morosov, at a regional level plant productivity largely depends on climatic conditions, but at a local level mainly on soil conditions. On this basis Morosov proposed the principle of dividing Russian forests into silvicultural zones and subzones, domains and sub domains based on site differences (Kdesinkov 1960).

In Finland, Cajander (1926) proposed that identification of a site might also be based on understory species. He stressed the importance of geographic distribution (i.e. locality) and stand structure, especially the significance of undergrowth plants in indicating site quality, while Morozov paid more attention to soils and climate. Therefore he defined *site type* as stands with similar site quality and similar understory composition. This marks the foundation of forest (site) typology, and both Cajander and Morosov are seen as the founders.

After Tansley (1935) suggested his ecosystem theory, the *ecosystem* concept was widely accepted. A multi-factor approach was introduced into site studies. However, little attention was paid to the ecosystem approach until the 1970s when it was revitalised in North America. Krauss, of Germany, might be seen as the first person to assess forest sites using ecosystem principles. He introduced geology, geography, climatology, soil

science, plant geography and sociology, and even pollen analysis, and forest history into site into the Baden-Württemberg models (Spurr and Barnes 1980). Subsequently, site evaluation methods similar to those of the Baden-Württemberg model have been widely used in some other countries such as America (Spurr and Barnes 1980), Canada (Hills 1952; Hills and Pierpoint 1960; Rowe 1971), and Australia (Christian *et al.* 1960; Lewis *et al.* 1976).

#### **2.2.4 Development in the Last Five Decades**

It could be said that the development of site concepts and principles mainly occurred in the last half of this century. Major developments currently focused on technical improvements and expansion of research scales. The scope of study expanded from local regions to entire countries. Although there are some differences in the site attributes used, most studies use a multi-factor approach. For example, starting from the 1940s, using ecosystem principles, Hills and his associates further proposed the concept of *total site* (ecosystem) and his ecological approach to site classification and evaluation was successfully used in the Ontario Region of Canada (Hills 1952b; Hills and Pierpoint 1960). It is usually called “ecological and/or biological site evaluation” today (Boissonneau and Pala 1978; Franklin 1980). Their method allows extensive application of airphoto interpretation in the classification, mapping, and evaluation of large, often inaccessible land areas.

Wakeley (1954) proposed a growth-intercept method to build site index curves. This site quality assessment method has been widely accepted and used to assess site quality of plantations in many countries (see Ferree *et al.* 1958; and Alban 1972). Since the 1980s, there has been growing awareness of worldwide pollution and unexplained forest deterioration has been identified throughout extensive areas, in the industrially advanced countries in particular. Fernandez (1986) suggested that this pollution should be taken as a site factor in evaluating forest resources and their sites.

Due to the development of calculation technologies (such as digital computers), site quality evaluation has evolved from traditional single factor and/or qualitative descriptions to multi-factor and quantitative modelling. The multivariate analysis technique is now widely applied in ecological research and it has been introduced into site quality assessment. For example, Carmean (1965) used multiple regression techniques to model black oak site quality and soil and topography in south eastern Ohio, USA. Similar studies were conducted by a number of authors (e.g. Kinloch and Page 1966; Page 1970; McNab 1987 and 1990; Worrell and Malcolm 1990a & 1990b; Hairston and Grigal

1991). In addition to soil and topographic factors, McNab (1987) and McNab and Merschat (1990) also introduced geological variables. In one case the correlation between tree height and geological variables was as high as 0.91.

Techniques of ordination and grouping were used to order (or rank) forest sites to reflect an underlying gradient in physiography, soils, or vegetation. This method can be seen in a number of studies (Curtis and McIntoch 1951; Whittaker 1967; Carleton *et al.* 1985; Roberts and Cristensen 1988; Chang and Gauch 1986; Radloff and Betters 1977). Such ordinations have proved useful for determining the influence of various site factors on forest composition and productivity. Grouping (or clustering) were employed to group similar sites for the purpose of classification (Barnes *et al.* 1982; Pregitzer and Barnes 1984; Nowacki *et al.* 1990). Grouping is often done in conjunction with ordination to produce classification systems that can be used for stand management prescriptions (Spies and Barnes 1985, Hix 1988, and Burton *et al.* 1991). Ordination and classification can be achieved using a variety of multivariate analysis methods, including correspondence analysis, principal components analysis, principal coordinates analysis, clustering analysis and canonical discrimination analysis. Such methods produce graphical displays of the distance or dissimilarity among samples, which may be used to detect patterns or gradients in the data. McNab (1990), for instance, developed prediction models of forest types from topographic variables (i.e. elevation, aspect, index of landform and land surface shape), accounting for over 97 percent of variation in location of forest type centroids in a canonical discriminant analysis.

In recent years, increasing attention has been paid to multiple use of forest resources. Forest managers are often faced with several estimates of site productivity. Not only are there different measures of productivity, such as site index or mean annual increment at some fixed age, but estimates of each may be obtained from several sources, including site classification systems, site-forest relationships, and growth measures from young stands.

Using correlations among the habitat classification systems, soil site equations and growth and yield equations, Reed (1989) proposed a new method of assessing alternative estimates of plantation site productivity and mean annual increment in the absence of observations of the true values, through a quantitative evaluation of the alternative productivity estimates. His method was successfully used for the productivity estimates for young red pine plantations.

The application of remote sensing technology may be the most significant development in site quality estimation and classifications since the 1940s. The early application of aerial-photography technology has proven to be useful in identifying forest sites because of the exceptionally detailed information on topography and forest structure contained in them (Seely 1960). For instance, during the 1940s air-photographs were successfully used in site quality classification and mapping based on soil types and/or topography (Losee 1942). With the development of photo-interpretation techniques, aerial photographs have been successfully used in estimating forest stand variables. Forest site quality estimation therefore developed from early qualitative classification to quantitative estimation (Spurr 1960; Choate 1961; Colwell 1970; Heller and Ulliman 1983; Howard 1991).

The launch of the first Landsat satellite in 1972 caused a revolution in site information collection, after which satellite-based digital imagery was introduced into forest inventory. The applications have advanced from early forest land cover/use classification and mapping to estimation and prediction of various forest stand structure attributes, phenological, physiological and chemical parameters. Moderate success has been achieved in forest (site) type classifications and mapping at regional scales (see Section 2.5 of this chapter), but only limited success in direct site quality estimation (e.g. Getter and Tom 1977; Tom and Miller 1978 and 1980; Driscoll *et al.* 1982; Häme 1984; Vanclay 1988; Vanclay and Preston 1990) and site degradation assessment (Johnston and Barson 1990). In the early stage the studies were concentrated on the use of digital imagery data alone. More recently, studies have been characterised by incorporation of ancillary data into satellite-based imagery using computerised spatial modelling, analysis and mapping techniques through GIS, knowledge-based spatial data analysis and decision-making systems (including expert systems, artificial intelligence, and/or neural network techniques) (Hollenbaugh 1987; Hart *et al.* 1987; Hodgson *et al.* 1988; Klock 1989; Rauscher *et al.* 1989; Skidmore 1989; Lowell 1990; Davis and Dozier 1990; Kourtz 1990; Bolstad 1992). Applications of satellite technology in site studies will be discussed in more detail in Sections 2.4 and 2.5.

### **2.2.5 Summary Implications**

The above review of the historical development of forest site evaluation shows that there has been progress from perceptual to theoretical abstract knowledge. This development process may be broadly summarised as the following four stages:

- (1) *Perceptual Knowledge* This stage, which lasted for more than 2000 years, from primitive society to about the 18th century AD was characterised by perceptual



and subjective descriptions of the superficial phenomena of forests and their sites, e.g., the evaluation of forest sites was based mainly on the appearance of forests and/or their growth locality. Although lacking precise concepts, this stage conveyed the idea of differences of site quality in different site conditions.

- (2) *Single-factor Site Evaluation* The main features of this stage is that site classification and assessment were based on one or a few site attributes (such as soil, location, geomorphology or climates) to express site productivity. Most work done before the appearance of Cajander's forest typology (1940s), Tansley's ecosystem and Sukachev's biogeocenosis may be seen as single site evaluation.

Compared with perceptual knowledge, the single-factor site evaluation qualitatively describes site quality by one or a few site attributes. It clarifies the concepts of site and site quality. As it is relatively simple to use and successful in local (small) areas, single-factor site evaluation is still stressed and used today (see Zonneveld 1981). However, in areas where site conditions are more complex, a single-factor site attribute cannot reveal the complex relationships between sites and forests. This disadvantage stimulated the development of the multi-factor approach.

- (3) *Multi-factor Site Evaluation* This stage stresses site as an ecosystem (i.e. total site or biogeocenosis) influenced by many site factors or combinations of ecological factors. Sites are classified and evaluated using the principle of ecology and other sciences. The main characteristic is that many disciplines contribute to the site study; the site evaluation is based on environmental and/or plant analysis. The ecosystem approach is a typical representative of this stage in the evolution of site evaluation and it is used at present.
- (4) *Comprehensive forest site evaluation and site mapping* This stage is characterised by the combination of qualitative and quantitative methods to evaluate forest site quality. It stresses forest site as the sum of many site factors. Apart from the conventional site information collected from permanent and/or temporary sample plots, the information collected for site classification and evaluation can be acquired by remote sensors and/or computers. Methodologically, ecosystem site classification and evaluation approaches are widely accepted, and technically, multivariate analysis spatial modelling, GIS, expert systems, and artificial intelligence techniques have been widely introduced into site evaluation. Site quality is expressed by graphs, tabular and site maps, and can be stored in

computer disks so that it is relatively indexed. This stage quantitatively and mathematically reveals the interrelationships between trees and their site environment. This represents the future of site productivity evaluation and defines the direction for future forest site studies.

### 2.3 MAIN APPROACHES FOR EVALUATING FOREST SITE QUALITY: A BRIEF OVERVIEW

As reviewed above, because of the great practical importance attached to the effective evaluation of forest site quality, much effort has been devoted to the development of techniques for evaluating site quality, and therefore a number of site classification systems and assessment methods have been developed. These many methods and approaches are summarised in Figure 2.1.

VIEWS	METHODS	
	<i>Direct Approaches</i>	<i>Indirect Approaches</i>
<i>Stand Variables</i>	Yield Volume Biomass Height (Site index) Mean annual increment Growth-intercept Other stand variables	Indicative plants Overstorey interspecies relationships lesser vegetation characteristics Other vegetation characteristics
<i>Site Variables</i>	Measures of availability of soil chemical elements Soil moisture photosynthetic active radiation	Climate variables Topographical variables Soil variables Geological variables Other environmental variables
<i>Holistic</i>	Combinations of both stand and site variables	

Figure 2.1 Approaches for estimating site quality and relationships among them.

Figure 2.1 shows that all methods of site quality estimation are based upon three views: stand and site variables or both. Under these views, two common methods, usually called direct and indirect methods (Rennie 1963; and Clutter *et al.* 1983), have been developed for expressing and rating site quality. The stand variable view assumes that stand variables are the direct and ultimate measures of site quality. Although a number of measures from stands have been proposed to indicate site quality, the best measure of site quality may be stand volume or biomass. Because of the practical difficulties of direct measurement of total stand volume, the site index has been the most commonly

used measure, as it is strongly correlated with stand volume. Indirect methods concentrate on specific vegetation (e.g. understory) sensitive to site quality.

The site variable approach assumes that site quality depends mainly on the soil, climatic, geological and topographic attributes, and that an accurate knowledge of these site attributes supplies a basis for estimating the amount of stand volume or yield from an area. Direct methods involve use of properties of the site itself as indicators of site quality. This approach is predicated on the idea that site quality is determined by variables such as temperature, light, supply of soil water and available nutrients etc. However, few of these properties can be measured under practical forest inventory conditions. Many are measured through indicator variables such as the composition of ground vegetation.

The holistic approach assumes that a site can be seen as a ecosystem (total site), and any factors affecting this ecosystem can be seen as site quality factors. The stand variable approach can not be used in a unforested area, while the site variable approach cannot provide information on the quantity of a site for a species of interest. For instance, the site index approach can not be used until the stands reach the *index age*, and mean annual increment can not be truly observed without measuring volume at the age of interest. Using the correlations among the habitat classification system, soil site equations and growth and yield equations, Reed (1989) proposed a new method of assessing alternative estimates of plantation site quality and mean annual increment in the absence of observations of the true values. In Canada, site quality was evaluated and classified by incorporating stand variables (e.g. site index), soils, topographic and climatic variables (Burger 1976; Pojar *et al.* 1987).

There has been detailed discussion on these specific methods by many authors. For instance, Jones (1969) gave a comprehensive review of forest site evaluation work in North America. The work in the United States was again reviewed by Carmean (1975). Most text and reference books on silviculture, forest management, inventory, and forest ecology devote major chapters or sections to site evaluation (e.g. Spurr 1952, Spurr and Barnes 1980, Clutter *et al.* 1983; Shepherd 1986). Hägglund (1981) presents a review of research on site quality evaluation published after 1973, with emphasis on the site index approach. Clutter *et al.* (1983) gave a similar discussion, but they put more emphasis on site index curve construction. The comprehensive evaluation and classification methods used in Canada were summarised in a recent review by Burger and Pierpoint (1990).

## 2.4 FORESTRY APPLICATIONS OF REMOTE SENSING

### 2.4.1 Introduction

Since the launching of the first earth-observing civilian Landsat satellite in 1972, great efforts have been made to develop methods of forest inventory and management using digital satellite data. The aim is to eliminate time-consuming and expensive field work required to collect the data for various stand variables and to use computer-assisted interpretation techniques. Over the years advances have been achieved with the improvement of imagery resolution (spatial, spectral, radiometric and temporal) and the development of data processing and interpretation techniques. Forestry applications of satellite data have also been developed from simple mapping of forest types to detecting more subtle changes in forests over time and space.

Current trends in forest studies have been toward the integration of remotely-sensed data into GIS and/or expert systems. This integration allows satellite spectral data to be used beyond standard image processing. Furthermore, it allows for remotely-sensed data to be used in conjunction with spatially-referenced digital data such as site variables (e.g. elevation, slope, aspect, soils) as well as biological variables. In this way, information obtained from remote sensing of forests can be enriched, and the capacity of remotely-sensed data in detecting forest and site variations can be improved.

This section gives a review of the literature on some recent applications of remote sensing in forestry. The discussion is organised as (1) a discussion on the conceptions of remote sensing; (2) an overview of the technical development of remote sensing in forestry; and (3) a review of forestry applications of satellite data.

### 2.4.2 Definition of Remote Sensing

*Remote sensing*, or *téledétection* in French, *telepercepción* in Spanish, 遥感 in Chinese, and *fernerkundung* in German, is defined as “a technique in geography for location, classification and estimation of features in the environment” (Curran 1987). Early broad definitions call it a technique of “acquisition of information about an object without touch or direct contact with that object” (Richason 1978; Slama 1980; Moik 1980; Simonett 1983; and Sabins 1987), or “the group of techniques for collecting information about an object and its surroundings from a distance without physically contacting them.” (Lo 1986). Barrett and Curtis (1982) defined remote sensing as “the science of observation from a distance”, while Richason (1978), Dahlberg and Jensen (1986) and Curran (1987)

saw it as a technique rather than a subject, or discipline. In recent years it has grown into a very wide ranging technique (Curran 1985).

As a term, remote sensing is itself relatively new. It was first proposed in 1958, and was formalised and defined by Parker in 1962, at the first Symposium on the remote Sensing of Environment in Michigan, as “covering the collection of data about objects which are not in contact with the collecting device” (Zhao (赵宪文) 1983; Howard 1991). It was introduced to replace the traditional but more restrictive terms *aerial photography*, *photogrammetry* and/or *aerial photo interpretation*, which refer only to the acquisition and analysis of aerial photography acquired by the conventional photographic process (Slama 1980; and Simonett 1983).

The *object* in the above definitions usually means the earth’s surface. The *information* is typically in the form of electromagnetic radiation (EMR) that has either been reflected or emitted from the object. The earlier definitions of remote sensing were focused mainly on the acquisition of information. Remote sensing, however, has a broader meaning encompassing the acquisition and analysis of data from all portions of the electromagnetic spectrum, including the visible portion. Today, remote sensing is generally accepted as not only involving the collection of raw data, but also as involving manual and automated raw data processing, imagery analysis and presentation of the derived information. As stated by Luney and Dill (1970)

*Remote sensing denotes the joint effects of employing modern sensors, data processing equipment, information theory and processing methodology, communications theory and devices, space and airborne vehicles, and large-systems theory and practice for the purposes of carrying out aerial or space surveys of the earth’s surface.*

The definition was further detailed by Short (1982) as

*The acquisition of data and derivative information about objects or materials (targets) located at the Earth’s surface or in its atmosphere by using sensors mounted on platforms located at a distance from the targets to make measurements (usually multispectral) of the interaction between the targets and electromagnetic radiation.*

With the development of the concept of remote sensing, the term *photography* was replaced by the term *imagery*, which was defined as “a continuous or discrete record of a two dimensional view” (Curran 1985). Imagery, in a technical sense, refers to products made from electromechanical scanners and other devices measuring radiation beyond the visible portion of the spectrum. The term *photointerpretation* becomes *image interpretation* or *image processing*. Although taking on discipline dependent meanings, remote sensing now usually refers to “the use of electromagnetic radiation sensors to

record images of the environment which can be interpreted to yield useful information.” (Curran 1985).

Developed from aerial remote sensing, satellite remote sensing is therefore defined by Harris (1987) as “the use of sensors, normally operating at wavelengths from the visible (0.4  $\mu\text{m}$ ) to the microwave (25 cm), on board satellites to collect information about the earth’s atmosphere, oceans, land and ice surfaces.” Commonly, the information is collected in two dimensional form either as a photographic image, such as the high-resolution images from the metric camera carried on the space shuttle, or as an array of digital data.

Satellite remote sensing may be best defined by its mode of operation (Harris 1987). Based on the altitude of platforms, it can be divided into *air-borne* (aircraft) and *space-borne* (satellite) remote sensing. Based on the origin of the energy it can also be classified into *passive* and *active* remote sensing. Most images are passive since the energy is from the sun. Active remote sensing occur when the energy is from the sensor itself, such as a radar image.

### **2.4.3 The Development of Remote Sensing in Forestry: An Overview**

Forestry has become one of the major applications of remote sensing technology. The early development of remote sensing as a scientific field was closely associated with developments in photography. The sensor systems were developed from the earlier simple cameras using the visible wavelengths to very sophisticated satellite sensors in a variety of portions of the spectrum. Simonett (1983) divided the development of remote sensing technology and practice into two time periods: prior to and since 1960. This section gives a brief review of the major development and applications of remote sensing in forestry summarised from Holter (1970), Hilborn (1978), Thomas and Gruner (1980), Simonett (1983), Harris (1987), and Howard (1970 and 1991). Based on the development of remote sensors, applications of spectral wavelength, the altitude of sensors, and the form of the photography and/or imagery, four phases are subdivided and discussed respectively, although these are a somewhat arbitrary division of an evolutionary process.

#### *Phase 1. Prior to 1945: The invention and simple applications of early photography*

According to Simonett (1983), the development of cameras stemmed from experiments over 2300 years ago by Aristotle with a *camera obscura*. Experiments were continued from the 13th through to the 19th centuries with advances in chemistry providing the knowledge of photosensitive chemicals and the invention of optical prisms. The first

successful photographs were taken from the air by cameras strapped to the breasts of pigeons in Paris in 1836 (Thomas and Gruner 1980). The first known popular interest in images of trees on photographs was in 1838 (Howard 1970). In 1849, aerial photographs were first used for topographic mapping in France (Elachi 1987). By 1858, balloons were being used to acquire photographs of large areas. Aerial photographs were taken from a balloon near Berlin in Germany in 1887 in order to examine the characteristics of beech, spruce and pine stands (Spurr 1960; and Heller 1972). Austrian foresters proposed, in 1892, to use remote sensing to map forests and vegetation, the corridors of avalanches, screes, rocks and counterlines in inaccessible alpine areas (Hildebrandt 1983). This was followed by the use of kites in the 1880s and pigeons in the early 1900s to carry cameras to many hundred metres of altitude.

The Wright brothers' airplane was developed in 1903, and the first aerial photograph from a plane was taken by Wilbur Wright in 1909 (Spurr 1960). Within ten years, aerial photographs were being successfully used for soil survey and mapping in the USA.

In the 1920s the techniques of aerial photography were used widely in agriculture and forestry. For instance, beginning in the 1920s, photointerpretation techniques were first introduced for forest inventory in Ontario, Canada (Craig 1920). The interpretation of the photographs was combined with field checking and the preparation of stock maps. The applications included estimation of stand volume, height, tree counts, and crown density measurements (see Heller and Ulliman 1983). In this period, as well as forest mapping, German foresters also used air-photography for inventory and forest management planning purposes (Hildebrandt 1983).

Many advances in photointerpretation techniques were made after World War II. Black-and-white (B/W) aerial photographs taken from aircraft platforms were widely used (mainly in the USA) on an experimental basis in forest inventory. Supplemented by ground checking, aerial photographs were interpreted to define and map forest types and major soil types between the 1940s and the 1950s (Spurr 1948 and 1960).

### *Phase 2. 1945-1960: Applications of nonphotographic Imagery*

The most significant advances in this phase were the use of colour photographs and non-photographic image-forming systems (such as radar) for detecting radiation reflected or emitted (or both) from remote scenes. This innovation overcame the limitations of conventional photographs in the visible wavelength. Nonphotographic sensors operate in portions of the electromagnetic spectrum from the microwave to the ultraviolet region.

Panchromatic aerial photography became more widespread, and the applications of its products spread from topographic and other thematic mapping to include estimating many stand variables, including tree size measurements, density, tree height, tree quality, growth rate, and site quality. Colour photography began to be used for land and soil classification and mapping. Descriptions of applications of aerial photography in forestry can be found in Spurr (1948 and 1960) and Loetsch and Haller (1964). The photo-interpretation techniques developed in this phase have played, and will continue to play, a significant role in forest inventory, especially at the national forest inventory (NFI) level (Thallon 1979; Köhl and Sutter 1991). Comprehensive reviews on the applications of remote sensing in forestry in this stage can be found in Seely (1960).

### *Phase 3. 1960-1972: Applications of Spaceborne (Satellite) Imagery*

The major advances in this phase were the birth of satellite remote sensing and the application of laser technology. The phase began with the launch of the weather satellite TIROS (Television InfraRed Observation Satellite) and the invention of the laser in 1960. Besides the visible wavelengths, the satellite era also saw investigation of other portions of the spectrum, notably the thermal infrared (TIR). Colour photography, including visible, colour infrared (CIR), near infrared (NIR), panoramic photography and sideways-looking airborne radar (SLAR) imagery, were widely used for detection of changes such as disease, identification of tree species (composition), and estimation of stand variables (Colwell 1970; and Heller 1976). The scales in mapping vary from small-scale (about 1:120,000 or smaller) and global coverage by ESSA (Environmental Science Service Administration) and NOAA (National Oceanic and Atmospheric Administration) series satellites to large-scale air-photography (1:2000 or greater) for detecting morphological and phenological characteristics of trees (Heller and Ulliman 1983).

### *Phase 4. 1972-present: Applications of Digital Satellite Remote Sensing Imagery*

This phase began with the launch of the Landsat-1 (initially named ERTS-1) satellite in 1972, and the development of multiple spectral scanner (MSS) images in digital form. The greatest improvement made in this phase was to focus all energy through a single aperture and record all wavebands simultaneously. Prior to 1971, only the visible and NIR wavebands were recorded through one aperture. The second generation of satellite remote sensors with higher spectral and spatial resolutions and more spectral bands (“a selection of wavelength portions of the electromagnetic spectrum” (Aldrich 1979)) were developed in the 1980s, including Landsat-4 (1982) and Landsat-5 (1984), SPOT-1 (1986) and



SPOT-2 (1989), and NOAA-7-11 AVHRR (1982-1989) (see Section 2.4.5). Computer-aided image interpretation and processing techniques have been extensively used in forest inventory, for detection of changes, mapping and making estimates of many forest, ecological, morphological, phenological, physiological and environmental (site) variables (Section 2.5).

Recent developments in digital remote sensing include introduction of the imaging spectrometer and radio systems. In particular, low altitude airborne scanners (or spectrometers) can provide images with higher spectral (i.e. more spectral bands with narrower bandwidth, such as 10.0 nm, having up to 224 channels) and higher spatial resolution (2.5 m or smaller pixel size). These data types have improved recognition capability and they have been used to measure forest stand parameters and to estimate vegetation canopy characteristics constituents and pigments (e.g. fluorescence and chlorophyll a and b). For instance, the Airborne Visible/Infrared Imaging Spectrometer (AVIRIS) became operational in 1989, operating in the visible and near infrared (NIR) region from 0.4 - 2.5  $\mu\text{m}$ . It has been used for estimating physiological variables (e.g. fluorescence of chlorophyll) in vegetation canopies (Elvidge *et al.* 1993; Hamilton *et al.* 1993; Vane and Goetz 1993; and Vane *et al.* 1993). This technique is not yet used commercially in forestry due to its cost.

The review above showed that the development of remote sensing has been an evolutionary process stemming from increased information captured in terms of space, time, and radiance. This evolutionary process is summarised in Table 2.1.

Table 2.1 Remote sensing timeline. Some of the important dates in civilian remote sensing programs.

Phases	Time	Sensors Systems and Applications
Phase I	1830s 1859 1862 1910 1920s	Niepcé takes first photographs of nature First aerial photographs - captive balloon over the French countryside Forest mapping from aerial photographs Wilbur Wright takes first photographs from an airplane systematic forestry mapping from aerial photography in Canada and the United States.
Phase II	1940s	Forest inventory and stand variable estimates using photography and/or nonphotography.
Phase III	1960 1962 1966	TIROS-1 first operational meteorological satellite Prototype multispectral camera constructed by Zaitor and Tsuprun Digital image analysis for agricultural applications
Phase IV	1972 1975 1979 1982 1984 1986 1989 1990s	Landsat 1 (ERTS 1) MSS Landsat 2 MSS Landsat 3 MSS, NOAA-6 AVHRR Landsat/TM 4 Landsat/TM 5 SPOT-1 Airborne imaging spectrometer (e.g AVIRIS), NOAA-11 MERIS, HIRIS, Landsat/TM-6 (missing), 7, SPOT -2, 3, 4, 5, ADEO 1, 2

## 2.4.4 Remote Sensing of Vegetation: an Overview

Remote sensing uses radiation in different parts of the electromagnetic spectrum (EMS) as the carrier of information regarding various phenomena of the Earth and in the atmosphere. In principle, remote sensing systems could measure energy emanating from the earth's surface in any sensible range of wavelengths. However, technological considerations, the selective opacity of the earth's atmosphere, scattering from atmospheric particles and the significance of the data provided exclude certain wavelengths. The major ranges of wavelengths used for earth resources sensing are between about 0.4 and 12  $\mu\text{m}$  (referred to below as the visible/infrared range) and between about 30 to 300 mm (referred to below as the microwave range). In the microwave bands it is often more common to use frequency rather than wavelength to describe ranges of importance (Richards 1986). Visible and reflected infrared radiation is the most frequently used range of EMS for vegetation.

Figure 2.2 shows typical reflectance characteristics for green vegetation, water and soil over the wavelength interval from 0.4 to 12.5  $\mu\text{m}$  and corresponding system parameters of the four common satellite remote sensors (Landsat TM, MSS, SPOT and AVHRR systems). All of the reflectance spectra of plant leaves (including conifers) have the same reflectance shape. Differences appear only in the magnitude of the reflectance (Goillot 1980). Dependent upon the optical properties of leaves, four spectral regions are usually considered for digital satellite remote sensing: visible, near-infrared (NIR), middle-infrared (MIR) and thermal-infrared (TIR).

### 2.4.4.1 Visible Region (0.4 – 0.7 $\mu\text{m}$ )

As shown in Figure 2.2, the reflectance curve in this region shows that the leaf reflectance is low in the blue band (about 0.45 to 0.52  $\mu\text{m}$ ), peaks in the green-yellow region (about 0.52 to 0.55  $\mu\text{m}$ ), and decreases to a minimum in the red (about 0.63 to 0.70  $\mu\text{m}$ ). Typically, about 70-90% of blue and red light is absorbed to provide energy for photosynthesis (Carolis and Amodeo 1980), with the absorption maxima at 0.435 and 0.67  $\mu\text{m}$  respectively. This low reflectance (less than 15%) in the blue and red regions is generally attributed to absorption by leaf pigments such as chlorophyll and xanthophyll, carotenoids and anthocyanins (Gate 1970; Rock *et al.* 1986; Goyut 1990; Moya *et al.* 1992).

Gates (1970) and Carolis and Amodeo (1980) stated that chlorophyll, carotenes, and xanthophylls absorb radiation in the blue region (around 0.445  $\mu\text{m}$ ), but only chlorophyll absorbs radiation in the red waveband (near 0.645  $\mu\text{m}$ ). Yamada and Fujimura (1988)

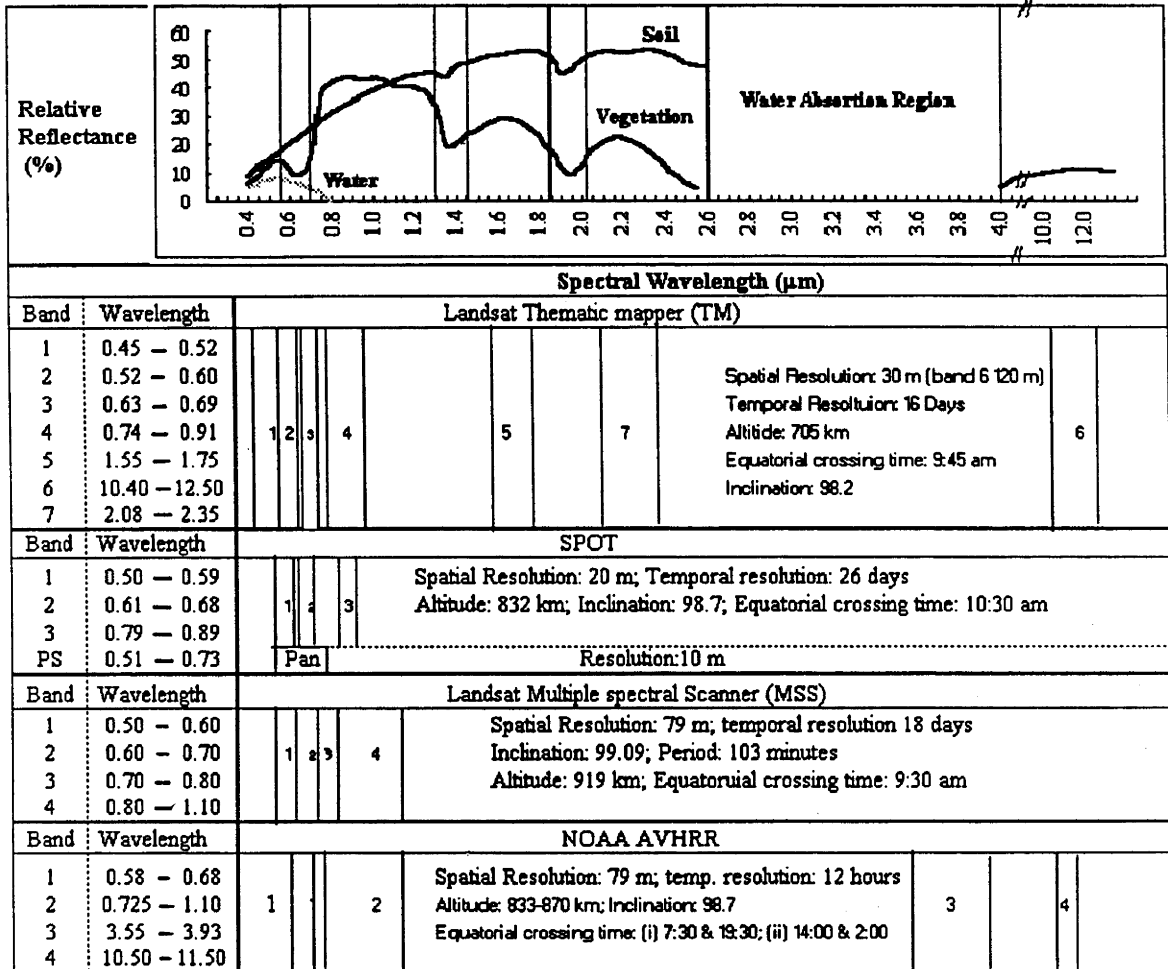


Figure 2.2 Spectral reflectance curves of typical green vegetation, soil and water. Also shown are the system parameters of the four most common digital satellite remote sensing systems: SPOT, TM, MSS, and AVHRR.

considered the reflectance of leaves to be a function of chlorophyll pigment content. For this reason, any changes of reflectance intensity of leaves occurring in these wavebands may indicate a subtle change of canopy, stand structure and/or stand conditions. There is a slight peak in the green, which is why growing vegetation appears green. The sharp increase in the curve (Figure 2.2) between about  $0.68 \mu\text{m}$  and the NIR plateau is called *red edge*<sup>1</sup>. The slope and position of this red edge have been directly correlated with leaf chlorophyll concentration (Horler *et al.* 1983). An important feature of the visible radiation is that the relationship between reflectance and amount of green vegetation (biomass, LAI, and height of trees) is usually negative.

#### 2.4.4.2 Near-Infrared Region (about $0.7 - 1.3 \mu\text{m}$ )

In this spectral region, leaf pigments and the cellulose of leaf cell walls are transparent, therefore leaf absorption is very low (less than 10%) and incoming radiation is either

<sup>1</sup> The red edge is the sharp transition region between the red and the near-infrared wavelengths (see Figure 2.2)

reflected or transmitted (Goyut 1990; Barrett and Curtis 1992). About 50% of NIR light is reflected in the *infrared-plateau* (see reflectance curve in Figure 2.2). The reflectance level depends largely upon the anatomical structure of the leaves, and usually increases with the number of cell layers (Gates 1970; Rock *et al.* 1986). Westman and Price (1988) showed reduced cell volume could reduce NIR reflectance. This reflectance property is useful in detecting the changes of canopy cover and biomass by LAI (Tucker 1979; Tucker *et al.* 1975; and Curran 1985). However, this analysis of the reflectance properties of vegetation in the NIR is not necessarily suited to coniferous canopies. Many studies (e.g. Colwell 1974; Danson 1987; Poso *et al.* 1987; Häme 1991) have indicated that there exists a strong negative correlation between canopy cover and NIR reflectance. This means that the reflectance intensity of coniferous canopy in all wavelengths, including the NIR band, usually decreases with accumulated stand growth. Like visible light, NIR reflectance also has a strong negative correlation with the amount of vegetation. This may be attributed to effects of increasing canopy shadows resulting from crown expansion. This will be discussed in more detail in Chapters 5 and 6.

#### **2.4.4.3 Middle-Infrared Region (1.3 – 2.5 $\mu\text{m}$ )**

The optical properties in the MIR wavelength are influenced somewhat by internal (cellular) structure but more particularly by water concentration within the leaves (Tucker 1980; Barrett and Curtis 1992; Wessman 1989; and Danson *et al.* 1992). MIR is therefore usually called the “water-absorption” region. As can be seen from the reflectance curves in Figure 2.2, leaf reflectance decreases with increasing wavelength, with the minimum near 1.40 and 1.85  $\mu\text{m}$ , and becomes negligible beyond 2.5  $\mu\text{m}$ . The levels of the absorption of light in these two spectral portions vary according to leaf water content. Landsat TM bands 5 and 7 are centred on these two regions and it has been suggested that the data obtained in them could be used for detecting the various levels of water-related stress in vegetation (Guyot *et al.* 1985; Rock *et al.* 1986; Westman and price 1988). The upper limit of 2.5  $\mu\text{m}$  is a result of the decrease of sun radiation with wavelength and the absorption of radiation by atmospheric water vapour. This may be why the remote sensing of vegetation is generally restricted to the spectral region from 0.4 to 2.5  $\mu\text{m}$ .

#### **2.4.4.4 Thermal-Infrared Region (about 3 – 20 $\mu\text{m}$ )**

The thermal-infrared (TIR) portion of the EMS extends from about 3 to 20  $\mu\text{m}$ . Atmospheric water vapour strongly absorbs radiation in much of this region. Strong atmospheric absorption occurs between 3.5 to 4.5  $\mu\text{m}$ , the level of absorption depending

mainly on the water content of the atmosphere. Within this region, radiation naturally emitted from all objects is easily detectable and is related to their surface temperature (Olsson 1987). Advance Very High Resolution Radiometer (AVHRR) band 4 (10.3 - 11.3  $\mu\text{m}$ ) and 5 (11.5 - 12.5  $\mu\text{m}$ ), Landsat TM channel 6 (10.4 - 12.5  $\mu\text{m}$ ), and Heat Capacity Mapping Radiometer (HCMR) band 2 (10.5-12.5  $\mu\text{m}$ ) are centred on this region, and the data are usually used for plant heat stress management. However, the effect of atmospheric water absorption significantly reduces in the spectral range from about 8 to 14  $\mu\text{m}$  (Jackson 1986). Data obtained in this wavelength region usually have much coarser spatial resolution (120 m for Landsat 4/5 TM band 6, 1100 m for AVHRR 6/7 and 500 - 600 m for HCMR); the measured radiating temperature is compounded of vegetation and soil temperature, and it is difficult to separate the vegetation component from the total thermal radiation. The emissivity of a vegetation canopy and soil surface vary in time and space (Olsson 1987). For a review of TIR remote sensing from satellites see Lynn (1986).

#### **2.4.4.5 Microwave Region (about 30 $\mu\text{m}$ - 1 m)**

The microwave region of interest to remote sensing is usually restricted to 5 to 500  $\mu\text{m}$  and the most common sensing systems working in this band are RADAR (Radio Detection And Ranging) instruments. Radar is an active remote sensing technique, where the radiation is transmitted towards the surface of the object, by the instrument. The returning radiation is then measured in terms of the time interval between the transmittance and return and the properties of the returning signal. RADAR imaging systems (such as SEASAT SAR (Synthetic Aperture Radar) and Side-Looking Airborne Radar system (SLAR)) can provide an all-weather day-and-night imaging capability as they are neither blocked by clouds nor dependent on solar radiation. Three characteristics of the surface being sensed are: surface roughness, conductivity and slope (or incidence angle). Different vegetation and/or different parts of a tree have different sensitivity to radar wavelengths. This means that the data obtained from a radar system can provide information on vegetation type (e.g. Bush and Ulaby 1978; Shanmugam *et al.* 1983) as well as vegetation conditions (Ulaby *et al.* 1984; Paloscia and Pampaloni 1984). Bush *et al.* (1976) reported that radar returns from deciduous trees in the spring are much higher than those in autumn (Smith 1983). Radar data have proved useful in detecting soil degradation (e.g. soil salinity) (Smith 1983). The data are also useful in soil and site diagnosis for silvicultural management. Details on the principles, imaging systems,

analysis procedures and applications of radar can be obtained from Smith (1983), Simonett and Davis (1983), and Elachi (1988).

#### 2.4.4.6 Some General Features of Reflectance of Forest Canopies

As indicated above, the intensity of reflectance of the forest canopy is affected by both the internal structure of leaves and the external conditions. Canopy structure factors (such as branch and canopy layers, depth and shadows) also have significant effects on the intensity of reflectance (Williams 1991). These factors, however, usually change over time. For instance, pigment (e.g. chlorophyll and carotenoid) concentrations may vary, and additional pigments may build up within leaves in response to stress. Such variations can appear as subtle spectral changes in the visible and red edge portions of reflectance curves from vegetation in decline and can be used to detect forest damage (Jackson 1986). For instance, the internal structure of leaves changes with their increasing age (e.g. more spongy mesophyll, higher chlorophyll concentration and senescence) and therefore significantly influences the intensity of the forest canopy (Ajai *et al.* 1983; Mather 1987).

In general, the leaf absorption coefficient is lowest (i.e. highest reflectance) in young leaves in the visible wavelengths and highest in the NIR range (Wanjura and Hatfield 1988). During leaf senescence, starch, chlorophyll and protein are degraded. Usually light reflectance increases markedly (especially in the visible region (e.g. 0.55  $\mu\text{m}$ ) when chlorophyll degradation takes place (Barrett and Curtis 1992) and leads to a negative correlation with leaf age. However, leaf optical properties change significantly only during the juvenile and senescence stages. During the major part of the growth processes of deciduous trees their leaves have practically constant optical properties (Guyot *et al.* 1989).

The optical properties of conifer needles (pine, fir or spruce) change slowly as a function of their age (from year to year) with increasing pigment and water content (Westman and Price 1988; Guyot 1990). LAI has been one of the major factors estimated from remotely-sensed imagery since it has a strong relationship with plant productivity (see Section 2.5.5).

As shown in Figure 2.2, the reflectance of non-vegetation surfaces shows different patterns with wavelength. Water reflects only about 10% or less in the blue-green range, a small percentage in the red and no energy after the NIR range. Soils and/or non-green parts of vegetation typically increase monotonically with wavelength. As seen in the figure, soils show an approximately linear reflectance with wavelength, however, with

dips centred at about 1.4  $\mu\text{m}$ , 1.9  $\mu\text{m}$  and 2.7  $\mu\text{m}$  respectively, owing to moisture content. These water absorption bands are almost unnoticeable in very dry soils and sands (Richards 1986). All soils show the same reflectance pattern, but the reflectance level (pixel intensity) may be very different due to soil properties such as moisture content, colour, texture, and physical and chemical properties (Ritari and Saukkola 1985; Mulders 1987). Based on these optical properties of soils, remote sensing can be used to detect the soil-based site quality over unforested sites. For instance, the red light reflectance of the A horizon of a podsolised soil at normal moisture content was approximately 2.5 times the reflectance of the undergrowth of medium rich site type (Mulders 1987).

Williams (1991) found that conifer forests, in general, are more absorptive of radiation than broadleaved, deciduous hardwood forests. He also found that the magnitude of reflectance throughout the visible and NIR wavelength regions decreased dramatically for the conifer species as scene complexity increased from the needle, to the branch, to the canopy level. DeGloria and Benson (1987) have done a series of interpretation tests to determine the interpretability of spectral data from different bands of advanced SPOT film products for forest and agricultural survey in California, USA. They suggested that the best data for interpreting renewable resources were from the spectral bands sensitive to the red, NIR, and MIR.

#### **2.4.4.7 Three Basic Characteristics of Forest Cover**

Forest remote sensing is based on interpreting measurable variations in the *spectral*, *temporal* and *spatial* characteristics of forest cover types of interest. The capability of remote sensing to detect the changes of forest structure or growth is generally decided by the three basic characteristics briefly described below:

- (a) *Spectral characteristics* (or signature) of the target are the unique spectral reflectance for each specific earth feature. Different land cover types show different reflectance *intensity* and therefore can be differentiated. The reflectance levels depend upon a wide range of factors relating to the structure and condition of a particular land cover type.
- (b) *Temporal characteristics* Temporal effects are any factors that change the spectral characteristics of a feature over time. For example, the spectral characteristics of many tree species are in an almost continuous state of change throughout a growing season or whole growing process and these changes must be accounted for when interpreting the satellite data for a particular application. Another example is the use of seasonal thermal data to infer information about the cover

types. Temporal effects influence virtually all remote sensing operations. These effects normally complicate the issue of analysing spectral reflectance properties for forest resources. However, temporal effects might be the keys for generating the information sought in an analysis. For instance, the growth and/or change of a stand is predicated on the ability to measure temporal effects.

(c) *Spatial characteristics* that are used involve shapes and relative sizes as well as absolute sizes of objects. The term *spatial effect* also applies to factors that cause the same types of features at a given point in time. An example of this type of spatial effect is the change in leaf morphology, leaf angles and location of trees when they are subjected to some form of stress.

## **2.4.5 Applications of Satellite Data to Forests**

### **2.4.5.1 Introduction**

This section is a review of recent literature on the applications of remote sensing in forestry. The applications before the 1980s have been reviewed in great detail by Heller and Ulliman (1983). The discussion here will focus mainly on some recent applications of the data from the US Landsat MSS and TM, NOAA AVHRR, and the French SPOT, since these four data sources are most commonly used in forestry. The spectral, spatial and temporal resolution and other system parameters of these four sensors were summarised in Figure 2.2. More details on their characteristics can be found in Curran (1985), Harris (1987), Mather (1987), Arnaud and Leroy (1991), Barrett and Curtis (1992), Torlegård (1992), and Richards (1993). Reviews on the forestry applications of other remote sensing systems can be found in Leckie (1990).

The objective of this section is to briefly review the ways in which satellite remote sensing can be useful in delineating and evaluating the structural characteristics of forests which are required for forest management and planning. The discussion is organised with regard to (1) some general features of forestry applications of satellite data; (2) forest (site) type mapping; (3) forest inventory; (4) evaluation of stand variables; (5) assessment of forest (site) productivity; and (6) detection of forest changes.

### **2.4.5.2 Some General Features of Forestry Applications**

Forestry needs information about general growing conditions, forest resources and changes within them. Traditionally, information on forests is from inventories. Therefore, forest inventory has become the basis for forestry information acquisition systems.



Inventories are generally defined in terms of their function which is to determine the extent, scale, quantity, quality, and the locations of the forest resources. Inventories are classified in many different ways, depending on their objectives. FAO (1982) presented a classification of forest inventories used in various planning situations (Table 2.2). Table 2.3 lists some typical information requirements for these forest inventory and management activities. Most forestry information requirements that can be met by satellite remote sensors arise within the context of forest inventory, environmental monitoring and related special surveys. Not all data acquired by remote sensing systems can meet such information requirements (Table 2.3), nevertheless satellite remote sensing has become an increasingly important information source on forests. Detailed discussion on the requirement for forest information can be found from many forest inventory and forest management textbooks (e.g. Spurr 1952; Davis 1966). Sayn-Wittgenstein (1986), Cicone *et al.* (1977), and Ahern and Leckie (1987) also gave detail on the information requirements in respect of remote sensing. Aldrich (1979) listed various USDA Forest Service remote sensing user's requirements, desired ground resolution and/or preferred film (data) type, and recommendations for photographic remote sensing.

Table 2.2 Classification scheme for forest inventories (FAO 1982).

Type of Inventory (example)	Area coverage	Time Horizon (years)	Smallest Unit of Interest	Relative emphasis on inventory element (priority classes)							
				Landuse Pattern	Forest Area	Topography & Soil	Ownership	Accessibility & Costs	Volume Quantity	Growth & Site Class	Drain
world Forest Inventory	Region	10	Country	I	I	III	I	II	I	III	I
National Forest Inventory	Country	10-50	Country/ Civil District	I	I	II	I	II	I	I	I
Enterprise Inventory	Estate	10-20	District/ Range		I	II		I	I	II	I
Pre-investment survey	Potential Supply Area	10-20	District/ Range Catchment		I	II	II	I	I	II	I
Land-use survey	Country/ Civil District	10-50	Village	I	I	I	I	III	III	II	II
Working plan Survey Logging	District/ Range	0-10	Forest Stand (Tree)		I	I		I	II	II	I
Regeneration	District/ Range	0-10	Forest Stand		I	I				II	
Stand/stumpage Appraisal	Forest Stand	0-2	Forest Stand (Tree)		I	I		I	I		

Priority Classes: I - very important, needed in detail (or according to detailed stand classes); II - general estimate; III - little emphasis or can be eliminated.

Although forestry applications have many features in common with other land applications, they differ from the other major land application fields in a number of ways, such as their large area covering capacity and long time periods and therefore great usefulness of multi-temporal and multi-spectral data. Forestry applications are

Table 2.3 Forestry information requirement and possible forestry applications of remote sensing.

1. Reconnaissance Mapping	<i>Pre-inventory stratification</i> <i>Special purpose mapping</i> <i>Ecosystem and wildlife habitat</i> <i>Forest fuel maps</i> <i>Overview maps</i>
2. Detailed Forest Inventories	<i>Forest</i> <i>Stand (forest) types</i> <i>Stand boundaries</i> <i>Stand structure variables</i> <i>Species composition</i> <i>Height classes</i> <i>Age (or age classes)</i> <i>Density (including canopy closure, stocking)</i> <i>Diameter (or basal area)</i> <i>Volume (or yield)</i> <i>other stand variables</i> <i>Location</i> <i>Status (conditions, alive or cut)</i> <i>Non-forest</i> <i>farm land, water, rock, roads and tracks, etc</i>
3. Forest Change (inventory update)	<i>Decreasing</i> <i>Cutover</i> <i>Damage</i> <i>Insect and disease damage assessment</i> <i>Other damage assessment (wind fall, waterkill, etc)</i> <i>Increasing</i> <i>Natural regeneration</i> <i>Plantings (plantations)</i>
3. Forest Protection	<i>Fire protection</i> <i>Fire detection</i> <i>Fire mapping</i> <i>Fuel types for the protection</i> <i>Insect attack</i> <i>Pollution</i>
4. Site Evaluation	<i>Site quality</i> <i>Soil (e.g. soil physical conditions, fertility, parent rock)</i> <i>Climate (temperature and rain)</i> <i>Topography (slope, aspect, elevation, brief)</i> <i>Site Index, yield, or other site quality measures</i> <i>Site (forest type) classification and mapping</i>
5. Other information requirements relevant to forest management	<i>Vegetation Science</i> <i>Various vegetation indices</i> <i>Biomass</i> <i>Global change</i> <i>Species diversity</i> <i>Soil science</i> <i>Soil classification and mapping</i> <i>Soil type mapping</i> <i>soil erosion</i> <i>soil salinity</i> <i>Geology (rock type)</i> <i>Geography and geomorphology</i> <i>Climate</i> <i>Environmental impact studies</i>

characterised by a number of phenological, ecological, economic, long time horizontal, and large area land (site) management features, which together will ensure that remote sensing has and will continue to play an increasingly important role in forest type mapping, forest inventory, and monitoring, especially at national and even global levels. For one thing, the community interested in the remote sensing of forestry areas is large and diverse, including scientists, forest managers, government bodies and international organisations (e.g. FAO, UNESCO, and UNEP), as well as many consulting organisations and many large and small public companies concerned with forest resource, ecosystem and environmental management. Then again, forest management *per se* also involves different levels of planning (see Tables 2.2 and 2.3).

In forestry, strategic and operational planning are the two basic levels of planning activity (Davis 1966). The information required for strategic planning includes forest area, timber volume, timber growth, and health and mortality by strata. Strata are usually defined by tree species composition, age classes, size-class, site type and accessibility. The operational planning helps management determine (1) where, when and how much to cut; (2) the need and kind of silvicultural treatments; and (3) the need for, and location of logging roads, drainage and fertilisation. The information needed for operational planning is provided by forest maps which define the locations, shapes and area of each operative unit (e.g. compartment, block, stand etc). Also needed is information on timber volume, species composition, age, and growth rate, as well as soil and site quality. Thus there is a large and diverse demand for information, and varied applications of remote sensing in forestry and the areas relevant to forestry involving renewable and non-renewable resource survey and management applications are required. The role of forestry applications of remotely-sensed images at national and/or international levels is obvious, but there will also be an increasing role for them in forest planning and management at local levels. The following sub-sections will review the applications of remotely-sensed data to meet these information requirements.

#### **2.4.5.3 Mapping of Forest (Site) Types**

A forest type is a forest area which exhibits a general similarity in tree species, composition and structural characters. According to forest type theory (Cajander 1926 and 1949), biologically equal sites have similar vegetation cover and productivity (site quality) and therefore belong to the same forest type. Ecologically, a forest type is treated as an ecosystem unit and is classified using the ecosystematic approach (Clark *et al.* 1986; Mackinnon *et al.* 1992). Due to their large area scale and the difficulties of and high costs

of obtaining information in the field, using remotely-sensed data to classify and map forest types has historically been and continues to be the most frequent use of remotely-sensed data. In fact, the first forestry application of Landsat MSS data was forest cover type classification and mapping which began immediately after the launch of the ERTS satellite in the USA (Landgrebe *et al.* 1972; Latham and McCarty 1972).

Spectral data (pixels) can be classified into classes (usually called *information classes* or *spectral classes* in remote sensing) according to their reflectance values measured by satellite remote sensors. In forest inventory (sampling, for instance), forest cover type classification usually means stratification. The spectral classes may represent forest types (usually called strata). The desired forest cover type maps can be produced by displaying the classified and interpreted pixels with an appropriate presentation format (such as labels, colours and text).

There are two main categories of satellite data analysis procedures that may be followed to create a forest type map from a remotely-sensed image: *image enhancement* and *image classification* (Estes *et al.* 1983; Curran 1985; Hoffer 1986; Mather 1987). The objectives of image enhancement, also called "image optimisation" in some literature (e.g. Kaufmann and Pfeiffer 1988), is to transform and display the multidimensional (multispectral) data such that ground features of interest are accentuated. The imagery is then interpreted visually using tone, grey-scale, texture, pattern, boundaries, shape, colours, and context. A variety of image enhancement techniques, such as ratio, principal component analysis, spatial filtering, stretching, transformations, and band combinations, have been developed to increase the image contrast in the range of reflectance of the forest types of interest and produce a colour image highlighting these forest types (Leckie 1990).

In general, image enhancement can visually differentiate forest cover types at lower levels (usually Level I and II) and may meet the reconnaissance purpose. In the early examples, Howard (1976) and Jaakkola (1976) successfully mapped forest and non-forest classes. In Australia, using Landsat MSS data, Jones (1976) successfully mapped in the New England district in New South Wales several forest cover types (Level II) which included rain forest, wet sclerophyll forest and dry sclerophyll forest. Ahern and Bennett (1985) developed a standard enhancement procedure for Landsat MSS data for forest mapping in Canada. A review of digital enhancement of Landsat MSS data was given by Beaubien (1986). The applications he reviewed covered forest vegetation classification and forest type, biomass and inventory mapping. The most recent development of image

enhancement technique is the integration of enhanced digital satellite data with digital topographic data in a GIS. This image enhancement approach has proved to be valuable in improving land cover mapping accuracy in complex and rugged territory (Walsh *et al.* 1990).

Two principal types of automated classification procedure can be used to create forest type maps: *supervised classification* and *unsupervised classification* (Swain and Davis 1978; Tom and Miller 1984; Richards 1986; Mather 1987; Howard 1991). In supervised classification, the spectral characteristics of each forest cover type (class) are defined by statistics (e.g. mean pixel intensity in each band, and the covariance matrix) derived from within a known area of that cover type called a "training" sample. The analyst then assigns specific pixels to classes (cover types) according to the statistical similarity of their spectral values. The data analyst in a sense "supervises" the establishment of decision boundaries by providing the training samples, and "teaches" the classifier to recognise the information classes. Therefore, the classification accuracy from the supervised approach, to a great extent, depends on the knowledge of the analyst about the interest areas and the numbers and representativeness of training samples (Thomas *et al.* 1987; Fukue *et al.* 1988).

Unsupervised classification is based on a specific algorithm (such as clustering) to separate the spectral data of the entire image into classes. It is then up to the analyst to label these classes as to cover types. During the classification processes the analyst has little control over the establishment of the decision region. The classes are independent of any *a priori* assumptions about what ground covers they actually represent. To complete the analysis the spectral classes produced from unsupervised algorithms must eventually be converted to information classes by identifying the ground cover which corresponds to each spectral class (e.g. water has unique reflectance characteristics so that it can be discriminated easily by its spectral signature). Because of the analyst's reduced control over the classification processes, unsupervised classification is not generally as effective a method of characterising information classes as is supervised classification. This is particularly true when the spectral classes are only marginally separable in the measurement space (e.g. two tree species and age stages of the same species which have only subtle spectral reflectance differences). When based entirely on unsupervised classification, analysis can be expected to produce reliable results only when the spectral classes are easily discriminated in the image. While in complex terrain where there are many cover types and therefore many spectral classes, it may be difficult to classify forest

types (Townshend and Justice 1980), or even impossible to identify land-cover types of interest (Evans and Hill 1990).

A discussion of the capabilities and limitations of some most commonly used supervised and unsupervised approaches was given by Hoffer (1986). In view of the advantages and disadvantages of supervised and unsupervised approaches, a hybrid approach (the combination of both supervised and unsupervised classifications) was proposed to improve classification and mapping capabilities of spectral data by incorporating two or more decision rules rather than using only one of these techniques (Walsh 1980; Thomas 1980; Thompson *et al.* 1980; Hoffer 1986; Mather 1987; Chuvieco and Congalton 1988).

Spectral data of all resolutions have been employed to generate forest type maps, from high resolution of SPOT and TM to mid resolution MSS and to coarse resolution AVHRR maps (see below). Mapping accuracy, however, varied greatly between locations, terrain conditions, growing seasons (dates), resolutions and data qualities, processing and classification algorithms, scales, and detail degrees (classification levels), ranging from very low (less than 50%) to very high (greater than 95%) accuracy.

Landsat MSS data have performed successfully in classifying and mapping land cover and forest types at Levels I (e.g. forest and non-forest) and II (e.g. coniferous and deciduous forests), with 80% or higher mapping accuracy in many studies (e.g. Landgrebe *et al.* 1972; Howard 1976; Jaakkola 1976; Jones 1976; Carneiro and Hildebrandt 1978; Kan and Weber 1978; Beaubien 1979; Walsh 1980; Hill and Kelly 1986; Kelly and Hill 1987; Karteris 1988; Hall *et al.* 1989 and 1991). However, the mapping accuracy of Landsat MSS data at higher classification levels (III-IV) has been typically below 80% (Dodge and Bryant 1976; Strahler *et al.* 1978; Häme 1984). The limitations of the Landsat MSS data prevent the extraction of much of the detailed information foresters require. These limitations include deficiencies in spatial and radiometric resolution, spectral bands of the sensor, frequency and timing of image acquisition and lack of flexibility of illumination and viewing geometry.

The spectral and spatial resolution of TM data have been increased over the original MSS data to improve the data quality and products. Anuta *et al.* (1983) identified six categories of level II-III land covers with Landsat 4 TM data, with classification accuracy ranging from 76.6% to 98.5% and overall accuracy 88.4%. These six categories are: (1) medium-aged slash pine (10-20 years old); (2) medium-aged loblolly pine; (3) young pines (<5 year old); (4) uneven and mixed natural longleaf-loblolly pines; (5) hardwood-pine; and (6) non-forest. Coleman *et al.* (1990) could differentiate 5 age groups (i.e. 0-1, 2-5, 6-10,

11-20, and >20) of pine plantations with TM data in Louisiana, USA. The classification accuracy ranged from 68% to 74% using band combination 5, 4, and 3, and could be as high as 98% in some sites. Lillesand *et al.* (1985) obtained 93% overall and 90% average class accuracy for an area which included hardwoods, jack pine, red pine, lowland conifers, and three levels of jack pine defoliation. Similar species separation was also obtained by Shen *et al.* (1985) with simulated TM (TMS) data of a Minnesota study area (USA). They discriminated forest covers from non-forest (level I) classes with as high as 98% mapping accuracy. Bradbury *et al.* (1985) used both Landsat TM and MSS data to classify woodland in southern Wales. Their study area comprised stands of spruce, larch and pine on the uplands and oak, ash, beech and elm on the poorer soils and steeper slopes. The data showed the classification accuracy from TM data were better in most cover types (about 20% higher) than that from MSS data. Superiority of TM data over MSS data is also apparent in many reports (e.g. DeGloria 1984; Williams *et al.* 1984; Franklin 1986; Hopkins *et al.* 1988; Hall *et al.* 1989; Evans and Hill 1990; Arai 1992). Toll (1985), Hopkins *et al.* (1988) and Evans and Hill (1990) attributed better mapping results to better spectral discrimination of TM data (especially bands 1, 3, & 5).

TM data are superior to MSS data in mapping of level III but not necessarily of levels I and II. Dottavio and Williams (1982) classified a southern US. pine plantation into four classes, (i.e. clearcut, young pine, mature pine and hardwood) and found that the overall classification accuracy from Landsat MSS data was 71%, and that from TMS data 77%. When the pine classes were subdivided (i.e. pine: 1-5, 6-10, 11-25 years old and mature, and mixed pine/hardwood) the overall accuracy dropped to 30% for Landsat MSS and to 60% for TMS. Benson and DeGloria (1985) evaluated digitally enhanced Landsat 4 TM data of a California study area. The classes included in this study were high density conifer, hardwood/conifer, hardwood, brush, meadow, grassland, bare ground, and rock. Overall classification results varied with sensor and band combination. General results were as follows: high density conifer—TM 62-85% correct, MSS 80%; hardwood/conifer—TM 23-57% correct, MSS 47%; brush—TM 22-80%; MSS 20% correct; low density conifers—50-70%, MSS 90%; hardwood—TM—20-37%, MSS 40%; and grassland—TM 60-70%, MSS 43%. Keil *et al.* (1990) obtained varied mapping accuracies in level II (deciduous forest 86%, pine 80%, and mixed deciduous and coniferous 69%) and III (species subclasses 52-71%). Similar varied results have been obtained by many other researchers (e.g. Toll 1985; Hudson 1987; Parks and Petersons 1987). The data show that MSS data are more interpretable than TM data for certain cover types.

Evans and Hill (1990) found that TM data were superior to MSS data for identification of longleaf-slash pine, loblolly shortleaf pine and hardwood stands in the Kisatchie National Forest, Louisiana, but no significant differences were observed between TM and MSS supervised classification of pines and hardwoods. By statistical analysis, Williams and Nelson (1986) found that the differences in classification accuracy lie in the nature of the land cover classes desired: for classification of finer, higher levels (levels III, IV or higher), the higher spatial resolution of TM is beneficial; whereas for classification of coarser, lower levels (Level I and II), TM has disadvantages unless the spatial context of a pixel is incorporated into the classification procedure. As pointed out by Townshend and Justice (1981), classification accuracy could sometimes be improved by coarser resolution of sensor data, since internal variations (e.g. sensor noise) decline within each single class. Woodcock and Strahler (1987) showed that local variance of a forest type sharply decreased with pixel cell sizes from 30 m to 120 m. Recorded variations caused by the reflectivity differences between tree crowns and their shadows are increased as the spatial resolution is made finer, but are average when the spatial resolution is coarse (Howard 1991). Maxwell (1976), Toll (1985), Cushnie (1987) and Justice *et al.* (1989) found higher spatial resolution imagery has higher internal variability within homogenous land-cover types than coarser resolution and therefore a poorer classification accuracy. At higher resolution forest stands look less homogeneous as areas of varying species or crown closure become distinct units. This causes greater variance in the reflectance from a forest stand and difficulties in classifying forest type. It is therefore useful sometimes to degrade the recorded signals by averaging groups of pixel values (e.g. 3 x 3 window) within each segment which is being digitally analysed; but the risk is that more mixed pixels are introduced into the classification.

The capability of SPOT data in classifying forest types has received mixed reviews. In an urban study in Athens, Georgia, SPOT data were found to increase the accuracy of level II and III classifications by 15 to 20% over that of TM data (Welch 1985). Skidmore and Turner (1988) discriminated five age classes in radiata pine plantations in Australia with an 87% mapping accuracy. In assessing the capability of species recognition of SPOT data in northern Belgium, Borry *et al.* (1990) could map the forest cover types at level II with 95% accuracy and 60-95% at level III information details. In Kenya, SPOT imagery was used to identify and to delineate the boundaries of land systems, in which the plantation boundaries could be mapped at a scale of 1:10,000. Within the compartment, the planted species, height classes, age classes and crown cover could often be inferred from variations in hue (colour), tone and texture (see Howard 1991). In a recent study of



subtropical vegetation classification using SPOT data, Franklin (1993) showed varied classification results at levels I and II. Low separability was found in an area with sparse and variable vegetation.

SPOT and TM data showed approximately equal capability for forest type mapping, but the SPOT system has fewer spectral bands and therefore statistically provides less spectral information than TM data (Parks and Peterson 1987; Chavez and Bowell 1988). Büttner and Csillag (1989) showed that the spectral separability and classification accuracy of soils was better with TM imagery owing to its MIR band (TM5), compared to those of SPOT imagery. Manière and Courboulès (1989) showed that TM5 data allowed better identification of tree species, whereas TM1 (blue band) data were useful to separate species in terrain shadow zones. Chavez and Bowell (1988) stated that SPOT data may not necessarily produce higher accuracy in land cover classification than TM data, but that they may be better in cartography and area estimation. Welch (1985) suggested that SPOT data were more suitable for cartographic mapping at a smaller scale (e.g. 1:24,000 or smaller) than TM data, but may be less helpful for forest type mapping because of reduced spectral resolution (fewer bands) relative to TM which may obscure vegetation differences. Parks and Peterson (1988) reported that both TMS and SPOT data have the same capability in identifying level III categories of different vegetation species, age classes and cover density using supervised classification techniques. They also stated that TM data could provide better opportunities for high resolution monitoring of vegetation, moisture, and geology through its many spectral band combinations and its extensive coverage; whereas SPOT data were more useful for acquiring information on spectrally and spatially complex ground features occupying small areas. In particular, SPOT has advantages in vegetation analysis through its limited spectral band combinations, its frequent coverage, and nadir and off-nadir viewing.

NOAA AVHRR data are usually used for forest type classification and mapping on a large area scale, such as national, continental and even global levels, because of their coarser spatial resolution. Since the mid-1980s, there have been several studies using AVHRR data for forest vegetation classification and mapping at the continental level. For instance, Justice *et al.* (1985) produced a continental digital image composite at the level of plant formations/pan-formations for Latin America using AVHRR data. Tucker *et al.* (1985) used AVHRR data to classify vegetation communities in Africa based on eight composite observations from an 11-month period. These composites were created by producing images composed of the maximum normal difference vegetation index (NDVI) values for each pixel during contiguous 21-day periods. Such compositing and use of

multitemporal data are feasible at continental scales only with coarse resolution, high frequency coverage. Townshend *et al.* (1987) created a vegetation map of South America in which 16 vegetation classes were differentiated, several with accuracy greater than 90%. Clark *et al.* (1986) used AVHRR data to classify ecological units at a 1:250,000 scale (Level I: forest and non-forest areas; Level II: coniferous, deciduous, and mixed forest types) using colour enhancement methods with AVHRR. In comparison with Landsat MSS data, Gervin *et al.* (1985) produced a land-cover map for the Washington, DC, area with AVHRR data. In this study, classification accuracy at level I obtained from AVHRR was similar to classification accuracies for Landsat MSS data (71.9% and 76.8% respectively). The accuracy for the predominant classes was similar for both sensors, and land-cover discrimination for less commonly occurring and/or spatially heterogeneous classes was improved with MSS data. They concluded that the AVHRR data performed as well as, or better than, MSS data in classifying large homogeneous areas. Given mapping accuracy, lower processing cost and more temporal frequency, AVHRR imagery provides an attractive and reliable alternative to the higher resolution data for regional forest cover mapping. A comprehensive review of the applications of AVHRR data in ecological surveys, including stratification, inventory, and condition assessment, and detection of changes, has been made by Roller and Colwell (1986).

In site productivity/type mapping at the regional scale, Getter and Tom (1977) developed a multivariate discriminant model for classifying the site productivity of 14 coniferous species using Landsat MSS band data and ancillary data (i.e. elevation, slope, aspect, and airphoto-derived vegetation data) in Colorado, USA. The overall classification accuracy was 92% on the ten site index classes, while a classification accuracy of only 68% was obtained without using spectral data (Tom and Miller 1978). The ancillary variables (e.g. topographic data) were found to be generally more useful discriminators than spectral data. The work was continued by Tom and Miller (1980) by combining the four MSS bands and all their various band ratio combinations and topographic data, resulting in a training set accuracy of 97.3% for nine site index classes (i.e. 97.3% of 37 field site lots could be correctly assigned to their known site productivity class). Häme (1984) reported that, by using numerical interpretation of Landsat MSS data combined with colour infrared photography and map data, it is possible to map forest site types faster and with lower costs than by using traditional methods. Eleven of thirteen site types could be recognised from imagery, and mapping accuracy ranged from 0 to 100% with an average of 59%. Site type mapping using MSS data has been used in practice for forest taxation purposes in Finland (Lovén 1986). A recent investigation showed that net primary

productivity (NPP) (tons/ha/year) could be mapped with moderate accuracy in continental scale with AVHRR data (Chong *et al.* 1993).

With respect to mapping scales, Krebs (1982) produced forest type maps at 1:250,000 scale at Level I information detail (75% correct) and Level III information detail (52% correct) and the interpretation cost was only 1%, which is lower than other photo-interpretation techniques (aerial photographs and colour infrared). Keil *et al.* (1990) produced 1:200,000 scale forest type maps from Landsat MSS data with 69-86% accuracies for level II and 52-71% accuracy at level III. Mead and Meyer (1977), working with boreal forest types in Minnesota, concluded that 1:123,000 was the smallest acceptable scale when working with Landsat MSS data. Howard (1991) stated that Landsat MSS data favour forest mapping at a scale of 1:100,000 and map revision at a scale of 1: 50,000 or larger. Using manual interpretation, Karteris (1988) could map forest land at levels I and II at 1:50,000 scale using four Landsat MSS images in southwestern Michigan from winter and fall growing seasons. He obtained an accuracy of 79.9-88.3% for mapping, and 86-95% for identification, with winter imagery showing better accuracy. In Ireland TM data has been demonstrated experimentally to be suited to forest stock mapping at a scale of 25,000, but with the species information mainly provided from other sources; and for stock map revision of wind throw and clear felling at scales up to 1:10,500 using a GIS overlay of forest compartment and sub-compartment boundaries (MacSiurtain *et al.* 1989). In comparing the mapping capability of satellite imagery from several sensors, Konecny (1990) suggested 1:200,000 scale for Landsat MSS data, 1:100,000 for TM and 1:15,000 for SPOT panchromatic data (cited in Torlegård 1992). Gugan and Dowman (1988) developed a topographic mapping model using SPOT imagery. The mapping accuracy with this model was compatible with that of mapping at 1:50,000 with 25 m contours and about 80% of the information content required by 1:50,000 scale mapping could be extracted. Hall *et al.* (1991) showed that SPOT panchromatic band data were able to map forest cutover at 1:15,000 scale as accurately as from traditional aerial photographs at the same scale. Based on Markham and Townshend (1981), smaller map scales (such as 1:10,000 or smaller) may be obtained using higher spatial resolution images (e.g. SPOT Panchromatic band 10 m resolution, or low altitude imaging spectrometer) since mapping scale can be seen as a function of spatial resolution.

Many efforts have been made to improve classification accuracy by (1) development of new classification and enhancement techniques or discrimination roles; (2) application of ancillary data, (3) application of multi-temporal or multi-sensor data; and (4)

improvement in data quality by error corrections. To improve forest site mapping accuracy, Pu and Miller (1991) developed a classification method using fuzzy sets theory by incorporating TM and ancillary data, obtaining an accuracy of 78%, which is close to that derived from site index. Fisher and Pathirana (1990) suggested that a fuzzy classifier may enable the extraction of information about individual pixels and about sub-pixel phenomena not addressed by other classifiers. Wang (1986a, b), Lees and Ritman (1991), and Moore *et al.* (1991) showed better classification and mapping accuracy using a decision-tree classifier. Skidmore (1989) developed an expert system classifier to map eucalypt forest types in Australia and concluded that it could improve forest type mapping accuracy. Kanellopoulos *et al.* (1992) proposed an artificial neural network based on the multilayer-perception model to classify land-cover types using two-date SPOT data. The average classification accuracy was 91%, exceeding the performance of a maximum-likelihood classifier by 28%. Another example of using the neural network classifier can be found in Salu and Tilton (1993). Plumb (1993) improved the mapping accuracy of vegetation types in Big Bend National Park, Texas, from 42% by traditional supervised classification to 72%, using knowledge-based digital mapping techniques. Using landform and vegetative factors, Satterwhite *et al.* (1984) could improve land cover classification of Landsat MSS data from level II to III and at times to level IV. Lynn (1986) and Hill and Aifadopoulou (1990) suggested that application of multi-sensor data could improve classification accuracy. Merged images of different spatial and spectral resolution have been used to enhance interpretability (Welch and Ehlers 1987) and merged images from different growing seasons have shown more ability to make land cover classifications than single date images (Fuller and Parsell 1990). Multi-temporal data are especially useful in discriminating land cover types in extremely complex and heterogeneous environments where the surfaces are barely identifiable spectrally (Conese and Maselli 1991; Fleischmann and Walsh 1991; Thomson 1992). The mapping capability of coarse spatial resolution data (e.g. AVHRR) can be improved by incorporating higher resolution data sources (Iverson *et al.* 1989; Marsh *et al.* 1992). Skidmore *et al.* (1986) and Richards *et al.* (1987) showed improved mapping accuracy by combining SIR-B radar and Landsat MSS data. Strahler *et al.* (1978), Tom and Miller (1980), Satterwhite *et al.* (1984), and Moore and Bauer (1990) showed improvement in classification results when combining spectral and ancillary data.

To improve data quality, Chen (1984) developed a topographic correction procedure for Landsat MSS data using the DTM data over the same area. The corrected Landsat MSS data showed better classification accuracy than the original data. Yu and Chen (1990)

showed that topographically-corrected TM data give better information on vegetation in mountainous regions than uncorrected data. Kawata *et al.* (1988) proposed a radiometric correction method for removal of atmospheric and topographic effects on Landsat MSS data. Hall-Könyves (1987) showed that the topographic effects on the spectral responses of cultivated fields in gently undulating terrain (0-15°) were weak. Itten and Meyer (1993) showed that in complex terrain, TM data corrected geometrically (slope-aspect) and/or atmospherically-corrected could increase classification accuracy by 10 to 30%, geometrically-corrected data having better accuracy than atmospherically-corrected data. The data showed that in terrain with 5° or higher degrees of slope the spectral responses were significantly affected. Similar error correction methods have also been used for improving the quality of SPOT data (Senoo *et al.* 1990; Yang and Vidal 1990; and Baker *et al.* 1991) and AVHRR data (Singh and Saull 1988; Teillet and Staenz 1992).

The current trend in improving classification accuracy is the use of GIS to integrate digital biogeographical data with satellite remotely-sensed data and the introduction of knowledge-supported data analysis techniques. The data sources can be from multi-sensors, multi-temporal, multispectral, or multi-resolution data sources. The most widely used ancillary data are from digital terrain models (DTM) which include elevation, slope, aspect and slope position data. The variation in the topographic configuration of an area can produce a complex reflectance geometry that can increase the probability of misclassification, and this can be more important in altering spectral responses than crown size and crown density (Walsh 1987). By incorporating DTM data, the shadowing effects caused by sun angle can be corrected. For instance, topographic variables were integrated with TM data to increase the accuracy of classifications of vegetation communities in the Rocky Mountain terrain (Frank 1988). Increase in accuracy of classification has also been reported by a number of other authors (e.g. Skidmore 1989; Janssen *et al.* 1990; Kanellopoulos *et al.* 1992; Chagarlamudi and Plunkett 1993).

#### **2.4.5.4 Forest Inventory**

Using remotely-sensed data for forest inventory purposes has become a common forestry practice, especially for the purposes of inventory data base update (Hegyí and Quenet 1982 and 1986; Poso *et al.* 1987; and Pilon and Wiart 1990). Jaakkola (1986a and 1986b) gave a broad summary of applications of Landsat MSS data to forest inventories and forest management in the European countries, especially in the Nordic countries. The applications are directed to inventory sampling designs (e.g. two-stage and multi-stage sampling), forest site type mapping, forest cover (type) classification, estimating stand

variables, and monitoring forest changes. Applications of Landsat MSS for regional forest resource inventory and management in North America were summarised by Leckie (1986).

Multi-stage sampling procedures (also called multi-phase sampling, double sampling, photo-plot sampling, two-stage, or three-stage sampling in some work) have been used in studies associated with forest inventories with satellite data. Since sampling from imagery and/or photographs is far quicker than ground sampling, it is advantageous to sample in the field on a fraction of the plots sampled on the imagery and then to collect field data, which cannot be otherwise obtained. Usually remotely-sensed data are used for forming the sample of the first stage in multiphase sampling. This is accompanied by several stages of sub-sampling using low and/or high altitude photography and/or ground data acquisition to check the first-stage interpretation (e.g. Heath 1974; Kalensky *et al.* 1979; Hegyi and Quenet 1986; Jaakkola 1986a; Poso *et al.* 1984 and 1987; Peng 1987; and de Gier and Stellingwerf 1992). Refer to van Genderen *et al.* (1978), Nelson *et al.* 1987, and Skidmore and Turner (1989) for detailed discussion on sampling designs for accuracy assessment of maps from satellite data.

A three-stage sampling model for large-area timber inventories was developed at the University of Freiburg (Jaakkola 1986b). In this study, Landsat MSS imagery was used to create the first-stage sampling units resulted in identification of forest type covers such as hardwood and conifer forests. Second-stage sampling units were selected (at 5% sampling error) from 1:50,000 scale CIR-film by applying the PPS (probability proportional to size) sampling method based upon the timber characteristics: age, crown closure, height, crown diameter, and stocking. A total of 320 photo points were measured in the field in the third stage of the inventory. The results showed strong agreement in forest area estimate (compared with the actual area); the standard error of volume estimate of principal tree species was 5%. The disadvantage of the three stage sampling method is the requirement for <sup>a</sup> full coverage of aerial photographs, which may not always be available.

Poso *et al.* (1987) presented a two-phase sampling procedure for estimating stand variables using Landsat TM data. By integrating Landsat TM data with permanent sample plots, Peng (1987) proposed a continuous forest inventory method for compartmentwise estimation. An example of successful multiphase sampling is provided by the Alaskan multi-resource vegetation inventory (LaBau and Winterberger 1988). The sampling design uses three levels of remote sensing information: Landsat MSS data classification, small scale CIR aerial photographs (1:60,000) and macro-scale CIR photographs (1:3,000 to 1:7,000). The fourth phase is provided by field plots.

Stratification, correlation and regression modelling are three basic approaches used for estimating stand variables in multi-phase forest inventory. The major purpose of sampling stratification is to reduce the standard error of the estimate (Strahler 1981), while correlation and regression are used to establish the relationships between the estimated and true values. Kirby and Van Eck (1977) used Landsat MSS data to stratify forest into cover types as a first stage during conifer forest inventories. Jaakkola and Saukkola (1979) used Landsat MSS data to develop regression models for timber volume estimation in the forest stands dominated by Scots pine in northern Finland. The means of the block volumes were 80.1 m<sup>3</sup>/ha (measured) and 79.7 m<sup>3</sup>/ha (model-estimated) respectively. Strahler and Li (1981a and 1981b) reported studies using Landsat MSS data to estimate stocking and height in sparse to moderately stocked ponderosa pine forests.

Nelson *et al.* (1987) reported a statistical procedure which utilised Landsat MSS data in a stratified random sampling design to assess continental or sub-continental forest resources. In their study, sample blocks were analysed from MSS imagery selected throughout the continental USA in order to estimate the areas of conifer and broadleaved forests. Misclassification errors reduced the reliability of the estimates. The accuracy of estimates was significantly improved after improving the sampling design procedures by incorporating aerial photo-interpretation information to "correct" or "adjust" Landsat-based estimates of coniferous and broadleaved forests (Nelson *et al.* 1989). The sampling procedure, according to the authors, was useful for assessment of continental (e.g. whole country) or sub-continental (e.g. forest types) forest resource.

Poso *et al.* (1984) proposed a stratification model for compartmentwise estimation with Landsat MSS data. He found the best stratification was obtained from the first principal component. The stand variables estimated by the model showed high correlation with the same variables measured in the field. The correlation between the first principal component and stand age was 0.82 and between the first principal component and stand volume 0.78 for the two best sites. This work was continued three years later by using both Landsat MSS and TM data for plotwise and compartmentwise estimation of stand characteristics (Poso *et al.* 1987). Again the best stratifications were obtained from the first principal component images, with a correlation of about 0.85 for stand volume, age and mean height. Similar procedures and results were reported by Peng (1987).

A forest classification and inventory system (FOCIS) was designed by Franklin *et al.* (1986) at the University of California for stratified sampling. They combined Landsat MSS data with DTM data for timber stratifications. The overall accuracy of stratification and estimates of timber for a large area was about 87%, with standard errors ranging from

6.7 to 24.4. The results suggested that FOCIS can produce a softwood timber volume estimate for very large areas with an accuracy comparable to estimates produced by conventional means, but at significantly lower cost than conventional methodologies.

As discussed earlier, Landsat MSS have been shown to be capable of classifying forest land into cover types (or stratifications) at levels I and II with reasonable accuracy. In some cases, this level of stratification is adequate for an initial reconnaissance of unmapped, poorly mapped or inaccessible areas. The improvements in the accuracy of broad level classification with better spatial resolution data (such as TM and SPOT) make the results more acceptable as a source of reconnaissance-level forest information than the results from the coarser spatial resolution data (such as Landsat MSS data). Hall *et al.* (1989) used both Landsat TM and MSS data for mapping and estimating area of forest cutover, obtaining an approximately equal mapping accuracy (89.5% for TM and 86.9% for MSS data respectively). Roller and Colwell (1986) and Hall *et al.* (1991) suggested that NOAA AVHRR data may be more useful and cost-effective for stratifying broad land cover types prior to sampling, whilst the combinations of AVHRR and TM data may increase the accuracy of stratification.

Bercha *et al.* (1990) developed a multi-sensor airborne forest inventory system in Alberta, Canada. The system provided a three-dimensional description of forest using the spectral information from vertical and horizontal planes recorded by Laser and multispectral camera (video) sensors. The forest description included principal stand characteristics such as species composition, forest condition, crown density, height, vertical stratification and foliage density. The system provided an economical and efficient technique for obtaining forestry parameters ranging from pre-inventory surveillance to detailed inventories and monitoring of changes in the forests in different conditions.

Reich and Hussin (1993) used a two sampling design for estimating stand above-ground biomass on a regional basis using L-band radar backscatter imagery. Two models were derived to estimate stand biomass by comparing three estimations in a simulation study using four sample sizes (25, 50, 100 and 200 stands). Model 1 estimated average stand biomass as a function of the amount of radar backscatter, while Model 2 estimated biomass as a function of the radar backscatter and basal area. The F-test and t-test showed that no significant differences existed between the model-estimated and ground measured biomass ( $\alpha < 0.05$ ). Model 2 showed better estimate accuracy than Model 1. Mean square error (MSE) dramatically decreased from 100-650 to 10 - 64 as sample sizes increased from 25 to 200.



#### 2.4.5.5 Evaluation of Stand Variables

Remotely-sensed data have been used with varying degrees of success to quantify various stand variables such as canopy closure, density, diameter, basal area, height, tree age, volume, biomass, and LAI. In general, the technique is to relate the forest structure variables of interest obtained from ground measurements to the spectral data at the same location. The spectral values can be original data or various combinations and transformations. The most common method is correlation analysis and/or regression modelling (including simple, multiple and/or stepwise regression techniques). Virtually all studies have focused on coniferous forests, especially plantations, which tend to be more uniform and more distinguishable from other vegetation types than are deciduous forests.

Canopy closure of coniferous forests in Sequoia National Park in California, USA, correlated well with the spectral values of several bands or band combinations of TMS data, with correlations ( $r$ ) ranging from 0.62 to 0.69 ( $n = 123$ ) irrespective of forest type (Peterson *et al.* 1986). Total basal area, however, was poorly related to the spectral data ( $r < 0.5$ ). They found that stratification by forest type could significantly improved the correlation with basal area. The data analysis suggested that the relationships between total basal area and spectral values will be strongest in young, low density, even-age managed plantation stands. In another study of California coniferous forests, TMS visible bands (Bands 1, 2, and 3) were found to be most strongly correlated with basal area and leaf biomass (Franklin 1986), but the correlations were relatively low ( $r^2 = 0.29 - 0.30$ ). The best result was obtained from the band 3 with log-linear equation ( $r^2 = 0.64$  and  $0.67$  for basal area and biomass respectively).

A relatively high negative correlation between TMS and canopy closure was found for the pine-aspen forests in southwest Colorado, USA (Butera 1986). The correlation coefficients were -0.76 (TM1), -0.66 (TM2), -0.67 (TM3), -0.09 (TM4), 0.80 (TM5), -0.60 (TM6) and 0.76 (TM7) respectively. By using a regression model, she created a map of forest canopy closure for the area. The accuracies of the map were 71%, 74% and 54% for percent canopy closure classes of 0-25%, 25-75% and 75-100% respectively. Jensen *et al.* (1991) obtained much higher correlation between canopy closure of mangrove and SPOT XS data (NDVI) ( $r = 0.91$ ) in southwest Florida, USA.

Spanner *et al.* (1984b) used a classification method to study the capability of TMS data to differentiate crown closure and tree size classes in a fir-dominant forest in Idaho, USA. They obtained a classification accuracy of 60% in differentiating canopy closure classes

of 10-39%, 40-69%, and 70-100%; with lower accuracy on the sites of very low canopy closure (0-10%). Saw timber and pole size classes were also classified with 72-87% accuracy. Based on the classification accuracy, the bands in these analysis were ranked in order of TMS bands  $4 > 7 > 5 > 3$ .

A regression model was built to estimate stand volume of Scots pine in Finland with Landsat MSS data (see Jaakkola 1986b). The correlation between volume and combined band data (i.e.  $Ch4 + Ch5 \cdot (Ch6 + Ch7)$ ) ( $r^2$ ) was 0.88 at forest block level. But the estimate at pixel-by-pixel level was low ( $r^2 = 0.41$ ). The model was tested in a timber inventory by visual checking and correlation analysis which resulted in correlation coefficients from 0.8 to 0.92. According to the authors, the model is applicable in forest inventory for estimating the regional distribution of timber volume. Forest management planners can use the results as such, or as a first step in a more sophisticated inventory.

Ardö (1991) investigated the relationships between Landsat TM data and the volume ( $m^3/ha$ ) of forest compartments in a coniferous forest dominated by Scots pine in southern Sweden. The correlations ( $r$ ) between TM band data and compartment volume ranged from -0.50 to -0.80 ( $n = 99$ ).

Li and Strahler (1981; 1985; 1986a; 1986b and 1992), Strahler and Li (1981a and 1981b), and Strahler and Jupp (1990) and Nilson and Peterson (1991) have taken different approaches to the study of satellite data of coniferous forests by using forest canopy reflectance models to investigate the potential of estimating forest canopy and stand parameters. Using the Li-Strahler geometric-optical canopy reflectance model, Woodcock *et al.* (1990) could estimate size and density of trees with Landsat TM data. Using the same models, reasonable estimates of woody biomass on a regional scale could be given with TM data (Franklin and Strahler 1988).

Franklin *et al.* (1991) correlated tree canopy cover of blue oak woodland and wooded grassland (semi-arid woodlands) in California, USA, to TM data over two seasons. The correlations ( $r$ ) ranged from -0.76 (TM4) to -0.83 (TM3) for the raw band data of the September image, and -0.67 (TM4) to -0.77 (TM1) for the December image. The correlations were improved (about 2-7% increase) when using the canopy cover plus modelled canopy shadow cover. In a recent study in young conifer stands in Oregon, USA, a very high correlation was obtained between TM band data and stand ages of Douglas-fir dominated stands (2 to 35 years old) (Fiorella and Ripple 1993) with linear correlations ( $r$ ) ranging from 0.82 to 0.96 (except TM4). Log-linear regression modelling showed that the TM4/TM5 ratio could explain 91% of stand age variation.

Many studies have related the LAI of coniferous forests to satellite data. Running *et al.* (1986) correlated LAI of coniferous forest stands along a transect across the mountains of Oregon, USA, to airborne Thematic Mapper (ATM, i.e. TMS) data by linear regression analysis. The strongest positive correlation was produced between the LAI and NIR/red band ratio ( $r^2 = 0.76$ ,  $SE = 0.38$ ,  $n = 18$ ). The correlation was improved to 0.82 ( $SE = 1.187$ ) after correction for atmospheric effects. The LAI for these stands ranged from 0.6 to 16.0  $m^2/m^2$ . In another study by Peterson *et al.* (1987), a log-linear equation fitted the asymptotic characteristics of the relationship better, explaining 89% of variation for the red and 91% for the NIR/Red band ratio respectively. Inverse curvilinear relationships were observed between LAI of temperate coniferous forests in the western US and TM data by Spanner *et al.* (1991), the best correlation being obtained from TM5 ( $r = 0.74$ ), and improved to 0.80 by topographical and atmospheric correction. However, the estimate accuracy of LAI at sub-regional scale is generally low (Memani *et al.* 1993).

Sader *et al.* (1989) examined the relationships between forest structure and biomass and TM-derived vegetation indices in three forest types (tropical, subtropical and warm temperate forest biomes) in Puerto Rico and the USA. The *normalised difference vegetation index* (NDVI), calculated from low altitude aircraft TMS data, was found significantly correlated with forest age classes ( $r = 0.67$  and  $0.65$  respectively), but the TM-derived NDVI was not correlated with the same age classes ( $r = 0.11$ ). Moreover, biomass differences were found undetectable with NDVI. They concluded that NDVI computed from TM data does not appear to be a good predictor of stand structure variables or total biomass in uneven age, mixed broadleaf forest, especially in areas with complex terrain conditions. Memani *et al.* (1993) and McGwire *et al.* (1993) also showed a low relationship between TM-derived NDVI and LAI. The correlation between LAI and NDVI could be somewhat improved by correction for canopy closure using the MIR band (Memani *et al.* 1993), or by reducing the effects of spatial autocorrelation in sampling design (McGwire *et al.* 1993).

Larson (1993) established predictive models for estimation of canopy cover of Acacia woodland in eastern Sudan using the NDVI computed from Landsat MSS, TM and SPOT data. The correlation coefficients ( $r$ ) between field-measured canopy cover and the satellite sensor derived NDVI were 0.552, 0.698 and 0.718 for MSS, TM and SPOT data respectively. The best correlation and estimate were obtained from SPOT data.

Spanner *et al.* (1990) related LAI from 19 coniferous stands in Oregon, Washington, Montana, and California, USA, to NDVI of multi-temporal AVHRR data. The NDVIs of the summer images were found best correlated LAI ( $r^2 = 0.70$  for July 1986 image and

0.79 for July 1987 image). They concluded that AVHRR NDVI could be used to detect seasonal differences in all of the forest stands. These seasonal differences were related to: a) phenological changes in LAI caused by climate; b) proportions of surface cover types contributing to the spectral reflectance; and c) large variations in the solar zenith angle. Curran *et al.* (1992) found seasonal LAI of coniferous forests could be estimated using Landsat TM data.

Turner *et al.* (1987) related SPOT-1 data to stand variables of radiata pine in Canberra, Australia. They found that only the NIR band (XS3) was significantly correlated with stand age and dominant height ( $r^2 = 0.5$  approx.). Danson (1987) correlated SPOT data with five stand variables of Corsican pine in England and found strongly significant correlations of SPOT NIR band (XS3) to tree density ( $r = 0.65$ ,  $n = 29$ ), mean diameter at breast height (DBH) ( $r = 0.79$ ), mean tree height ( $r = -0.83$ ) and age ( $r = -0.67$ ), but not to canopy cover. The correlations between green (XS1) and red (XS2) and stand variables were relatively low ( $r < 0.48$ ). Similar correlation patterns were also reported in a recent study with ATM and SPOT data (Danson and Curran 1993), where ATM band 7 and SPOT XS band 3 were found most strongly negatively related to stand age, tree density, mean tree height, DBH (ATM 7:  $r = -0.60$  to  $-0.76$ ; SPOT XS3:  $r = -0.66$  to  $-0.84$ ).

Stenback and Congalton (1990) examined the understory of mixed coniferous forests in northern California, USA with TM data. They found that TM data could be used to recognise the presence or absence of vegetated understory in three canopy closure classes: sparse (< 30%), moderate (30-70%), and dense (> 70%). The best classification accuracy was obtained from a combination of TM bands 2, 3, 4, 5, and 7.

SPOT and TM data were used to estimate tree density of sparse oak (*Quercus ilex* and *Q. suber*) woodlands in southern Spain (Joffre and Lacaze 1993). The regression analysis showed that TM data were less successful than SPOT data. SPOT panchromatic band data explained about 72% of variation of tree density. The explanatory power could be improved to 88% through a 0-100 binary coding of panchromatic data, called thresholded Laplacian Index (TLI). TM data could explain only about 37% or less variation.

Westman and Paris (1987) developed a model to estimate 31 structural features and the biomass of forests of pygmy cypress (*Cupressus pygmaea*) and pine (mainly *Pinus contorta* ssp. *Bolabderi*) near Mendocino, Canada with great success using C-band radar (4.75 GHz) data. The model enabled independent testing of the effects of tree stem, branch, and leaf branch biomass, branch angle, and moisture content on radar backscatter. Tree LAI was strongly correlated with vertically polarised power backscatter ( $r = 0.94$ ),

while branch mass per unit area was highly correlated with crosspolarised backscatter ( $r = 0.93$ ).

An airborne pulse laser system, called the Light Detection and Ranging (LIDAR) system, has been used by Nelson *et al.* (1988) to predict total tree volume and green weight biomass of a pine plantation in Georgia, USA. They were able to estimate overall tree volume to within 2.6% and mean biomass to within 2.0% (based on 38 test plots), but were not successful in predicting volume or biomass on a site by site basis. Their earlier study (Nelson *et al.* 1984b) showed that airborne laser data were highly correlated with canopy closure ( $r^2 = 0.82$ ), but less well correlated with tree height.

A knowledge-based expert system was developed to assess vegetation characteristics from spectral albedo and biogeographical information (Kimes *et al.* 1991). This system can be used for inferring and evaluating the physical and biological characteristics of a forest stand including ground cover, biomass, LAI, and photosynthetic capacity. The inferences from this system were significantly more accurate and robust estimates of vegetation characteristics than conventional data analysis (information extraction) techniques.

#### **2.4.5.6 Estimation of Site Productivity**

As discussed in Chapter 1, the productivity of a forest site is the productive capacity (or actual production) of an area of land for a given forest type or tree species. In forestry it is commonly designated as site index, yield and/or mean annual increment of timber volume; whereas in ecological studies, it is usually measured with biomass weight of a unit area (e.g. tonne/ha). Using satellite data, forest productivity is generally assessed by means of ways of (1) digital classification and mapping of forest type or site classes and (2) estimation of productivity variables such as volume, yield, site index, mean annual increment, and/or biomass through correlation and regression modelling. Although classification and mapping of site productivity (or site types) based on satellite data have been produced at broad levels with some success, the successful direct estimates of forest productivity using satellite data are rare.

Fox *et al.* (1985) developed a discriminant model for predicting forest productivity with moderate success using satellite and biogeographical data (18 variables) in northwestern California, USA. Three broad productivity classes delineated by wood volume classes ( $> 85 \text{ ft}^3/\text{acre}/\text{year}$ ,  $50\text{--}84 \text{ ft}^3/\text{acre}/\text{year}$ , and  $< 50 \text{ ft}^3/\text{acre}/\text{year}$ ) could be predicted using vegetation cover data obtained from Landsat MSS data classification and combining it with topographic data and ecological zone information. The mapping of the productivity classes produced from the model showed an overall accuracy of 86.6% at one site and

73.7% at another. However, these productivity classes are too general to show the real differences between site classes. For instance, site classes I to IV of Douglas-fir were all classified into the first, while class V was in the second productivity class and none were in the third productivity class.

In another study, predictive models of mean increment of timber volume in three study sites of the United States (southern Illinois, eastern Tennessee, and northwestern New York) were developed using TM data and digital biogeographical data on forest productivity and soils, DTM, solar radiation, vegetation type in a GIS (Cook *et al.* 1987; Cook *et al.* 1989). In general, forest productivity was more accurately predicted with a combination of TM and biogeographical variables than with either data type alone. The best regression models in each of the three study sites were statistically significant ( $p < 0.002$ ). However, the correlations were generally low ( $r = 0.30 - 0.64$ ).

Iverson *et al.* (1988) used AVHRR data to estimate site productivity (i.e. mean increment of timber volume) at regional levels in Illinois and Tennessee, USA. A multiple regression technique was used to derive the predictive models by relating AVHRR data to the TM-derived estimates of forest productivity mentioned above (i.e. Cook *et al.* 1987; and Cook *et al.* 1989). The predictive models were employed to estimate the site productivity of each AVHRR pixel for creating regional maps of forest productivity. The results were then compared with the forest productivity estimated by the US Forest Service at county levels. For the 428 counties in the southern Illinois region, the correlation ( $r$ ) between the two productivity estimates was 0.71. For the 168 counties in the eastern Tennessee region, the correlation was 0.52. The data suggested that forest productivity could be predicted with moderate accuracy (about 60 to 70% of total variance) at the continental scale by stratification of sites within ecological regions.

Predictive models were derived to estimate site quality with limited success using Landsat 5 TM data in tropical moist forests of northeast Queensland, Australia (Vanclay and Preston 1990). Site quality, defined as growth index (GI) derived from stand variables (e.g. DBH, diameter increment, basal area, and tree species) was strongly correlated with TM data ( $r = 0.293 - 0.719$ ). The best correlation was obtained from band 5. Geological variables were found helpful for improving the performance of TM data for site quality estimation.

In Finland, satellite data have been used to rate site productivity with some successes (Häme and Saukkola 1982; and Häme 1984). An operative forest productivity class estimation method, called KAUKO, was developed to determine site quality classes using

Landsat MSS imagery (Häme and Saukkola 1982). The site quality classes which represent the timber growth potential of each site were defined based on lesser vegetation according to Cajander's (1909) forest type theory. Tomppo (1992) improved the method, called KAUKO2, and used it to estimate site fertility applying Landsat TM and DTM data. The results obtained were very close to that from inventory sampling and have been used by Finland Government for forest income taxation. The method developed could save 14 to 60% cost and 20-30% of the time compared to conventional methods.

Estimation of vegetation productivity has proven to be globally applicable. Box *et al.* (1989) have shown that the AVHRR-derived NDVI has as strong a relationship with net primary productivity (NPP) as climate-based productivity models do, and the relationship is reliably consistent over most ecosystems ( $r^2 = 0.81$  based on measurements of annual NPP from different biomes,  $n = 94$ ). NDVI is also related to actual evapotranspiration (AET) across a range of biomes ( $r^2 = 0.87$ ) (Box *et al.* 1989). Running *et al.* (1989) also determined that AET and PSN (net photosynthesis) estimates from AVHRR-derived NDVI closely matched ground measurements ( $r^2 = 0.90$ ), even in mountainous terrain. Forest productivity, the productivity (NPP) of coniferous forests in particular, was found most strongly correlated with NDVI; while above ground annual NPP was found to be the best indicator of productivity (Box *et al.* 1989). However, the correlations varied greatly with scales, indicators of productivity and vegetation types. For instance, in the example mentioned above (Box *et al.* 1989), the NPP-NDVI correlations were relatively low at regional levels.

#### **2.4.5.7 Detection of Forest Changes**

##### *2.4.5.7.1 Introduction*

Remote sensing is a useful tool for detecting, determining and evaluating changes in a variety of surface phenomena over time. The information about changes in forests is especially important for updating forest resource maps and forest statistics. Two major types of change appear in forests: natural and man-made. Natural changes are consequences of seasonal variations, growth, mortality and damage (e.g. water stress, insect and disease damage). Man-made changes involve cutting, road construction, silvicultural treatments, and man-made damage (such as burning). Milne (1988) noted that common types of change detectable in remotely sensed data are those associated with the clearing of natural vegetation, increased cultivation, urban expansion, changing surface water levels, post-fire vegetation regeneration, and soil disturbances resulting from mining, landslides and overgrazing. Satellite data are therefore very suitable for

monitoring the kind, quality, distribution, and condition of natural vegetation found on range and forest lands (Milton and Mouat 1989).

A key technique for detecting changes in the forest is the use of two or more satellite images of the same area, preferably acquired from the same sensor at the same phenological period but in different years. The multi-temporal satellite images can be obtained from different sensors, but must be geometrically and atmospherically corrected and merged to make a new multiple band combination data set for change detection use. Many digital analysis techniques have been developed for studying remotely sensed data for change detection purposes. Milne (1988) divided these techniques into five broad groups: (1) visual interpretation; (2) differencing images and ratioed images; (3) classification routines; (4) data transformation (e.g. principal component analysis, albedo differencing images); and (5) regression analysis. Discussion of the principles and methodologies of these techniques can be found in reviews by Milne (1988) and Hobbs (1990). Singh (1989) gave a discussion on these different change detection techniques. Mouat *et al.* (1993) reviewed the applications of combinations of various data sources for forest change analysis. Hallum (1993) proposed a sampling and stratification procedure for "change estimation". Several examples of detection of forest changes with remotely sensed data: deforestation (clear cutting, cutover), forest damage, forest declines, forest stand dynamics; and seasonal variation of stand variables are reviewed below.

#### 2.4.5.7.2 Deforestation

Monitoring changes in forest cover over time is, perhaps, one of the most important applications of satellite data. In Brazil, AVHRR and/or Landsat MSS were used to estimate deforested areas and deforestation rates with moderate success at a regional level (Malingreau and Tucker 1987; Nelson and Holben 1986; Nelson *et al.* 1987; Woodwell *et al.* 1987). By comparing the Landsat MSS and TM derived forest cover maps produced from manual interpretation in a GIS in three regions in western Victoria, Australia (Mildura, Horsham and Portland regions), Frisina *et al.* (1991) identified the area of forests cleared and the amount reforested between 1987 and 1990. They also determined the gross rate of forest clearing on freehold land for the three years.

Comparing the forest cover maps derived from Landsat MSS data of 1977 and 1983, forest cover in Costa Rica was found to be significantly decreased (Sader and Joyce 1988). Furthermore, four of the 11 Costa Rican forest zones have disappeared completely: dry tropical forest, moist montane forest, moist lower montane forest and wet montane forest. They also found that a close relationship existed between road building and



deforestation by overlaying transportation network maps with forest cover maps. In another study using Landsat MSS data from 1973 to 1988 in the Mabira Forest in southeastern Uganda, Westman *et al.* (1989) found a net forest removal of 29% during the 15-year period.

#### 2.4.5.7.3 Forest Damage

Damage is any loss, either biological or economic, due to environmental factors (called "stress" in some literature) capable of inducing injury to a plant (Murtha 1982). Damage caused by insects and/or diseases has been evaluated successfully using remotely-sensed imagery (e.g. Heath 1974; Dottavió and Williams 1983; Nelson 1983; and Häme 1991). Work by Dottavió and Williams (1983) showed that Landsat MSS imagery was capable of indicating where areas of heavy gypsy moth (*Lymantria dispar* L.) defoliation occurred but was only partially capable of resolving areas of moderate defoliation. Since 1983, annual defoliation of hardwood forests by gypsy moth in the mid-Atlantic states has been regularly mapped from high altitude panoramic CIR aerial photos (Ciesla *et al.* 1989). By comparing the capability of SPOT-1 data with high altitude CIR panoramic aerial photos in mapping the defoliation of hardwood in the same regions, Ciesla *et al.* (1989) showed that 86% agreement could be obtained between the two map products, but SPOT data were cheaper and easier to interpret. They concluded that the visual interpretation of SPOT data could provide the general location of defoliated areas and produce reliable statewide or regional maps showing defoliation, but was less reliable for estimating intensity of defoliation on a site specific basis.

Cohen (1991) detected the changes caused by water stress of vegetation using Landsat TM data and obtained a relatively high correlation ( $r = 0.84$  for NDVI). Damage to hardwoods caused by pear thrips (*Taeniothrips inconsequens* Uzel) in 1984 and 1988 was evaluated using Landsat TM data in southern Vermont and northwestern Massachusetts, USA (Vogelmann and Rock 1989). The image analysis by using band ratioing and subtracting techniques showed that in approximately 0.33 million ha of deciduous forest in the study area, 39.4% was classified as medium damage, and 9.7% was high damage. By comparison, the damage in 1988 was higher than in 1984. In their early study using airborne NS-001 TMS data in the spruce-fir forests in the same region, the ratios of 1.65/1.23 and 1.65/0.83  $\mu\text{m}$  reflectance were found to be strongly correlated with ground-based measurements of forest damage, with correlation coefficients ( $r^2$ ) being as high as 0.95 (Vogelmann and Rock 1986). Several investigations have also used satellite data to

map and assess forest damage caused by other insects (e.g. Leckie and Ostaff 1988; Mukai *et al.* 1987; Nelson 1983).

A comprehensive study was conducted in Finland to detect the changes in both coniferous and deciduous forests resulting from thinning, clear cutting, damage and growth using multi-temporal SPOT and TM data (Häme 1991). The results of this work showed that using multi-temporal spectral data and knowledge about changes in forests, changes resulting from thinning (e.g. thinning intensity), clear cutting and growth could be detected, and the degree of forest damage could be estimated and predicted, but changes due to site preparation methods could not be separated. The NIR band was most sensitive to forest damage. The study suggested that satellite-aided detection of change can be used for updating forest map systems, aiding normal treatment planning, updating sampling inventory results and giving information for ecological investigations. An automated system for monitoring forest changes can be created using multi-temporal spectral data combined with knowledge about changes in forests.

Brockhaus *et al.* (1993) successfully estimated forest decline by combining Landsat TM with topographic data in the boreal montane forests in the Black Mountains of North Carolina, USA. Correlation coefficients between the single TM band data and field estimates of defoliation taken from 21 one-ha field plots were low ( $r = 0.10 - 0.54$ ). However, the correlation could be improved to 0.85 by introducing topographic data (elevation, slope, and aspect). The model was shown to be applicable in predicting conditions through the ecosystem. A forest decline class map could be created by applying the model. TM band 4 was the only band significantly related to needle loss.

#### 2.4.5.7.4 Change Dynamics

Using a visual interpretation technique, Sader and Winne (1992) were able to track changes in a forest of the Great Pond, Maine, US, from 1978 to 1987 resulting from natural causes (e.g. spruce budworm damage) and from silvicultural and management activities (e.g. harvesting, regenerating, clearcut, road building, etc.) by using multi-temporal Landsat MSS and TM data. Stand history maps were created and shown to be very useful for inventory stratification and updating forest resource information. Walker *et al.* (1986) successfully used Landsat MSS data to examine the forest structure gradient of semi-arid eucalypt woodlands in southern Queensland, Australia. The data showed that the various successional stages of poplar box woodlands (a simple vegetation type) in the study area could be detected, based on the differences in a structural gradient from 0 to 50 years since clearing.

#### 2.4.5.7.5 Seasonal or Interannual Changes

Studies have shown that seasonal and/or inter-annual changes of vegetation can be detected and predicted using satellite data. For instance, Spanner *et al.* (1990) and Curran *et al.* (1992) indicated that the seasonal and inter-annual changes of LAI could be detected using multi-temporal imagery. They compared the LAI of slash pine plantations in northern Florida, USA estimated from Landsat TM data recorded at different growing seasons, and found that the LAI of slash pine plantations varied greatly through the year.

Choudhury and Tucker (1987) utilised AVHRR data recorded from 1982 to 1984 and scanning Multi-channel Microwave Radiometer data (Nimbus-7 satellite) from 1979 to 1985, to differentiate seasonal and inter-annual vegetation variations on three large deserts, the Kalahari in Africa, and the Great Victoria and Great Sandy Deserts in Australia using NDVI and the 37 GHz<sub>2</sub> brightness temperature. The temporal variation of the difference of the brightness temperature followed the phenology of the regional vegetation. Results of their study indicated that NDVI values calculated for the two Australian deserts were identical in the time series, proving the evaluation technique to be valid for determining the aridity of the deserts.

Running and Nemani (1988) could detect seasonal changes of forest productivity with low to moderate success by relating seasonal patterns of the AVHRR vegetation index (NDVI) to simulated photosynthesis and transpiration of forests in different climates. An ecological simulation model, called the FOREST-BGC model, was developed to estimate seasonal above-ground net primary production (ANPP) and rates of transpiration (TRAN) and photosynthesis (PSN) using weekly AVHRR NDVI data for 1983-1984. The correlations for annual data ( $r^2$ ) ranged from 0.72 to 0.87, but they were lower and more variable for weekly data. They concluded that estimates of vegetation productivity using the global vegetation index (GVI) can be done only as annual integrations until unsubsampling local area coverage NDVI data can be tested against forest PSN, TRAN and ANPP, measured at shorter time intervals.

#### 2.4.5.7.6 Land Quality and Degradation Changes

Robinove *et al.* (1981) showed that the relative annual change in the land quality of arid and semi-arid environments can be assessed by monitoring changes in albedo estimates of the landscape with the Landsat MSS data. Albedo is the ratio of the amount of EMR reflected from a surface to the amount of radiation incident on the surface. The authors concluded from field investigations at the Desert Experimental Range in southwestern Utah, USA that annual changes in albedo, as measured with successive fall-to-fall

Landsat images, are related to land quality changes. In another study in the same region, Frank (1984) showed that the changes in land quality and degradation caused by soil erosion and changes in vegetation productivity are predictable using Landsat MSS data using residual difference and/or ratio difference images. A regression model could explain about 50% of the variance. A comprehensive discussion on the use of remote sensing techniques in land degradation studies in Australia before 1990 can be found in Johnston and Barson (1990).

#### **2.4.5.8 Conclusion**

Satellite data from Landsat MSS, TM, SPOT and AVHRR systems have been used extensively by foresters in understanding the nature and dynamics of forest ecosystems. Most forestry applications have understandably focused on forest cover classification and mapping. The accuracy of forest type mapping has been improved with increased resolution (spatial, spectral, radiometric and temporal) and data processing techniques. There are also some successful examples of practical forestry applications. For example, classifications have been successfully used to generate fuel type data for a decision support system for forest fire prediction and fire growth modelling in Canada (Kourtz 1984) and have assisted forest site type mapping for taxation purposes in Finland (Höme 1984; Tomppo 1992). However, the accuracy of forest type classification and mapping of digital images has not been consistent and it is data dependent. Most of the accuracies reported for forest and site type classification seem disappointingly low (less than 80%). According to Anderson *et al.* (1976), a classification accuracy of 85% should be the minimum acceptable when utilising remotely-sensed data. Based on this standard, the forest type maps created from image classifications cannot be used for direct forest management purposes, especially at the operational planning level, where more detailed information is needed.

Successful forest management begins with the compilation of a detailed management inventory. As in forest type classification and mapping, the successes in forest inventory using satellite data have been at a broad (regional) scale only. The data may be detailed enough for strategic planning, but it is still inadequate for operational planning purposes. Because of the detailed information requirement (see Tables 2.2 and 2.3), current satellite remote sensors seem unable to provide significant information for new forest management inventories. Repeatedly, studies of forest stratification and classification using satellite data have shown that the spectral data can only provide stratum information which is too general for forest inventory requirements.

The results of estimating forest stand structure parameters and site productivity with satellite data are very encouraging in that they show that statistically significant relationships between various forest stand variables and spectral data generally do exist. The results are frustrating, however, because the established relationships are not consistent and vary greatly between species, locations and data recording date (seasons), especially at a per pixel scale. The correlations are generally not high enough to provide accurate estimates of various stand variables. Due to these weaknesses, the relationships are unacceptable to most forest managers. Nonetheless, in some cases, the relationships may be used to accurately estimate the mean or median of a given forest stand (type) over a large region. For more accurate estimates of stand variables at a small local scale, further studies concerning the use of satellite data with finer spectral, radiometric and temporal resolution are needed.

Forest ecosystems are the most complex ecosystems to classify, detect, measure and predict because of their heterogeneity and the many factors affecting their spectral response. The information required on forests is also diverse. Although satellite remote sensing, at least at the present time, can not meet all of these diverse requirements, research has suggested that satellite data will prove extremely useful in extracting spatial information on forest ecosystem attributes with the further development of remote sensing technology. Because satellite sensors record information about ground surface on a pixel basis, they may not be as useful as finer resolution data if information on site specific stand parameters is required.

Satellite imagery offers a promising means for making forest management and planning more efficient. To what extent the imagery can be used for these purposes at the operative level is still not clear. The results obtained so far usually do not meet the detailed information requirements of the forestry community. Consequently, only a few countries, most in Northern Europe and the North America region, have had serious, long-term research projects on the application of satellite remotely sensed data. To approach the operative use of satellite data in forestry, many of the spectral, spatial, temporal, physiological, ecological and phenological relationships among various forest phenomena and spectral data remain to be further explored.

## 2.5 SUMMARY AND CONCLUSION

Forest site quality evaluation has a long history and it has been, and continues to be, seen as “the iron law” in forestry due to its extreme importance in silvicultural management. Many methods and approaches have been developed for forest site quality evaluation and classification purposes. Many measures have been used to express site quality, but no consistently applicable index of quality has been standardised. As stated in the open introduction in Chapter 1, most of the established methods for site information collection involve very time-consuming and very expensive direct field measurements of a large number of temporary or permanent sample plots and trees. To date, foresters have been seeking ways of accurately estimating site quality using modern technologies in site information collection and analysis. These include the application of modern remote sensing, geographic information systems (GIS) and other computer-aided spatial analysis, mapping and modelling techniques.

Satellite data have been used extensively by foresters in understanding the nature and dynamics of forest ecosystems. Innumerable examples exist for using such data to map and quantify forest stand structure variables (see Sections 2.4.5.3 to 2.4.5.6). Patterns of changes in forests over time have been assessed with multi-temporal data. Satellite data have also been used to evaluate forest stress and/or damage due to diseases, insect attack, drought, and pollution (see Section 2.4.5.7). Forest productivity or biomass estimates have been made for several forest ecosystems with a variety of satellite remote sensors (see Section 2.4.5.6). However, very little work has been reported for directly estimating forest site quality and stand variables at local scale (such as an area of 5 x 5 km). No study has been reported in the literature on estimating radiata pine forest growth and site quality with satellite data.

There seems to be no doubt about the capability of satellite data in classifying and determining forest stand variables at large regional scales. However, accuracy of estimation at the sub-regional level, especially the accuracy at the local scale, has been generally low and therefore there is no direct operational use at a local level. This study will focus on addressing the relationships between various stand variables and satellite data on a local scale (see Chapter 5 and 6), and developing methods to estimate forest variables and site quality with satellite data in conjunction with biogeographical data (see Chapter 7).

## Description of Study Site

### 3.1 INTRODUCTION

Selection of a suitable research site is a vital part of any research project to effectively use remotely sensed data and the corresponding ancillary data sources available. Based on the research assumptions and objectives set up in Chapter 1, any site under consideration for this study had to include most of the forest vegetation characteristics stipulated for the research project so that procedures developed could be extrapolated to other areas. In addition, the sites selected had to be in the area where required data sources were available. These data sources may include satellite remotely sensed data with different resolutions, aerial photographs of higher quality taken at the same location and time, and other ground maps or data sources available. Importantly, the sites selected had to be readily accessible for field procedures. The basic objectives of this study were to explore the relationships between stand variables and satellite data, and on that basis to estimate site quality at a local scale, satellite data of high resolution and forest stands with a relatively complete age class structure were required.

Having regard to these considerations, Kowen Forest (also called Kowen District) in the Australian Capital Territory (ACT), Australia, was selected for this study as it has large stands of pine plantations in ages ranging from newly-planted to forty-five years. The forest comprise mainly radiata pine (*Pinus radiata* D. Don) stands (covering about 98% of the total plantation area) with a small area of other pine plantation stands such as *P.*

*ponderosa* Lawson and *P. jeffreyi* Grev. and Balf. The site quality and plantation productivity are diverse, ranging from poor to good sites for *P. radiata* growth. Most of the compartments are easily accessible by road.

In addition, SPOT High Resolution Video (HRV) (XS and PS modes) and Landsat 5 Thematic Mapping (TM) data were available for the area selected. Some other ground information on the area such as historical records of the pine plantations, meteorology, geology, soils, aerial photographs and maps were also available.

The object of this Chapter is to give a broad description of the study area, including geographic location and physiographic characteristics. The satellite remotely sensed data and corresponding ground truthing of the study area are described in Chapter 4.

## 3.2 LOCATION OF THE STUDY AREA

Kowen Forest occupies the northeastern corner of the Australian Capital Territory, about 14 kilometres east of Canberra City (Figure 3.1). It juts into New South Wales (NSW) north of Queanbeyan as a shoe shaped projection covering about 80 square kilometres. The western boundary is defined by the Sutton Road and the southern boundary by the Goulburn-Bombala railway line. The northern boundary follows a ridge line varying between 820 and 900 m above sea level (Figure 3.2). The area of interest for this study is situated at latitude 35° 15' S to 35° 21' S and longitude 149° 12' E to 149° 22' E. This area covers Fairbairn Block in the west, extends to the Mountain Block in the east and follows the ACT—NSW border up to the northern end of Kowen Forest, and down to the Molonglo River in the south.

## 3.3 SITE CHARACTERISTICS

### 3.3.1 Geology

The rocks of the area are diverse and generally old (Öpik 1954; Strusz 1971; Strusz and Henderson 1971). The eastern part of the study area mainly consists of Upper Ordovician sandstone and shales, with some outcrops of Upper Silurian Porphyry; while the western part of the area (Fairbairn) is dominated by Middle Ordovician shale, sandstone and quartzite<sup>1</sup>. Surficial Quaternary sediments can be found on hillsides and some valley floors (Öpik 1954; Dijk 1959; Sleeman and Walker 1979). On ridge crests, where erosion

---

<sup>1</sup> Source: 1:50,000 Geological Map and Explanatory Notes, Canberra City, A.C.T., Bureau of Mineral Resources, Department of National Development, Canberra, Australia.



is dominant and rock outcrops common, lithosols and shallow earths tend to occur irrespective of the nature of the parent rock but are invariably gravelly when underlain by metamorphic rocks.

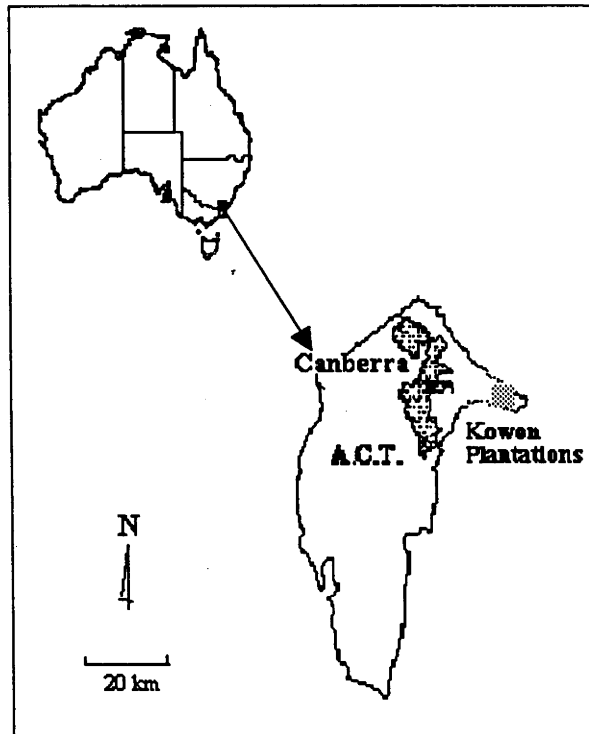


Figure 3.1 Location of the study area

In addition, some other rock types<sup>2</sup> occur in the western part of the study area, including Middle Silurian, Lower Devonian, and Lower Silurian rock types (Strusz and Henderson 1971). The hills are over folded sedimentary rocks (inclined shales and sandstone) of which outcrops frequently occur, and minor volcanics (e.g. quartzite). The undulating “lowland” area is also over sedimentary rocks, but less severely folded.

### 3.3.2 Soils

The 1:2,000,000 soil map<sup>3</sup> shows that the dominant soils in the area are “hard setting loamy soils with mottled yellow clay, neutral to alkaline reaction trends with bleached A2 horizon” (from Atlas of Australian Soils, 1965). The main soil groups found in the area are lithosols (skeletal soils), red and yellow earths and podzols (Sleeman and Walker 1979).

<sup>2</sup> Geological series sheet Canberra SI-16, Bureau of Mineral Resources and Geological Survey of New South Wales, 1964, Second Edition, Dominion Press, Box Hill, Victoria, Australia.

<sup>3</sup> Source: Atlas of Australian Soils (Sheet 3): Sydney-Canberra-Bourke-Armidale Area (NMP/62/053), compiled by K. H. Northcote et al, 1965, CSIRO, Published by Division of National Mapping, Department of National Development, Canberra, ACT, Australia.

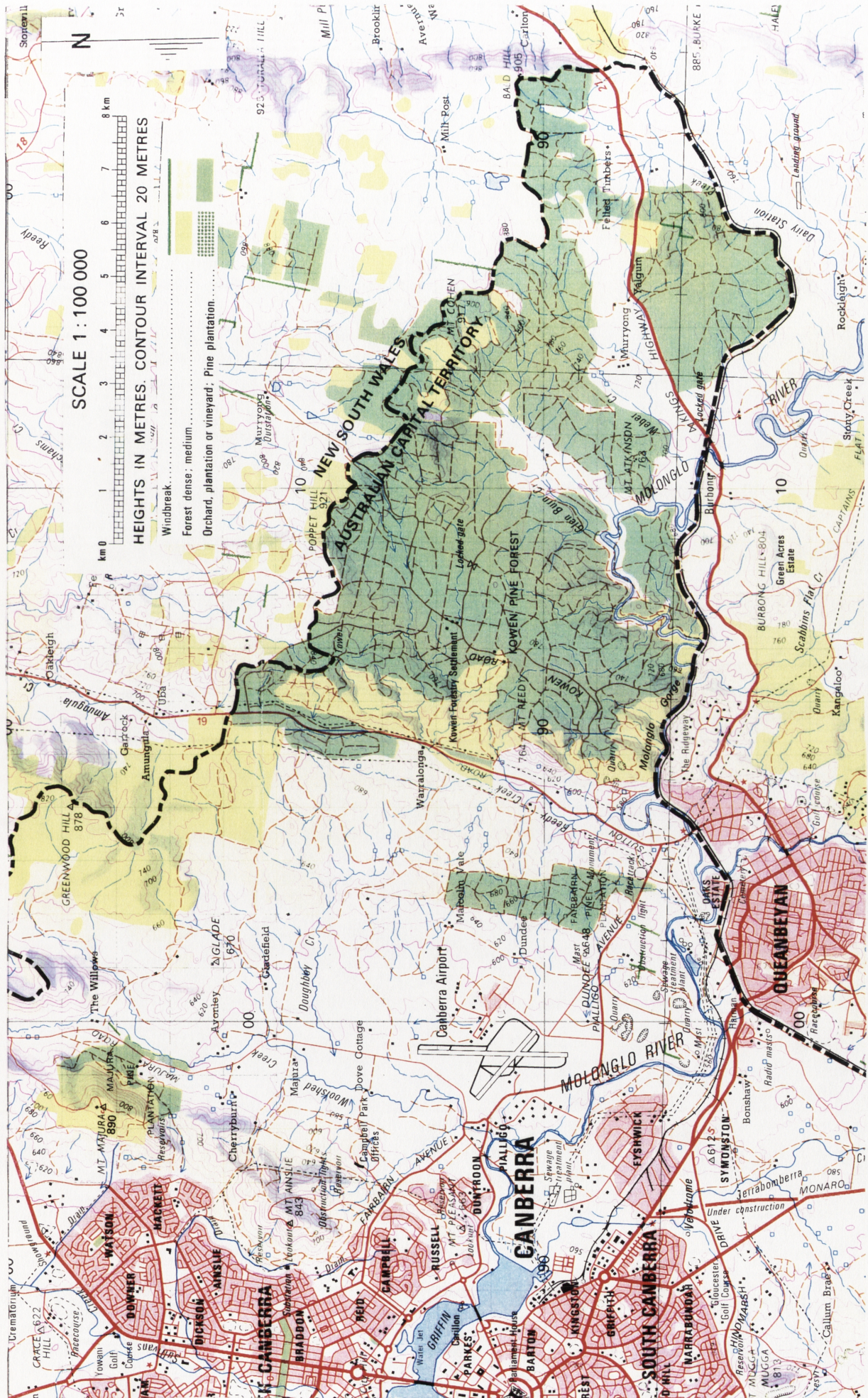


Figure 3.2 Radiata pine plantation stands over the study area (adapted from AUSMAP CSU 89/011, Edition 4, AUSLIG 1989).

Both deep massive-earth, and uniform coarse to medium-textured soils are found in the study area. The latter are characteristically stony and gravelly, shallow, lacking of differentiation and of low natural fertility (Gunn and Story 1969; Byron 1971) and they often occur on the highest ridges and steepest slopes where there are extensive rock outcrops. Generally, shallow sands, loams and clay loams containing a large proportion of coarse textural material in the form of fragmented shales and gravel, interspersed with numerous outcrops of inclined shale and quartzite, predominate in the area, except in the alluvial beds (Sleeman and Walker 1979; and Waring [unknown]). The deep massive earths usually occur in hilly and rolling to undulating terrain and on the terraces of the intermediate level in alluvial landscapes associated with site drainage conditions. Most soils of the area are slightly acid to neutral in reaction throughout (pH value from 5.5 to 6.5) and salt content is low.

In general, the soil conditions in the area are relatively poor. However, the radiata pine can still grow well, since the drainage condition on the slopes is apparently quite good and the rock is well broken so that tree roots penetrate easily to the fragmented shales and to the moister subsoils.

### **3.3.3 Climate**

The main climatic factors of the study area were summarised in Table 3.1. According to the records over 48 years<sup>4</sup>, the mean annual rainfall ranges from 625 mm at Canberra Airport (near the Fairbairn Block, about 1.2 km away from Kowen) to 660 mm at Kowen. Mean annual maximum and minimum temperatures at the Kowen Forest area are 19.4 and 6.3° C respectively. Mean annual evaporation from a class 'A' pan is 1664 mm, and there are 83 days of frost annually. Absolute maximum temperature is 41.9° C, recorded in 1939 and absolute minimum is -7.8° C, recorded in 1935. The mean monthly maximum temperature is in January and minimum temperature in July.

### **3.3.4 Topography**

Much of the ACT would be regarded as geomorphologically mature with mainly gently rolling hills and broad valleys having gentle slopes (Noakes 1954). The topography of the Kowen Area varies from gently undulating low land surfaces (slope < 5°) to rather steep (slope > 40°), hilly country on the north-eastern boundary of the ACT and the southern border. Elevation ranges from 570 m in the southwestern part (Fairbairn) to 930 m in the northeastern part. Lowest elevation is 558 m at the Molonglo River and the highest at the

---

<sup>4</sup> Climatic Average: Australia, Bureau of Meteorology, Australian Government Publishing Centre, April, 1988

Table 3.1 Mean and median monthly and annual rainfall (mm), raindays (no.), humidity(%) and temperature (°C)<sup>1</sup>

Station <sup>2</sup>	Jan.	Feb.	Mar.	Apr.	May	June	July	Aug.	Sept.	Oct.	Nov.	Dec.	Annual
<b>Rainfall (mm) and Raindays (Airport: 1939-1987; Kowen: 1927-1985)</b>													
Canberra	66	57	54	49	48	37	39	48	52	69	61	51	625
Airport	49	57	34	40	41	29	34	47	51	53	55	36	630
Kowen	60	54	55	50	50	45	44	53	54	74	64	57	660
	53	56	41	40	43	36	36	51	50	64	58	45	634
<b>Mean Raindays Number (Airport: 1939-1987; Kowen: 1927-1985)</b>													
Canberra	8	7	7	8	9	9	10	11	10	11	9	8	107
Kowen	6	6	6	5	5	7	6	7	7	8	6	6	75
<b>Temperature (C) (1939 - 1986)</b>													
Canberra	27.7	26.9	24.5	19.7	15.1	12.0	11.0	12.8	15.9	19.2	22.5	26.0	19.4
Airport	12.9	12.9	10.7	6.5	2.9	0.8	-0.3	0.8	2.9	5.9	8.4	11.1	6.3
Mean	20.3	19.9	17.6	13.1	9.0	6.4	5.4	6.8	9.4	12.6	15.5	18.6	12.9
<b>Mean Relative Humidity (%) (1939-1986)</b>													
Canberra	60	67	68	75	82	84	84	79	72	65	60	56	71
Airport	34	39	41	45	55	59	59	53	49	46	40	34	46
Mean	47	53	55	60	69	72	72	66	61	56	50	45	59

1. Source: Bureau of Meteorology, Canberra (1991).

2. Station details: Canberra AMO, 1939-1987, Location: 35° 19' S, 149° 12' E, Elevation: 571.0 m.  
Kowen, 1927 - 1985, Location: 35° 18' S, 149° 17' E, Elevation: 765.0 m.

top of Cohen Hill on the northeastern boundary. Most of the study area is higher than the surrounding district, as implied in its common name "Kowen Plateau"<sup>5</sup>.

### 3.3.5 Vegetation

Most of the area (about 98%) is now covered by *Pinus radiata* plantation stands, most of the remainder being *P. ponderosa* plantation stands. The surrounding indigenous mixed eucalypt forest comprises the following species: *Eucalyptus melliodora*, *E. polyanthemos*, *E. macrorhyncha*, *E. maculosa*, *E. rossi*, *E. dives* and *E. stuartiana*, with an average height of 12 m, rising to a maximum of 21 m. in the gullies, and with an average DBH (diameter at breast height) of 25 cm (Shoobridge 1951). Poor quality, dry sclerophyll eucalypt forest with sparse coverage can still be seen on adjacent unplanted sites. The sparse undergrowth of sclerophyllous shrubs is about 1 - 1.5 m in height.

### 3.3.6 Land Capacity Classes

Based on the conditions of geology, soils and physiographical characteristics of the area and the land classification systems proposed by Gunn *et al.* (1969a and 1969b), Byron (1971) and Enchelmaier (1973) classified the Kowen Forest area into two land systems - Gundaroo and Woolcara Land Systems. The former is usually located in the undulating lowlands on folded sedimentary rocks with well-textured massive earths. The latter land system usually occurs on folded paleozoic sedimentary rocks with minor volcanics, with shallow gravelly uniform, medium-textured soils.

According to the site quality (SQ) class standards for radiata pine growth in ACT (Appendix A) suggested by Lewis (1967), Duffy (1968 and 1969), Galloway (1969), and Lewis *et al.* (1976), the site quality class of Gundaroo Land System was estimated from III to VII (i.e. the site index<sup>6</sup> (SI) estimated from about 24 to 38 m), with a volume mean annual increment (MAI) of about 8-30 m<sup>3</sup>/ha/year. The SQ of Woolcara Land System was approximately from V to VII, and productivity varies from about 11 to 16 m<sup>3</sup>/ha/year of MAI. The land capacity classes and their corresponding productivity criteria were set out by Lewis *et al.* (1976) (See Appendix A).

<sup>5</sup> Kowen Cultural Resource Survey and Management Plan Final Report, Prehistory and Anthropology Department, the Faculties, Australian National University, 1990.

<sup>6</sup> Site index (SI) is taken as the height of 220-30 of the tallest trees in the forest land at 20 years of age, minus 2 meters. This is equivalent to the stand mean height at 20 years of age (Duffy 1969).

## 3.4 SILVICULTURAL CONDITIONS

### 3.4.1 Establishment of Kowen Forest

Kowen Forest is owned by the Commonwealth of Australia, and managed by the Forest Branch of the ACT Administration. It presently appears to be well managed, and it is mainly used for the purpose of timber production.

The establishment of softwood plantations in the ACT commenced in 1915, but the purpose of this early planting was largely to enhance the landscape and to control soil erosion<sup>7</sup>. By 1925 only 650 acres had been planted (Shoobridge 1951). The success of these plantings led to a continuing program of plantation establishment in the same region commencing in 1926 and using a number of exotic coniferous species. The first planting of the Kowen Forest was carried out in 1927 (Carron 1967), primarily as an erosion measure and an attempt to control blackberry. During the 1930s it was apparent that *Pinus radiata* was the most successful of many species tried and was capable of relatively fast growth. Consequently, a major program aimed at wood production from this species was initiated. The stands of interest cover about 3,000 ha, with planting year ranging from 1945 to the present.

### 3.4.2 Site Preparation

Before the 1940s, little site preparation was undertaken because of limited labour. Occasionally the eucalypt woodland or forest was salvage logged for firewood or timber prior to clearing. A broadcast burning of the debris was the only practical form of site preparation in the early years of plantation establishment at Kowen. Site preparation methods such as clearing, ripping and ploughing were first introduced in 1945, and have been widely used in the ACT for many years. Since the 1960s plantation establishment techniques have included deep ripping to 40 cm depth (using Caterpillar D7s and D8s), and fertilising at the time of planting. These practices have resulted in a very high survival rate of 90% in the first year of growth. Since then, ripping-heaping-burning has been the most used site preparation technique.

---

<sup>7</sup> Source: A Resource and Management Survey of the Cotter River Catchment, Resource and Environment Consultant Group, Department of Forestry, Australian National University, Canberra, ACT 1973.

### 3.4.3 Planting and Tending Techniques

Until 1945, almost all planting at Kowen had been in ten-inch (25 cm) deep holes dug with a double-ended mattock. Since 1945, 'slit' and/or 'split' techniques have been more popular, with the seedlings planted in the middle of the rip furrow (Scott 1972). There is very little difference in radiata pine growth with respect to these two planting methods (Clarke 1956).

Since 1941 standard initial spacing has been 2.4 by 2.4 m (8 by 8 ft) to 2.7 by 2.7 m (9 by 9 ft); prior to 1941 it was mainly 12 by 12 ft. The spacing of existing stands is mainly 2.7 by 2.7 m. During the 1950s, thinning was carried out first at 15 years of age and every 3 years thereafter.

The field investigations (see next chapter) found some wind damage and windthrow occurring in areas where soils are shallow (such as at the uphill and/or top of the hills).

## 3.5 PREVIOUS WORK ON STUDIES OF SITE QUALITY AT KOWEN: A BRIEF OVERVIEW

As stated in Chapter 4, extensive studies have been conducted on site quality evaluation for the purposes of timber production, environmental conservation, education and scientific research at Kowen. Initially, six site quality classes (see left side of Table 3.2) set by Gray (1945) were used and subsequently seven site classes (right side of Table 3.2) (Gunn *et al.* 1969; and Lewis 1976) defined by site index and mean annual increment. In Carron's (1955) work, the site evaluation was based on a relationship between mean height at 20 years and site index defined by the conventional graphical method. Based on the "Australian equation" developed by Stoate (1945) (cited in Spurr 1952; and Carron 1967), he also constructed a volume (V) equation from stand top height (STH) and basal area over bark (BAOB) at Kowen, *i.e.*

$$V = -1.9205 - 0.3645 \cdot BAOB + 0.0407 \cdot STH + 0.3342 \cdot BAOB \cdot STH$$

Further studies on the "height-age" relation in the same area were carried out. Carron (1967) constructed a family of anamorphic curves on age of trees from 12 to 37 years in 50 plots in radiata pine plantations, and used them to classify site quality at Kowen. Scott (1972) built a series of a site index curves for five stand top height levels. A site index estimation equation was derived to estimate site quality for Kowen forest by Bary and Borough (1978) and Ferguson (1979). This model was applied in this study to calculate site index from stand top height and stand age (see Chapter 4). In a recent study, West *et*

al. (1988) developed a series of simulation models for predicting the growth of radiata pine plantations in the Australian Capital Territory (ACT).

Table 3.2 Site classes of radiata pine defined by top height (TP) at 20 years of age (Gray 1945), site index<sup>1</sup> (SI) and mean annual increment<sup>2</sup> (MAI) of volume (Gunn *et al.* 1969; and Lewis *et al.* 1976)

Site Quality and Land Capacity Class	by top height at 20 years of age (from Gray 1945)		by SI & MAI (from Gunn <i>et al.</i> 1969; and Lewis <i>et al.</i> 1976)	
	TP class & mean Top height (ft)	Limits of class (ft)	SI (m)	MAI (m <sup>3</sup> /ha/yr)
I	100 (30.48 m)	105.0 - 95.0 (32.00 - 28.96 m)	38	30
II	90 (27.43 m)	94.9 - 85.0 (28.95 - 25.91 m)	36	27
III	80 (24.38 m)	84.9 - 75.0 (25.90 - 22.86 m)	34	24
IV	70 (21.34 m)	74.5 - 65.0 (22.85 - 18.91 m)	32	21
V	60 (18.29 m)	64.9 - 55.0 (19.90 - 16.76 m)	30	17
VI	50 (15.24 m)	54.9 - 45.0 (16.75 - 13.72 m)	27	13
VII			24	8

<sup>1</sup> Predominant height: mean height of 75 tallest trees per hectare at age 30.

<sup>2</sup> Cubic meters to 10 cm top per hectare per year; rotation 50 years

In determining the effects of site factors on the growth of radiata pine in Pierces Creek Forest (about 25 kilometres away from Kowen), Heberle (1968) suggested that at least 27 site variables should be considered in predicting site index of the species in the area. Similar conclusions were reached by Kloeden (1969) at Mt. Stromlo of ACT (about 12 km from Kowen). He concluded that the depths of the soil horizons, slope position, slope steepness and altitude were the most important factors to take into account for rating site quality. Based on a study in Kowen, Byron (1971) suggested that aspect, slope steepness and soil depth should be taken into account in evaluating the site potential of radiata pine at Kowen.



## Data Sources

### 4.1 INTRODUCTION

Site quality is an expression of the average capacity or productivity of a designated land area for growing trees. Measures of site quality attempt to bring together in a single expression the combined, interacting and interdependent effects of all the environmental factors operating at the site. From the viewpoint of remote sensing, site quality can be seen as an expression of the average response of a tree species or stand to specific conditions at a specific site. Consequently, site quality evaluation by remote sensing, in a general sense, becomes the evaluation of the spectral-vegetation-environment interaction. The capture of vegetation and environmental information influencing the spectral responses is a prerequisite for evaluating this interaction.

Traditionally, site quality is evaluated by (see Figure 2.1 in Section 2.3):

1. The measurement of one or more of the individual site factors which are closely associated with tree growth and which will permit practical field or photo (or image) recognition. These include geological, soil and topographical characteristics.
2. The measurement of some characteristics of the trees or other vegetation considered expressive of site quality. These include the quantity of wood (e.g. timber volume) produced per unit of land area, size characteristics of trees and the plant species naturally occurring on the area.

3. A combination of the above two. Site quality is evaluated through establishing the relationships (or models) between site quality measures and site factors. This requires measurement of some characteristics of trees as well as some site factors.

As this study is not concerned with testing the relationships between tree growth and environmental factors, but rather with determining the relationships between remotely sensed data and stand growth parameters, and then indirectly expressing the site quality from spectral responses, the third method above will be considered. The conditions of the study site were described in Chapter 3. Because no recent stand and site data were available for the study area, field sampling and measurements were made to obtain the variables related to site quality. This chapter focuses mainly on the data preparation. Specifically, the major objectives of this Chapter are to:

- Select the site factors and stand variables related to stand growth and site quality respectively;
- describe the field measurement and calculation procedures for the site variables selected;
- describe the methods and procedures for digitisation of site information, i.e. the generation of digital terrain models (DTM);
- describe the satellite data selected; and
- describe how the data were combined.

## **4.2 SITE AND STAND VARIABLES**

### **4.2.1 Selection of Sample Points**

Previous work has shown that great variations in site quality of *Pinus radiata* plantation stands occurred within a small area due to the influence of soil and topographical factors (Heberle 1968; Scott 1972; and Turvey 1987). Therefore the selection of sample plots should reflect these variations of sites and stands. Due to the limitations of labour and costs for detailed measurements of stand and site variables, the point sampling (also called temporal angle-count sampling) method was chosen as the easiest to perform in the field. The accuracy of the method was considered to be adequate for the purposes of the investigation.

In point sampling, the probability of a tree being tallied is proportional to its stem basal area. Large trees tend to be sampled in greater proportion than smaller trees with lesser

The major purpose of this study was to develop models to estimate SQ with satellite and ancillary data. The major measure used to indicate SQ was SI which was derived from height-age relation. The key parameter in the field measurements was stand top height. Purposive sampling method was used to locate sample plots in the stands to be representative of corresponding age classes and site conditions. No attempt was made to choose random samples to accurately estimate other stand parameters. Therefore the representativeness of sample points became very important (Paragraphs 3-5).

volume and height. The sample points are analogous to plot centres, and an angle gauge (Relaskop) is used to subtend a fixed angle of view to “sight in” a tree (Avery 1967; Avery and Burkhart 1983). Point sampling produces very acceptable results compared to other methods if the sample is representative (Phillips and Saucier 1981). Therefore, in selecting the sample points, the following four aspects were considered for the selection and distribution of sampling points:

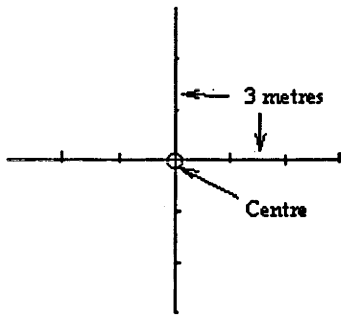
- *Representativeness* A sampling point must be representative of the stand. Before choosing sample points, the stands to be measured were examined. In order to obtain better estimates, at least two sample points were selected in each stand investigated.
- *Comprehensiveness* The distribution of sample points needs to include stands of different ages and/or showing possible differences in stand growth and site potential. For example, sample points were chosen at different positions on the slope, or on different soil types.
- *Non-disturbance* The sample points should be selected in stands in which there has been little or no disturbance because disturbances such as recent thinning, pruning, and/or damages (e.g. winthrow) may affect the intensity of stand spectral reflectance.
- *Locatability and recognisability* The sample points must be easy to access and to locate on the corresponding imagery.

In order to locate the sample points accurately, the satellite data were registered to ground truth maps (i.e. compartment maps by ACT Forests) and displayed on the same scale of the compartments and aerial photos (see Section 4.4 in this chapter). Each sample point was located at least one pixel (about 20 meters) away from stand boundaries in order to avoid the effect of the stand edge. This was done by overlaying the compartment maps on the false colour imagery maps with the same scale, and then marking all sample points on the compartment and air-photos and imagery maps.

#### 4.2.2 Measurements of Stand Variables

The major stand parameters measured at a sample point were stand top height, basal area and stand mean diameter at breast height over bark (DBHOB). As the top height is defined as the mean height of the 40 tallest trees in a hectare, the 4 tallest trees were selected in an area of 0.1 hectare (i.e. sample size).

Canopy coverage was estimated using the canopy density scale from aerial photographs. Understory coverage was estimated using the following method. two lines of 18 metres were established at rightrangles to each other, passing through the sampling point (centre of plot - see the figure below). Along each line, six points were defined at 3-m intervals. A point was recorded as '1' if it fell beneath understory cover, otherwise it was recorded as '0'. The percentage understory coverage was estimated by dividing the 12 selected points by the number of points beneath understory. For example, if 8 points fell selected points by cover, the coverage was estimated by  $8/12 * 100 = 66.67\%$ .



Although attempts were made to measure overstory and understory coverage, these estimates are not considered to be very accurate.

(attached to Page 82, Paragraph 2).

The distribution of the sample points at each age level was presented in the following table (attached to Page 82, Paragraph 5).

The distribution of sample points at different age.

Age	Point Number
9	2
10	2
11	2
12	3
14	2
16	5
20	3
21	3
23	3
24	4
25	4
26	5
27	4
28	11*
29	3
30	3
32	3
34	3
42	3

\* The stands of 28-year old covered a very large area in the study area. They showed differences in growth because of the differences in site conditions (e.g. slope position and soils). 11 points were therefore selected at different site conditions.

The stand basal area ( $\text{m}^2/\text{ha}$ ) was determined by the Bitterlich Angle Count Method. The principle of this method is that an estimated measure of basal area can be obtained by counting, in a sweep (plot), the number of trees whose diameter at breast height is greater than the width of an angular field of view, and multiplying it by a basal area factor (BAF). This factor is dependent on the angle of view. The details of the methods can be found in Hüggarð and Owen (1960) and Bitterlich (1984). In this work, each site was sampled with a Spiegel Relaskop with  $\text{BAF}=4$ . Two to three angle sweeps with the Spiegel Relaskop were performed at each sample site to ensure accuracy of measurements.

All trees in the angular field of view were measured for DBHOB. The four tallest trees within the 0.1-hectare sample point were selected for measuring top height. A Blume-Leiss altimeter was used for measuring the top height. In order to calculate canopy depth (green index), the height from the ground to the first green branch of the trees selected for measuring top height was also measured. The canopy coverage, undergrowth height and coverage (as percentages) were subjectively estimated at each point.

In addition to the measurements of stand variables, two soil profiles were obtained with a soil auger from each sample plot to determine soil parameters. The soil parameters measured are described in Section 4.2.4.1. The method of soil profile measurement was based on Northcote (1979) and Turvey (1987).

Other factors measured at each sample point included slope, elevation, aspect and position on slope. The elevation above sea level in meters at each sample point was measured using a pocket aneroid barometer. The field data sheets for soil and stand measurements are presented in Appendices B and C.

A total of sixty-eight sample points were measured in stands aged from 9 to 42 years in the study area. The methods and procedures of the field measurements are described in the following sections. | The field work was conducted from March to September 1989.

### **4.2.3 The Measures of Site Quality for Radiata Pine**

In Australia, several measures have been proposed to express radiata pine site quality (SQ). These includes site index, site quality classes, and mean annual increment (MAI). Among these measures, site index is the most commonly used measure of site quality in radiata pine plantation management as other measures are affected by stand density (or planting spacing) and used only for references in practice. Site index was therefore used as the measure of site quality in this study. Twenty years was selected as the standard age. In addition, several stand variables and their ratios to stand age, termed *mean annual*

*increment* (MAI), were also tried in data analysis. These measures and corresponding concepts are defined as follows:

(1) *Site Index* (SI)

The equation developed by Ferguson (1979) for the ACT region was used, i.e.

$$SI = H' + \left[ \frac{1 - e^{-\alpha_1 A'(1-\alpha_2)}}{1 - e^{-\alpha_1 A(1-\alpha_2)}} \right]^{\frac{1}{1-\alpha_2}} \quad (4.1)$$

where *SI* - site index in metres

*H'* - measured top height in metres

*A* - standard age (20 for radiata pine in Australia)

*A'* - stand age in years

$\alpha_1$  and  $\alpha_2$  - formula parameters, in Kowen  $\alpha_1 = 0.119$ , and  $\alpha_2 = 0.442$

(2) *Top Height* (TH)

Stand *top height* is defined here as the mean height of the tallest trees in the stand at a rate of 40 per hectare (Lewis *et al.* 1976). In this study, the mean value of the four tallest trees selected within 0.1-ha circular sample points was used as stand top height. The methods of selection and measurements are described in Sections 4.2.1-2 above.

(3) *Height Index* (HI)

The height index is defined as the ratio of measured stand top height and stand age, i.e.

$$HI = \frac{\text{TopHeight}}{\text{Age}} \quad (4.2)$$

where *HI* is equivalent to mean annual increment in height (MAI<sub>h</sub>)

(4) *Volume* (V)

The stand volume (m<sup>3</sup>/ha underbark) of each stand was estimated from basal area (m<sup>2</sup>/ha) and top height using the equation developed by Carron (1968), i.e

$$V = N(-0.03818 + 0.00223T - 0.0001414T^2) + G(0.4145 + 0.3390T) \quad (4.3)$$

where *V* — stand volume under bark (to 10 cm d.u.b.) of trees 13 cm DBHOB and larger

*N* — number of trees in stand (per hectare)

*T* — stand top height in meters

*G* — stand basal area over bark in m<sup>2</sup> (trees 13 cm DBHOB and larger)

In even-aged plantation stands such as the Kowen Forests, there did not exist great differences between dominant and codominant trees. Therefore the canopy depth calculated from top height trees may be close to the mean stand level (attached to Page 84, Paragraph 2).



(5) *Volume Index (VI)*

Like the height index, the volume index was defined as the ratio of stand volume per hectare and corresponding stand age (i.e. mean annual increment in volume (MAI<sub>v</sub>)):

$$VI = \frac{\text{Volume}}{\text{Age}} \quad (4.4)$$

(6) *Canopy Depth (CD)*

In remote sensing of vegetation, canopy depth (or crown size) is an important canopy parameter in determining the canopy reflectance (or absorption). Because it affects the number of leaves and the size of shadows, it is generally highly correlated with spectral reflectance (See Chapter 2) and was selected as one of stand variables in this study.

$$CD = TH - Hb \quad (4.5)$$

where *CD* — canopy depth in metres

*TH* — Total height in metres

*Hb* — the height from ground surface to the first green branch of the trees.

(7) *Canopy Index (CI)*

$$CI = \frac{\text{Canopy Depth}}{\text{Stand Age}} \quad (4.6)$$

(8) *Basal Area Index (BAI)* (i.e. mean annual increment in basal area (MAI<sub>b</sub>))

$$BAI = \frac{\text{Basal Area}}{\text{Stand Age}} \quad (4.7)$$

(9) *Diameter Index (DI)* (i.e. mean annual increment in diameter)

$$DI = \frac{\text{Mean Diameter}}{\text{Stand Age}} \quad (4.8)$$

(10) *Other Stand Parameters*

In addition to the eight parameters listed above, several other stand variables were tested to determine their relationships with satellite data. These stand variables included density (number of trees per hectare), basal area (m/ha), mean stand diameter, stand age in years, canopy percentage coverage, and undergrowth coverage.

#### 4.2.4 Selection and Field Measurements of Site Variables

For a given tree species, site quality is mainly determined by growth responses to physical environmental factors - soil, climate and terrain. The climate factor may be relatively important for site productivity assessment in a large region. In a small area, however, it can be ignored as climate does not vary over a short distance (micro-climate may be different, but it is very difficult to measure). Therefore, the variation of site quality may be mainly due to changes of soil and local terrain (landform). The temperature and moisture conditions may differ from location to location, but these differences arise from the differences in topography and soil. Thus this study mainly concentrates on the effects of soil and terrain conditions on tree growth.

##### 4.2.4.1 Soil Variables

The soil attributes selected are those thought by Turvey (1987) to be important for silvicultural activities. He classified *Pinus radiata* plantations by coding the soil attributes. As this study was concentrated in a small area, the main soil properties considered were depth, structure, moisture, and texture. Other soil factors tested and recorded in the field were pH values, colour, parent rock, and content of gravel (diameter > 5 mm). The definitions of soil factor attributes were based on Northcote (1979), Turvey (1987) and Murtha (1988). A brief summary of the attributes investigated in the field follows.

##### (1) *Soil Depth*

Radiata pine growth has been found to be very strongly correlated with soil depth (Raupach 1967; Jackson and Gifford 1974; Turvey 1983 & 1986; Grey 1989a). Depth here refers to the vertical depth to any layer in the soil which impedes root extension, such as rock, dense soil, an indurated pan, or the influence of permanent or prolonged seasonal waterlogging. This depth is sometimes referred to as the "effective soil depth" for distribution of most plant roots (Jackson and Gifford 1974; and Murtha 1988). This usually includes only the combined thickness of the A and B horizons. Due to difficulty in preparing soil profiles, this field investigation concentrated on measurement of the "effective depth". The field investigation included measurement of sub-horizons (i.e. O - O<sub>1</sub> and O<sub>n</sub>) (above the mineral soil surface), A (A<sub>n</sub> and A<sub>2</sub>) and B (B<sub>1</sub> and B<sub>2</sub>). The definition of these soil horizons can be found from Charman (1978) and McDonald *et al.* (1984a).

## (2) *Texture*

The texture of a soil profile and the changes in texture within it are important determinants of the physical and chemical environment of the root zone (Turvey *et al.* 1986; and Turvey 1987). Field measurement methods used were those of Northcote (1979). An approximate estimate was made of the clay content (%) of each texture grade within the profile (including the uppermost 10 cm of soil).

## (3) *Structure and Pedality*

Soil structure refers to the distinctness, size and shape of peds (Murtha 1988). The grade of structure and the stability of the ped are of major importance for air and water entry to the soil. It was measured in the field for each layer of the soil profile. The definitions were taken from Northcote (1979) and Turvey (1987).

## (4) *Soil Colour*

Soil colour was defined in terms of hue, values and chroma using Fujihara Industry Company colour charts (1966). No special colour names were used, only the value/chroma rating and hue.

## (5) *Gravel or Stone Contents*

The gravel contents of the A and B horizons were measured. It was estimated from a Visual Percentage Estimation Chart (see Northcote 1979).

## (6) *Field pH Value*

Since acid soils are high in exchangeable hydrogen and alkaline soils are high in exchangeable bases, the pH reflects, in a general way, the base status of the soil and gives an indication of the availability of plant nutrients. The pH values of the A and B horizons were measured. Field kits for measuring pH employ a mixture of indicator dyes. The pH values were read from the Van der Burg Universal Indicator with a range of pH from 5 to 9.

## (7) *Others*

Other soil-related attributes recorded in a sample point (or soil profile) included parent rock, the condition of the uppermost 10 cm of soil and the nature of the subsoil as defined by Turvey (1987). In addition, lower boundaries between soil horizons, moisture and organic matter (i.e the distribution of plant roots) were estimated visually from the soil profile.

#### 4.2.4.2 Topographic Variables

The topographic conditions usually influence forest growth by changing the features of soil and climatic conditions. Tree growth is significantly different in different types of terrain. Studies have indicated the growth of radiata pine is significantly related to elevation, slope and aspect variables (Ballard 1971; Woollons and Hayward 1985). Consequently, terrain conditions are important site factors influencing tree growth and can be used to indicate site quality. On the other hand, because of their effects on spectral responses from the ground surface (such as azimuth angle and slope shadows), terrain factors can also be used to improve classification accuracy in remote sensing (Hall-Könyves 1987; Kawata, *et al.* 1988; Thomson and Jones 1990; Conese and Maselli 1991).

Terrain attributes recorded at each sample point were elevation height above sea level, aspect, slope, and topographic position (position on slope). The elevation in meters was read from an altimeter. A compass was used to measure the aspects in degree. The slope in degree was measured with a Blume-Leiss altimeter. The topographic position of each sample point was recorded according to its specific position in relation to the surrounding geomorphological and landform types (e.g. distance from top of hill) that may cause differences in tree growth (see McDonald *et al.* 1984b; and Speight 1984). Five topographic position grades were recorded in the field (see Table 4.1).

Aspect was recorded from 0 to 360 degrees clockwise from N. Four aspect grades were classified based on their possible influences on growth of trees in the study area, with each covering 90 degrees (see Table 4.1).

The grid-based digital topographic data covering the whole study area were generated by digitising and interpolation (see Section 4.4).

Table 4.1 The category division levels of qualitative site variables (aspect and topographic positions) over the study area. The division levels are used for '0-1' coding and quantitative analysis in Chapter 7.

Qualitative Variables	Levels	Descriptions
Aspect	<i>ASP1</i>	0° - 90°
	<i>ASP2</i>	91° - 180°
	<i>ASP3</i>	181° - 270°
	<i>ASP4</i>	271° - 360°
Topographic Positions	<i>TP1</i>	Top of Hill
	<i>TP2</i>	Upper slope
	<i>TP3</i>	Lower slope
	<i>TP4</i>	Level area (No aspect)
	<i>TP5</i>	Gully, Valley or drainage line

### 4.3 SATELLITE DATA

Four satellite data sets of the study area were obtained. Two were acquired from the SPOT satellite system one on September 11, 1986 and the other on January 24, 1987. A broad panchromatic band (PS mode) of 0.51 - 0.73  $\mu\text{m}$  was included in the SPOT scene in 1987 to provide a 10 x 10 meter resolution. Some cloud shadows occurred in the SPOT scene in 1986 and partly obscured the study area. The other two data sets were obtained from Landsat TM with 6 bands and 30 x 30 meters resolution in Bands 1, 2, 3, 4, 5 and 7, 120 x 120 meters in Band 6. The first TM data were recorded on February 8, 1988, and the second on April 21 in the same year. The system parameters of these two satellite systems are shown in Figure 2.2 (Chapter 2).

A sub-image of 800 x 500 pixels over the study area was used for data pre-processing. In order to locate exact features, both SPOT and TM images had to be incorporated with digital ground maps (see Section 4.4). As there is geometric distortion, digital image data were geometrically corrected by establishing mathematical relationships between the addresses of the pixels in the images and the corresponding coordinates of those points on the ground (via a digital map). This was done using the microBRIAN programs mCNTRL, mSIEVE, mMODEL and mMAPPR. A total of 24 ground control points (GCPs) were selected. The model error (mMODEL) was limited to below 0.8. The AFINE model in program mMAPPR was chosen for geometric correction. The principles and resampling procedures are explained by the CSIRO Division of Water Resources (1988).

After image registration, all data outside the radiata pine plantation stands were cut off, producing a subimage of 576 x 375 pixels covering the stands of interest. The 1986 SPOT image was used only for producing colour composite maps for field work but not for further data analysis as parts of the stand were cloud shadowed. The three images were then combined together into a data set of multi-sensor, multi-temporal and multi-resolution and multi-spectral images. The basic statistics of these three images are summarised in Table 4.2, and their frequencies of pixel intensity in each wavelength bands were presented in Figure 4.1. They were respectively named as the January-24 SPOT image (24/1/1987 SPOT data), the February-9 TM image (9/2/1988 TM data), and the April-21 image (21/4/1988). The first two are referred to as the Summer images and the last the Autumn image. Figure 4.2 is a false colour composite map produced with SPOT Panchromatic band and the February-9 TM band 4 and 5. The radiata pine plantations are shown in green colour with compartment boundaries around them.

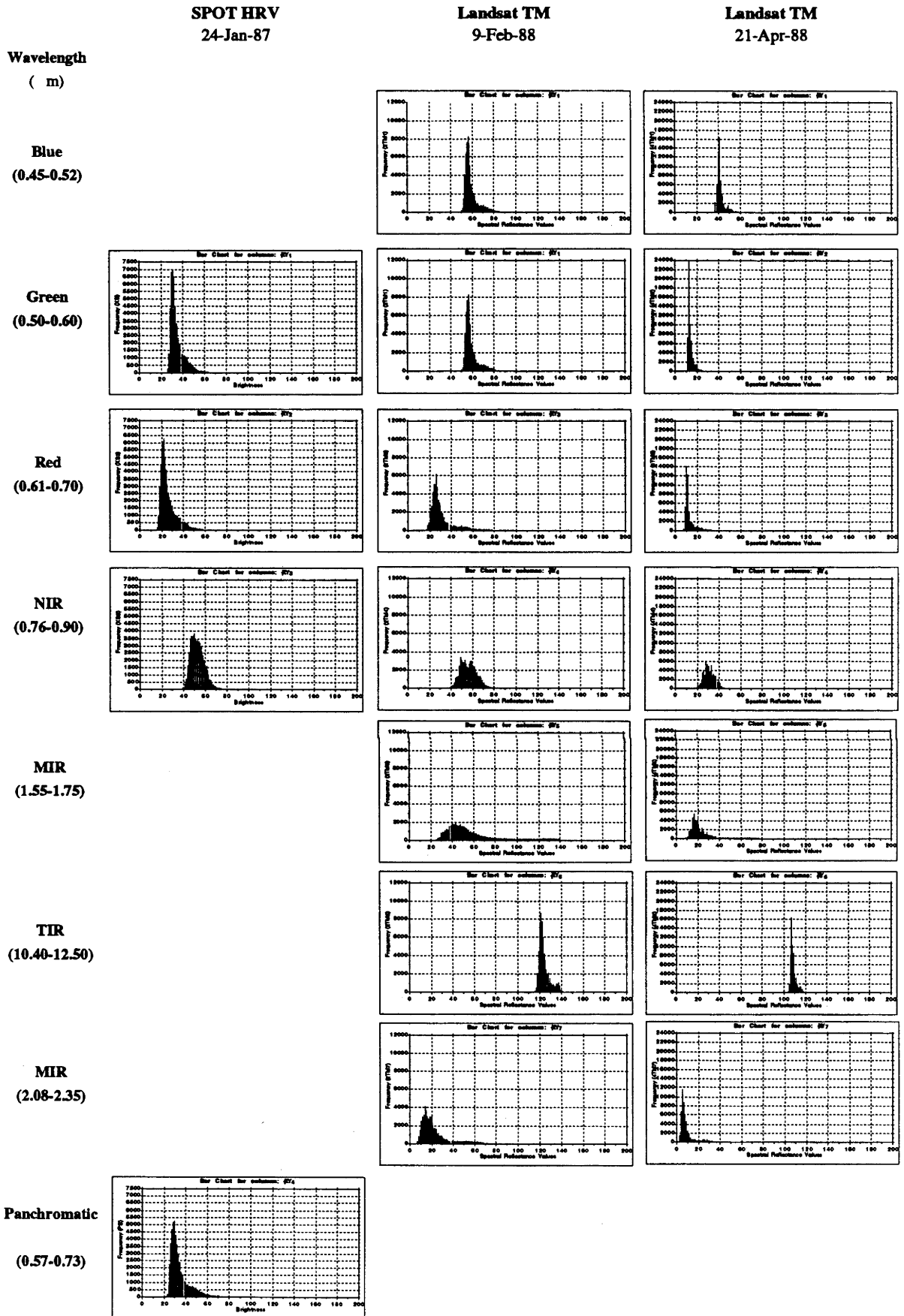


Figure 4.1 The frequency of spectral values over the study area (576 x 375 pixels).



Figure 4.2 Radiata pine plantations in the study area. The map was produced with SPOT panchromatic band and the February-9 TM bands 4 and 5. The pine plantations are dark green in colour surrounded by compartment boundaries.

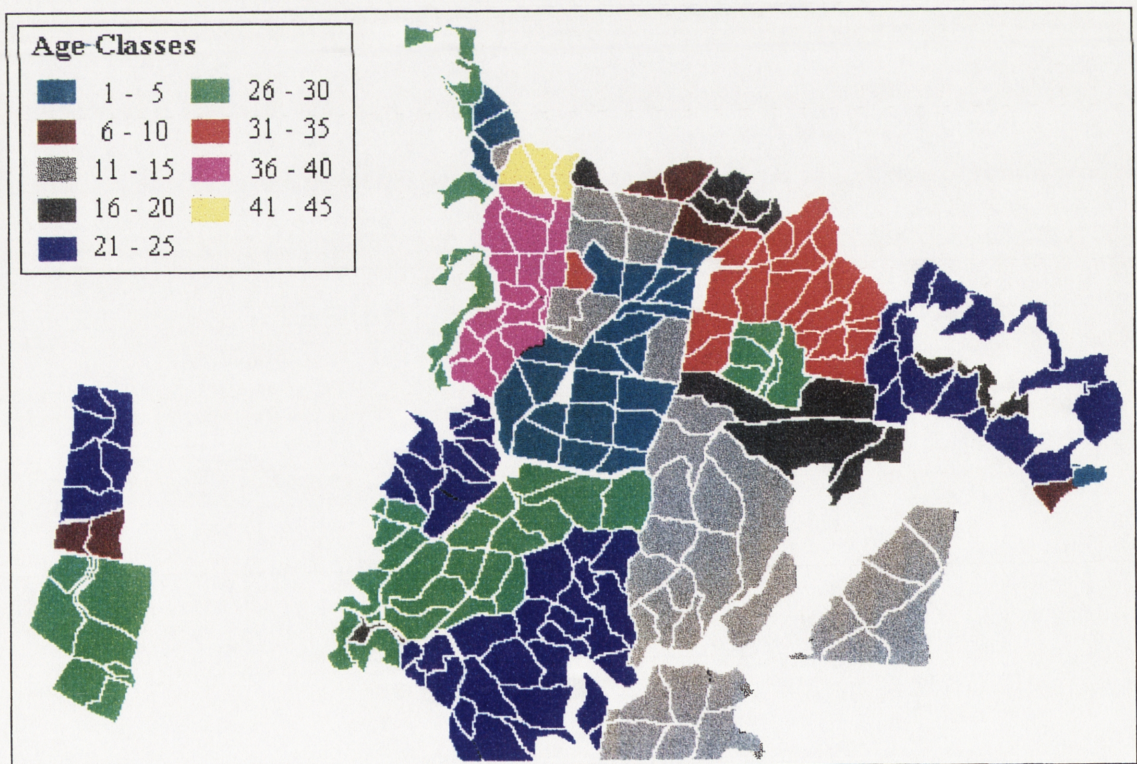


Figure 4.3 The digitised 5-year age class map of the radiata pine plantation stands in the study area. The area and percentage of each age level are summarised in Table 4.4.

Table 4.2 The basic statistics of imagery data over the whole study area. The total pixel number is 216000 (576 x 375). SD - Standard deviation, CV - coefficients of variation (%).

Systems (data sets)	Bands	Wavelength ( $\mu\text{m}$ )	Mean	SD	Min	Max	VC (%)
SPOT HRV (24-Jan-1987)	XS1	0.50 - 0.59	41.72	9.15	1	220	21.93
	XS2	0.61 - 0.69	35.13	11.07	1	220	31.51
	XS3	0.79 - 0.90	57.75	8.35	1	197	14.46
	PS	0.51 - 0.73	45.77	13.44	20	191	29.36
Landsat TM (9-Feb-1988)	2TM1	0.45 - 0.52	69.07	9.95	49	157	14.41
	2TM2	0.52 - 0.60	32.19	7.68	18	90	23.86
	2TM3	0.63 - 0.69	44.46	16.28	15	90	36.62
	2TM4	0.76 - 0.90	59.59	9.29	2	129	15.59
	2TM5	1.55 - 1.75	99.38	46.12	6	210	46.41
	2TM6	2.08 - 2.35	130.43	8.33	115	155	6.39
	2TM7	10.40 - 12.50	42.80	23.48	3	113	54.86
Landsat TM (21-Apr-1988)	4TM1	0.45 - 0.52	48.84	5.57	3.6	115	11.40
	4TM2	0.52 - 0.60	19.11	4.09	11	62	21.40
	4TM3	0.63 - 0.69	19.13	6.20	9	76	32.41
	4TM4	0.76 - 0.90	34.23	6.72	6	75	19.63
	4TM5	1.55 - 1.75	47.14	23.90	6	205	50.70
	4TM6	2.08 - 2.35	113.38	4.45	104	128	3.92
	4TM7	10.40 - 12.50	20.00	11.33	2	131	56.65

## 4.4 GENERATION OF DIGITAL GROUND TRUTH AND DIGITAL TERRAIN MODELS

### 4.4.1 Need for Digitising

Forest data are usually collected by administrative or forest management units with distinct boundaries. Site information (such as soil, climate and terrain) is usually shown in attribute maps (e.g. soil maps, contour and landform maps, etc). Consequently, any remotely sensed data have to be related to these site attributes and forest area units by associating each pixel with the administrative units at the specific geographic locations to which they belong. Site information in a digital form is suitable for input into a computer and can be incorporated into other data sources, such as satellite remotely sensed imagery data, for computerised forest management and planning through a GIS.

As noted earlier in this chapter, age is an important variable for prediction of forest productivity. In order to locate stands of different ages, the compartment maps showing the stand boundaries and stand age after planting at different locations had to be in digital form for incorporation into corresponding imagery data at the same locations.

Topographic parameters such as surface elevation, slope, aspect and topographic position are important site factors influencing both the growth of trees and the spectral reflectance of the ground surface. This site information also had to be in digital form and combined with remotely sensed data. The following section gives a description of the methods and



procedures for generation of a digital stand age map and a digital terrain model for the study area.

#### **4.4.2. Digitisation of Compartment Maps**

Kowen Forest is divided into management blocks and compartments (polygons), each with clear boundaries (roads) around it. The input data used in this study were taken from the Kowen Forest compartment map of 1:25,000 scale (revised in 1987) obtained from the Forestry Division of the ACT Administration, Canberra. The digitised area covered from 49° 12' 30" - 149° 21' 30" E and -35° 15' 20" - -35° 20' S.

The digitising was performed using a PC-based ARC/INFO system (PC Network Version 3.3, Environmental System Research Institute (ESRI), 1989) in the Department of Geography, the Australian National University. The digitising equipment used was the Tektronix 4958 tablet with a 4-button mouse puck attached. Other software used for data conversion and editing included IDRISI and microBRIAN.

A total of 219 polygons (stand compartments) was input. Each polygon was assigned a value (i.e stand age). The input polygons covered stands from 3 to 42 years of age. In order to produce digital grid data that could be incorporated with other data sources, the digitised coverage was converted from ARC/INFO format (rational) into the data format required by setting up a correct grid spacing value. The programs LINEGRID and POLYGRID, as the names imply, were used for grid line (compartment boundaries) and polygon (tree age within a compartment) data interpolation respectively. Based on the maximum and minimum values of the digitising coordinates and the corresponding ground distance (calculated from the base map), the grid spacing values can be calculated for determining grid pixel size. With the grid data used in this study, the grid spacings of 0.035 were specified to produce an approximate 20 x 20 meter grid interval (pixel size) to match SPOT XS data.

The digitised compartment map is displayed in Figure 4.3, with different colours showing 5-year age classes of the radiata pine plantation stands ranging from 3 to 42 years of age. The area and percentage of each single age level and age classes are given in Table 4.3.

#### **4.4.3 Generation of Digital Terrain Data**

Digital terrain data can be produced in several ways, such as by the use of optical-mechanical stereo plotters, automatic electro-optical mappers, extraction from satellite data and/or mathematical interpolation of irregular data. In this study, the mathematical interpolation method was used.

Table 4.3 The digitised stands at different age levels. Pixel size is 20 x 20 meters (0.04 ha).

Stand Age	Pixel Numbers of Each Single Age	Stand Area of Each Single Age ha)	Proportions of Each Single Age	Proportions of Each 5-year Age Class
3	813	32.82	1.34	1 - 5: 10.11%
4	3397	137.12	5.58	
5	1944	78.47	3.19	
6	694	28.01	1.14	6 - 10: 2.42%
9	778	31.40	1.28	
11	52	2.10	0.09	11 - 15: 24.53%
12	4644	187.46	7.63	
13	504	20.34	0.83	
14	9031	364.54	14.84	
15	699	28.22	1.15	
16	3069	123.88	5.04	16 - 20: 7.30%
18	401	16.19	0.66	
19	246	9.93	0.40	
20	730	29.47	1.20	
21	2899	117.02	4.76	21 - 25: 21.68%
23	6838	276.02	11.23	
24	3940	159.04	6.47	
25	969	39.11	1.59	
26	2169	87.55	3.56	16 - 30: 18.60%
27	495	19.98	0.81	
28	2347	94.74	3.86	
29	2694	108.74	4.43	
30	3525	142.29	5.79	
31	947	38.23	1.56	31 - 35: 7.45%
32	2327	93.93	3.82	
33	857	34.59	1.41	
34	230	9.28	0.38	
35	173	6.98	0.28	
36	400	16.15	0.66	36 - 40: 4.75%
37	733	29.59	1.20	
38	938	37.86	1.54	
39	614	24.78	1.01	
40	205	8.27	0.34	
41	362	14.61	0.59	41 - 45: 0.93%
42	257	8.27	0.34	
Total	60921	2457	100%	

#### 4.4.3.1 Hardware and Software Used

The hardware system used for digitising was the VAX/VMS Cluster computer with a Tektronix 4113 workstation and a digitising tablet 4958 (including a 10-button mouse puck) connected in the Computer Service Centre of the Australian National University. In addition, a Hewlett Packard (HP) 7586 flat bed plotter was used for map plotting. The software system used for input of irregular point and line data was MAPDIG<sup>1</sup>. The

<sup>1,2,3,4,5,6</sup> Programs MAPDIG, ANUDEM (original version is SPLIN2H), DIGINV, GRDCON, ANUMAP and INTGRD were written by Dr. M. Hutchinson (Centre for Resource and Environmental Studies

program ANUDEM<sup>2</sup> (version 3) was used for grid data interpolation of irregularly spaced data. Several FORTRAN programs were written to check the input strings and points data. The conversion of coordinates was done with program DIGINV<sup>3</sup>. The program GRDCON<sup>4</sup> was used to produce input contour files for running program ANUMAP<sup>5</sup> which produced plot files for HP plotter. The program INTGRD<sup>6</sup> was used to interpolate and subset the data output from ANUDEM. The slopes and aspects were computed using MAP<sup>7</sup> on VAX/VMS. MicroBRIAN<sup>8</sup> (Version 2.3, MPA 1989), IDRISI<sup>9</sup> (Version 3.0, Eastman 1991) and ORSER<sup>10</sup> were used for geometric correction, editing and combination.

#### 4.4.3.2 Data Sources for Digitising

Two 1:25,000 scale mapsheets were used for input of irregular point and line data. The first was the topographic series map (Bungendore 8727-II-N; Central Mapping Authority of NSW 1980). The other was orthophoto series map (Canberra 8727-III-N). Both maps contained relatively detailed information on local relief, main roads and the distribution of plantations and compartment boundaries, as these were important for defining ground control points (GCPs) for data resampling. The interval of the contour lines is 10 meters. The digitised area covered from 149° 12'30" to 149° 21'30" E and 35° 20'00" to 35° 15'20" S). In order to avoid edge effects, the digitised area was expanded 1' in four directions (i.e 149° 11'00" - 149° 22'00" E/35° 21'00" - 35° 15'00" S).

#### 4.4.3.3 Digitising Procedures

The program ANUDEM accepts five data types, i.e. contour, streamline, point, polygon and sink point data. The first four data types can be produced from digitising equipment, and the sink point data was produced by the program ANUDEM. Contours, streamlines, points and polygons were input separately using a digitising tablet. All contour lines in sparse contour line areas and every second or third contour line in the dense contour line areas were digitised (a total of 12985 points). Streamlines were defined by line segments

---

(CRES), the Australian National University (ANU). The program MAPDIG was revised by Mr. David Moore, Department of Forestry, ANU.

<sup>7</sup>MAP (Map Analysis Package) is a set of computer programs running on VAX/VMS that provide for the input, output and transformation of cartographic data (see Tomlin 1987). It is a GIS system and can be used to process multilayer satellite data and all kind grid-based data sources

<sup>8</sup>microBRIAN is a PC-based image processing systems developed by the CSIRO Division of Water Resources, Canberra, Australia

<sup>9</sup>IDRISI is a grid-based geographic information system for running on IBM PC or compatible developed by the Graduate School of Geography at Clark University, Worcester, Massachusetts, USA.

<sup>10</sup>ORSER (Office for Remote Sensing and Earth Resources) is a image processing systems (GIS) running on VAX/VMS developed by Turner *et al.* (1982)

with the starting point and end point each having an associated elevation label. All streamlines were digitised (a total of 3910 points). The point data (a total of 468 points) were input from the local maxima (e.g. hilltops), local minima (e.g. saddles or sink points) and wherever there were abrupt changes in elevation. Polygons (compartments) were also digitised. The polygon data were used to define ground control points for defining the GCPs for the purposes of geometric correction of the DTM data.

#### 4.4.3.4 Interpolation

Data preparation for input to ANUDEM included data checking, co-ordinate transformation and calculation of grid spacing. The data checking included elimination of error labels, wrong strings and repeatedly digitised points. FORTRAN programs were written to "close" each polygon. As the program ANUDEM uses a meridian coordinate system, the input data from MAPDIG were transformed from a Cartesian coordinate system into a meridian coordinate format by means of the program DIGINV.

The interpolation of irregularly spaced elevation points is a process of assigning an appropriate elevation value to each grid point at a specified grid spacing. As the linear distances of a degree in longitude and latitude are different, that is the linear distance of a degree of longitude decreases as the latitude increases (closer to the poles), the grid spacings need to be calculated from the global coordinate system and corresponding ground distance. The linear distance of a degree of longitude at any place on the earth can be calculated from the following formula:

$$\text{The distance in longitude} = 111.2 \text{ km} / \text{Cos} (| \text{latitude} |) \quad (4.9)$$

where 111.2 km is the distance of a degree of latitude.

In the study area, the latitude and longitude limits of the grid are:

Longitude: 149.18333° - 149.36667°E.

Latitude: -35.25° - -35.35°S.

The central point coordinates of the study area are: 149.275°E / -35.30°S

As the compartment map was used as the base map for data registration, the distance of a degree was calculated from the 1:25,000 scale maps. The mean length of a degree of latitude is 109.853 km. Using the equation (4.9), the distance of a degree of longitude in the digitised area equalled 90.7545 km. Therefore, for 20-metre grid data, the grid spacing values were calculated as follows:

$$\text{Grid spacing in longitude} = 20 \times 1/90.7545 \times 1000 = 0.0002204^\circ$$

$$\text{Grid spacing in latitude} = 20 \times 1/109.8536 \times 1000 = 0.0001821^\circ$$

Unfortunately, the program ANUDEM accepted only one grid spacing value. Therefore, the mean value (i.e.  $0.0002^\circ$ ) of the two grid spacing values was used. A grid point output from ANUDEM therefore represents approximately 18 x 22 meters on the ground. i.e.

$$0.0002^\circ \text{ of longitude} = 18.1625 \text{ m ( i.e. } 0.0002 \times 90.8125 \times 1000)$$

$$0.0002^\circ \text{ of latitude} = 21.9907 \text{ m (i.e. } 0.0002 \times 109.853571 \times 1000)$$

The drainage enforcement algorithm used in ANUDEM imposes a global drainage condition to automatically remove from all spurious sink points which have not been identified in the fitted grid (Hutchinson 1990). The action of the algorithm can be modified in practice through the specification of three elevation tolerances. Therefore, the degree of sink point removal and DTM accuracy depends, to a great extent, on these three specified tolerances. The first tolerance is a measure of the elevation accuracy of the data. Elevation differences between data points not exceeding this value are judged to be insignificant with respect to drainage. Thus data points which block drainage by no more than this tolerance are removed. The second tolerance is a measure of local relief which is set to the contour interval when inputting contour line data. And the third tolerance is simply used as a final checking of drainage clearances which would entail very large changes to the grid (Hutchinson 1990). In this work, these three tolerances were specified as 2.5, 10.0 and 50.0 respectively.

The contour line data were input in two formats, i.e. line format and point format. The sink point data output from ANUDEM was also re-input into the program for removal of the sink points. The final output data were produced from contour line format data, which can significantly increase data accuracy.

#### **4.4.3.5 The Calculation of Slope and Aspects**

A data subset of 800x500 pixels was obtained with the INTGRD program and input to MAP for computing slope and aspects. The slope was calculated in degrees and the aspects were in 8 directions clockwise from N with 45 degrees in each direction. Then the DTM data (elevation, slope, and aspect) were resampled using microBRIAN. A three-dimensional topographical map was produced by overlaying elevation and aspect (Figure 4.4). Figures 4.5, 4.6 and 4.7 respectively display the elevation, slope and aspect using the DTM data of the radiata pine plantation areas.

## 4.5 DATA COMBINATION

As shown above, a pixel of DTM data represents an area of 22 x 18 metres of ground surface area. Therefore, the DTM data were corrected to match the corresponding base map—compartment map. This was performed using the microBRIAN program mMAPPR. A total of 37 GCPs was selected. The relationship model of the two coordinate systems was established via the AFINE model between common GCPs using program mMODEL (The model error was limited to below 1.0). The geometrically-corrected DTM data were then combined with other geobiographical data and satellite data, producing a new multi-layer data base in a GIS.

## 4.6 SPECTRAL DATA OF SAMPLING POINTS

After resampling, all data from different sources were combined into a multi-layer data set. All sample points were located on the multi-channel image. Because of the difficulties in locating a single pixel onto a 0.1-ha sample point, the mean reflectance value of each sample point was calculated from a 3 x 3 pixel window (9 pixels). This is equivalent to an area of 60x60 m in ground size (since all images were resampled and registered to a 20x20 m pixel size). The mean values of the pixel windows could be seen as a reliable estimate of spectral values of the sample points because the status of the forests surrounding the sample point did not have much difference in density and coverage. The spectral values of each sample point were used later for further analysis and modelling in the following chapters.

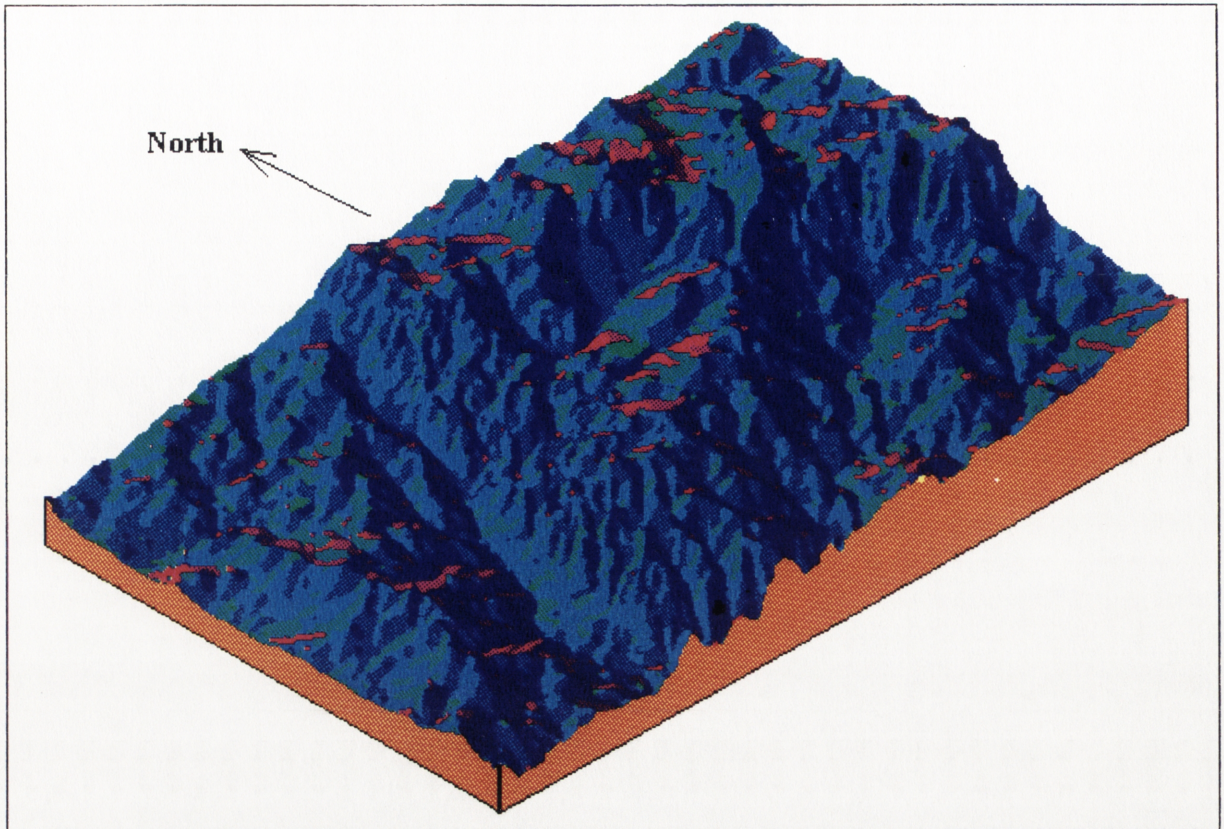


Figure 4.4 The terrain and geomorphological map of the study area. The map was generated from digital terrain model (DTM).

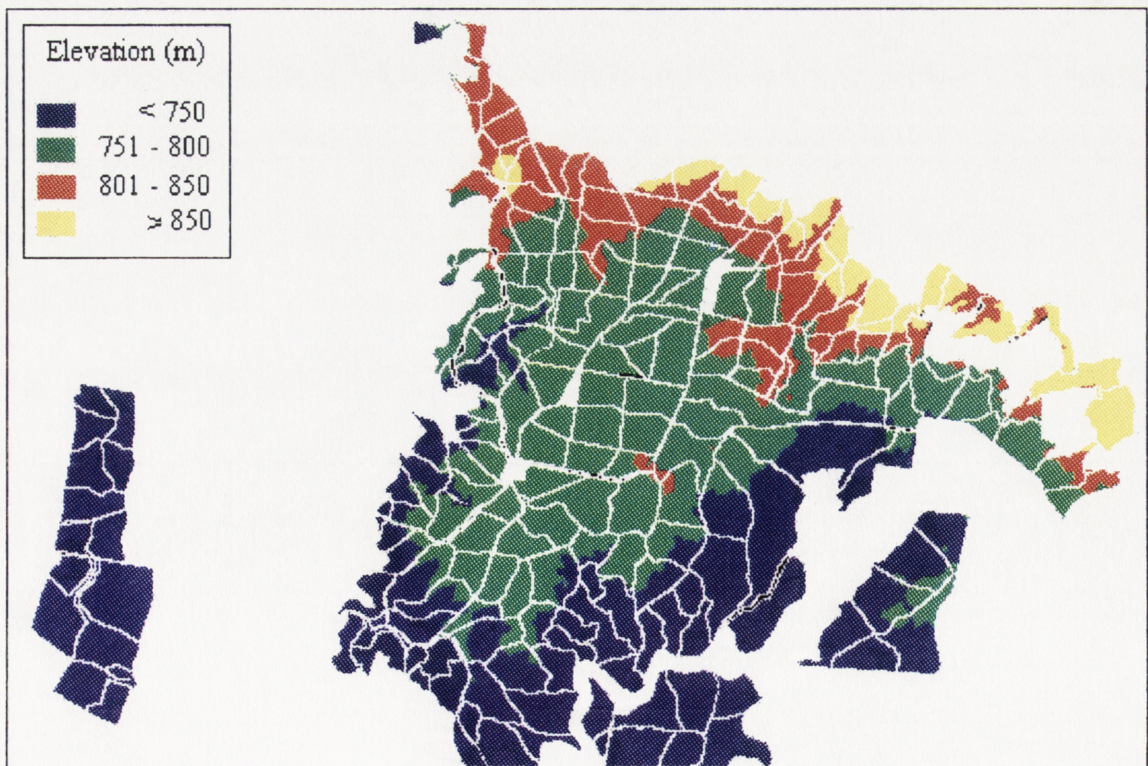


Figure 4.5 The elevation (m) of the radiata pine plantation area.

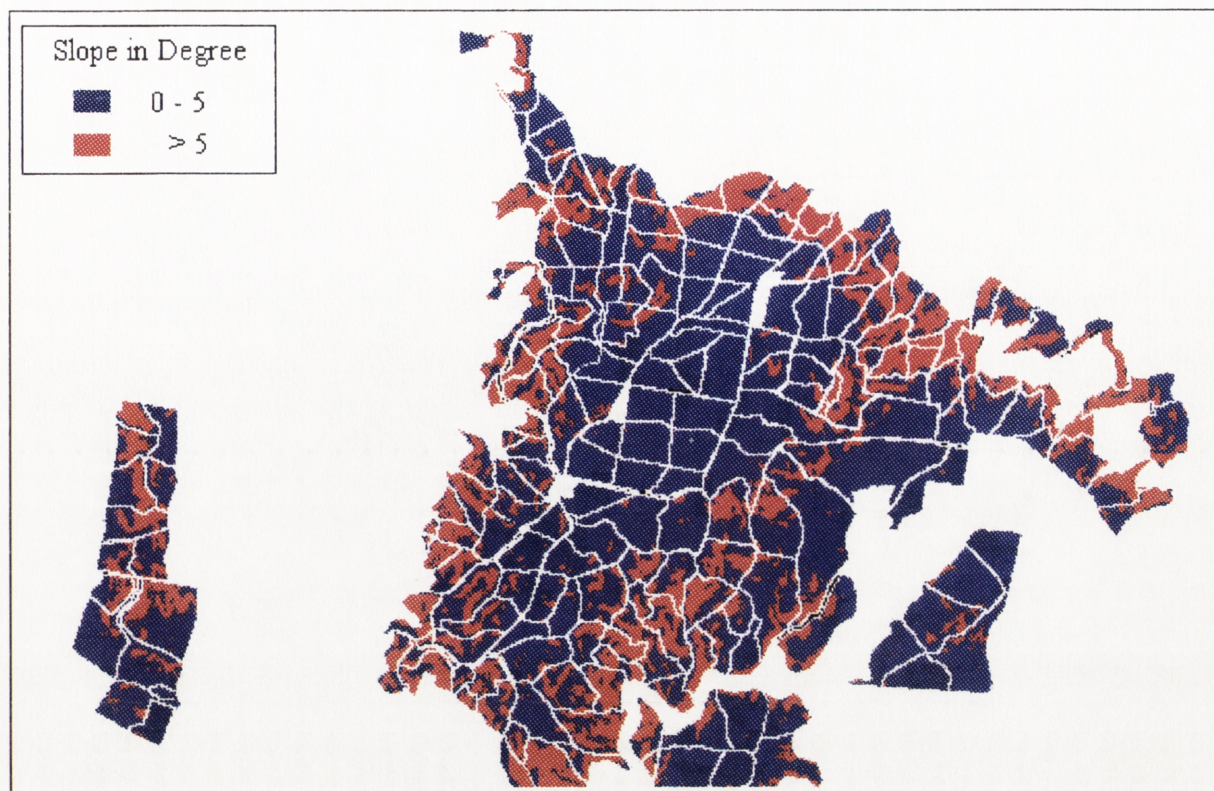


Figure 4.6 Slope ( ° ) of the radiata pine plantation area.—

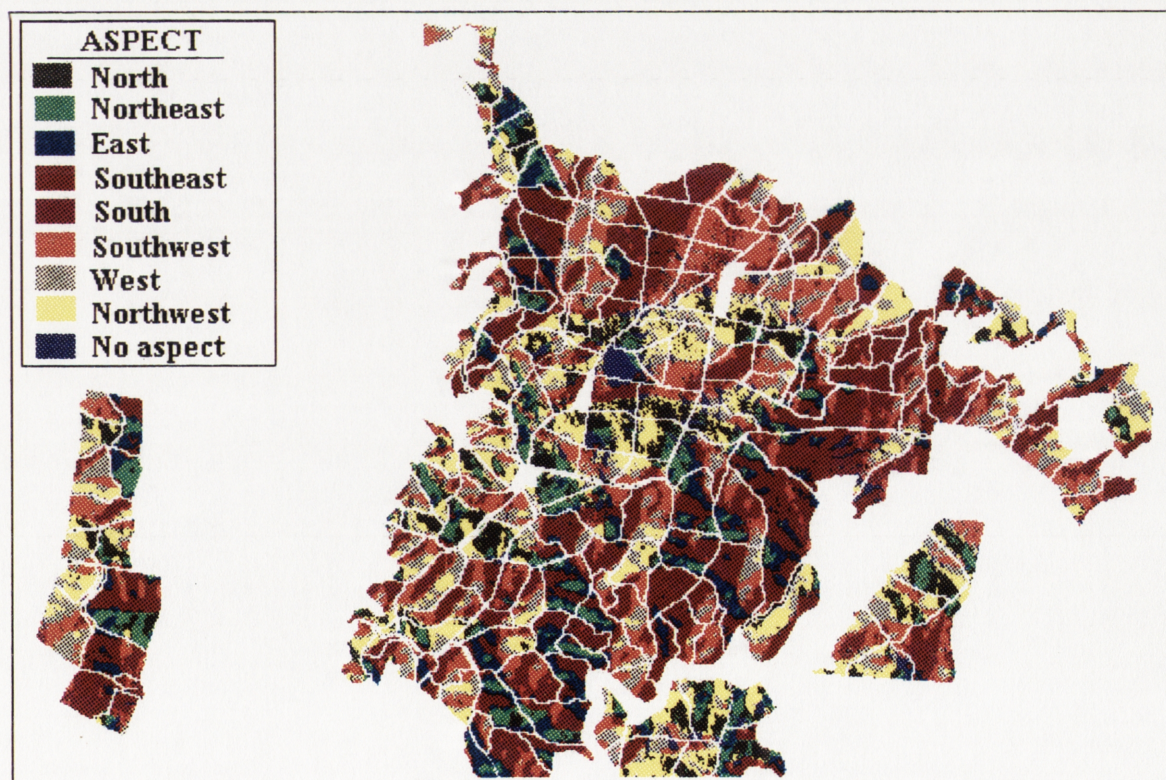


Figure 4.7 Aspect over the radiata pine plantation area. It is displayed in eight directions, each 45° clockwise from north.



# **Relationships Between Spectral Characteristics of SPOT And TM Data And Age of a Coniferous Forest**

## **5.1 INTRODUCTION**

The successful monitoring of forest resources by remote sensing depends on its ability to determine forest tree species (or forest types), growth rate, tree size, and other stand parameters from canopy reflectance measurements. In forestry, the determination of site quality is usually suggested by tree size, yield or volume per unit area, and/or soil type. Due to difficulty with measurement and the effects of stand density, volume is not usually used as the measure of site quality (see Chapter 2). In practice, foresters generally use top height at a designated age as a site index. Therefore, the "height-age" relation becomes the basis of site quality evaluation. For forest site productivity evaluation with remote sensing techniques, three basic attributes of forest stands need differentiation: density, height and/or volume (or yield). Further study is needed to determine whether remotely sensed digital data can give meaningful site quality information, either directly or indirectly by calculation. Because of the effects of canopy shadows, it is relatively difficult to describe site quality from soils using remote sensing techniques. This leads to the question of whether the site quality may be indirectly predictable from a "*reflectance-canopy-age*" relationship.

Previous work by numerous authors has shown that remotely sensed data may be used to detect subtle changes of vegetation. Most of these studies, however, have concentrated on

annual or biennial plants, such as winter wheats, cottons and grasses (e.g. Tucker 1979 and 1980; Liu and Zheng 1990). The details have been discussed by several authors (Colwell 1983; Guyot 1990; King and Meyer-Roux 1990). A great number of studies in forestry have also found that there are significant correlations between spectral reflectance and canopy closure expressed by leaf area index or percent canopy coverage (Kharin 1973; Lodwick 1979a and 1979b; Horler and Barber 1981; Holmes 1981; Butera 1986; Badhwar *et al.* 1986; Scrafini 1986). Some authors have concluded that high resolution remotely sensed data can be used to detect changes in stand structure, with particular emphasis on forest canopy parameters (Butera 1986; Dottavio 1981; Franklin *et al.* 1986; Petersons *et al.* 1986; Danson 1987; Williams *et al.* 1987; Goel and Reynolds 1989; Palter 1990; Walter-Shea and Biehl 1990; Häme 1991).

In studies of the "reflectance-age" relations, Gausman (1974) and Gausman *et al.* (1970; 1971; 1973; and 1976) found significant correlations between the age of cotton leaves and light reflectance, transmittance and absorption. In investigating the sensitivity of satellite remotely sensed imagery data to forest stand age structures, Werte *et al.* (1986) found that multi-date Landsat MSS and TM data could be used to detect up to four forest regeneration ages. Leckie (1984) was able to discriminate high and medium conifer regrowth using cross-polarised C-band synthetic aperture radar data. Knepeck and Ahern (1987) reported that high spatial resolution MEIS-II pushroom scanner data (1 to 5.5 m resolution) were sensitive to juvenile stand conditions (brush, young conifers). These studies, however, were mainly concentrated on age-class classification purposes.

Spectral data have been found to be related to tree age by several authors. The correlations, however, vary greatly with data sources, species and places. With Landsat MSS data, Poso *et al.* (1984) obtained a correlation coefficient between spectral values and stand age for pine ( $r = 0.39$ ), spruce ( $r = 0.36$ ) and broadleaves ( $r = 0.34$ ). They found that the Band 5 (0.6 - 0.7  $\mu\text{m}$ ) data produced the highest correlations with pine and spruce age. Band 7 (NIR) data showed the highest correlation with stand age of broadleaf species. Danson (1987) reported the correlation between SPOT XS data and the age of Corsican pine (*Pinus nigra* var. *maritima*), with only 28 samples and a correlation of -0.42 to -0.67. In a recent investigation, Conese and Maseli (1991) also concluded that multi-temporal TM data can describe vegetation phenological cycles and had better discrimination performances for stand recognition and classification than single date data.

Age is generally considered to be the most important independent variable in growth and yield studies (Buchman 1962) and was the only independent variable in many forest growth

models. Because of its ease of measurement, it is the most commonly used independent variable in predicting site quality and stand yield. As the study area provides a relatively complete age distribution of even-aged plantation stands (see Chapter 3 and 4), it is possible to detect the changes of imagery data with stand ages before studying the relationships between site quality and satellite remotely sensed data. The relationships between the imagery data and other stand variables is examined in later chapters. The major objective of this chapter is to examine the ability of SPOT and Landsat TM data to detect the variation of even-aged plantation stands at different growth stages. More importantly, the studies also determine the information content of each individual spectral band and their combinations and indicate the best bands and optimal age periods for detecting changes of stand structure.

## **5.2. METHODOLOGY**

### **5.2.1 Data Generation**

#### **5.2.1.1 Stand Age**

The characteristics of the study site and the stands were described in Chapters 3 and 4. The study area has a relatively complete age structure, ranging from newly-planted to old stands (i.e. 2-51 years old). This complete stand age gradient provided the possibility of evaluating the changes of spectral reflectance values with stand age.

The locations of pine stands at different ages had been defined on the digitised compartment map by referring to compartment records. The stand age data were assigned to corresponding stands based on the 1:10,000 scale compartment maps and compartment records and by referring to corresponding air-photographs (black/white and colour) at the same scale taken in 1986 and 1987. The stands selected for data analysis ranged from 3 to 42 years of age.

#### **5.2.1.2 Satellite Data**

In order to locate the tree age on the compartment map accurately, all the geometrically-corrected images of SPOT and TM were registered onto the grid-based compartment maps produced by digitising (see Chapters 3 and 4). The compartment boundary map was overlaid onto the images so that the stands could be easily recognised on the screen. The pixels of the radiata pine stands aged from 3 to 42 years were respectively extracted and used for calculating the mean spectral values. This was undertaken using the grid-based GIS IDRISI program (Eastman 1990). Several FORTRAN programs were written to

calculate the statistics of imagery data of the stands aged from 3 to 42 years. The stands ranging from 3 to 42 years of age are summarised in Table 5.1. The distributions of age and age classes are shown in Figure 5.1. The spectral data characteristics of each age or age classes are presented in Appendices D-G.

## 5.2.2 Data Analysis

### 5.2.2.1 Basic Statistics

Calculating basic statistics helps understanding of the characteristics of the data sets used for data analysis. This includes calculating the means, standard deviation (SD), standard error (SE), variance and coefficients of variation (CV) of the raw data of each band. These parameters were computed respectively for all the pixels of the study area covering the stands of interest and the pixels at each age level and/or age class.

### 5.2.2.2 Data Combinations and Transformations

SPOT and Landsat TM data from separate dates were superimposed and made into a “multi-temporal” data set (18 channels; see Chapter 4). The images of difference and mean images were computed from the two separate date TM data, producing a new multi-channel (21 channels) imagery data set. The images of difference and average were computed as follows:

$$D_i = 2TM_i - 4TM_i$$

$$M_i = \frac{2TM_i + 4TM_i}{2}$$

where  $D_i$  — difference of two Landsat TM data in  $i$ th band;

$M_i$  — the mean values of two Landsat TM data in  $i$ th band;

$2TM_i$  — the  $i$ th band of the February-9 TM image; and

$4TM_i$  — the  $i$ th band of the April-21 TM image.

$$i = 1, 2, \dots, 7.$$

In addition to the “between-image” band combinations for the two TM data sets, combinations and transformations among the spectral bands within a single date image were also tried. This included logarithmic, reciprocal and principal component transformations (see below).

Table 5.1 General statistics of the radiata pine stands selected to calculate spectral values aged from 3 to 42 years.

No.	Stands Age	Symbols	Pixels Numbers	Area in hectare	% of the total area	5-year Age Classes	
						Age Classes	Pixel No
1	3	a	813	32.52	1.33	1 - 5	6154
2	4	b	3397	135.88	5.58		
3	5	c	1944	77.76	3.19		
4	6	d	694	27.76	1.14	6 - 10	1472
5	9	e	778	31.12	1.28		
6	11	f	52	2.08	0.09		
7	12	g	4644	185.76	7.62	11 - 15	14930
8	13	h	504	20.16	0.83		
9	14	i	9031	361.24	14.82		
10	15	j	699	27.96	1.15	16 - 20	4446
11	16	k	3069	122.76	5.04		
12	18	l	401	16.04	0.66		
13	19	m	246	9.84	0.40	21 - 25	14646
14	20	n	730	29.2	1.20		
15	21	o	2899	115.96	4.76		
16	23	p	6838	273.52	11.22	26 - 30	11230
17	24	q	3940	157.6	6.47		
18	25	r	969	38.76	1.59		
19	26	s	2169	86.76	3.56	31 - 35	4534
20	27	t	495	19.8	0.81		
21	28	u	2347	93.88	3.85		
22	29	v	2694	107.76	4.42	36 - 40	2890
23	30	w	3525	141	5.79		
24	31	x	947	37.88	1.55		
25	32	y	2327	93.08	3.82	41 - 45	619
26	33	z	857	34.28	1.41		
27	34	!	230	9.2	0.38		
28	35	@	173	6.92	0.28	Total	
29	36	#	400	16	0.66		
30	37	\$	733	29.32	1.20		
31	38	%	938	37.52	1.54		
32	39	&	614	24.56	1.01		
33	40	*	205	8.2	0.34		
34	41	?	362	14.48	0.59		
35	42	<	257	10.28	0.42		
Total			60921	2457			

\* the symbols representing stand ages are used in PC plots in Figure 5.6

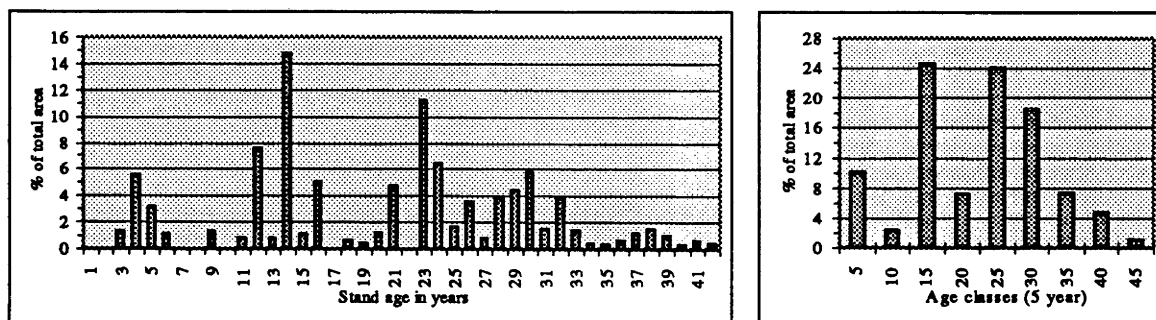


Figure 5.1 Proportions of the radiata pine plantation stands at the different age levels (a) and 5-year age classes (b).

### 5.2.2.3 The Computation of Vegetation Indices

Due to the differences of spectral bands in their responses to vegetation and the effects of terrain on spectral reflectance, the combinations of bands (such as band ratios and differences) are usually computed and used to reduce the topographic effects and to give some indication of the amount of radiation absorbed or reflected by green vegetation. These combinations of bands, usually called vegetation index (VI), have been widely used to predict crop yield or forest biomass (Tucker *et al.* 1980; Tucker 1979 and 1986; Barnett and Thompson 1983; Gardner *et al.* 1985; Prince 1990; Liu and Zheng 1990; Sader *et al.* 1989; and Kanemasu *et al.* 1990). At least fifty such transforms or indices can be found in remote sensing literature, but most are functionally related. A concise review of the use of the transforms and indices for the estimation of some vegetation parameters can be found in Jackson (1983) and Jackson *et al.* (1983). Among these transforms, ratios or indices, normal difference vegetation index (NDVI), agricultural vegetation index (AVI), and relative vegetation index (RVI) are the most commonly used indices in estimating vegetation parameters. These indices are defined from red and near-infrared (NIR) wavebands using the following formulae:

- (1) Normal Difference Vegetation Index (NDVI)

$$NDVI = \frac{NIR - Red}{NIR + Red}$$

- (2) Agricultural Vegetation Index (AVI)

$$AVI = NIR - Red$$

- (3) Relative Vegetation Index (RVI)

$$RVI = \frac{NIR}{Red} \cdot 100$$

These three vegetation indices have been reported to be related to several stand variables including leaf-area-index (LAI) (Tucker 1986; Peterson *et al.* 1987; Spanner *et al.* 1984b and 1990; Running *et al.* 1986; and Clevers 1989), and biomass (Sader 1987; Sader *et al.* 1989). In this study, the above three NIR-related band combinations (ratios and differences) were used in assessing their relationships with stand age. It is assumed that stand ages may have significant effects on these vegetation indices. The inferences that might be drawn from this study are that these three vegetation indices may be related to stand ages and may be used to estimate stand variables and site quality. The work reported in this chapter was to evaluate the relationships between the vegetation indices and stand

ages. The relationships to other forest growth and site parameters are evaluated in the following chapters.

#### **5.2.2.4 Difference Test**

The paired spectral reflectance differences of the three data sets recorded from SPOT and Landsat TM on different dates were analysed using paired t-test and F-test methods. The former method was used to test the differences in mean reflectance, and the latter the variances. The methods and procedures of computation can be found in Eaton (1983), Nelson (1990), and SAS Institute Inc. (1989).

#### **5.2.2.5 Scatter Plots**

The mean spectral reflectance of each band and their combinations were each plotted against stand age to view the general trend of change in the spectral reflectance in each spectral band. In addition to single age levels from 3 to 42 year of age, the 5-year age classes were plotted against the mean spectral values of the stands of the same age classes.

#### **5.2.2.6 Principal Component Analysis**

Principal component analysis, also referred to as principal component transformation, eigenvector transformation, the Hotelling transformation and the Karhunen-Loève (K-L) transformation, is a commonly used multivariate statistical technique that linearly transforms an original set of variables into a substantially smaller set of uncorrelated variables that represents most of the information in the original set of variables (Jolliffe 1986). Its main goal is to reduce the dimensionality of the original data set. A small set of uncorrelated variables is much easier to understand and use in further analysis than a large set of correlated variables. In remote sensing image analysis and pattern-recognition fields, it is used not only for determining the underlying dimensions of multi-channel image data (also called data compression or spectral redundancy reduction by some authors) (Ready and Wintz 1973; Schowengerdt 1983; Anuta *et al.* 1984; Poso *et al.* 1984 and 1987; Peng 1987; and Häme 1991), but also for image enhancement (Donker and Mulders 1977; Gillispie 1980; Canas and Barnett 1985; Walsh *et al.* 1990; and Lee and Hoppel 1992), for digital change detection (Byrne *et al.* 1980; Ingebritsen and Lyon 1985; Horler and Ahern 1986; Fung and LeDrew 1987; Richards 1984; Singh 1989; and Fung 1990), classification and mapping (Conese *et al.* 1988; Loughlin 1991; Franklin 1992), separation of ground cover information (Crist and Cicone 1984), and for characterising seasonal changes in cover types (Lodwick 1979a and 1979b; and Lu 1988). The technique essentially consists of choosing uncorrelated linear combinations of the variables in such a way that each

successively extracted linear combination, called principal component (PC), has a smaller variance. If the variables have significant linear inter-correlations, the first few components will account for a large part of the total variance. The principal components (PCs) are computed by:

$$PCs = a_{1i}x_1 + a_{2i}x_2 + \dots + a_{Ni}x_N = a_i^T X$$

where  $a_j^T = [a_{1j}, a_{2j}, \dots, a_{Nj}]$  is the transpose of the normalised eigenvectors (i.e.  $a_i^T a_j = 1$ ) of the variance-covariance matrix of the original data. Principal components have several characteristics, some of which are of special interest in remote sensing:

- (1) The total variance is preserved in the transformation (Dunteman 1989), i.e.

$$\sum_{i=1}^N S_i^2 = \sum_{i=1}^N \lambda_i$$

where  $S_i^2$  is the variance of  $j$ th original variable, and  $\lambda_i$  are the eigenvalues of variance-covariance or correlation matrix.

- (2) The principal component scores are jointly uncorrelated (Rao 1964; and Kshirsagar 1972). This is the only transformation that produces uncorrelated coefficients (Moik 1980).
- (3) The first principal component has the largest variance of any unit-length linear combination of the observed variables (bands). The last principal component has the smallest variance of any linear combinations of the original variables (Jolliffe 1986; and SAS Institute Inc. 1989).

A detailed mathematical description and discussion of principal component analysis can be found in Rao (1964) and Jolliffe (1986), and statistical treatments can be referred to in Kshirsagar (1972) and Mardia *et al.* (1979).

As there existed strong inter-relations between spectral band data, the principal component analysis technique was employed to reduce the dimensionality of multi-band images. The principal component images produced were then used for the evaluation of relationships with stand age and other stand variables (see the following chapters). This is a relatively important technique to overcome multi-collinearity in multiple regression of multi-channel imagery data. This will be discussed in more detail in Chapter 7. Principal component images can also be used for classifications and detection of changes of the stands but the applications are not discussed here. Six principal component analyses were performed on the three single dates data sets and their combinations, including calculations of the loading, eigenvalues and production of principal component images. In this chapter, the



principal component transformations are performed using variance-covariance matrices, as the images have the similar unit-length of data (i.e. 0-255).

### 5.2.2.7 Correlation Analysis

Correlation analysis includes computing correlation matrices between the wavebands and regression analysis between stand age and the reflectance values in each band. The former was used to test the inter-correlations within the images. The latter was used to evaluate the relationships between spectral values in each waveband spectral region and stand ages. As the change patterns of spectral reflectance with stand age are not simply linear, several non-linear functions were employed to examine the changes of spectral reflectance values of each band and their combinations with stand age, i.e

$$\text{Polynomial} \quad y = a + bx + cx^2 \quad (5.1)$$

$$\text{Log Polynomial} \quad y = a + b \cdot \log(x) + c \cdot [\log(x)]^2 \quad (5.2)$$

$$\text{Power} \quad y = a \cdot x^b \Leftrightarrow \log(y) = a + b \cdot \log(x) \quad (5.3)$$

$$\text{Exponential} \quad y = a \cdot e^{bx} \Leftrightarrow \ln(y) = a + bx \quad (5.4)$$

$$\text{Reciprocal} \quad y = a + b \left(\frac{1}{x}\right) \quad (5.5)$$

$$\text{Logarithm} \quad y = a + b \cdot \log(x) \quad (5.6)$$

In fitting these functions, the <sup>reflectance</sup> values of each band of SPOT and TM image data were used as the dependent variable ( $y$ ) and stand age as the independent variable ( $x$ ). The data were fitted for stand ages ranging from 3 to 42 and 5 to 35 years old respectively. The single date and the combination of multi-date Landsat TM data (i.e. differences and means of the two TM data sets), and logarithmic and reciprocal data transformations were also tried. The relationships between the first two principal components (see Section 5.2.2.6) and stand ages were also evaluated by simple and polynomial regression analysis.

### 5.2.2.8 Cluster Analysis

As the imagery data cover stands from 3 to 42 years of age, it was thought likely that the reflectance values for some age periods might be the same or similar. Clustering was performed to classify the stands into spectral reflectance homogeneous classes (age groups) based on the similarities (or distance) between the spectral reflectance values of the stands at each single stand age. The similarity between the spectral bands was also detected by clustering algorithms. A FORTRAN program was written to calculate distance and similarity (e.g. Euclidean distance, Pearson Product Moment Correlation (PPMC), Cosine Theta (normalised distance), and standardised Euclidean distance). Several

clustering algorithms were also tried, including centroid, farthest and nearest neighbour (single linkage). The classification process was demonstrated in a dendrogram. The theory and methods of cluster analysis can be found from a number of sources (e.g. Everitt 1980; Pielou 1977 & 1984; Gordon 1981; Hartigan 1975; Späth 1980; and Fung and Pan 1982).

## 5.3 RESULTS

### 5.3.1 Data Characteristics

The means, standard deviations (SD), coefficients of variation (CV), minimum and maximum and data ranges of the spectral data over the radiata pine plantation stands are displayed in Tables 5.2 and 5.3. The two summer images showed higher values in variance, standard deviation, and data range than the autumn image. The relative variation for the green, red and NIR bands respectively of the three data sets were similar, with the highest for the red bands and lowest for the NIR bands. For the TM data, the February-9 image (2TM) had higher pixel values than the April-21 image (4TM). Standard deviations, variances and data ranges (maximum - minimum) were also higher in the 2TM data. In particular, the data ranges in this image were nearly twice as large as those for the 4TM data. However, the two TM images showed similar CVs, with the highest in Band 7 (CV > 63.29 % for 2TM7 and 66.79% for 4TM7) and lowest in Band 6 (CV < 4.2%). In comparison, the mean TM images produced higher standard deviations and variance but lower CVs than the difference image (Table 5.3).

Table 5.2 The data characteristics of SPOT and Landsat TM imagery data of the radiata pine plantation stands aged from 3 to 42 years. The total pixels on radiata pine plantation stands were 60869<sup>a</sup>.

Bands	Mean	SD	Variance	CV	Min	Max	Range
XS1	34.41	6.51	42.43	18.93	21	89	68
XS2	25.80	7.50	56.21	29.06	15	91	76
XS3	52.77	6.42	41.24	12.17	16	92	76
PS	34.36	9.22	85.01	26.83	20	191	171
2TM1	59.69	5.99	35.90	10.04	50	96	46
2TM2	25.07	4.71	22.21	18.79	18	60	42
2TM3	29.26	10.24	104.94	35.01	15	107	92
2TM4	55.18	7.60	57.82	13.78	26	105	79
2TM5	57.39	26.76	716.29	46.64	20	203	183
2TM6	123.02	5.11	26.09	4.15	115	144	29
2TM7	21.66	13.71	188.03	63.29	3	99	96
4TM1	42.99	3.22	10.34	7.48	36	66	30
4TM2	15.42	2.53	6.37	16.37	12	34	22
4TM3	13.62	4.03	16.25	29.60	9	44	35
4TM4	32.06	5.10	25.98	15.90	13	55	42
4TM5	26.23	14.12	199.50	53.84	6	99	93
4TM6	109.63	2.43	5.90	2.22	104	123	19
4TM7	10.33	6.90	47.66	66.79	2	48	46

<sup>a</sup> 2TM1 to 2TM7 represent bands 1 to 7 of February-9 TM image, and 4TM1 to 4TM7 represent bands 1 to 7 of the April-21 TM image.

Table 5.3 Summary of the mean ( $M_1$  to  $M_7$ ) and difference ( $D_1$  to  $D_7$ ) images of the two TM data sets over the radiata pine plantation stands ranging from 3 to 42 years of age (see Section 5.2.2.3).

Band Combinations	Mean	SD	Variance	CV	Min	Max	Range
<i>Difference of Two TM imagery Data</i>							
$D_1$	16.62	2.35	5.50	14.12	11.44	23.51	12.07
$D_2$	9.53	1.92	3.68	20.13	5.33	14.82	9.49
$D_3$	15.44	4.90	24.03	31.74	6.88	29.45	22.57
$D_4$	22.09	3.01	9.04	16.61	15.24	27.81	12.57
$D_5$	30.13	10.46	109.48	34.73	6.42	59.78	53.36
$D_6$	12.96	2.24	5.03	17.30	8.50	18.36	9.86
$D_7$	10.96	5.59	31.23	50.98	1.00	28.21	27.21
<i>Mean Reflectance of two TM Imagery Data</i>							
$M_1$	51.39	3.46	11.94	6.72	48.33	62.83	14.50
$M_2$	20.32	2.65	7.04	16.06	17.96	28.77	10.81
$M_3$	21.76	5.15	26.52	23.67	17.20	37.70	20.50
$M_4$	41.83	3.82	14.61	9.14	36.29	49.55	13.26
$M_5$	42.12	15.05	226.51	35.73	26.00	91.57	65.58
$M_6$	116.37	2.91	8.44	2.50	112.55	124.875	12.33
$M_7$	16.35	7.84	61.52	47.99	8.82	43.61	34.79

The two MIR bands of TM data showed higher data ranges, standard deviations and variances than the visible bands (Tables 5.2 and 5.3). This result implies that the MIR bands may be more sensitive to the stands.

The basic statistics of the spectral values of the stands aged from 3 to 42 years for the three data sets are summarised in Appendices D-F. The same statistical parameters of the spectral values at 5-year age classes are given in Appendix G. The coefficients of variation of spectral values in XS1 and XS2 of the SPOT data and Bands 1, 2, 5, 6 and 7 of the TM data were found to be slightly higher in the young stands than in the older stands (> 10-15 years old), but this was not obvious in XS3 of the SPOT data and Bands 3 and 4 of the TM data. The standard deviations in all bands decreased with increased stand ages in younger stands (< 15 years old) and fluctuated after 15 years of age. The spectral values of the 5-year age classes showed a similar trend of changes, with the standard deviations and coefficients of variation being higher for younger stands (i.e. 5, 10 and 15 age classes) (see Appendix G).

### 5.3.2 Comparison of Spectral Data

The results of a two group paired  $t$ -test on mean values and F-test on equal variances of the images are presented in Table 5.4. All individual bands showed highly significant differences in mean spectral values of the corresponding spectral bands between the three data sets on the same area but with different recording dates and systems ( $p < 0.0001$ ). Significant differences also existed in variance. The comparison in red, green and NIR bands of SPOT and TM images indicated that there were significant difference in variances of the SPOT and the April-21 image, with the significance level  $P = 95\%$  or higher (99%).

In the comparison of SPOT and the February-9 TM data, the red bands were significantly different but the green and NIR bands did not show differences in data variances. The results of difference tests between the mean image of the two date TM and SPOT images in the corresponding spectral bands showed no significant differences in variances of the red and the NIR bands, but significant difference in the green band ( $p < 0.01$ ).

### 5.3.3 Change of Spectral Values with Stand Ages

The scatter plots of the original SPOT and TM data against stand age in years are shown in Figure 5.2. The images of differences and means of the TM data for two dates were plotted against stand age as shown in Figure 5.3. In Figure 5.4 shows the mean reflectance values by 5-year age classes plotted against corresponding age classes. It can be seen that, except for the NIR band, the spectral values followed an approximate reverse J-shaped data distribution. The spectral values were highest in the youngest stands (age 1-4), and sharply decreased from age 3 to 5 years, then gently decreased from age about 5 to age 20. Between age 20 and 35, the spectral values were constant after which they increased slightly. The difference and mean images of the TM data for the two dates displayed the same patterns of change with stand age (Figure 5.3). Smoother changes occurred in the plots showing relationships between the 5-year age classes and corresponding reflectance values (Figure 5.4).

Table 5.4 Difference significance test on mean reflectance ( $t$ -test) and equal variances test ( $F$ -test) of the three data sets recorded by SPOT and Landsat TM on three dates.  $n = 36$

Band Comparison	Paired T-test			Variance Homogeneous Test	
	Mean Difference	Paired t value	Prob. (2 Tail)	Paired F Values	Prob.
The comparisons between the February-9 and the April-21 TM images					
1 - 1	16.58	43.06	0.0001	3.50	0.01
2 - 2	9.54	29.60	0.0001	3.97	0.01
3 - 3	15.23	18.74	0.0001	6.57	0.01
4 - 4	21.50	66.06	0.0001	2.33	0.01
5 - 5	29.28	19.98	0.0001	3.22	0.01
6 - 6	13.10	35.35	0.0001	3.91	0.01
7 - 7	10.67	12.47	0.0001	3.70	0.01
The comparisons of green, red and NIR bands of SPOT and the February-9 TM data					
Green	8.35	40.74	0.0001	1.20	+
Red	4.39	7.59	0.0001	1.66	0.05
NIR	2.31	9.58	0.0001	0.62	+
The comparisons of green, red and NIR bands of SPOT and the April-21 TM data					
Green	17.89	48.01	0.0001	4.75	0.01
Red	10.84	27.95	0.0001	2.40	0.01
NIR	19.19	63.92	0.0001	1.44	0.05
The comparisons of green, red and NIR bands of SPOT and mean TM data					
Green	13.12	51.67	0.0001	2.21	0.01
Red	3.22	11.58	0.0001	0.80	+
NIR	8.44	38.62	0.0001	0.94	+

+ the difference was not significant in variance, i.e.  $P > 0.1$ .

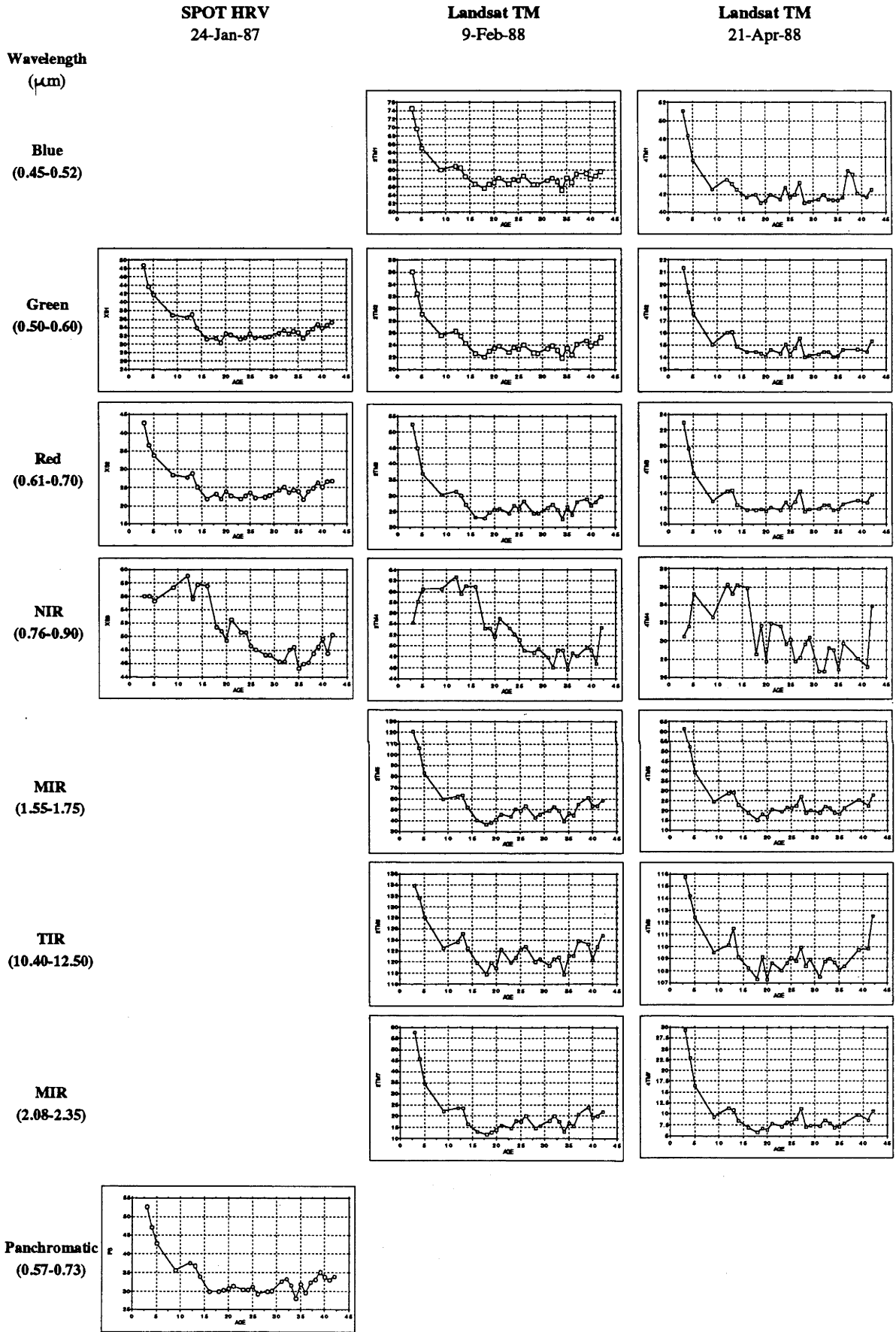


Figure 5.2 Relationships between spectral band data and stand age.

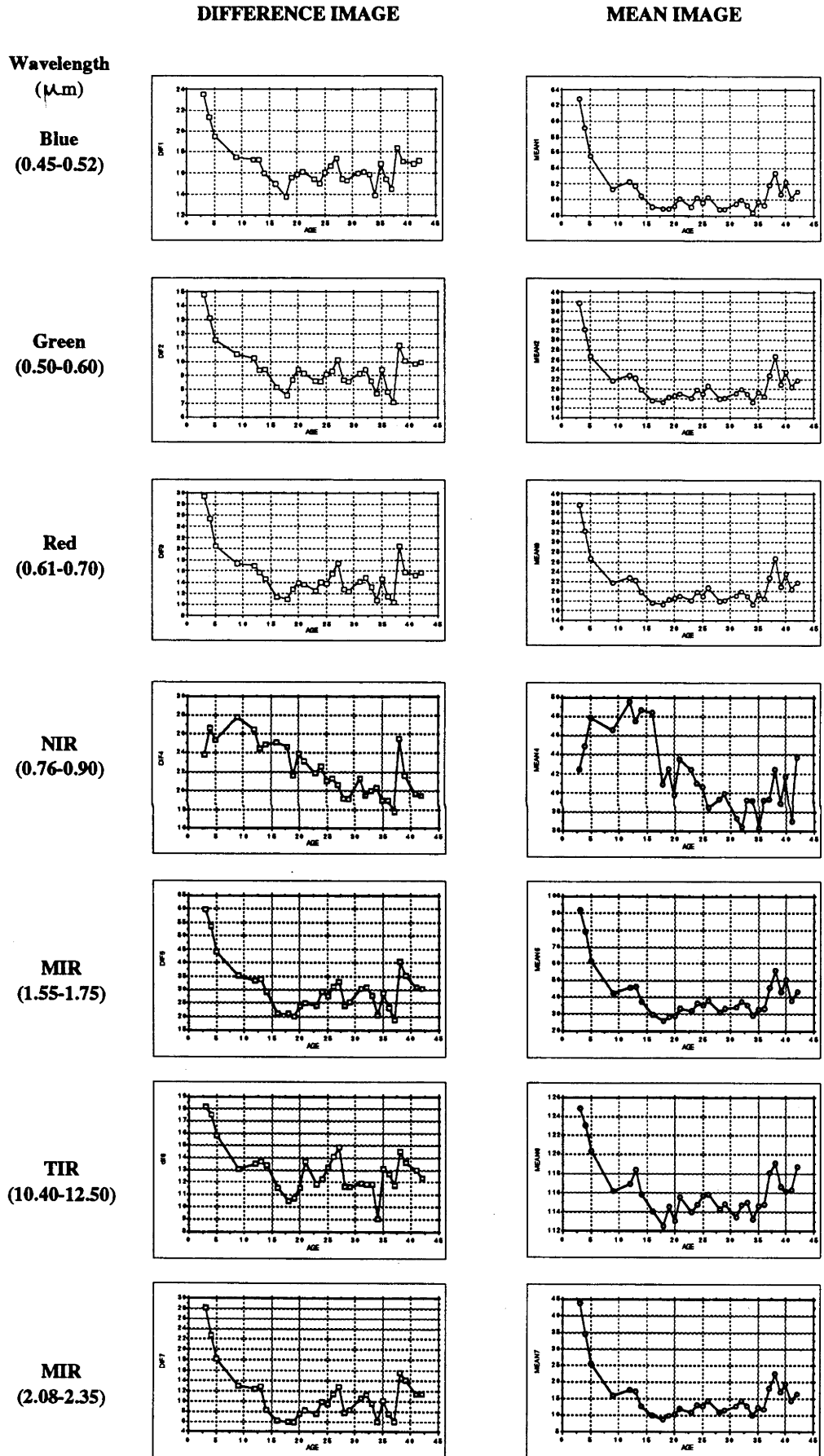


Figure 5.3 Relationships between the difference and mean spectral values of the two TM data sets for two dates and stand age.

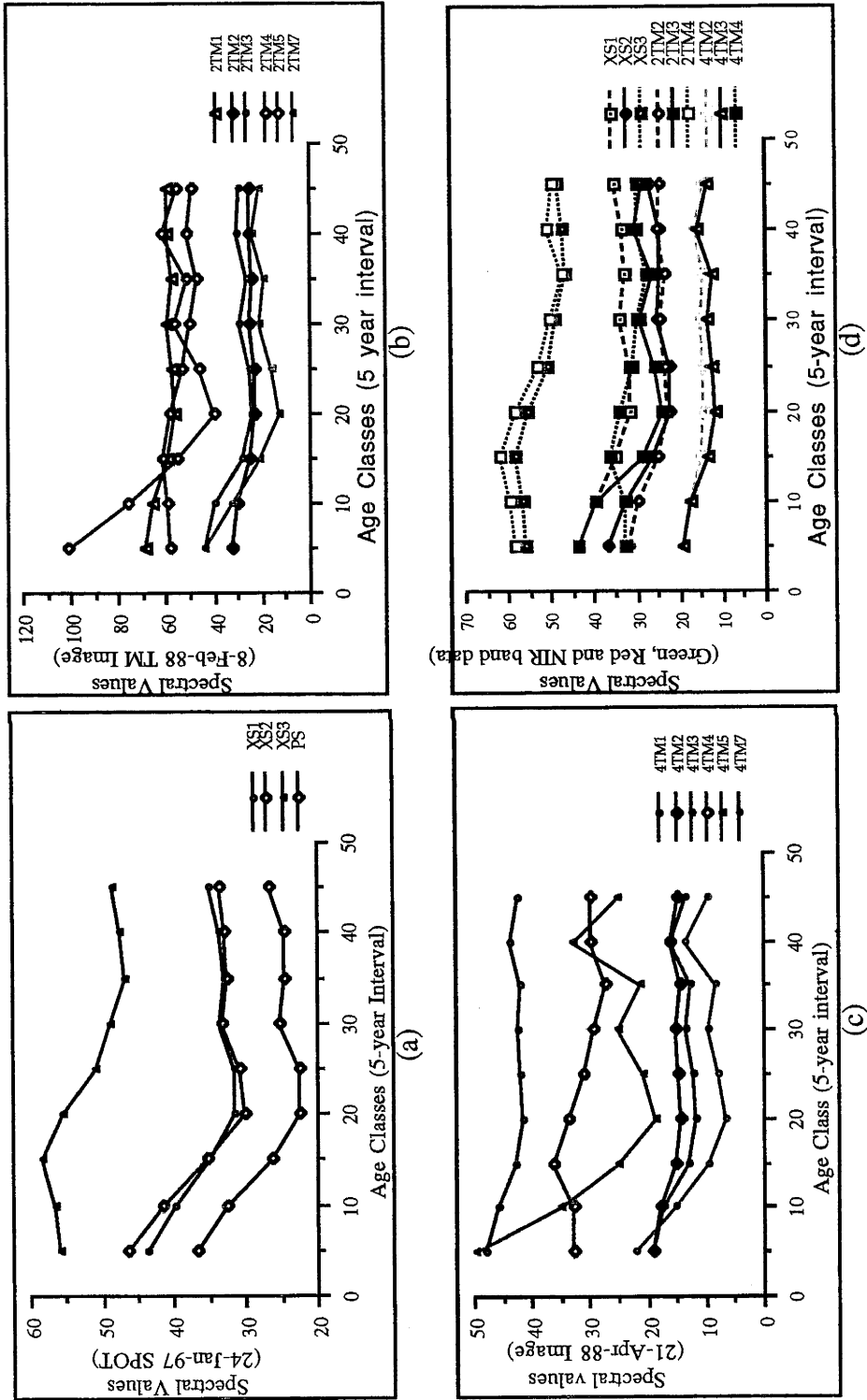


Figure 5.4 Relationships between 5-year age classes and mean spectral values of the January-24 SPOT data (a); the February-9 TM data (b) and the April-21 TM data (c). (d) is the comparison of the three similar bands, the green, red and NIR, of the three data sets,

The NIR band showed a different pattern of changes as stand age increased. The reflectance values increased from age 2 to about 12, and then showed an approximately linear decrease from age 12 to about 32 and stayed constant or slightly increased after about age 33.

The changes of three defined vegetation indices (AVI, NDVI, RVI) with increasing stand ages are indicated in Figure 5.5. The vegetation indices significantly increased from age 3 to 5, then gently increased from age 5 to about 20. The peaks of the VI-age curves were located at about age 15. All vegetation indices gently decreased with increasing stand ages after about 15 years of age.

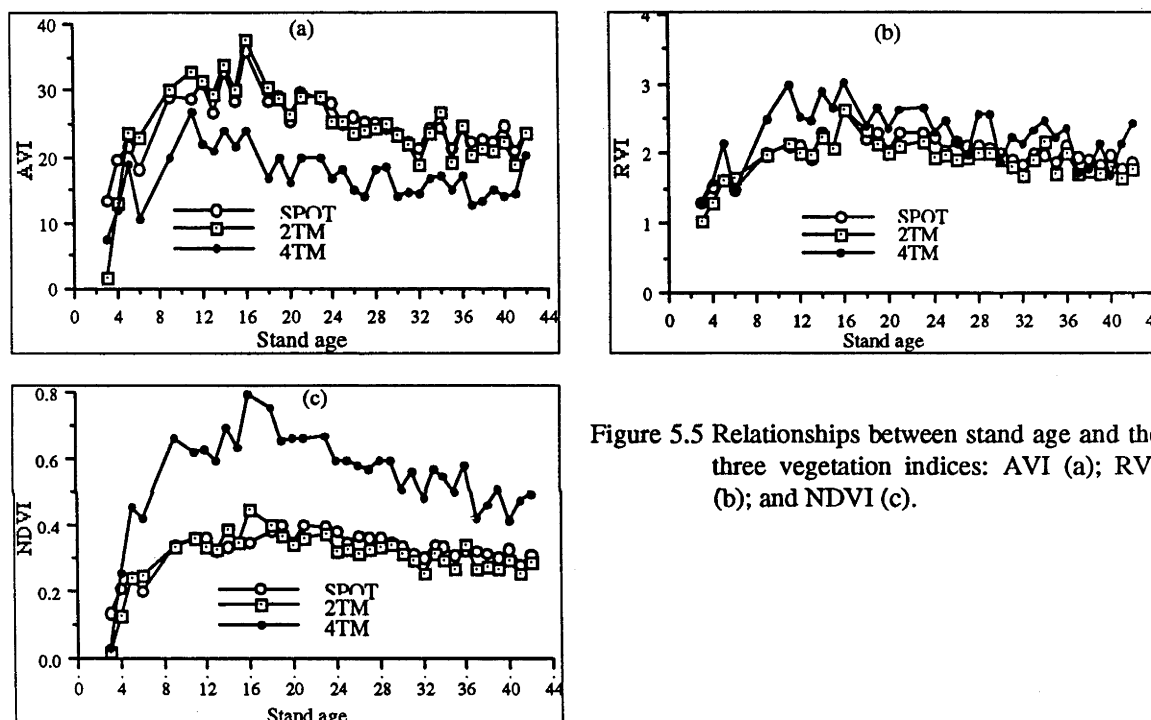


Figure 5.5 Relationships between stand age and the three vegetation indices: AVI (a); RVI (b); and NDVI (c).

### 5.3.4 Principal Component Analysis

Six principal component analyses (PCA) were carried out using the spectral values over the radiata pine plantation stands. The data sets used for each PCA included the three single date SPOT and TM data, the difference and mean images of the two TM data, and all three data sets together. The results of the principal component analysis are presented in Tables 5.5 to 5.10. All principal components (PCs) were computed and then correlated with stand ages.

In the SPOT data, PC1 explained 81.56 % and PC1+PC2 together explained 99.88 % of the total variance in the spectral values of the three XS mode bands. XS2 produced the highest loading in PC1 (0.692), while XS3 showed the highest loading in PC2 (0.909), about three times larger than those for XS1 (0.252) and XS2 (0.333) (Table 5.5).



Table 5.5 Results of PCA for SPOT XS data.

Bands	PC1	PC2	PC3
XS1	0.589	-0.252	0.768
XS2	<b>0.692</b>	-0.333	-0.641
XS3	0.417	<b>0.909</b>	-0.022
Eigen Values	46.00	10.34	0.07
Variance Explained (%)	81.56	18.33	0.12
Cumulative (%)	81.56	99.88	100.00
Correlation with Age	-0.69**	-0.49**	0.04

\*\* significant at 99.9% confidence level. Total variance = 56.40

The PCA results for the two TM data sets are given in Tables 5.6 and 5.7. PC1 of the February-9 image explained 93.82% of the total variance, and PC1 and PC2 together explained 97.73% (Table 5.6). The PC1 of the April-21 image contained 93.42% of the total variance, and the first two PCs together as high as 99.06% (Table 5.7). The PCs from the mean image were very close to those of the original TM data, with PC1 explaining 94.17% of the total variance and PC2 explaining 4.41% (PC1+PC2 = 98.58%) (Table 5.9). Since PC3 to PC7 showed very little information content (< 2%), further data analysis was concentrated on the first two PCs.

Table 5.6 Results of PCA for the February-9 TM data.

Bands	PC1	PC2	PC3	PC4	PC5	PC6	PC7
2TM1	0.1819	-0.0137	0.1077	0.3258	0.0231	0.8080	-0.4423
2TM2	0.1398	0.0132	0.0805	0.3444	-0.0588	0.2988	0.8732
2TM3	0.2973	-0.0524	0.1919	0.7572	-0.0806	-0.5037	-0.1962
2TM4	0.0818	<b>0.9731</b>	0.2022	-0.0434	-0.0497	-0.0235	-0.0246
2TM5	<b>0.8003</b>	-0.1654	0.3466	-0.4437	-0.1165	-0.0351	0.0216
2TM6	0.1571	0.0365	0.0081	0.0238	0.9843	-0.0480	0.0469
2TM7	<b>0.4326</b>	0.1460	-0.8854	0.0517	-0.0680	-0.0032	-0.0136
Eigen Values	553.17	23.00	8.84	3.33	1.06	0.17	0.02
Variance Explained (%)	93.82	3.90	1.50	0.57	0.18	0.03	0.00
Cumulative (%)	93.82	97.73	99.22	99.79	99.97	100.00	100.00
Correlation with Age	-0.50**	-0.64**	-0.07	-0.14	0.18	-0.31	-0.09

\*\* significant at 99.9% confidence level. Total variance = 589.58

Table 5.7 Results of PCA for the April-21 TM data.

Bands	PC1	PC2	PC3	PC4	PC5	PC6	PC7
4TM1	0.1833	-0.0334	0.5132	0.1363	0.4285	0.5883	-0.3920
4TM2	0.1414	-0.0018	0.3382	0.2079	0.0233	0.1868	0.8871
4TM3	0.2307	-0.0720	0.4650	0.3960	-0.6733	-0.2417	-0.2384
4TM4	0.0679	<b>0.9850</b>	0.1216	-0.0530	0.0096	-0.0831	-0.0256
4TM5	<b>0.8344</b>	-0.0204	-0.2821	-0.3591	-0.2057	0.2286	0.0159
4TM6	0.1455	0.1109	-0.5412	0.7998	0.0932	0.1539	-0.0390
4TM7	<b>0.4137</b>	-0.1041	0.1371	0.0994	0.5581	-0.6912	-0.0109
Eigen Values	167.70	10.12	1.06	0.037	0.009	0.006	0.003
Variance Explained (%)	93.42	5.64	0.59	0.18	0.13	0.03	0.01
Cumulative (%)	93.42	99.06	99.65	99.83	99.96	99.99	100.0
Correlation with Age	-0.36*	-0.44**	-0.36*	-0.05*	-0.58**	-0.09	-0.16

\* and \*\* significant at 95% and 99.9% confidence levels. Total variance = 179.50.

Table 5.8 Results of PCA for the difference image of the two TM data sets.

Bands	PC1	PC2	PC3	PC4	PC5	PC6	PC7
$D_1$	0.1710	0.0328	-0.0593	0.2322	0.0068	0.8341	-0.4652
$D_2$	0.1375	0.0417	0.0073	0.2641	-0.1649	0.3781	0.8599
$D_3$	0.3529	0.1278	-0.0551	0.7479	-0.3332	-0.3896	-0.1845
$D_4$	0.1310	0.2410	<b>0.9601</b>	-0.0189	0.0306	0.0166	-0.0364
$D_5$	<b>0.7709</b>	0.3647	-0.2033	-0.4770	-0.0404	-0.0434	0.0186
$D_6$	0.1585	0.1038	-0.0665	0.2961	0.9258	-0.0800	0.0920
$D_7$	0.4369	<b>-0.8826</b>	0.1605	-0.0381	0.0447	-0.0303	0.0052
Eigen Values	170.59	10.04	5.22	1.59	0.71	0.17	0.04
Variance Explained (%)	90.57	5.33	2.77	0.85	0.38	0.09	0.02
Cumulative (%)	90.57	95.90	98.67	99.51	99.89	99.98	100.00
Correlation with Age	-0.55*	-0.01*	-0.59**	-0.14	-0.04	0.00	0.08

\*\* significant at 99.9% confidence level. Total variance = 188.36.

Table 5.9 Results of PCA for the mean image of the two TM data sets.

Bands	PC1	PC2	PC3	PC4	PC5	PC6	PC7
$M_1$	0.1835	-0.0076	0.1907	0.3745	-0.0665	0.7984	-0.3844
$M_2$	0.1405	0.0109	0.1337	0.3448	-0.0257	0.2030	0.8953
$M_3$	0.2723	-0.0643	0.2773	0.6888	0.1551	-0.5457	-0.2204
$M_4$	0.0716	<b>0.9882</b>	0.1093	-0.0112	-0.0598	-0.0456	-0.0266
$M_5$	<b>0.8131</b>	-0.1080	0.3080	-0.4615	-0.1293	-0.0495	0.0129
$M_6$	0.1539	0.0660	-0.1168	-0.1060	0.9630	0.1374	0.0298
$M_7$	<b>0.4271</b>	0.0569	-0.8651	0.2052	-0.1525	-0.0095	-0.0198
Eigen Values	317.75	14.89	2.34	1.77	0.56	0.10	0.01
Variance Explained (%)	94.17	4.41	0.69	0.52	0.17	0.03	0.02
Cumulative (%)	94.17	98.58	99.28	99.80	99.97	100.00	100.00
Correlation with Age	-0.46*	-0.59**	-0.04	-0.24	-0.24	-0.35	0.12

\*\* significant at 99.9% confidence level. Total variance = 337.42.

As shown in Tables 5.5 to 5.9, all spectral bands had positive loading values in PC1. For the SPOT data the information in PC1 was mainly contributed by the visible bands, with more emphasis on the red band (XS2) (Table 5.5). For the TM data, the information in PC1 was mainly contributed by the two MIR bands (TM5 and TM7), with the TM5 band showing the highest loadings (0.8003 for 2TM5; and 0.8344 for 4TM5) (Tables 5.6-5.7). All other TM bands contributed very little information to PC1 since they all showed relatively small PC loadings. NIR had a very high positive loading on PC2 (0.9731 for 2TM4, and 0.9850 for 4TM4), from 4 to 10 times larger than the loadings of any other bands. Similar information contents were found for the PCs of the mean image (Table 5.9).

The principal components computed from the difference image had different information contents, with PC1 having less and PC3 having more than those from the raw TM and mean images (Table 5.8). PC2 contained 5.33% of the total variance (188.36), but it had no correlation ( $r = -0.01$ ) with stand age (Table 5.8). As in the original data, the differences in Band 5 ( $D_5$ ) and 7 ( $D_7$ ) showed higher positive loadings in PC1. The information of PC2 was mainly from the  $D_4$ , as it produced a very large negative loading

in PC2 (-0.8826). The difference in Band 4 (D<sub>4</sub>) contributed the most information to PC3 as it had a very large positive loading (0.9601). PC4 to PC7 of the difference image contained negligible information (< 1%) on the stands.

The final principal component analysis was conducted using the three data sets together (18 channels) to compare their contributions to the total variation. As shown in Table 5.10, the PC1 could explain 89.24% and PC1 and PC2 taken together accounted for over 94% of the total variation. The remaining 16 PCs contained less than 6% of the total information and had no significant correlations with stand age and can be considered negligible.

Table 5.10 Results of PCA for the three data sets together (18 channels).

Bands	PC1	PC2	PC3	PC4	PC5	PC6	PC7
XS1	0.1409	0.0498	-0.0709	0.1805	0.2789	-0.3022	0.0645
XS2	0.1650	0.0408	-0.1066	0.2426	0.4083	-0.3004	0.0907
XS3	0.0675	0.5168	0.0525	0.2557	0.0574	-0.1056	-0.3323
PS	0.1959	0.0649	-0.0844	0.3160	0.3679	-0.1587	0.2103
2TM1	0.1543	0.0002	-0.0921	0.0962	0.1107	0.2302	0.0651
2TM2	0.1186	0.0162	-0.0697	0.0752	0.1287	0.2509	0.0417
2TM3	0.2517	-0.0290	-0.1677	0.1442	0.1488	0.6679	0.0649
2TM4	0.0692	<b>0.7032</b>	0.0524	0.0051	-0.2126	0.1962	-0.1201
2TM5	<b>0.6782</b>	-0.0898	-0.3125	0.1063	-0.5550	-0.2035	-0.0744
2TM6	0.1324	0.0320	-0.0807	-0.0738	-0.1372	0.0977	0.6292
2TM7	<b>0.3648</b>	0.0851	-0.1548	-0.7857	0.3881	-0.0309	-0.2131
4TM1	0.0829	-0.0189	0.1227	0.1012	0.1057	0.1468	-0.1049
4TM2	0.0627	-0.0136	0.1161	0.0567	0.0821	0.1228	-0.0123
4TM3	0.0991	-0.0712	0.2226	0.0797	0.1039	0.2567	0.0178
4TM4	0.0270	<b>0.4092</b>	0.2669	-0.1897	-0.0022	-0.0794	0.4933
4TM5	<b>0.3657</b>	-0.1681	0.7381	0.0137	-0.0631	-0.0832	-0.0559
4TM6	0.0660	0.0054	0.1107	-0.1252	-0.0443	-0.0923	0.2907
4TM7	0.1842	-0.1059	0.3082	0.0427	0.0930	0.0713	-0.1369
Eigen Values	765.31	43.58	24.31	11.92	5.01	3.62	1.74
Variance Explained (%)	89.24	5.08	2.83	1.39	0.58	0.42	0.20
Cumulative (%)	89.24	94.32	97.16	98.55	99.13	99.55	99.76
Correlation with Age	-0.49**	-0.67**	0.14	-0.12	-0.18	-0.20	-0.16

\*\* significant 99.9% confidence level. Total variance = 857.58

As can be seen from Table 5.10, the 2TM5 band shows the highest contribution to the PC1 as it has the highest PC loading (0.6782), two to three times larger than any of the other 17 channels. 2TM7 (0.3648) and 4TM5 (0.3657) also had higher PC1 loadings, but they were much lower than 2TM5. This means the information on PC1 was mainly contributed by the MIR bands. The information of PC2 was mainly contributed by the three NIR bands, with the loadings in PC2 being 0.7032 for 2TM4, 0.5168 for XS3 and 0.4098 for 4TM4. All other spectral bands had very small loadings in PC2 (< 0.1).

Figure 5.6 displays the plots of PC1 against PC2 from the three original data sets. The figures show that the young stands from ages 3 to 6 (a, b, c and d respectively in the

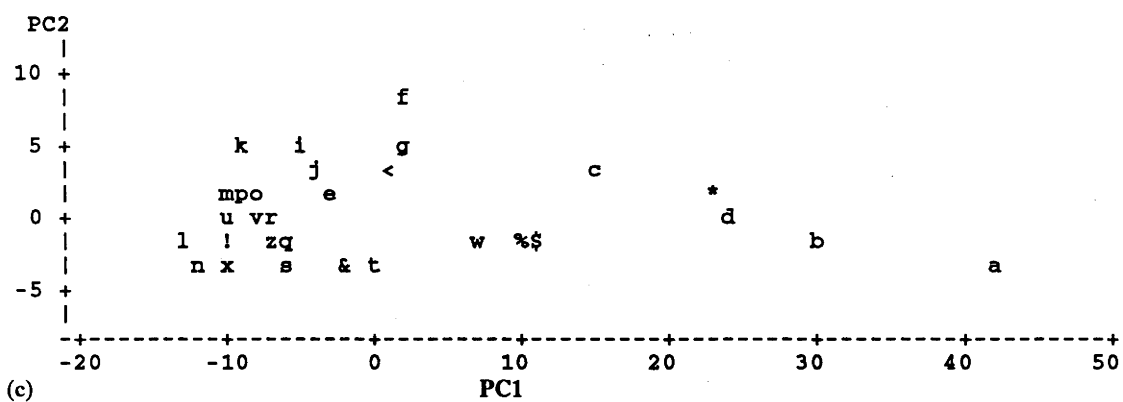
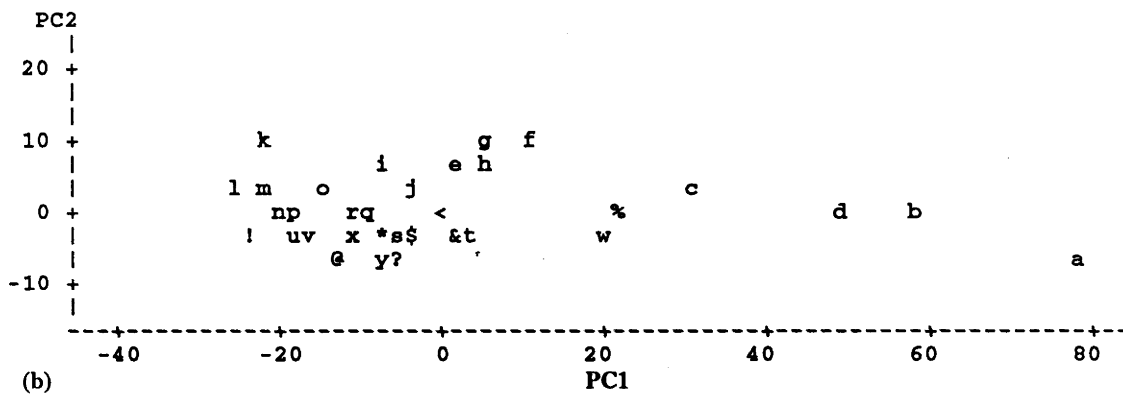
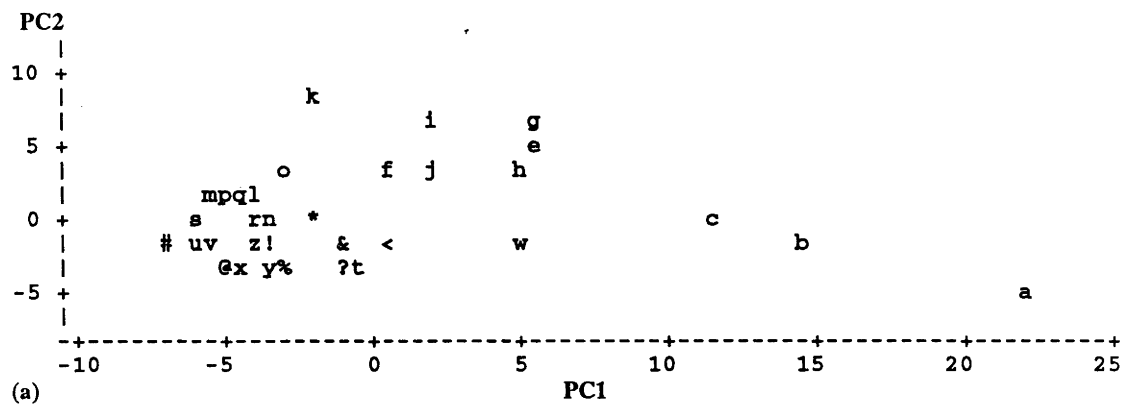


Figure 5.6 Plots of PC2 against PC1 calculated from the images of the January-24 SPOT data (a), the February-9 TM (b) and the April-21 TM (c). The characters from a to z and several other symbols represent the stands aged from 3 to 42 years (see Table 5.1).

plots (see Table 5.1) are at the extreme right, with higher positive values in PC1 and lower values in PC2 (in absolute terms). For the stands between 9 and about 15 years old (the symbols: e, f, g, h, i, j in the plots), the data show a lower positive loading values in both PC1 and PC2 than the data of the younger stands (age < 9). From about 16 to 25 years of age (symbols: k, l, m, n, p, q, r), the stands have negative loadings in PC1 but low positive loadings in PC2. The stands from age 25 usually shows negative loadings in PC1 and PC2 after about 20 years of age (symbols: s, t, u, v, x, y, z, !, @, #, \$, %, &, \*, ?, and <).

### 5.3.5 Correlations

#### 5.3.5.1 Inter-correlations within and between Images

Correlation matrices of data within the images and between the SPOT and TM images are displayed in Table 5.11. The green, red and panchromatic bands of the SPOT data were highly inter-correlated across the 60869 pixels covering the radiata pine stands aged from 3 to 42 years, with a range of correlation coefficients ( $r$ ) from 0.979-0.997, while the NIR band showed a relatively lower correlation with other bands ( $r = 0.537$ -0.555).

All TM bands were strongly inter-correlated ( $r = 0.946$ -0.996 for 2TM;  $r = 0.877$ -0.994 for 4TM), with the exception of the NIR band which showed a lower correlation with other bands ( $r < 0.43$  for 2TM, and  $r < 0.37$  for 4TM). Similar correlation patterns (i.e. high correlations between the visible and MIR bands and lower correlations with the NIR bands) also occurred between the three data sets (Table 5.11). In comparison, the SPOT data in all bands were better correlated with the February-8 TM data than with the April-21 TM data. This implies the two summer imagery data may be similar in their correlations with the stand parameters.

#### 5.3.5.2 Correlations between Raw Spectral Values and Stand Ages

The correlation coefficients between the raw spectral values and stand ages are presented in Table 5.12. The spectral values in all bands were negatively correlated with stand age (significant at 95% or larger confidence levels), with a range of correlation coefficients:  $r = -0.57$  to  $-0.83$  for the SPOT image,  $-0.46$  to  $-0.78$  for the February-9 TM image and  $-0.31$  to  $-0.54$  for the April-21 TM image. The visible, MIR and TIR bands showed very close correlations with stand ages. The highest correlation coefficients were found in the NIR bands ( $r = -0.82$  for XS3,  $-0.78$  for 2TM4 and  $-0.54$  for 4TM4 respectively).

Table 5.11 Correlations within and between the three data sets

Images	SPOT (14-Jan-1987)				2TM (9-Feb-1988)							4TM (21-Apr-1988)							
Bands	XS1	XS2	XS3	PS	2TM1	2TM2	2TM3	2TM4	2TM5	2TM6	2TM7	4TM1	4TM2	4TM3	4TM4	4TM5	4TM6	4TM7	
XS1	Within SPOT Image																		
XS2	1																		
XS3	0.997	1																	
PS	0.555	0.537	1																
	0.979	0.982	0.558	1															
	Between SPOT and 2TM																		
	Within 2TM Image																		
2TM1	0.955	0.955	0.484	0.969	1														
2TM2	0.950	0.952	0.497	0.966	0.996	1													
2TM3	0.931	0.936	0.445	0.949	0.993	0.996	1												
2TM4	0.438	0.411	0.940	0.445	0.403	0.421	0.379	1											
2TM5	0.949	0.944	0.445	0.953	0.980	0.970	0.972	0.371	1										
2TM6	0.903	0.897	0.444	0.918	0.959	0.946	0.948	0.396	0.962	1									
2TM7	0.952	0.950	0.417	0.957	0.988	0.979	0.981	0.332	0.995	0.956	1								
	Between SPOT and 4TM																		
	Between 2TM and 4TM																		
4TM1	0.887	0.885	0.458	0.908	0.924	0.922	0.917	0.356	0.910	0.857	0.918	1							
4TM2	0.867	0.865	0.446	0.891	0.905	0.904	0.900	0.354	0.891	0.850	0.899	0.994	1						
4TM3	0.816	0.816	0.343	0.842	0.867	0.868	0.872	0.262	0.860	0.821	0.870	0.978	0.989	1					
4TM4	0.275	0.238	0.793	0.286	0.211	0.225	0.176	0.837	0.194	0.253	0.154	0.294	0.329	0.268	1				
4TM5	0.859	0.848	0.384	0.868	0.883	0.874	0.872	0.295	0.907	0.857	0.904	0.968	0.974	0.974	0.302	1			
4TM6	0.840	0.829	0.384	0.828	0.847	0.837	0.836	0.330	0.885	0.887	0.874	0.877	0.893	0.892	0.365	0.940	1		
4TM7	0.878	0.871	0.376	0.888	0.909	0.902	0.900	0.276	0.920	0.866	0.925	0.981	0.981	0.979	0.255	0.995	0.925	1	

As can be seen from Figure 5.3, both difference and mean images of TM data showed a similar change trend over stand age as did the raw band data. They were therefore used in data analysis to check whether or not they could provide any useful information on stand variables (attached to Page 122, Paragraph 2).

When the correlation coefficients were calculated using the values from the stands of aged from 5 to 30 years, the correlations were only slightly improved in the visible and MIR bands, but the correlations in the NIR were significantly improved, with correlation coefficients ( $r$ ) increasing from -0.82 to -0.87 for the SPOT data, from -0.78 to -0.91 for the February-9 TM, and from -0.54 to 0.78 for the April-21 TM data (Table 5.12).

The difference and mean data of the two TM images showed a similar correlation pattern as did the original single date TM image. The correlation coefficients with stand age in all bands were only slightly higher than those computed from the raw February-9 TM data, but much better than those from the April-21 TM data (Table 5.12). However, the correlations calculated using the spectral values of stands aged from 5 to 30 years, the correlations were lower in the visible, MIR and TIR bands than those in the same bands of original February-9 TM data, but much higher in the same bands of the raw April-21 TM data, especially in the NIR bands (Table 5.12).

Table 5.12 Correlations between stand ages and the raw spectral values and the combined TM data. The correlation coefficients were computed with the values from stands aged from 3 to 42 and 5 to 30 years respectively.

Correlations between the Raw Spectral Band Data and Stand Age			Correlations between the Combined TM Imagery Data and Stand Age		
Bands	age: 3-42	age: 5-30	Combinations	(age: 3-42)	(age: 5.30)
XS1	-0.57**	-0.58**	$D_1$	-0.57**	-0.45*
XS2	-0.56**	-0.55**	$D_2$	-0.59**	-0.51*
XS3	-0.82**	-0.88**	$D_3$	-0.59**	-0.49*
PS	-0.57**	-0.53**	$D_4$	-0.80**	-0.85**
2TM1	-0.54**	-0.53**	$D_5$	-0.56**	-0.41*
2TM2	-0.54**	-0.56**	$D_6$	-0.57**	-0.40
2TM3	-0.50**	-0.49**	$D_7$	-0.54**	-0.46*
2TM4	-0.78**	-0.91**	$M_1$	-0.58**	-0.55*
2TM5	-0.47**	-0.49**	$M_2$	-0.58**	-0.57**
2TM6	-0.46**	-0.52*	$M_3$	-0.54**	-0.40*
2TM7	-0.51**	-0.52**	$M_4$	-0.77**	-0.87**
4TM1	-0.46**	-0.57**	$M_5$	-0.51**	-0.52*
4TM2	-0.43**	-0.58**	$M_6$	-0.49**	-0.55*
4TM3	-0.31*	-0.50**	$M_7$	-0.50**	-0.54**
4TM4	-0.54**	-0.78**			
4TM5	-0.34*	-0.56**			
4TM6	-0.31*	-0.57**			
4TM7	-0.37*	-0.53**			

\* and \*\* denote the correlation coefficients are significant at 95% and 99% levels.  $n = 35$

### 5.3.5.3 Correlations between Principal Component Images and Stand Ages

The correlations between stand ages and the PC images were computed and are shown in Tables 5.5-5.10 (see Section 5.3.4). Table 5.13 gives only the correlation coefficients of PC1 and PC2 with stand ages, as these two PCs were generally strongly correlated with the changes of stand ages, with correlation coefficients ( $r$ ) ranging from 0.36 to 0.67. PC1 showed higher correlation coefficients with stand age than PC2 in SPOT data, but TM images or their combinations showed a reverse pattern, with PC2 showing higher



correlation coefficients. Other PCs did not show significant correlations with stand ages (Tables 5.5-10).

By comparison, PC2 of the February-9 TM data showed the highest correlation ( $r = 0.67$ ) with stand age. The PC images produced from the multi-temporal data, either the two TM data sets (14 channels) or three data set (18 channels) together, showed correlations with stand age very close to those of the February-21 TM data. These results imply that the selection growing season or recording date is most important in detecting the stand variation using spectral data.

Table 5.13 Correlations between the first two principal components and stand ages (3 - 42).

Images	PCs	Correlations with age
SPOT Image	PC1	-0.66 ***
	PC2	-0.54 ***
February-9 TM Image	PC1	-0.53 ***
	PC2	-0.67 ***
April-21 TM Image	PC1	-0.36 *
	PC2	-0.44 **
TM Difference Image	PC1	-0.55 **
	PC2	-0.01
	PC3	-0.59 ***
TM mean Image	PC1	-0.42 *
	PC2	-0.59 ***
SPOT + 2TM + 4TM (18 Channels)	PC1	-0.49 **
	PC2	-0.67 ***
All TM images (14 bands)	PC1	-0.51 **
	PC2	-0.68 ***

\*, \*\* AND \*\*\* - significant at 95%, 99% and 99.9% of confident levels.

Further information on the correlations between the PCs and stand age was given by plotting PC1 and PC2 images against stand ages (Figure 5.7). It can be seen that PC1 showed a similar pattern of change to the original images in visible, middle and thermal bands. PC2 also showed a very similar pattern to the NIR raw image data. At young stand ages (< 6), PC1 values sharply decreased with increasing stand age and then gently reduced from age 7 to about 17. After 18 years of age, the PC1 became negative, was lowest at about 20 years of age, and slightly increased from age 22 to 25. After 25 years of age, the PC1 values fluctuate around zero (Figure 5.7). The PC2 values showed a reverse change pattern with the changes in age, with PC2 values significantly increasing with age from 3 to 6 years old, then more gently increasing from ages 7 and to about 16. PC2 shows the highest value at about age 17 and then shows a gentle decrease with increasing stand age to about age 30 after which they fluctuated about zero.

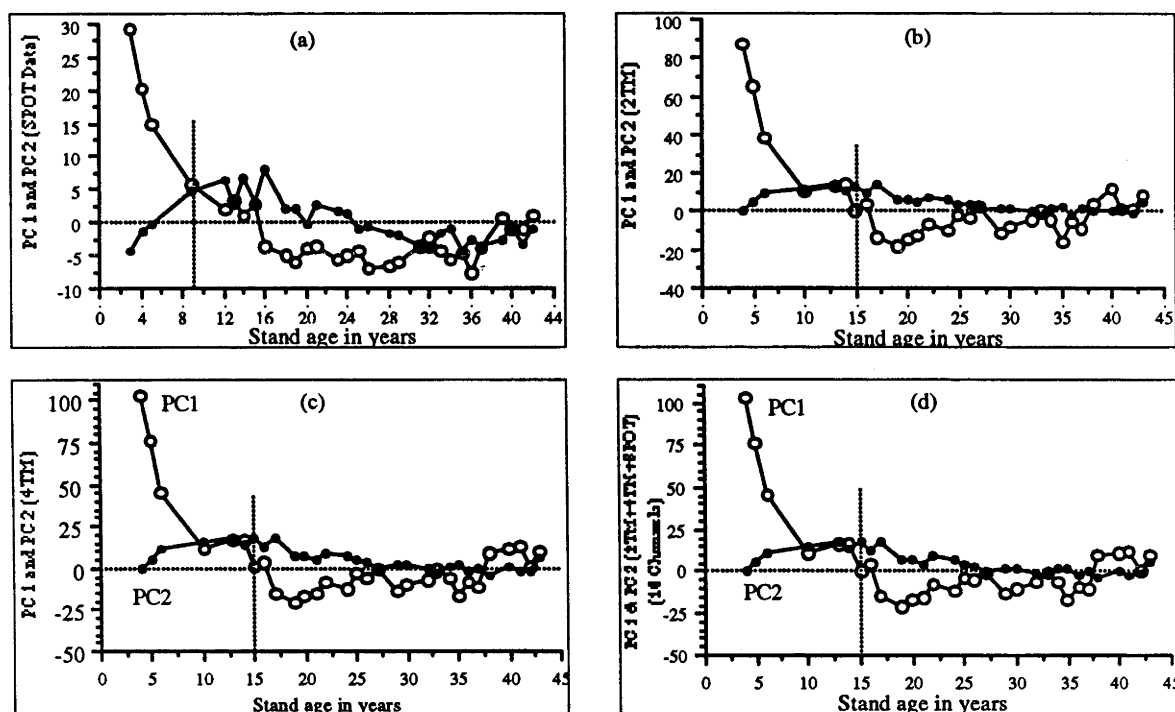


Figure 5.7 Relationships between stand age and the first two PCs of the January-24 SPOT data (a); the February-9 TM data (b); the April-21 TM data (c); and the three data sets together (d).

#### 5.3.5.4 Non-linear Correlations

The simple linear relationships between stand ages and the spectral values and their combinations and/or transformations have been shown in the earlier sections. However, the relationships between spectral responses of the stands and their ages are not linear. Regression analysis was undertaken using the six equations listed in Section 5.2.2.7. The simple linear function was also used for comparison with the non-linear functions. The results of regression analysis using the original band data, difference and mean images are presented in Table 5.14.

The non-linear regression analysis showed that all bands were strongly correlated with stand ages. For the visible, MIR and TIR bands, the lowest correlations were obtained from the linear function. The highest correlations were obtained from the polynomial function (Eq. 5.2) using logarithmically transformed age variables (significant at 99% confidence level), with  $r^2$  ranging from 0.73-0.90 for the SPOT image, 0.66-0.86 for the February-9 TM image and 0.30-0.78 for the April TM image. The visible and MIR bands showed the closest fitting results, with the best fit obtained from the green band for the SPOT data ( $r^2 = 0.90$ ), and the second MIR band (TM7) for the two TM data ( $r^2 = 0.86$  and 0.78 respectively). The NIR bands showed the lowest  $r^2$  in the log polynomial function (Eq. 5.2). In comparison, the summer images fitted better than the autumn image.

The models with the mean images of the TM data for two dates showed better fitting than with the difference images (Table 5.14), except for the power function model (Eq. 5.3). The correlations obtained from the mean image were nearly equal to those from the February-9 TM data.

Table 5.14 Regression models relating spectral values to stand age. The models listed in the table were defined in Section 5.2.2.7.

Models	Linear	Polynomial	Log Polynomial	Power	Exponential	Reciprocal	Log
Bands	$r^2$	$r^2$	$r^2$	$r^2$	$r^2$	$r^2$	$r^2$
XS1	0.33	0.88	0.90	0.67	0.36	0.65	0.84
XS2	0.31	0.86	0.88	0.65	0.34	0.62	0.82
XS3	0.69	0.73	0.73	0.84	0.70	0.64	0.41
PS	0.33	0.85	0.87	0.67	0.32	0.59	0.82
2TM1	0.28	0.77	0.84	0.61	0.33	0.60	0.79
2TM2	0.29	0.77	0.81	0.60	0.33	0.59	0.76
2TM3	0.24	0.71	0.77	0.54	0.26	0.51	0.71
2TM4	0.61	0.61	0.66	0.50	0.60	0.50	0.26
2TM5	0.22	0.76	0.85	0.54	0.20	0.44	0.75
2TM6	0.21	0.70	0.73	0.48	0.24	0.47	0.65
2TM7	0.26	0.74	0.86	0.53	0.17*	0.41	0.76
4TM1	0.21	0.70	0.75	0.49	0.24	0.48	0.67
4TM2	0.18	0.69	0.70	0.45	0.21	0.43	0.62
4TM3	0.09+	0.62	0.63	0.32	0.13*	0.32	0.50
4TM4	0.28	0.28*	0.30*	0.21	0.25	0.22	0.10+
4TM5	0.12	0.70	0.74	0.37	0.10+	0.30	0.58
4TM6	0.10+	0.74	0.69	0.30	0.10+	0.30	0.50
4TM7	0.13*	0.70	0.78	0.40	0.11+	0.32	0.63
D1	0.27	0.59	0.67	0.31	0.27	0.48	0.65
D2	0.31	0.58	0.64	0.32	0.29	0.46	0.62
D3	0.30	0.62	0.68	0.32	0.29	0.47	0.66
D4	0.60	0.63	0.67	0.62	0.61	0.51	0.30
D5	0.26	0.56	0.65	0.24	0.21	0.34	0.62
D6	0.25	0.51	0.55	0.29	0.26	0.43	0.54
D7	0.29	0.61	0.71	0.17*	0.13*	0.37	0.67
M1	0.26	0.77	0.84	0.31	0.27	0.58	0.77
M2	0.26	0.77	0.80	0.29	0.26	0.56	0.74
M3	0.20	0.71	0.76	0.21	0.18*	0.46	0.68
M4	0.51	0.51	0.56	0.49	0.45	0.41	0.20
M5	0.19	0.77	0.84	0.16*	0.12+	0.40	0.71
M6	0.18*	0.74	0.74	0.19*	0.15*	0.43	0.62
M7	0.23	0.75	0.86	0.15*	0.11+	0.62	0.74

\* means the regression models are significant at 95% confidence level; + means the regression is not significant. All others are significant at 99% or higher confidence levels..

### 5.3.5.5 Correlations Between Vegetation Indices and Stand Ages

The changes of the vegetation indices with stand age are displayed in Figure 5.5. Table 5.15 presents the correlations between the stand ages and the three vegetation indices. The linear correlations between vegetation indices and stand ages were very poor ( $r < 0.23$ ). When fitting the regression model using the non-linear functions, the correlations ( $r^2$ ) were as high as 0.90. The best results were obtained using the polynomial function- $VI = a + b \cdot \log(\text{age}) + c \cdot \log^2(\text{age})$ . The highest correlation coefficient was found between the normal difference vegetation index (NDVI) and stand age. In the comparison of the three data sets, the vegetation indices computed from SPOT data showed the best correlations. The

correlation coefficients calculated from the February-9 TM image were found to be higher than those from the April-21 TM image. Many other combinations of the bands and data transformations were also tried, but did not improve the correlations.

Table 5.15 Relationships between vegetation indices and stand age. The regression was computed using equation:  $VI = a + b \cdot \log(\text{age}) + c \cdot \log^2(\text{age})$ ,  $n = 36$ .

Data Sources	Vegetation Indices	Simple Linear Correlations ( $r$ )	Regression analysis with log polynomial function ( $r^2$ )
SPOT Image (January-24,1987)	NDVI	0.22	0.90
	AVI	-0.12	0.82
	RVI	0.14	0.85
The February-9 TM Image	NDVI	0.14	0.82
	AVI	0.10	0.80
	RVI	0.03	0.77
The April-21 TM image	NDVI	0.03	0.71
	AVI	0.20	0.58
	RVI	0.01	0.70

### 5.3.6 Clustering and Grouping of Spectral Values of Stands

The similarity among the mean spectral values of the stands at different stand ages were compared and grouped using clustering algorithms. The first cluster analysis was carried out to compare the similarity among the spectral bands. The relationships between the spectral bands were clustered according to the Pearson Product Moment Correlation similarity coefficients and the nearest neighbour (also called single linkage) methods (Johnson 1967). It can be seen from Figures 5.8a to 5.8c that: (1) the NIR band showed the lowest similarity (i.e. low correlation in Table 5.11) to the other bands and was classified as a single group; (2) the visible bands (including Panchromatic band in SPOT data) showed the highest similarity and could be classified into a spectral band group; (3) the two MIR bands (TM5 and TM7) and the TIR (TM6) were closer to the visible bands than to the NIR and could be grouped into the visible band groups. When using the three data sets together (18 channels), three spectral band groups could be delineated based on their similarity (Figure 5.8d): (1) all the NIR bands, 4TM2, 4TM3, 4TM5, and 4TM7; (2) 4TM1 and 4TM6; and (3) the rest of the spectral bands. In comparison, 2TM4 was closer to XS3 than to 4TM4, while the rest of the February-9 TM bands were closer to the SPOT XS1, XS2 and PS bands.

The relationships between the mean spectral values from the single date images of the stands aged from 3 to 42 years are shown in Figure 5.9a-c. In general, four spectral classes can be classified: age 3-6, 7-16, 17-25, and 25-42. Similar classification results could also be obtained by using the three data sets together (18 channels: SPOT + 2TM + 4TM) (Figure 5.9d). These classification results are very similar to the pattern of changes of the raw spectral values and principal component values with stand age described in

Sections 5.3.3 and 5.3.4. Although SPOT data showed a similar classification pattern to the TM data sets, they produced some mixed age groups (Figure 5.8c). In comparison, TM data showed better classifications. The best classification was obtained using the multi-temporal data (Figure 5.9d).

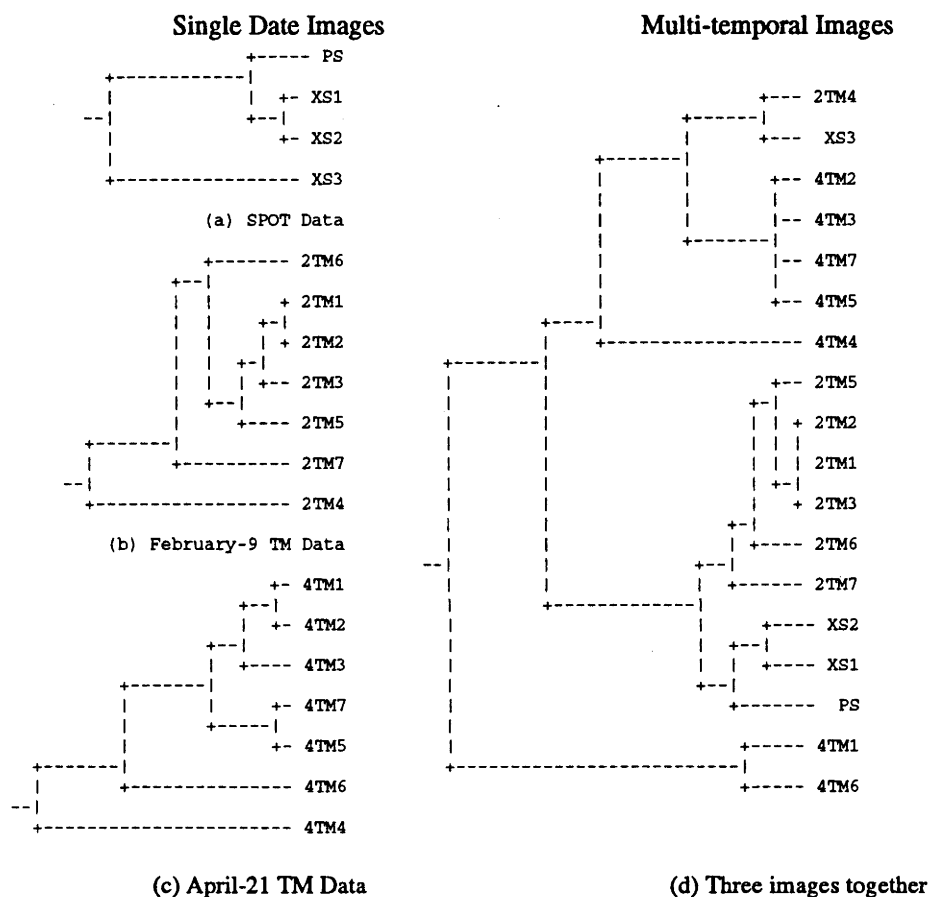


Figure 5.8 Clustering dendrograms showing the resemblance between the spectral bands of the three single date images (a) - (c) and showing the relationships among the three images and corresponding spectral bands (d).

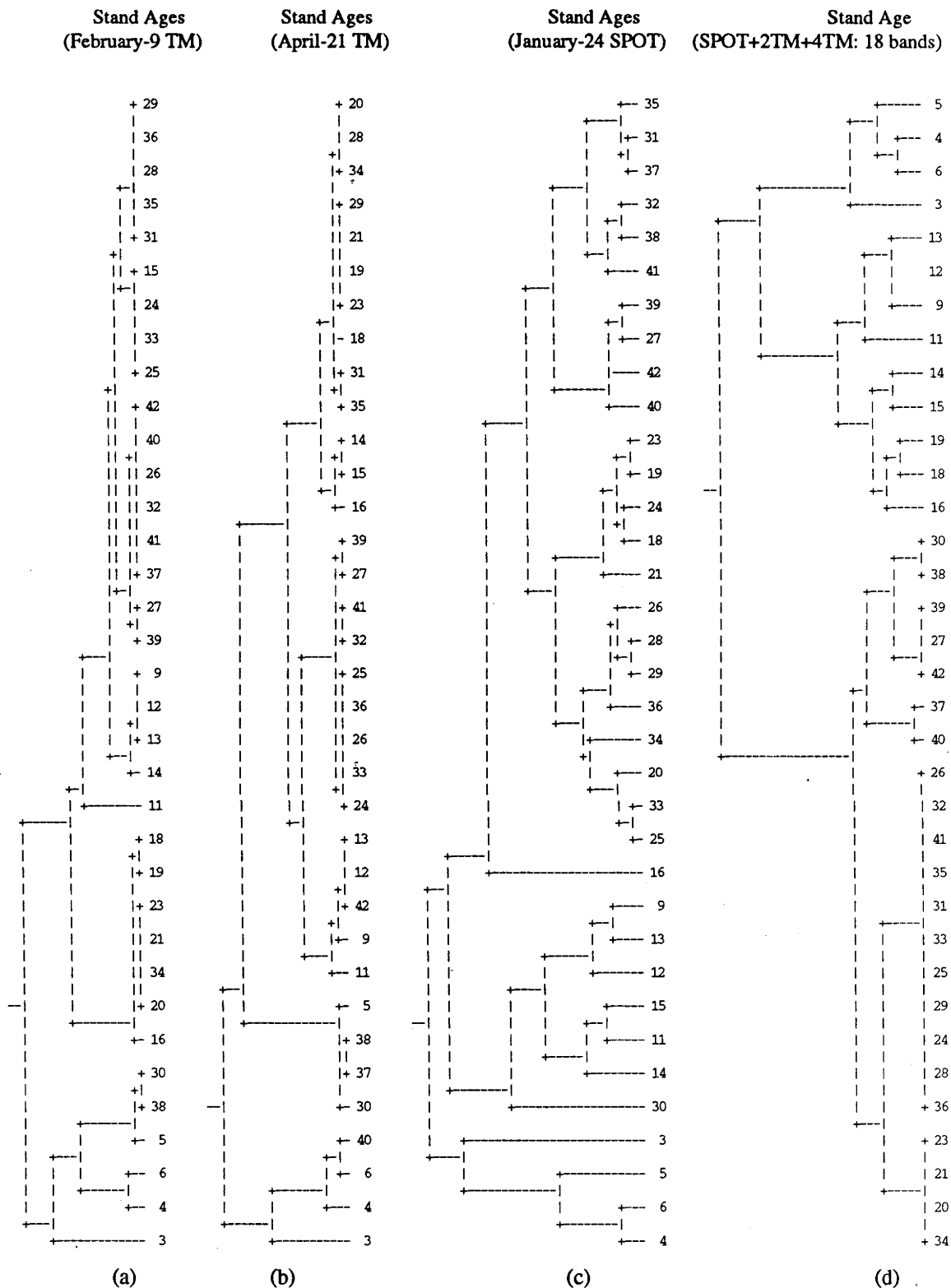


Figure 5.9 Clustering dendrograms of the mean spectral values of stands aged from 3 to 42 years. The number at the right of each diagram is the stand age in years. The figures show the classifications of the mean spectral values of the stands computed from the February-9 TM data (a), the April-21 TM data (b), the January-24 SPOT data (c), and the three data sets together (i.e. SPOT+2TM+4TM: 18 channels) (d).

## 5.4 DISCUSSION

### 5.4.1 Variation of Spectral Values

As shown in Tables 5.2 and 5.3, although recorded at the same location, the three data sets taken on different dates showed significant differences in mean values, data ranges, and variances. Even the two TM data with the same system parameters showed significant differences due to different recording dates (75 days interval). These variations in radiance have been attributed to the effects on the spectral reflectance of the ground targets, atmospheric effects, wavelength and the angular relationships between sensors, target and sun (Swain and Davis 1978). Discussion of these sources of variation can be found in papers by Hoffer (1978), Duggin (1983); Curran 1985; Guyot 1990; and Boissard *et al.* 1990). Milne (1983) also attributed the variations to the effects of physiological/phenological and silvicultural conditions on the total spectral reflectance of vegetation. Environmental conditions such as moisture and temperature conditions which vary between dates could also significantly affect the vegetation reflectance (Knipling 1970; Jackson 1986).

The differences between the February and April-21 TM images may be mainly ascribed to the changes of sun angle and weather conditions. On the other hand, they may also be attributed to changes in the ground cover. In general, lower reflectance means higher canopy absorption and therefore higher amounts of ground cover as estimated by leaf area index. The tree stands may not significantly change in such a short time period, but the changes of undergrowth coverage and other factors such as the weather and moisture conditions may cause a different spectral reflectance at different growing seasons.

SPOT and Landsat TM are different sensor systems, with great differences in scanning angles, wavelength width, scanning times and therefore azimuth angles of the sun in Landsat TM and SPOT images. SPOT images (vertical) are approximately two hours later than the TM images. These differences become more significant in rugged areas, since change in azimuth angle relocates the slope shadows and the penetration distance of sun light (Hall-Könyves 1987; Kawata *et al.*, 1988; Thomson and Jones 1990; Conese and Maselli 1991).

The differences in spatial resolutions and width of spectral wavelength in SPOT and TM systems also cause differences in spectral values (Häme 1991). For instance, a 10x10 meter pixel of a SPOT panchromatic image may cover several tree crowns in a normal stand. If the forest canopy is not closed, a pixel value will be a combination of the reflectances of

the undergrowth, possibly bare soils, rocks and/or pruning debris, tree stems and branches and leaves.

Besides the variation in the images recorded from different dates, systems and wavelengths, the variations of spectral reflectance also occurred at different growth stages. As can be seen from Appendices D-G, the younger stands (< 10 years of age) generally showed higher values in data ranges, standard deviations and the coefficients of variation than the older stands. This is probably because of the very different reflectance properties of tree crowns and bare soil within a stand, as bare soil produces higher reflectance, while tree crowns show higher absorption and lower reflectance in visible bands.

In fact, because of the existence of various random noise, the variation seems to be unavoidable. Häme (1991) listed twelve factors that may affect the spectral reflectance, which he defined as *pixel intensity* and expressed as the function of these twelve factors. Indeed, some of the “noise factors” are uncontrollable. If these random “noise factors” are not considered, the variations may be attributed to changes of stand conditions at different growth seasons (Summer from January-March, and Autumn from April to June), such as stand undergrowth, needle amounts (i.e. needle falling) and stand physiological characteristics. In predicting forest growth using satellite remotely sensed data, the emphasis should be on the description of the variation of the spectral values because of the changes of growing seasons and growing periods.

#### **5.4.2 Changes of Spectral Values with Stand Age**

In general, the major factors influencing the spectral absorption and reflectance of a stand are leaf amount (or perhaps pigment concentration) and canopy shadows (See Häme 1991; Tucker 1978). As shown in Figures 5.2 to 5.4, the spectral values in all bands decreased with increasing stand age due to the stand growth. The stands in the juvenile growth stage (age 1-4) usually produced the highest spectral reflectance, since at this growth stage, the canopies of trees are separate and there are large spaces between the trees, causing higher ground and lower canopy reflectance. Thus the spectral reflectance in young coniferous stands is usually from bare soils, rocks and/or herbs (grass and shrubs), and the trees are distinguishable only by canopy shadows (Kneppeck and Ahern 1987). This high variation in canopy cover in this stage also results in higher data variation (e.g. higher data range, standard deviation). After the juvenile growth stage, stands enter an adolescent stage of rapid growth (age 5 to 10), creating a series of changes in stand structure (e.g. less understory, denser canopy cover and larger amount of leaf and concentrations of chlorophyll, etc) (Ovington 1971), and canopy shadows therefore also increase. This



significantly increases the canopy absorptions and dramatically reduces reflectance in the juvenile growth stage. In the stands between ages 10 and 20, the main changes of a closed stand relate to the deeper canopy and sparse understory. In particular, continuing canopy growth and increase in amount of leaves during this age stage significantly reduce the reflectance of stands.

Generally, the reflectance of the NIR waveband increases with increasing biomass (Tucker *et al.* 1975; Tucker 1978 and 1979). Thus, with stands growing with increasing stand age, one would expect that mean reflectance values would increase in the NIR band as occurs from age 3 to 10 (Figure 5.2). However, growth with age in coniferous forests is usually accompanied by a decrease in spectral reflectance in all bands, including the NIR band. This decrease in the NIR reflectance is usually attributed to the effects of canopy shadows on spectral reflectance (Danson 1987; Poso *et al.* 1987; Häme 1991; Brockhaus and Khorram 1992). The reasons for a decreasing NIR reflectance in conifers with growth are discussed by Danson (1987) and Häme (1991).

A constant reflectance level occurred in visible and MIR bands after about 20 years of stand growth and in the NIR band after about 32 years. Mature stands have a high and stable total leaf area index and variability in the relationship between leaf area index and spectral reflectance is related to short-term changes in chlorophyll concentration (Curran and Milton 1983). Therefore, after the coniferous plantations enter the mature and stable growth stage, their reflectance may fluctuate within a certain reflectance level. After the mature growth stage, continuing stand growth usually results in changes of stand structure such as less canopy depth, density, needle amount and therefore less canopy shadows. This may possibly be the reason for increased reflectance after the stands entered the mature growth stage.

Studies of vegetation index (VI) have shown a strong correlation with leaf area index and crop yield. In this study, both the reflectance-age and VI-age relation curves are very close to the growth pattern of radiata pine trees described by Jacobs (1937) (Table 5.16). As shown in Figure 5.5, the three vegetation indices (NDVI, AVI and RVI) had a reverse change pattern as did the raw spectral values (Figure 5.2-4). The vegetation indices significantly increased with tree growth from age 3 to about 6 and then gently increased from age 7 and reached their peaks at about age 17. Similarly in the reflectance-age curves, the spectral values decreased and reached a minimum at about age 20. The similarity can also be seen in principal components and age relation curves (Figure 5.7). The PC values

sharply decreased with age from 3 to 5, gently decreased from 7 to about 15. The PC values became negative after 16 years of age and reached the lowest at age 18 to 20.

Table 5.16 Growth patterns of radiata pine plantation stands (from Jacobs 1937)

Growth Stages	Upper Limits of Ages	Growth Characteristics (Buds and Leaves)
1. Juvenile stage:	1 - 4	Most primary leaves photo synthetically active buds all juvenile
2. Adolescent stage:	4 - 8	Primary leaves active on some parts of shoots, modified to scarios bracts on other parts. Buds, mixed, leading bud usually mature, side buds juvenile
3. Bulbous Stage:	6 - 10*	Primary leaves rarely active. Buds mature
4. Mature stage:	20 - 40	Primary leaves all modified. Foliar duties done by fascicles. Buds all mature
5. Senescent stage:	**	Primary leaves modified. Buds all mature

\* Upper limit of age at the bulbous stage varies with spacing of trees; \*\* varies with freedom of crown from less than 20 where severely restricted to 100 or more where completely free.

### 5.4.3 Correlation Analysis

The similarity of the changes in pattern with stand age between the visible and MIR and bands led to a strong and close inter-correlation between these bands ( $r > 0.90$ ) (Table 5.11). These highly inter-correlated bands (i.e. XS1 and XS2, TM1-3 and 5-7) produced approximately equal and low linear correlations with stand ages. However, they showed relatively high non-linear correlations with stand ages (see Table 5.14).

The spectral values in all bands were strongly negatively correlated to stand age ( $p < 0.001$ ). The NIR bands showed a stronger linear correlation with stand age, as they showed approximately linear changes over a wider age range than all other bands (see Figures 5.2 and 3). As discussed above, the responses for younger stands (age  $< 5$ ) did not reflect the real changes of stands because the reflectance was mainly from bare soils before the canopies achieved full ground cover. After 30 years of age, the reflectance values in all bands became constant or slightly increasing. Thus it is relatively difficult to describe the stand characteristics at juvenile and/or overmature (age  $> 35$ ) stand growth stages. This is presumably because the spectral responses were more significantly affected by stand canopy depth, as the canopy depth increased with increasing stand age in the 5-30 age period.

As shown in Figures 5.2 to 5.4, the spectral responses to stand age in most wavebands, however, were not linear. The linear correlation may not reflect the real changes of reflectance of stands from ages 3 to 42 years. In fact, compared with the simple linear correlation coefficients, all non-linear transformations significantly improved the correlation coefficients, including those for the NIR bands. The best results were obtained from the polynomial function using logarithmically transformed age variables (Table 5.14).

The NIR band was best correlated with radiata pine stand ages. Similar results have been reported using TM data by Hord (1982) and SPOT data by Danson (1987) and Turner *et al.* (1987). Tucker (1978) concluded that the NIR band was especially sensitive to changes in vegetation density, biomass and chlorophyll content. Using a SPOT image recorded in October, 1986, Turner *et al.* (1987) reported the NIR band data showed a correlation of only 0.5 ( $r^2$ ) with radiata pine stand age, while green and red bands showed no significant correlations. This might be due to the representativeness of samples selected and the data quality, as some cloud shadows occurred in that scene. The results obtained in this work showed that there are significant correlations and that they are also at a higher level than those reported by Turner *et al.* (1987).

A decrease of spectral reflectance values with an increase of stand age corresponds to the growth pattern expected for radiata pine forests in south-east Australia. It should be noted that the above discussion assumes that all stands grow in the same manner. In practice, however, this is not true. Therefore the reflectance values selected from different stands at corresponding ages may show different patterns, even at the same age, due to different position, terrain and soil background. These factors should be considered when evaluating the relationships between spectral reflectance values and stand age and are considered later.

As discussed in Chapter 2, green vegetation (chlorophyll a and b) usually shows a low red reflectance and a high NIR reflectance, and by contrast bare ground surfaces do not show such sharp distinctions. Thus, the indices based on the ratio of NIR to Red reflectance gives high values for healthy green vegetation and low for bare area (Harris 1987). The three main vegetation indices, NDVI, AVI and RVI, used in this work, were strongly correlated (non-linearly) with stand age, with  $r^2$  values of 0.82-0.9 in the SPOT image, 0.77-0.82 in the February-9 TM image and 0.58-0.71 in the April-21 TM image. The NDVI showed the highest correlation coefficients (Table 5.15). These three vegetation indices are usually believed to be sensitive to coniferous forest leaf area index (Spanner *et al.* 1984a, and Running *et al.* 1986), and biomass (Sader *et al.* 1989). Band ratios have been used by some researchers to reduce the effects of topography (see Richards 1986; Schowengerdt 1983), thus RVI (NIR/Red) may reflect the real changes of canopy depth regardless of different topography. The NDVI, however, has to be used with caution in rugged terrain, as the variations in NDVI were found by Thomson and Jones (1990) to be significantly correlated with slope (but not aspect). Nevertheless, NDVI could be useful for reflecting the changes in stand structure parameters, and canopy depth in particular, as it is significantly related to radiata pine stand volume growth (see Chapter 6).

As both of the red and the NIR bands are sensitive to green vegetation, the difference of these two bands, AVI, may be useful for identifying vigorous stands. As shown in Figure 5.10, The 'gap' (band difference) between the two curves increased from age 3, reached the peak at about age 9 and then decrease from ages 9 to 30 and became constant after age 30. Thus the stands at adolescent (ages 4-8) and bulbous (ages 6-10) growth stages may be highlight.

Although it has higher spatial resolution (10 m) the SPOT panchromatic band data did not have a higher correlation with stand age. Its correlation with stand age was very close to that for the green and red band data, and it showed a similar response to green vegetation in this wavelength region. Thus, while panchromatic band data may be useful in classification and land-cover mapping, it does not necessarily increase the prediction accuracy.

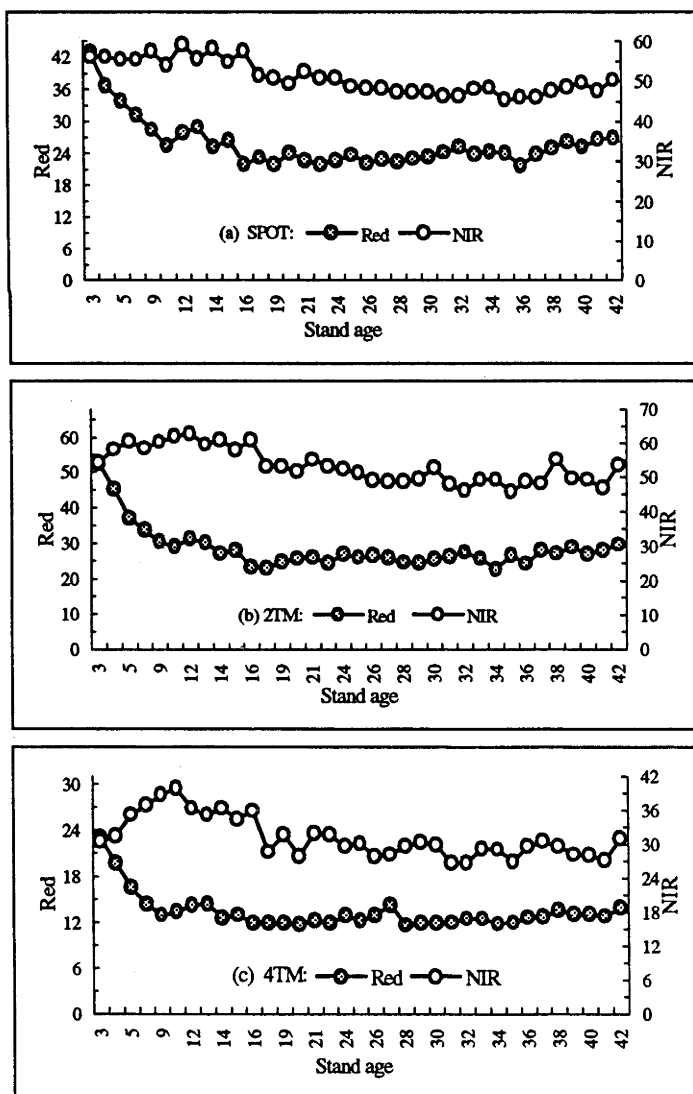


Figure 5.10 Curves of changes in spectral values in the red and NIR bands with increasing stand age.

#### 5.4.4 Principal Component Transformation

In remote sensing using multi-bands and/or multi-temporal data, the loadings of the eigenvectors are usually used to describe the relative contributions of each original band to the transformed components. The bands (visible and MIR) having strong inter-correlations showed higher positive loadings of eigenvectors in the first principal component (PC1), which explained 90% or larger of the total variations. Experience has indicated that loadings in PC1 measure the "brightness", which indicates the overall reflectance of the object (Kauth and Thomas 1976), such as the nature of the terrain (Lodwick 1979a). The NIR band data, however, showed high positive loadings in PC2 due to the differences between the NIR and the other bands in responses to green vegetation. Kauth and Thomas (1976) also named PC2 as "greenness" which is a measure of green biomass. Thus it seems that PC2 is more important in detecting the structural changes of stands, as it is associated with the quantity and quality of vegetation. The first two principal components have explained up to 95% or more of the total variance, whereas the remaining principal components contained very little variance and were essentially noise (Santisteban and Munoz 1978).

The changes of the PC1 and PC2 image values showed some interesting results which may make PC1 in particular useful for stand classification and mapping. As shown in Figures 5.6 and 5.7, the spectral classes (or age classes) can be classified at the inter-section point (about 10 years of age), while from this point to the zero PC values (i.e. 10 to 16 years of age) and thereafter can be treated as another two spectral classes. These were very close to the results obtained from cluster analysis (Figures 5.8 and 5.9).

In principal component analysis, the contributions of any variables to the total variance are usually determined by their PC loadings; that is the higher the PC loadings, the more contribution to the total variation. Based on this principle, the importance of the spectral bands can be compared and selected. In general, the spectral information of vegetation in PC2 was mainly contributed by the NIR band, while in PC1 mainly by the visible band for SPOT data and the two MIR bands for TM data. The importance of multi-temporal or multi-sensor imagery can also be compared by the PC loadings. As shown in Table 5.10, The total variance of the three data sets together (18 channels) was mainly contributed by the two MIR bands (TM5 and TM7) of the February-9 TM in PC1 and the NIR band in PC2 for the same image. The SPOT and April-21 TM images contributed very little even negligible information to the total variance. These PCA results suggest that the image recording time (such as from different growing seasons) significantly influences the results when detecting the variations of forest using spectral data. Multitemporal data may not

necessarily improve the information content on perennial vegetation; furthermore the use of multi-temporal image will increase the costs.

#### 5.4.5 The Separability and Sensitivity of Spectral Reflectance of Stands

Spectral separability or divergence indices are often used to indicate which spectral bands are contributing to the discrimination of known cover classes, based on relatively large amounts of training data (Toll 1984). In this study, the spectral reflectance values did not show significant differences between the stands at any adjacent age levels (see Appendices D-F). However, the stands at different ages could be grouped into spectral reflectance homogeneous classes (age groups) based on the similarities between the spectral values. No significant difference could be found after 25 years old, since the spectral reflectance of stands becomes constant.

Radiometric resolution may be an important factor affecting the sensitivity of spectral reflectance to stand structure. The spectral reflectance values usually concentrated within a small data range. In this work, plantations covered from 3 to 42 years of age, but the data ranges (the difference between maximum and minimum reflectance) in all bands were relatively small (in fact much smaller than the age range) (see Appendices D-G and Figure 5.11). This means the radiometric resolution of both TM and SPOT data may not be sensitive enough to detect subtle changes in stands at short age intervals.

Cluster analysis and principal component analysis also showed that the mean reflectance values of the spectral values of the stands can be grouped into three or four spectral classes of 5 or larger age groups (Figures 5.7, 5.8, and 5.9). This again indicates that the capability of both SPOT and TM data in detecting the subtle variations of radiata pine stands is limited.

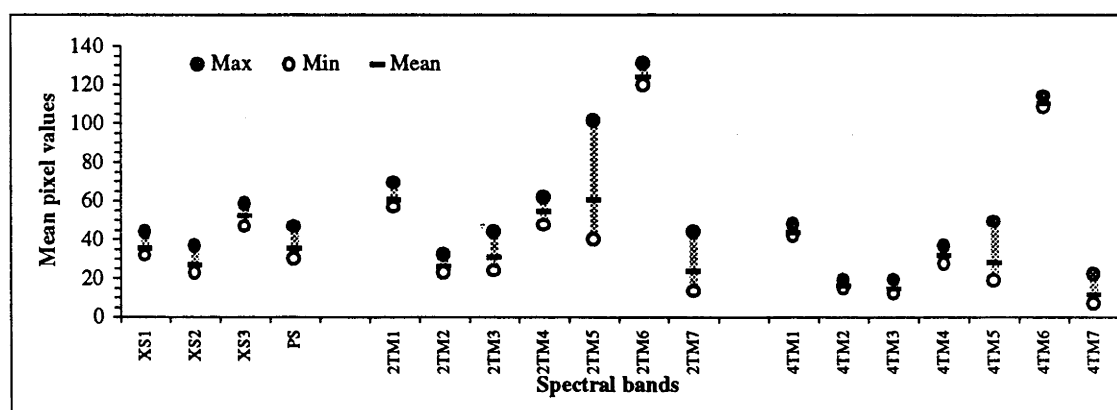


Figure 5.11 Band data ranges of the three data sets over the radiata pine stands aged from 5 to 42 years.

## 5.5 SUMMARY AND CONCLUSION

The basic aims of this chapter were to discover the patterns of change in spectral reflectance in pine forest and to evaluate the relationships between spectral reflectance and even-age plantation stands at different ages and growth stages. The work covered in this chapter included:

1. Testing the variations of spectral reflectance from separate dates and remote sensing systems;
2. Determining the separability and sensitivity of spectral reflectance at different stand ages and growth stages;
3. Evaluating the relationships between spectral values and stand age;
4. Evaluating and comparing the information content of SPOT and TM data on the radiata pine stands using principal component analysis.

As the study area covers stands at different growth stages, the results of the study gave information about spectral changes caused by the changes in stands due to age differences. Because changes in a stand occur at different times in the life of a stand, information about the general pattern of spectral responses to stands was obtained. From the results obtained, the conclusions reached in this chapter are as follows:

1. There are significant variations in separate data sets from Landsat TM or SPOT systems. The variations appear mainly related to the remote sensing systems' "noise" and the differences in stand undergrowth, as the changes of stands *per se* in a short time interval are slight, while the systems' "noise" (such as sun angle, atmospheric effects, soil types and terrain effects) may show significant differences with different recording dates.
2. Differences of spectral reflectance values between the adjacent ages or over short age intervals are very small. They could be grouped into spectral classes of 5 years or more age intervals.
3. The best age stage for investigating the changes of radiata pine stand structure is from 5 to 25 years of age when using SPOT and/or TM data. For the NIR band data, this can be extended up to about 30 to 35 years of age.
4. Both TM and SPOT images showed a similar sensitivity to radiata pine stand changes. The NIR bands in both images are the best bands for detecting changes in stands.

5. The change behaviour of spectral reflectance is very similar to the change of phenological growth with age. This makes TM and SPOT potentially useful in predicting forest growth and SQ.
6. The total variance of both SPOT and TM data over the radiata pine stands and all three data together can be explained by their first two principal components. The first principal component combined the information contained in the visible, MIR and TIR bands, whereas the information in the NIR bands was reflected by the second principal components. As for the original data, the second principal component is more sensitive to changes in stand growth processes.

It should be pointed out that the study described in this chapter did not establish what factors other than stand age are affecting the spectral reflectance . Age is indeed an indirect determinant of stand growth, and its relationships with spectral reflectance values are expressed by ecological and biological parameters. In this chapter it has been shown that the capability of SPOT and TM data in detecting subtle changes in stand growth is limited. This capability may be improved by integrating the spectral data with biogeographical variables. This will be further investigated in the following chapters.



# **A Correlation, Principal Component and Canonical Correlation Analysis of Stand Variables Versus SPOT and Landsat TM Images**

## **6.1 INTRODUCTION**

Understanding of the relationships between spectral reflectance and various stand attribute variables is the prerequisite for estimating, monitoring and predicting forest resources and management planning using satellite data. The study in Chapter 5 indicated that spectral response was strongly related to radiata pine plantation stand age. It also concluded that changes in the pattern of spectral reflectance are similar in timing to the growth changes in stands. This gives an indication of the potential of both SPOT and Landsat TM data for estimating and monitoring other stand parameters which are closely related to stand age. Therefore a further study was needed to test the relationships of the spectral response in different wavelength regions with various stand growth parameters. The work in this chapter was undertaken to test the capabilities of both SPOT and Landsat TM sensors and to develop analytical methods for using satellite remotely sensed imagery data to estimate forest stand growth parameters.

As reviewed in Chapter 2, previous work in the analysis of satellite remotely sensed imagery data related to forest stand variables is limited. Most investigations have been based on single date or single system images and a limited set of stand variables. The results reported have been data dependent, usually varying greatly with species, site

conditions, data types, data quality and even processing methods. Studies on estimating forest stand variables for practical management and planning purposes (especially at a local scale) are still in the experimental stage. Little has been reported on the relationships between spectral values and radiata pine stand variables.

The purposes of this chapter are (1) to examine the relationships between stand and spectral variables; (2) to determine what variables (stand and spectral variables) can be selected to develop models for estimating stand variables and SQ; and (3) to compare the capability of SPOT and TM data in detecting the variations of stand variables. This was done by using correlation analysis, principal component transformation (PCT), and canonical correlation analysis (CCA) techniques. The spectral variables include the raw band data and various band combinations (i.e. "between-image" and "within-image" band combinations and principal component images).

## 6.2 DATA COLLECTION

The data used in this study consisted of stand, site and spectral variables collected from sixty sample points (see Chapter 4). The stand variables included nine forest stand variables, four topographic variables and two soil variables. The stand variables include top height (TH), age, basal area (BA), mean diameter (MD) at breast height over bark, density (measured as stem number per hectare (SN)), canopy cover (CC), understory coverage (UC), canopy depth (CD) and volume (VOL) in cubic meters per hectare. The four topographic variables were slope (SLP) in degrees, aspect (ASP) in degrees from N, altitude (ALT) in meters, and top position (TP). The soil parameters included the depth of soil horizons A and B (AB), content of gravel (GC) larger than 5 mm in diameter. All these variables were defined in Chapter 4.

Three data sets of images were used for data analysis. The description of these three data sets was given in Chapter 4. The imagery values of each sample plot were calculated from a 3 x 3 pixel window. In addition to the individual band data, the data produced from principal components transformation were also used for correlation analysis. In addition, the "within-image" band combinations of the single date data and "between-image" band combinations of multi-temporal data were also used to compute correlation coefficients. The former are various band combinations done by addition, subtraction, multiplication and division between the spectral bands within a single date image, including the three well-defined vegetation indices — normal difference vegetation index (NDVI), agricultural vegetation index (AVI), and relative vegetation index (RVI) (see Chapter 5). The later "between-image" band combinations were the difference and mean images calculated from corresponding spectral bands of the TM data for two dates. Due to the

The words “similar pattern of change” were changed into “a strong inverse curvilinear relationship” (Page 141, last paragraph).

coarse spatial resolution in Band 6 of TM images, the results of this band were for comparative purposes,

## 6.3 DATA ANALYSIS TECHNIQUES

### 6.3.1 Correlation Analysis

Simple correlation (also called Pearson correlation) analysis was performed to determine the degree to which each stand variable was correlated with the imagery data. It was evaluated by computing linear correlation coefficients between the variables and by the significance test of each correlation coefficient, which measures the strength of the linear relation between two variables. i.e

$$r_{ij} = \frac{S_{ij}}{\sqrt{S_i^2 S_j^2}}$$

where  $S_i^2$  and  $S_j^2$  are the variances of variables  $i$  and  $j$ , and  $S_{ij}$  is the covariance. The correlation coefficient  $r_{ij}$  is tested under the null hypothesis  $H_0: r_{ij} = 0$ . Based on Finn (1974), if the statistic

$$t = \frac{r_{ij} \sqrt{N-2}}{\sqrt{1-r_{ij}^2}} > t(\alpha, N-2)$$

then the variables  $i$  and  $j$  can be considered significantly correlated, where  $t(\alpha, N-2)$  is the critical value at the degree of freedom ( $N - 2$ ) and confidence level  $\alpha$ , and  $N$  is the number of sample points.

### 6.3.2 Principal Component Transforms

The results obtained in the previous chapter indicated that the first two principal components (PCs) could explain 90% or more of the total variation of the data sets. Based on Kauth and Thomas (1976), Lodwick (1979b), Ingebritsen and Lyon (1985) and Horler and Ahern (1986), the first principal component (PC1) was explained as the measure of "brightness" which is related to the form and nature of terrain and in particular, its aspect. In Chapter 5, the first principal component (PC1) image showed a similar pattern of change with stand age to the raw data in visible, middle and thermal bands, i.e. a strong inverse curvilinear correlation ( $|r| \geq 0.73-0.93$ ) with stand age. The second principal component (PC2) was explained as the measure of "greenness" which is associated with the quality and quantity of vegetation and showed a strong linear

correlation with stand age ( $|r| > 0.55$ ). These two PCs might be useful for describing forest stand growth processes. Principal component analysis, in this chapter, was used to reduce the “redundancy” resulting from the strong inter-correlations within the images. The basic computation procedures can be found in the previous chapter.

### 6.3.3 Canonical Correlation Analysis

#### 6.3.3.1 Introduction

Forest remote sensing deals with relationships between spectral reflectance and forest cover and their interaction with environmental conditions affecting the reflectance. Consequently, many questions of interest to foresters in using remote sensing techniques may call for investigation of relationships between variables of two distinct but associated kinds. Such relationships may involve those, for example, between stand structure parameters and spectral bands data and/or between spectral reflectance and the physical environmental variables affecting the reflectance process. They might also involve, as in forestry and ecology, the connections between plant communities and their site conditions. Thus in testing these relationships between two sets of variables, the following three questions may arise and need to be investigated:

- To what extent can one set of two or more variables be predicted or “explained” by another set of two or more variables?
- What contribution can a single variable make to the explanatory power of the set of variables to which the variable belongs?
- To what extent can a single variable contribute to predicting or “explaining” the combination of the variables in the variable set to which the variable does not belong?

Simple and/or multiple correlation analysis techniques detect only the relationship of a single variable to the set of variables. Principal component analysis or factor analysis techniques analyse the inter-relationships within a set of variables. Canonical correlation analysis (CCA), also termed canonical variate, canonical transformation, canonical discriminant analysis and/or canonical analysis in some literature, is a data analysis technique that can quantitatively evaluate not only the relationships between the variables but more importantly the relationships between two sets of variables of different kinds. It can provide *proportion-of-shared-variation* measures to describe the relationships of two sets of random variables, each set consisting of multiple measures (Finn 1974). In addition, like principal component analysis, it can also reduce the redundancy

(dimensionality or variables) within a set of variables by a linear combination of within-set variables and determine the most correlated variables. The technique is useful for understanding the overlap of information content in two batteries of tests.

CCA is a good way of determining the best correlated variables between two sets of variables. Like PCA, it can be used to reduce the dimensionality of data space, and produce new combined variables (see below) which explain most of the variance in the variable groups. It can like correlation analysis detect the degree of association existing among the variables as well as variable groups. Based on the canonical coefficients (loadings) and canonical correlation, the importance (or contribution) of each single variable can be determined.

CCA has been widely used in biology, ecology and social science (see Thompson 1984; and Gittins 1985). In remote sensing, it has usually been used for classification purposes by defining a rotation of axes which give the greatest separation between classes (e.g. Lachowski *et al.* 1982, Harrison and Jupp 1988, and Häme 1991). In this study, CCA technique was employed to investigate the correlations between:

- stand variables and site variables (including DTM data);
- stand variables and SPOT image; and
- stand variables and TM images.

### 6.3.3.2 Some Basic Computational Procedures

CCA can be divided into five steps:

- derivation of variance-covariance or correlation matrices;
- computation of the eigenvalues and eigenvectors of matrix  $D = S_{xx}^{-1}S_{xy}S_{yy}^{-1}S_{yx}$ ;
- calculation of canonical correlation coefficients (canonical variates and their correlations);
- significance tests of canonical correlation coefficients; and
- redundancy analysis and interpretations of canonical variables.

Mathematically, let the partitioned vector  $G = [x_1, x_2, \dots, x_p \mid y_1, y_2, \dots, y_q]^T$  represent observations on two sets of variables, with each variable being measured about its respective mean and  $q \leq p$ . Let  $X = [x_1, x_2, \dots, x_p]^T$  and  $Y = [y_1, y_2, \dots, y_q]^T$  be jointly distributed with sample mean vector  $\mathbf{m}$  and variance-covariance matrix or other scalar-products matrix  $S$  (assuming  $S$  is positive definite matrix) partitioned as:

$$\mathbf{m} = \begin{bmatrix} \mathbf{0} \\ \mathbf{0} \end{bmatrix}, \quad \mathbf{S} = \begin{bmatrix} S_{xx} & S_{xy} \\ S_{yx} & S_{yy} \end{bmatrix},$$

where  $S_{xx}$  and  $S_{yy}$  are the “within-set” variance-covariance matrices of vectors  $X$  and  $Y$  respectively, and  $S_{xy}$  and  $S_{yx}$  ( $S_{xy} = S_{yx}$ ) are the “between-sets” variance-covariance matrices between vectors  $X$  and  $Y$ . These specify the relations between the two sets of variables  $X$  and  $Y$ . All the variance-covariance matrices  $S_{xx}$ ,  $S_{yy}$ ,  $S_{xy}$  and  $S_{yx}$  can be estimated as:

$$S_{xx} = \frac{1}{n-1} \sum_{k=1}^n (x_{ik} - m)(x_{ik} - m)^T \Leftrightarrow cX^T Y$$

$$S_{yy} = \frac{1}{n-1} \sum_{k=1}^n (y_{jk} - m)(y_{jk} - m)^T \Leftrightarrow cY^T Y$$

$$S_{xy} = S_{yx} = \frac{1}{n-1} \sum_{k=1}^n (x_{ik} - m)(y_{jk} - m)^T \Leftrightarrow cX^T Y$$

where

$\tau$ - denotes the transpose of a matrix,

$k = 1, 2, \dots, n$  observations (or sample size),

$i = 1, 2, \dots, p$  variables,

$j = 1, 2, \dots, q$  variables,

$c \leq 1$  and  $c \neq 0$

Hotelling (1935 and 1936) proposed the following as a measure of the correlation between the  $p$ -dimensional variable  $X$  and the  $q$ -dimensional variable  $Y$ . Consider a linear function of the  $x_1, x_2, \dots, x_p$ , i.e.  $u = a_1 x_1 + \dots + a_p x_p$ , and a linear function of the  $y_1, y_2, \dots, y_q$ , i.e.  $v = b_1 y_1 + \dots + b_q y_q$ . Then determine those values of the coefficients vectors  $a$  ( $p \times 1$ ) and  $b$  ( $q \times 1$ ) which maximise the correlation between  $u$  and  $v$ . More precisely, linear combinations of  $X$  and  $Y$  are usually sought, i.e.

$$u_k = a_k^T x$$

$$v_k = b_k^T y$$

with  $a_k$  and  $b_k$  scaled so that the linear combinations  $u_k$  and  $v_k$  have unit variance, i.e.

$$a_k^T S_{xx} a_k = 1,$$

$$b_k^T S_{yy} b_k = 1,$$

for which the correlation between  $u$  and  $v$

$$\text{cor}(u_k, v_k) = r_k \quad (\text{say})$$

is maximised subject to the constraints

$$E(u_k) = E(v_k) = 0, \quad s(u_k) = S(v_k) = 1,$$

$$\text{cor}(u_i, u_k) = 0, \quad \text{cor}(u_i, v_k) = 0, \quad \text{cor}(v_k, v_k) = 0,$$

where  $u_k$ ,  $v_k$  and  $r_k$  can be determined by eigenvalues and their corresponding eigenvectors of matrix  $D = S_{xx}^{-1}S_{xy}S_{yy}^{-1}S_{yx}$ . The statistical significance (or independence) of canonical correlation can be tested by making a null hypothesis of no relationships between the canonical variables. i.e. assume that the canonical correlation coefficients ( $r_k$ ) equal zero:

$$H_0: r_1 = r_2 = \dots = r_k = 0$$

The test of the  $H_0$  is usually done using Bartlett's (1941) Chi-square ( $\chi^2$ ) test. According to Finn (1974), the  $\chi^2$  value of  $j$ th pair of canonical variables can be calculated as follows:

$$\chi_j^2 = - \left[ n - 1 - \frac{1}{2}(p + q + 1) \right] \cdot \ln \Lambda_j$$

where  $n$  is the number of subjects (observation or sample size,  $n = 60$  in this study), and  $\Lambda_j$  can be estimated as:

$$\Lambda_j = \prod_{j=1}^k (1 - r_j^2) = (1 - r_1^2)(1 - r_2^2) \dots (1 - r_k^2)$$

where  $j$  denotes the  $j$ th pair of canonical variables ( $j = 1, 2, \dots, k, k \leq p$ ), and  $r_j^2$  is the canonical correlation coefficients estimated by the eigenvalues  $\lambda_j$ , with  $\lambda_1 > \lambda_2 > \dots > \lambda_k > 0$ .

As  $\chi^2$  obeys the Chi-square distribution at  $\alpha$  level critical value and the degree of freedom  $f = (p - j + 1) \cdot (q - j + 1)$ , therefore two canonical variables can be considered significantly correlated if

$$\chi_j^2 > \chi^2[\alpha, (p - j + 1) \cdot (q - j + 1)].$$

Bartlett's Chi-square ( $\chi^2$ ) test is discussed by Darlington *et al.* (1973) and Thompson (1984). The canonical correlation coefficients ( $r_j^2$ ) and the coefficients vectors of linear combinations (i.e.  $a_k^T$  and  $b_k^T$ ) were computed using the Statistical Analysis System (SAS) package (SAS Institute Inc., 1989).

In canonical correlation analysis, canonical redundancy analysis is usually used for interpretation of the variance of canonical variables (also called canonical variates). *Redundancy* is the proportion of the total variance in the variables in one set predictable from a linear composite of the other variables (Thompson 1984). The term "*redundancy*" is therefore synonymous with "*explained variance*". According to Gittins (1985), the redundancies of the canonical variable  $u$  and  $v$  can be written as:

$$U_{x/u_k}^2 = \sum_{i=1}^p s_{ik}^2 / p, \text{ and}$$



$$V_{y/v_k}^2 = \sum_{j=1}^q s_{jk}^2 / q$$

where  $s_{ik}^2$  is the correlation between the  $i$ th variable of  $X$  and the  $k$ th canonical variable of  $Y$ , and similarly  $s_{jk}^2$  the correlation between the  $j$ th variable of  $Y$  and the  $k$ th canonical variable of  $X$ .

In general  $U_{x/u_k}^2 \neq V_{y/v_k}^2$ . The redundancy associated with a canonical variable can be used as an index of the predictive or explanatory power of the canonical variable in relation to the other set of variables (Finn 1974). This is helpful in variable selection.

Canonical variables and their correlation coefficients have a number of properties, some of which are of considerable interest in remote sensing because they assist in understanding the relationships between the multi-band image and vegetation parameters:

- Canonical variables are dimensionless (when computed from correlation matrices). Consequently, they are invariant under non-singular linear transformations of the variables of either or both groups of variables.
- Canonical correlation coefficients can be interpreted as multiple correlation coefficients between a particular canonical variable of one domain and the complete set of variables of the other.
- The magnitude of  $r_k$  indicates the degree of linear correlation between the two canonical variables (i.e.  $u_k$  and  $v_k$ ). The squared canonical correlation coefficient,  $r_k^2$ , expresses the proportion of the variance of the  $k$ th canonical variable,  $u_k$ , say, that is explained by its conjugate,  $v_k$ , or *vice versa*. (Bartlett 1965; and Gittins 1985).
- Like the principal component transformations, the first few canonical correlation coefficients and their corresponding canonical variables have the largest contributions of the original variables.

Canonical correlation analysis was originally proposed by Hotelling (1935 and 1936) as a means of identifying the most predictable  $p$ -variate criterion. It has since been developed more mathematically (McKeon 1962; Mardia *et al.* 1979) and more intuitively (Seal 1964; Horst 1961). Comprehensive discussions of canonical correlation analysis are provided by most of the standard works on multivariate analysis (Mardia *et al.* 1979; Muirhead 1982). Practical applications in ecology and forestry can be found in, for example, Goldstein and Grigal (1972), Kowal *et al.* (1976), Pielou (1977), and Gittins (1985).

## 6.4 RESULTS

### 6.4.1 Data Characteristics

Table 6.1 is a summary of the stand variables computed from 60 sampling points. Stand age ranged from 9 to 42 years, with most points ranging between 10 and 30 years of age. Mean diameter at breast height over bark ranged from 14.3 to 47.0 cm, and the corresponding basal area from 9 to 42 m<sup>2</sup>/ha. The stand top height was between 9.7 and 28.9 meters. The stand density ranged from 139 to 1190 trees/ha. Canopy cover was estimated at from about 40% to approximately full cover (96%). The stand undergrowth cover was highly dependent on upper canopy cover and site conditions, ranging from little undergrowth cover (< 7%) in the stands with full upper canopy cover to almost full understorey cover (about 97%) in the stands with less tree canopy coverage. The canopy depth was between 8 and 25.25 meters, but it was highly dependent upon the stand density, stand average height and also the history of pruning. The volume of stands with mean diameter 13 cm or larger ranged from 21.5 to 429.9 m<sup>3</sup>/ha.

Table 6.1 Summary of the forest stand variables of 60 0.01-hectare sample plots.

Stand Variables	Mean	SD	SE	Variance	CV	Min	Max	Range
AGE	24.55	7.94	0.99	63.00	32.34	9.00	42.00	33.00
BA	26.56	9.04	1.12	81.68	34.04	7.50	52.00	44.00
TH	20.71	4.32	0.54	18.64	20.86	9.65	28.88	19.23
MD	29.21	6.23	0.81	42.58	21.33	14.29	46.98	32.69
SN	442.05	231.16	28.67	53436.32	52.29	138.45	1189.27	1050.82
CC	0.63	0.14	0.02	0.02	22.22	0.40	0.96	0.56
UC	0.52	0.24	0.03	0.06	46.15	0.07	0.97	0.90
CD	16.60	3.57	0.44	12.76	21.51	8.05	25.25	17.20
VOL	179.91	79.07	9.81	6251.74	43.95	21.47	428.95	407.49

The site characteristics summarised for the 60 sampling points is given in Table 6.2. All the points had slopes (SLP) between zero and 21 degrees. The altitude (ALT) was between 580 and 875 m above sea level. The aspect (ASP) of the sampling points ranged from 0 to 345 degrees. The mean depth (AB) of soil A and B horizons was 55 cm, ranging from about 21 to 120 cm. The gravel content (GC) (gravel diameter > 5 mm) of the soil was estimated at around 2-50%, with 21% as average. In addition, the topographic position (TP), which is not listed in the table, was also used for data analysis, being coded as numbers 1, 2, 3, 4, and 5, respectively representing level, downhill, uphill, middle hill and top of hill (see Section 4.2.4.2 of Chapter 4).

Table 6.3 shows the basic statistics of the imagery data selected for the same 60 sampling points on a 3 x 3 pixel window. Compared with the results summarised in Chapter 4 and 5, the statistical parameters calculated from 3 x 3 pixel windows of 60 sampling points

showed lower values in mean, standard deviation, variance, coefficient of variation and data range (see Table 5.2), as the sampling points covered a narrower age range (9-42) and were selected in the stands with full canopy closure and low disturbance.

Table 6.2 Summary of the site variables of 60 0.01-hectare sample plots.

Site Variables	Mean	SD	SE	Variance	CV	Min	Max	Range
SLP	8.40	5.31	0.66	28.24	63.21	0.00	21.00	21.00
ALT	739.43	56.51	7.01	3192.94	7.64	580.00	875.00	295.00
AB	54.45	22.11	2.74	488.91	40.61	21.00	120.00	99.00
ASP	170.17	105.48	13.08	11126.71	61.99	0.00	345.00	345.00
GC	0.21	0.11	0.01	0.01	52.38	0.02	0.50	0.48

As discussed in Chapter 5, the data range (i.e. the difference of maximum and minimum of the spectral reflectance values) may be seen as a measure of spectral sensitivity of the stands in different wavelengths, as the brightness gradient (radiometric resolution) from 0 to 255 shows the changes of spectral reflectance and absorption of an object. A higher data range may indicate greater sensitivity to changes within stands. Table 6.3 shows that the spectral values in all bands had a lower data range than the age range except for band 5 of the February-9 TM data. For instance, the data ranges of SPOT XS mode data are between 16.5 - 18.8. The February-9 TM images showed a data range of 8 - 50 and April-21 TM of 3.4 - 22.0. Green bands in the three data sets showed the lowest range of reflectance. In particular, the blue (TM1) and green wavebands of TM images showed a relatively low data range (3.4-12). In such cases, it is difficult to differentiate subtle changes in the stands as such a narrow data range could not contain all the stand information.

Table 6.3 The basic statistics of the 60 sample points of images on 3 x 3 pixel windows.

Variable	Mean	SD	SE	Variance	CV	Min	Max	Range
XS1	31.19	3.11	0.39	9.68	9.98	26.00	42.83	16.83
XS2	22.15	3.30	0.41	10.92	14.92	16.50	33.00	16.50
XS3	49.46	4.73	0.59	22.37	9.56	42.50	61.33	18.83
PS	30.18	0.50	0.62	24.99	16.60	24.00	52.75	28.75
2TM1	56.96	2.18	0.27	4.75	3.83	52.00	64.00	12.00
2TM2	23.07	1.62	0.20	0.61	7.00	20.00	28.67	8.67
2TM3	24.90	3.80	0.47	14.42	15.25	17.00	37.50	20.50
2TM4	52.11	6.40	0.79	40.94	12.28	42.00	66.00	24.00
2TM5	46.25	10.63	1.32	112.93	22.98	24.00	74.17	50.17
2TM6	121.70	2.81	0.35	7.89	2.038	117.00	130.00	13.00
2TM7	16.28	5.01	0.62	25.09	30.77	6.25	27.00	20.75
4TM1	41.27	1.26	0.16	1.58	3.04	38.89	46.00	7.11
4TM2	14.23	0.89	0.11	0.79	6.24	12.89	16.33	3.44
4TM3	11.94	1.33	0.17	1.78	11.17	10.00	15.50	5.50
4TM4	30.80	3.65	0.45	13.33	11.85	23.00	40.00	17.00
4TM5	20.82	5.05	0.63	25.47	24.24	13.00	35.00	22.00
4TM6	109.06	1.63	0.20	2.66	1.49	106.00	113.00	7.00
4TM7	7.69	2.11	0.26	4.46	27.46	4.75	14.00	9.25

## 6.4.2 Inter-Correlations Between the Stand Variables

Analysis of the ground data showed that several of the stand variables were highly inter-correlated (Table 6.4). Basal area, top height, mean diameter, volume and canopy depth all increased with stand age as they are related to tree growth. Stand density and canopy cover decreased and showed a negative correlation with age due to the management practice of thinning which involves the periodic removal of a number of trees. Stand density and canopy depth showed a weak negative correlation with stand age. Understorey cover showed a low negative correlation with age ( $r = -0.16$ ) as it is affected by upper canopy cover.

Table 6.4 Correlations between stand variables.

Variables	AGE	BA	TH	MD	SN	CC	UC	CD	VOL
AGE	1.00								
BA	0.37*	1.00							
TH	0.79**	0.48**	1.00						
MD	0.72**	0.34*	0.85**	1.00					
SN	-0.40*	0.38*	-0.44**	-0.65**	1.00				
CC	-0.35*	0.45**	-0.08	-0.22	0.48**	1.00			
UC	-0.16	-0.27	-0.24	-0.12	0.03	-0.25	1.00		
CD	0.62**	0.36*	0.83**	0.76**	-0.51**	-0.11	-0.18	1.00	
VOL	0.61**	0.90**	0.78**	0.62**	0.04	0.33*	-0.30	0.60**	1.00

\*and \*\* Significant at 99 and 99.9 per cent confidence levels respectively,  $n = 60$ .

Stand volume was strongly correlated with basal area ( $r = 0.9$ ), top height ( $r = 0.78$ ) and mean diameter ( $r = 0.60$ ) as they are the main determining factors of volume. Canopy depth (CD) increased with increased stand top height ( $r = 0.83$ ), mean diameter ( $r = 0.76$ ), and stand volume ( $r = 0.60$ ), but decreased with increased stem number ( $r = -0.51$ ) due to the effects of canopy competition.

## 6.4.3 Correlations Between Stand and Site Variables

The results of the correlation analyses between stand variables and site variables (i.e. topographic and soil) are given in Table 6.5. Basal area, top height, mean diameter, canopy depth, and stand volume were significantly negatively correlated with altitude (ALT) (significant at 99% confidence level). These five stand variables also showed a positive correlation with topographic position (TP) (significant at 95% confidence levels). The correlations between stand variables and slope, aspect, soil depth and gravel content were not significant. The lack of correlations may be explained by the relatively small differences in slope, aspect and soil characteristics in the study site. For example, most of the sample points were located on 15 degrees or less of slope.

Table 6.5 Correlations between stand and site variables.

Variables	ALT	SLP	ASP	TP	AB	GC
BA	-0.41**	-0.13	-0.08	0.28*	0.01	-0.05
TH	-0.46**	0.07	0.13	0.40**	0.06	-0.13
MD	-0.55**	-0.03	0.14	0.40**	0.25	-0.21
SN	0.26*	-0.11	-0.17	-0.14	-0.09	0.04
CC	0.07	-0.22	-0.13	0.35	0.13	-0.08
UC	-0.05	-0.22	0.09	-0.10	0.15	-0.18
CD	-0.49**	-0.01	0.21	0.28*	0.02	-0.07
VOL	-0.49**	-0.05	0.00	0.41**	0.08	-0.10

\*and \*\* Significant at 95 and 99 per cent confidence levels respectively,  $n = 60$ .

#### 6.4.4 Correlations Between Stand Variable and Raw Imagery Data

The results of correlation analyses between the reflectance values of each individual band and eight stand parameters are presented in Table 6.6. The visible, MIR and TIR bands of the three data sets showed no correlations with stand age ( $|r| = 0.01 - 0.23$ ). The NIR bands (XS3 and TM4) showed the highest correlation coefficients with stand age ( $|r| = 0.51 - 0.79$ ). This result supports the analysis of Chapter 5 which indicated strong negative linear relationships between stand age and the NIR band data. The correlation coefficients between the NIR bands and stand top height, mean diameter, and canopy cover were significant at the 99% confidence level. The correlations of canopy cover with the NIR (except TM4 of the April-21 TM image), MIR and TIR bands were significant at 95% or higher (99%) confidence levels, but the correlations with the visible bands were relatively lower.

Table 6.6 Correlations between raw imagery data and stand variables. 2TM and 4TM represents the February-9 TM and the April-21 TM images respectively.

Variables	AGE	BA	TH	MD	SN	CC	UC	CD	VOL
XS1	-0.13	-0.22	-0.42**	-0.33**	0.22	-0.16	0.25	-0.40**	-0.34**
XS2	-0.01	-0.13	-0.32**	-0.29*	0.21	-0.19	0.13	-0.33**	-0.23
XS3	-0.67**	-0.05	-0.40**	-0.37**	0.32*	0.38**	0.15	-0.31*	-0.21
PS	-0.10	-0.05	-0.36**	-0.24	0.16	-0.27*	0.27*	-0.30*	-0.17
2TM1	-0.09	-0.30*	-0.27*	-0.14	-0.07	-0.22	0.33**	-0.16	-0.30*
2TM2	-0.14	-0.41**	-0.32*	-0.22	-0.09	-0.29*	0.37**	-0.22	-0.41**
2TM3	-0.04	-0.43**	-0.22	-0.13	-0.16	-0.36**	0.41**	-0.15	-0.37**
2TM4	-0.79**	-0.25*	-0.52**	-0.49**	0.26*	0.38**	0.09	-0.36**	-0.39**
2TM5	-0.01	-0.47**	-0.27*	-0.13	-0.22	-0.48**	0.38**	-0.16	-0.43**
2TM6	0.12	-0.16	-0.05	0.08	-0.24	-0.36**	0.22	0.09	-0.14
2TM7	0.03	-0.41**	-0.25	-0.10	-0.20	-0.46**	0.35**	-0.13	-0.38**
4TM1	-0.08	-0.21	-0.29*	-0.16	-0.08	-0.27*	0.13	-0.15	-0.25
4TM2	-0.12	-0.24	-0.29*	-0.20	-0.08	-0.30*	0.19	-0.14	-0.28*
4TM3	0.08	-0.14	-0.17	-0.07	-0.14	-0.35**	0.16	-0.04	-0.17
4TM4	-0.51**	-0.11	-0.39**	-0.35**	0.17	0.23	-0.08	-0.26*	-0.24
4TM5	0.02	-0.20	-0.21	-0.11	-0.14	-0.32*	0.38**	-0.05	-0.26*
4TM6	0.23	-0.13	-0.08	0.00	-0.16	-0.41**	0.15	0.00	-0.14
4TM7	0.08	-0.15	-0.14	-0.07	-0.15	-0.34**	0.34	0.02	-0.20

\* and \*\* significant at 95 and 99 per cent confidence levels respectively,  $n = 60$

The three data sets showed very similar correlation patterns with other stand parameters. The visible bands of the SPOT data (XS1 and XS2) were significantly correlated with

mean diameter and canopy depth at the 99% confidence level, but these two stand variables showed no correlation with the visible bands of the TM images. Stand basal area was not significantly correlated with the SPOT image and the April-21 TM image ( $|r| < 0.24$ ), but it was significantly correlated with all bands of the February-9 TM image (95% or larger confidence levels). Understorey cover also showed a similar correlation pattern. Stand volumes were significantly correlated with all the bands (excluding TM6) of the February-9 TM image ( $|r| = 0.30-0.43$ ), but only significantly correlated with TM1, TM2 and TM5 of the April-21 TM image with lower correlation coefficients ( $|r| = 0.25 - 0.28$ ). Of the SPOT bands, only XS1 was significantly correlated with stand volume ( $|r| = 0.34$ ). All bands of SPOT data showed a negative correlation with canopy depth and mean diameter (except for the PS band) at a 95% confidence level, but only TM4 of the TM images was significantly correlated with canopy depth. Stand density did not show significant correlations with the three data sets, with the exception of the NIR bands in the SPOT and February-9 TM data.

In comparison, the summer images (i.e. the January-24 SPOT and the February-9 TM images) showed close correlations with stand variables, whereas the autumn image (the April-21 TM image) showed lower correlations. The correlation differences existing in the three data sets may be attributed to changes in the undergrowth and the effects of weather conditions and sun angle (see Chapter 5). Undergrowth vegetation cover (such as annual plants) could show differences from season to season and therefore influence the spectral responses, but the stands *pe se* could not show major changes in a short period of time. The comparison of the data ranges of the three data sets also showed the summer images were more sensitive to the variations of stands than the autumn image since the former had a wider data range (Table 6.3). These results imply that the time at which data are recorded may significantly affect the prediction accuracy. This will be further studied in the next chapter.

#### **6.4.5 Correlations Between Stand Variables and “Between-Image” Band Combinations**

The linear correlation coefficients between the nine stand parameters and the difference and mean images were calculated (Table 6.7). Both the difference and mean images of the two TM data showed close correlations in the corresponding spectral bands with stand variables. Compared with the results calculated from the raw imagery data, they are very much closer to the results for the February-9 image and much higher than those for the April-21 image. The results suggest that the data combinations of multi-temporal images

may be a better data source than single-date data for detecting the changes of stand structures as the combined images of multitemporal images, in a sense, may be able to reduce the effects of some random "noise".

Table 6.7 Correlations between the difference ( $D_1, \dots, D_7$ ) and mean ( $M_1, \dots, M_7$ ) imagery data and stand variables.

Variables	AGE	BA	TH	MD	SN	CC	UC	CD	VOL
$D_1$	-0.06	-0.24	-0.15	-0.07	-0.04	-0.10	0.31*	-0.10	-0.21
$D_2$	-0.08	-0.33**	-0.18	-0.12	-0.05	-0.14	0.32*	-0.17	-0.30*
$D_3$	-0.08	-0.43**	-0.17	-0.12	-0.12	-0.25	0.40**	-0.15	-0.35**
$D_4$	-0.71**	-0.27*	-0.42**	-0.41**	0.24	0.36**	0.20	-0.30*	-0.36**
$D_5$	-0.02	-0.49**	-0.21	-0.10	-0.19	-0.41**	0.23	-0.18	-0.40**
$D_6$	-0.03	-0.10	-0.01	0.10	-0.17	-0.14	0.16	0.12	-0.07
$D_7$	-0.01	-0.42**	-0.22	-0.08	-0.16	-0.37**	0.24	-0.18	-0.36**
$M_1$	-0.10	-0.31*	-0.31*	-0.16	-0.08	-0.27*	0.30**	-0.17	-0.32*
$M_2$	-0.14	-0.39**	-0.34**	-0.23	-0.10	-0.32*	0.34**	-0.21	-0.40**
$M_3$	0.00	-0.39**	-0.23	-0.13	-0.17	-0.39**	0.38**	-0.13	-0.35**
$M_4$	-0.73**	-0.21	-0.51*	-0.47**	0.25	0.35**	0.03	-0.34**	-0.36**
$M_5$	0.00	-0.40**	-0.27*	-0.13	-0.21	-0.45**	0.41**	-0.13	-0.40**
$M_6$	0.18	-0.16	-0.07	0.05	-0.23	-0.42**	0.21	0.06	-0.15
$M_7$	0.05	-0.35**	-0.23	-0.10	-0.20	-0.46**	0.38**	-0.09	-0.35**

\* and \*\* significant at 95 and 99 per cent confidence levels respectively,  $n = 60$

#### 6.4.6 Correlations Between Stand variables and Principal Component Images

PCA was performed using the spectral data on 60 sample points. It was done by using the spectral data of the three single-date images and also the combined two date TM images. Both the covariance matrix and correlation matrix were used to compute the principal components (PCs). The results of principal component analysis (PCA) and their correlations with stand variables are summarised in Tables 6.8-11.

The PCA was begun using the SPOT XS mode data (three channels) (Table 6.8). The PC1 explained 62% of the total variation of the covariance matrix and 68% of the correlation matrix, and PC1+PC2 together could explain up to 98%. PC1 computed from the covariance matrix was significantly correlated with stand age, top height, mean diameter and canopy depth ( $p < 0.01$ ) and volume ( $p < 0.05$ ), but not correlated with stand basal area, canopy cover or understorey cover. PC2 was only correlated with stand age or canopy cover. However, PC1 calculated from the correlation matrix was not significantly correlated with stand age, but correlated with top height, mean diameter and canopy depth ( $p < 0.01$ ) and volume ( $p < 0.05$ ), whereas PC2 showed a higher negative correlation with stand age ( $r = 0.65$ ,  $p < 0.001$ ) and canopy cover ( $r = 0.46$ ,  $p < 0.01$ ) than PC2 from the covariance matrix. Except for understorey cover which showed a correlation of 0.3-0.31, all other stand parameters showed no correlation with PC3.

Table 6.8 Results of PCA using SPOT data and correlation analysis between the stand variables and the principal component image.

Algorithms	By Covariance Matrix			By Correlation Matrix		
	PC1	PC2	PC3	PC1	PC2	PC3
PCs						
Var. Explained	61.62%	98.44%	100%	67.98%	97.83%	100%
Cumulative	61.62%	36.81%	1.56%	67.98%	29.86%	2.17%
AGE	-0.52**	0.44**	0.02	-0.22	-0.65**	0.01
BA	-0.13	-0.12	0.25	-0.18	0.03	0.25
TH	-0.49**	-0.04	0.14	-0.44**	-0.23	0.13
MD	-0.43**	-0.01	0.00	-0.37**	-0.23	-0.01
SN	0.35**	-0.04	0.07	0.28*	0.22	0.08
CC	0.18	-0.44**	0.10	-0.08	0.46**	0.11
UC	0.21	0.05	-0.31*	0.21	0.07	-0.30*
CD	-0.42**	-0.10	0.08	-0.41**	-0.14	0.08
VOL	-0.30*	-0.10	0.24	-0.31*	-0.08	0.23

\* and \*\* significant at 95 and 99 per cent confidence levels respectively,  $n = 60$

The PCs of the two TM data sets from the variance-covariance matrix made approximately equal contributions to the explanation of the total variance (see Tables 6.9 and 6.10). The first three PCs explain about 97% of the total variance. The correlations between PC1 of the February-9 TM image and basal area, top height, canopy coverage, stand volume and understory cover were significant at 95% or higher confidence levels, but not significant at 95% with stand age, mean diameter, stem number and canopy depth. PC1 of the April-21 image was significantly correlated with canopy cover, understory cover and volume ( $p < 0.05$  only). PC2 of the February-9 TM data was strongly correlated with seven stand variables - stand age, top height, mean diameter, density (stem number), canopy depth, volume and canopy cover ( $p < 0.01$ ). PC2 of the April-21 image, however, was correlated only with four stand variables - stand age, top height, mean diameter and canopy cover at a lower confidence level (95%) (except stand age at 99%). PC3 showed no significant correlations with any of these nine stand variables.

Table 6.9 Results of PCA using the February-9 TM data and correlation analysis between the stand variables and the principal component image.

Algorithms	By Covariance Matrix			By Correlation Matrix		
	PC1	PC2	PC3	PC1	PC2	PC3
PCs						
Var. Explained	74.19%	20.77%	2.19%	70.29%	15.24%	7.30%
Cumulative	74.19%	94.97%	97.15%	70.29%	85.53%	92.83%
AGE	-0.03	-0.79**	0.08	-0.05	-0.76**	-0.07
BA	-0.46**	-0.17	0.20	-0.40**	-0.16	0.14
TH	-0.28*	-0.50**	0.08	-0.27*	-0.46**	0.01
MD	-0.14	-0.51**	0.15	-0.15	-0.46**	0.07
SN	-0.20	0.38**	-0.06	-0.14	0.33**	-0.05
CC	-0.45**	0.48**	-0.01	-0.35**	0.49**	0.04
UC	0.39**	0.05	-0.07	0.41**	0.02	-0.10
CD	-0.16	-0.38**	0.19	-0.16	-0.35**	0.16
VOL	-0.43**	-0.33**	0.15	-0.39**	-0.29*	0.07

\* and \*\* significant at 95 and 99 per cent confidence levels respectively,  $n = 60$

As shown in Tables 6.9 and 6.10, the results of PCA from the correlation matrices differed somewhat from those from the variance-covariance matrices in variance



contributions of PCs and their correlations with stand variables. That is, the first two PCs calculated from the correlation matrices showed lower information content (lower explanatory power of total variance), and also lower correlations with stand variables, than the same PCs from the variance-covariance matrices. The third PCs, however, explained higher percentages of total variance than the same PCs from the variance-covariance matrices.

Table 6.10 Results of PCA using the April-21 TM data and correlation analysis between the stand variables and the principal component image.

<i>Algorithms</i>	By Covariance Matrix			By Correlation Matrix		
	PC1	PC2	PC3	PC1	PC2	PC3
<i>PCs</i>						
<i>Var. Explained</i>	72.52%	20.92%	3.43%	60.94%	16.30%	11.34%
<i>Cumulative</i>	72.52%	93.44%	96.87%	60.94%	77.23%	88.57%
AGE	-0.01	-0.53**	0.16	0.00	-0.42**	-0.36**
BA	-0.20	-0.05	-0.07	-0.22	-0.07	0.01
TH	-0.24	-0.34**	-0.03	-0.26*	-0.28*	-0.18
MD	-0.13	-0.33**	0.02	-0.15	-0.25	-0.21
SN	-0.13	0.22	-0.10	-0.13	0.17	0.17
CC	-0.31*	0.34**	-0.25	-0.37	0.23	0.32*
UC	0.34**	-0.20	-0.07	0.26*	-0.21	-0.06
CD	-0.07	-0.25	-0.02	-0.09	-0.23	-0.13
VOL	-0.27*	-0.16	-0.02	-0.28*	-0.12	-0.10

\* and \*\* significant at 95 and 99 per cent confidence levels respectively,  $n = 60$

Table 6.11 Results of PCA using the TM data for two dates (14 channels) and correlation analysis between the stand variables and the principal component image.

<i>Algorithms</i>	By Covariance Matrix			By Correlation Matrix		
	PC1	PC2	PC3	PC1	PC2	PC3
<i>PCs</i>						
<i>Var. Explained</i>	66.58%	19.09%	7.62%	55.99%	12.75%	9.92%
<i>Cumulative</i>	66.58%	85.67%	93.30%	55.99%	69.74%	79.67%
AGE	-0.03	-0.76**	0.17	-0.03	-0.73**	0.11
BA	-0.43**	-0.15	0.28*	-0.35**	-0.13	0.28*
TH	-0.29*	-0.47**	0.09	-0.29*	-0.45**	0.05
MD	-0.15	-0.46**	0.08	-0.15	-0.44**	0.04
SN	-0.20	0.29*	-0.02	-0.17	0.29*	0.01
CC	-0.44**	0.45**	-0.01	-0.41**	0.45**	0.00
UC	0.40**	0.00	0.02	0.35**	-0.07	-0.20
CD	-0.15	-0.32*	0.17	-0.13	-0.33**	0.12
VOL	-0.42**	-0.30*	0.18	-0.36**	-0.27*	0.18

\* and \*\* significant at 95 and 99 per cent confidence levels respectively,  $n = 60$

In the PCA of the multi-temporal TM images (14 channels), the variance contributions in the first three PCs were lower than those from single date TM images (See Table 6.11). Their correlations with stand parameters were close to the results obtained from the February-9 TM image. In addition, the PCA was also tried using the difference and mean images, but these did not give much higher correlations. The results were very close to those from the February-9 TM image. This is because most contributions (loadings of PCs) of variance were from the February-TM Image (see Chapter 5). This may further

indicate that the February-9 image is a better image for detecting the characteristics of radiata pine plantation stands.

### 6.4.7 Correlations Between Stand Variables and “Within-Image” Band Combinations

As different spectral bands have different optical properties and therefore different responses to the stand canopies (see Chapter 2), “within-image” band combinations may be useful in evaluating the relationships between stand variables and satellite images. The results of correlation analysis between the stand variables and the “within-image” band combinations are displayed in Tables 6.12-14. In addition to the three well-defined vegetation indices - AVI, RVI and NDVI, many other possible “within-image” band combinations (e.g. addition, subtraction and band ratios within images) were also tried. Most of the results obtained showed only marginal differences between the band combinations. Tables 6.12-14 list only the results of correlation analysis between stand parameters and the NIR-related band combinations as they show higher correlations than other band combinations.

Table 6.12 Correlations between stand variables and the “within-image” band combinations of SPOT image. XS3/1 and XS3-1 represent the ratio and differences of bands XS3 and XS1.

Stand Variables \ VI	AVI	RVI	NDVI	XS3/1	XS3-1
AGE	-0.60**	-0.41**	-0.41**	-0.47**	-0.59**
BA	0.04	0.11	0.08	0.17	0.10
TH	-0.16	0.05	0.04	0.02	-0.13
MD	-0.15	0.03	0.03	-0.03	-0.15
SN	0.16	0.03	0.01	0.11	0.18
CC	0.46**	0.41**	0.40**	0.46**	0.48**
UC	0.05	-0.01	0.00	-0.09	-0.02
CD	-0.07	0.13	0.11	0.08	-0.05
VOL	-0.04	0.09	0.07	0.12	0.01

Table 6.13 Correlations between stand variables and the “within-image” band combinations of the February-9 TM image. TM4-2, TM4/5, TM4/2 and TM4-1 denotes the differences and/or ratios of the corresponding band numbers.

Stand Variables \ VI	AVI	RVI	NDVI	TM4-2	TM4/2	TM4/5	TM4-1
AGE	-0.72**	-0.51**	-0.52**	-0.78**	-0.69**	-0.42**	-0.79**
BA	0.00	0.24	0.23	-0.15	0.03	0.33**	-0.15
TH	-0.37**	-0.16	-0.17	-0.46**	-0.31*	-0.05	-0.45**
MD	-0.38**	-0.21	-0.22	-0.45**	-0.34**	-0.14	-0.46**
SN	0.33**	0.34**	0.34**	0.30*	0.32*	0.38**	0.30*
CC	0.56**	0.59**	0.59**	0.47**	0.55**	0.64**	0.47**
UC	-0.14	-0.30*	-0.29*	0.00	-0.14	-0.28*	-0.02
CD	-0.25	-0.09	-0.10	-0.31*	-0.20	-0.03	-0.31*
VOL	-0.16	0.08	0.07	-0.30*	-0.12	0.20	-0.30*

\* and \*\* significant at 95 and 99 per cent confidence levels respectively,  $n = 60$

As can be seen from Table 6.12, the band combinations within the SPOT image were significantly correlated with stand age ( $|r| = 0.41 - 0.60$ ) and canopy cover (CC) ( $|r| =$

0.41 - 0.48) (significant at 99.9% confidence level), but not significantly correlated with any other stand variables ( $|r| = 0.02 - 0.17$ ). AVI and XS3-1 showed the highest correlation with stand age ( $|r| = 0.6$ ) compared with RVI and NDVI ( $|r| = 0.41$ ). The correlations of XS3/1 with the stand age and canopy cover were higher than with the three vegetation indices AVI, RVI and NDVI, but lower than with XS3-1.

Table 6.14 Correlations between stand variables and “within-image” band combinations of the April-21 TM image. For band combinations see Table 6.13.

VI Stand Variables	AVI	RVI	NDVI	TM4-2	TM4/2	TM4/5	TM4-1
AGE	-0.56**	-0.49**	-0.47**	-0.51**	-0.47**	-0.24	-0.50**
BA	-0.05	0.06	0.03	-0.05	0.05	0.29*	-0.05
TH	-0.33**	-0.19	-0.16	-0.34**	-0.25	0.08	-0.32*
MD	-0.33**	-0.23	-0.22	-0.32*	-0.26*	-0.04	-0.32*
SN	0.24	0.29*	0.26*	0.21	0.25	0.29*	0.20
CC	0.38**	0.47**	0.47**	0.33**	0.41**	0.48**	0.32*
UC	-0.15	-0.20	-0.19	-0.14	-0.19	-0.45**	-0.12
CD	-0.25	-0.18	-0.16	-0.24	-0.19	-0.01	-0.22
VOL	-0.18	-0.05	-0.05	-0.18	-0.08	0.25	-0.18

The results of correlation analysis between stand variables and the band combinations within the TM images were given in Tables 6.13 and 6.14. In addition to the strong associations with stand age and canopy cover, the band combinations were also correlated with several other stand variables. In general, the band differences (i.e. AVI, TM4-2 and TM4-1) showed better correlations with top height and mean diameter than the band ratios (i.e. RVI, NDVI, TM4/2 and TM4/5). Compared with the results from the original band data (Tables 6.5 and 6.6), the “within-image” band combinations were better associated with stand density (Tables 6.13 and 6.14). These band combinations, however, did not improve the correlations with stand volume, basal area, and canopy depth.

### 6.4.8 Canonical Correlations

Earlier sections have investigated the relationships between single stand variables and spectral values. This section focuses on the correlation analysis between two variable groups using canonical correlation techniques. Based on the computational procedures described in Section 6.3.3, four canonical correlation analyses were performed to test the correlations between the stand variables and the three original images and site variables (i.e. DTM and soil data). The analyses were undertaken by computing canonical correlations and canonical variables, significance tests, redundancy analysis and interpretation of corresponding canonical correlations and variables.

### 6.4.8.1 Canonical Correlations Between Stand Variables and SPOT Image

Table 6.15a presents the canonical correlation coefficients, eigenvalues and their variance proportion and the significance tests using SPOT data. The first canonical correlation (0.85) explained 78.57% of the total variance, and together with the second canonical correlation (0.58) up to 94.11% (Table 6.15a). The null hypothesis test showed the first two canonical correlations were significant ( $p < 0.005$  and  $0.025$  respectively) and no significant correlation in the third canonical variables. Thus further analysis was concentrated on the first two canonical variables. Based on the standardised canonical coefficients obtained, the canonical variables can be written as the linear combinations (the definition of variables  $x_i$  were listed in Table 6.15b):

$$\begin{array}{l}
 \text{The first pair of} \\
 \text{canonical variables} \\
 \\
 \text{The second pair of} \\
 \text{canonical variables}
 \end{array}
 \left\{
 \begin{array}{l}
 u_1 = 1.16x_1 - 0.67x_2 - 0.25x_3 - 0.48x_4 - 1.08x_5 \\
 \quad - 0.08x_6 + 0.03x_7 + 0.04x_8 - 1.54x_9 \\
 v_1 = -0.91y_1 + 0.23y_2 - 1.02y_3 \\
 \\
 u_2 = -1.08x_1 - 0.10x_2 + 1.02x_3 + 0.87x_4 - 0.73x_5 \\
 \quad + 0.16x_6 + 0.39x_7 + 0.31x_8 - 0.26x_9 \\
 v_2 = 2.00y_1 - 1.37y_2 + 0.17y_3
 \end{array}
 \right.
 \begin{array}{l}
 \text{For Stand Variables} \\
 \text{for SPOT XS data} \\
 \\
 \text{For Stand Variables} \\
 \text{for SPOT XS data}
 \end{array}$$

where  $x_1, \dots, x_9$  are the stand variables defined in Table 6.15b, and  $y_1, \dots, y_3$  represent SPOT XS bands 1 to 3.

Table 6.15a Results of CCA between stand variables and the SPOT (XS bands only) data.

Canonical Correlation					Significance test				
	Canonical Correlations	Eigen Values	Prop. (%)	Cum. (%)	$\Lambda_i$	$\chi^2$	DF	p	Decision
1	0.845	2.500	78.57	78.57	0.161	97.70	27	< 0.005	Reject
2	0.575	0.494	15.54	94.11	0.564	30.68	16	< 0.025	Reject
3	0.397	0.187	5.89	100.0	0.842	9.19	7	< 0.400	Accept

Table 6.15b Standardised canonical coefficients and correlations between the original variables and the canonical variables of opposite sets of variables.

Stand Variables					SPOT Data				
Standardised Canonical Coefficients for stand variables			Corr. Between Stand Var. & 1st two Cano. Var. of SPOT Data		Standardised Canonical Coefficients for SPOT Data			Corr. Between SPOT Data & 1st two Cano. Var. of Stand Var.	
$x$	$u_1$	$u_2$	$r_{v_1}$	$r_{v_2}$	$y$	$v_1$	$v_2$	$r_{u_1}$	$r_{u_2}$
TH ( $x_1$ )	1.158	-1.079	-0.103	-0.464	XS1 ( $y_1$ )	-0.907	2.002	-0.295	0.457
VOL ( $x_2$ )	-0.665	-0.098	0.042	-0.397	XS2 ( $y_2$ )	0.233	-1.372	-0.352	0.289
MD ( $x_3$ )	-0.246	1.023	-0.142	-0.334	XS3 ( $y_3$ )	1.024	0.169	0.644	0.339
SN ( $x_4$ )	-0.478	0.872	0.176	0.220					
BA ( $x_5$ )	1.084	-0.733	0.123	-0.268					
CD ( $x_6$ )	-0.089	0.160	-0.035	-0.386					
UC ( $x_7$ )	0.033	0.387	-0.050	0.356					
CC ( $x_8$ )	0.037	0.308	0.483	0.012					
AGE ( $x_9$ )	-1.544	0.259	-0.576	-0.350					

As shown above, the canonical variables are the linear combinations of the original variables, therefore the variables with the higher loadings (called canonical coefficients in

CCA) usually make higher contributions to the total variance. As can be seen from Table 6.15b, The first canonical variable ( $u_1$ ) for the stand variables was mainly contributed by stand age (-1.54), top height (1.16) and basal area (1.08), with most emphasis on stand age (age also showed the highest correlation with the first canonical variables (-0.58)). The first canonical variable for SPOT XS data ( $v_1$ ) was focused on XS3 (1.02) and XS1 (-0.91), with more emphasis on XS3. XS3 also had the highest correlation (0.64) with the first canonical variable of the stand variables. The second pair of canonical variables ( $u_2$  and  $v_2$ ) was mainly contributed by top height (-1.08) and mean diameter for the stand variables and XS1 and XS2 for the SPOT image. This result matched the result obtained in Section 6.4.4, where XS3 was shown to have a strong correlation with stand age (see Chapter 5), and top height was correlated with XS1 (see Table 6.6).

Table 6.15c Canonical redundancy analysis between stand variables and SPOT data.

<i>Standardised Variance of the Stand Variables Explained by</i>						
<i>Their Own Canonical Variables</i>			<i>The Opposite Canonical Variables</i>			<i>Decisions</i>
<i>Canonical Variables</i>	<i>Proportion (%)</i>	<i>Cumulative Proportion</i>	<i>Canonical R-Squared</i>	<i>Proportion (%)</i>	<i>Cumulative Proportion</i>	
1	10.06	10.06	0.714	7.25	7.19	None
2	33.69	43.75	0.331	11.18	18.33	*
3	14.24	57.99	0.158	2.30	20.58	None
<i>Standardised Variance of the SPOT XS Images Explained by</i>						
1	29.21	29.21	0.714	20.86	20.86	*
2	41.07	70.28	0.331	13.59	34.45	*
3	29.72	100.00	0.158	4.69	39.14	None

\* means that the canonical variables are good overall predictors of the opposite set of variables.

The canonical redundancy analysis (Table 6.15c) showed that the second pair of canonical variables for the stand variables was a good overall predictor of the opposite set of variables, the proportion of the variance explained being highest (11%) and much larger than the other two canonical variables (7% and 2%). The first canonical variable for SPOT XS data explained the highest proportion of the variance (21%). The results of CCA showed that the relationships between the nine stand variables and SPOT data were dominated by stand age, top height and basal area for the stand variables and XS3 and XS1 bands for the SPOT data, with more emphasis on stand age and the XS3 band. Based on the canonical coefficients (loadings), the importance of the variables in both sets of variables can be ranked as follows:

Order	1	2	3	4	5	6	7	8	9								
$u_1$ :	AGE	⇒	TH	⇒	BA	⇒	VOL	⇒	SN	⇒	MD	⇒	CD	⇒	CC	⇒	UC
$v_1$ :	XS3	⇒	XS1	⇒	XS2												
$u_2$ :	TH	⇒	MD	⇒	SN	⇒	BA	⇒	UC	⇒	CC	⇒	AGE	⇒	VOL	⇒	CD
$v_2$ :	XS1	⇒	XS2	⇒	XS3												

### 6.4.8.2 Canonical Correlations Between Stand Variables and TM Data

With the same analysis procedures, the results of CCA between the stand variables and the two date TM data sets are presented in Tables 6.16 and 6.17 respectively. The significance test of the canonical correlations for the February-9 TM data (excluding band 6) and stand variables showed that only the first two pairs of canonical variables were significantly correlated, with the canonical correlations being 0.87 and 0.65 respectively (Tables 6.16a). They explained 71% and 17% respectively of the total variances and 88% when combined. The canonical variables can be written as the following linear combinations:

$$\begin{array}{l}
 \text{The first pair of} \\
 \text{canonical variables} \\
 \\
 \text{The second pair of} \\
 \text{canonical variables}
 \end{array}
 \left\{
 \begin{array}{ll}
 \begin{array}{l}
 u_1 = 0.55x_1 - 0.47x_2 + 0.09x_3 + 0.08x_4 + 0.33x_5 \\
 \quad + 0.09x_6 - 0.14x_7 + 0.26x_8 - 1.16x_9 \\
 v_1 = -0.30y_1 + 0.0y_2 + 0.08y_3 + 1.01y_4 - 0.95y_5 + 0.68y_6
 \end{array} & \begin{array}{l}
 \text{for stand} \\
 \text{Variables} \\
 \\
 \text{for TM data}
 \end{array} \\
 \\
 \begin{array}{l}
 u_2 = -0.93x_1 + 0.66x_2 - 0.36x_3 - 0.37x_4 - 0.59x_5 \\
 \quad + 0.28x_6 + 0.32x_7 - 0.30x_8 - 0.02x_9 \\
 v_2 = -0.30y_1 + 0.22y_2 - 0.12y_3 + 0.37y_4 + 1.45y_5 - 0.43y_6
 \end{array} & \begin{array}{l}
 \text{for stand} \\
 \text{Variables} \\
 \\
 \text{for TM data}
 \end{array}
 \end{array}
 \right.$$

where  $x_1, \dots, x_9$  are the stand variables, and  $y_1, \dots, y_6$  represent TM band number.

As shown in Table 6.16b and above linear combinations, stand age ( $x_9$ ) had the highest loadings (-1.16) in the first canonical variable of the stand variables and also the highest correlation (0.74) with the first canonical variable of the opposite set of variables (i.e. the 2TM data). 2TM4 ( $y_4$ ) did the same in the first canonical variable of the February-9 TM data. Stand age and 2TM4 were therefore seen as the dominant variable in the first pair of canonical variables. The second pair of canonical variables were dominated by top height ( $x_1$ , -0.93) and 2TM5 ( $y_5$ ), as they both had the largest loadings (-0.93 and 1.45 respectively) and as well as the highest correlations with the canonical variables of the opposite sets of variables. Based on the canonical coefficients (loadings), the importance of the variables in the first two canonical variables may ranked as:

Order	1	2	3	4	5	6	7	8	9
$u_1$ :	AGE	⇒ TH	⇒ VOL	⇒ BA	⇒ CC	⇒ UT	⇒ CD	⇒ SN	⇒ MD
$v_1$ :	TM4	⇒ TM5	⇒ TM7	⇒ TM1	⇒ TM3	⇒ TM2			
$u_2$ :	TH	⇒ VOL	⇒ BA	⇒ SN	⇒ MD	⇒ UC	⇒ CC	⇒ CD	⇒ AGE
$v_2$ :	TM5	⇒ TM7	⇒ TM4	⇒ TM1	⇒ TM2	⇒ TM3			

The canonical redundancy analysis (Table 6.16c) indicates that the first two canonical variables for stand variables can be explained by the canonical variables for the February-9 TM data by 15.67% and 14.71% respectively, whereas the first canonical variables of the February-9 TM data could explain 14.64% and 23.93% of the stand variables. The emphasis in the stand variables was on stand age and top height, and in the February-9 TM data was on TM4, TM5 and TM7.

Table 6.16a Results of CCA between stand variables and February-9 TM data.

Canonical Correlation					Significance test				
	Canonical Correlations	Eigen Values	Prop. (%)	Cum. (%)	$\Lambda_i$	$\chi^2$	DF	p	Decision
1	0.866	2.999	70.88	70.88	0.094	120.334	54	< 0.005	Reject
2	0.652	0.739	17.46	88.34	0.375	50.077	40	< 0.100	Reject
3	0.494	0.322	7.62	95.96	0.643	22.524	28	< 0.450	Accept
4	0.345	0.136	3.20	99.16	0.851	8.256	18	< 0.900	"
5	0.147	0.022	0.52	99.68	0.965	1.793	10	< 0.990	"
6	0.115	0.013	0.32	100	0.987	0.679	4	< 0.990	"

Table 6.16b Standardised canonical coefficients and correlations between the original variables and the canonical variables of opposite sets of variables.

Stand Variables					The February-9 TM (2TM) Data (6 bands)				
Standardised Canonical Coefficients for stand variables			Corr. Between Stand Var. & 1st two Cano. Vars. of 2TM Data		Standardised Canonical Coefficients 2TM Data			Corr. Between 2TM Data & 1st two Cano. Var. of Stand Var.	
x	$u_1$	$u_2$	$r_{v_1}$	$r_{v_2}$	y	$v_1$	$v_2$	$r_{u_1}$	$r_{u_2}$
TH ( $x_1$ )	0.552	-0.928	-0.369	-0.445	TM1 ( $y_1$ )	-0.298	-0.299	-0.139	0.432
VOL ( $x_2$ )	-0.465	0.664	-0.178	-0.561	TM2 ( $y_2$ )	0.000	0.215	-0.133	0.520
MD ( $x_3$ )	0.089	-0.364	-0.401	-0.317	TM3 ( $y_3$ )	0.077	-0.121	-0.234	0.511
SN ( $x_4$ )	0.078	-0.366	0.349	-0.118	TM4 ( $y_4$ )	1.011	0.367	0.757	0.287
BA ( $x_5$ )	0.331	-0.586	-0.027	-0.538	TM5 ( $y_5$ )	-0.956	1.452	-0.319	0.590
CD ( $x_6$ )	0.090	0.277	-0.263	-0.285	TM7 ( $y_7$ )	0.678	-0.430	-0.335	0.536
UC ( $x_7$ )	-0.136	0.322	-0.102	0.370					
CC ( $x_8$ )	0.264	-0.297	0.568	-0.307					
AGE ( $x_9$ )	-1.160	-0.021	-0.744	-0.308					

Table 6.16c Canonical redundancy analysis for February-9 TM data and the stand variables.

Standardised Variance of the Stand Variables Explained by						
Their Own Canonical Variables			The Opposite Canonical Variables			Decisions
Canonical Variables	Proportion (%)	Cumulative Proportion	Canonical R-Squared	Proportion	Cumulative Proportion	
1	20.89	20.89	0.750	15.67	15.67	*
2	34.63	55.53	0.425	14.71	30.38	*
3	3.44	58.97	0.244	0.84	31.22	negligible
4	2.81	61.78	0.119	0.34	31.56	"
5	14.94	76.72	0.022	0.32	31.88	"
6	2.86	79.58	0.013	0.04	31.91	"
Standardised Variance of the February-TM Data Explained by						
1	19.52	19.52	0.750	14.64	14.64	*
2	56.32	75.84	0.425	23.93	38.56	*
3	1.62	77.46	0.244	0.40	38.96	negligible
4	13.75	91.22	0.119	1.64	40.60	"
5	6.28	97.49	0.022	0.14	40.74	"
6	2.51	100	0.013	0.03	40.77	"

\* means that the canonical variables are good overall predictor of the opposite set of variables.

The results of CCA between stand variables and the April-21 TM data were given in Tables 6.17a-6.17c. Only the first pair of canonical variables were significantly correlated ( $r = 0.74$ ,  $p < 0.007$ ), but it explained lower percentage of total variance (55.41%) than the same canonical variables of other two data sets (78.57% and 70.88% respectively, see Tables 6.15a and 6.16a). Stand age ( $x_9$ ) showed the highest loading (1.01) to the first canonical variable. In addition, basal area ( $x_5$ ) (0.86) and stand density ( $x_1$ ) (-0.78) also

showed higher loadings than other stand variables. The MIR band (TM5) contributed most information to the first canonical variables (Table 6.17b). Although the second pair of canonical variables was not significantly correlated ( $r = 0.56$ ,  $p < 0.34$ ), top height and the NIR band produced the highest loadings in stand variables and TM data.

$$\begin{array}{l}
 \text{The first pair of} \\
 \text{canonical variables} \\
 \\
 \text{The second pair of cano.} \\
 \text{variables}
 \end{array}
 \left\{
 \begin{array}{l}
 u_1 = -0.50x_1 - 0.50x_2 - 0.65x_3 - 0.78x_4 + 0.86x_5 \\
 \quad + 0.13x_6 + 0.54x_7 - 0.21x_8 + 1.01x_9 \\
 v_1 = -0.06y_1 - 0.10y_2 + 0.51y_3 - 0.68y_4 + 0.78y_5 - 0.12y_6 \\
 \\
 u_2 = -1.29x_1 + 0.89x_2 - 0.76x_3 - 0.92x_4 + 0.35x_5 \\
 \quad + 0.37x_6 - 0.04x_7 - 0.54x_8 - 0.61x_9 \\
 v_2 = 0.39y_1 + 0.42y_2 - 0.26y_3 + 0.61y_4 - 0.09y_5 + 0.24y_6
 \end{array}
 \right.
 \begin{array}{l}
 \text{for stand} \\
 \text{Variables} \\
 \\
 \text{for 4TM data} \\
 \\
 \text{for stand} \\
 \text{Variables} \\
 \\
 \text{for 4TM7 data}
 \end{array}$$

Table 6.17a Results of CCA between stand variables and the April-21 TM data.

Canonical Correlation					Significance test				
	Canonical Correlations	Eigen Values	Prop. (%)	Cum. (%)	$\Lambda_i$	$\chi^2$	DF	p	Decision
1	0.740	1.207	55.41	55.41	0.194	83.53	54	< 0.007	Reject
2	0.561	0.460	21.11	76.51	0.429	43.16	40	< 0.342	Accept
3	0.437	0.236	10.83	87.35	0.626	23.87	28	< 0.691	"
4	0.402	0.193	8.85	96.20	0.774	13.06	18	< 0.789	"
5	0.274	0.081	3.71	99.91	0.923	4.07	10	< 0.944	"
6	0.045	0.002	0.09	100	0.998	0.10	4	< 0.999	"

Table 6.17b Standardised canonical coefficients and correlations between the original variables and the canonical variables of opposite sets of variables.

Stand Variables					The February-9 TM (4TM) Data (6 bands)				
Standardised Canonical Coefficients for stand variables			Corr. Between Stand Var. & 1st two Cano. Vars. of 4TM Data		Standardised Canonical Coefficients 4TM Data			Corr. Between 4TM Data & 1st two Cano. Var. of Stand Var.	
x	$u_1$	$u_2$	$r_{v_1}$	$r_{v_2}$	y	$v_1$	$v_2$	$r_{u_1}$	$r_{u_2}$
TH ( $x_1$ )	-0.498	-1.290	0.075	-0.440	TM1 ( $y_1$ )	-0.060	0.386	0.277	0.405
VOL ( $x_2$ )	-0.496	0.891	-0.056	-0.342	TM2 ( $y_2$ )	-0.104	0.416	0.293	0.435
MD ( $x_3$ )	-0.647	-0.761	0.158	-0.346	TM3 ( $y_3$ )	0.514	-0.262	0.446	0.323
SN ( $x_4$ )	-0.776	-0.915	-0.269	0.055	TM4 ( $y_4$ )	-0.677	0.606	-0.316	0.453
BA ( $x_5$ )	0.861	0.355	-0.098	-0.230	TM5 ( $y_5$ )	0.778	-0.095	0.527	0.313
CD ( $x_6$ )	0.125	0.374	0.134	-0.255	TM7 ( $y_7$ )	-0.123	0.240	0.539	0.264
UC ( $x_7$ )	0.539	-0.038	0.363	0.085					
CC ( $x_8$ )	-0.206	-0.544	-0.495	-0.049					
AGE ( $x_9$ )	1.009	-0.608	0.409	-0.393					

The canonical redundancy analysis showed that the first two canonical variables for both sets of variables showed similar contributions to the canonical variables of the opposite sets of variables (Table 6.17c). Other canonical variables explained only small proportions of total variance (< 2.6%). The conclusion is that the dominated variables were stand age and top height for the stand variables and the NIR and MIR bands for the 4TM image. Based on the canonical coefficients (loadings), the importance of the variables in both sets of variables were ranked as follows:



Order	1	2	3	4	5	6	7	8	9
$u_1$ :	AGE	⇒ BA	⇒ SN	⇒ MD	⇒ UC	⇒ TH	⇒ VOL	⇒ CC	⇒ CD
$v_1$ :	TM5	⇒ TM4	⇒ TM3	⇒ TM7	⇒ TM2	⇒ TM1			
$u_2$ :	TH	⇒ SN	⇒ VOL	⇒ MD	⇒ AGE	⇒ CC	⇒ CD	⇒ BA	⇒ UC
$v_2$ :	TM4	⇒ TM2	⇒ TM1	⇒ TM3	⇒ TM7	⇒ TM5			

Table 6.17c Canonical redundancy analysis for April-21 TM data and stand variables.

<i>Standardised Variance of the Stand Variables Explained by</i>						
Their Own Canonical Variables			The Opposite Canonical Variables			Decisions
Canonical Variables	Proportion (%)	Cumulative Proportion	Canonical R-Squared	Proportion	Cumulative Proportion	
1	13.77	13.77	0.547	7.53	7.53	*
2	25.21	38.98	0.315	7.94	15.57	*
3	03.02	42.00	0.191	0.68	16.05	negligible
4	10.94	52.93	0.162	1.87	17.82	"
5	07.96	60.89	0.075	0.60	18.41	"
6	03.36	64.25	0.002	0.01	18.42	"
<i>Standardised Variance of the April-21 TM Images Explained by</i>						
1	31.38	31.38	0.547	17.16	17.16	*
2	43.90	75.28	0.315	13.83	30.99	*
3	13.65	88.92	0.191	2.61	33.59	negligible
4	01.19	90.01	0.162	0.18	33.77	"
5	02.90	92.91	0.075	0.22	33.99	"
6	07.19	100.00	0.002	0.01	34.00	"

\* means that the canonical variables are good overall predictor of the opposite set of variables.

### 6.4.8.3 Canonical Correlations Between Stand and Site Variables

The results of CCA between the eight stand variables (not including age) and six site variables are given in Tables 6.18a-c. Stand age is placed in the site variable groups for canonical correlation analysis, since it is strongly associated with stand variables but has nothing to do with site variables. The results of CCA are given in Table 6.18a-6.18c. The linear combinations of the first two pairs of canonical variables for the stand and site variable groups were written as:

$$\begin{array}{l}
 \text{The first pair of canonical variables} \\
 \left\{ \begin{array}{l}
 u_1 = 0.562x_1 + 0.09x_2 - 0.07x_3 - 0.29x_4 + 0.53x_5 \\
 \quad - 0.08x_6 + 0.032x_7 - 0.40x_8 \\
 v_1 = 0.004y_1 - 0.001y_2 - 0.303y_3 + 0.14y_4 - 0.16y_5 \\
 \quad - 0.10y_6 + 0.82y_7
 \end{array} \right. \begin{array}{l}
 \text{for stand} \\
 \text{Variables} \\
 \text{for site variables}
 \end{array}
 \end{array}$$

$$\begin{array}{l}
 \text{The second pair of canonical variables} \\
 \left\{ \begin{array}{l}
 u_2 = -0.65x_1 + 0.86x_2 + 1.92x_3 + 1.02x_4 + -1.72x_5 \\
 \quad - 0.05x_6 - 0.20x_7 - 0.92x_8 \\
 v_2 = -0.18y_1 + 0.08y_2 + 0.21y_3 + 0.59y_4 + 0.58y_5 \\
 \quad - 0.09y_6 - 0.05y_7
 \end{array} \right. \begin{array}{l}
 \text{for stand} \\
 \text{Variables} \\
 \text{for site variables}
 \end{array}
 \end{array}$$

where  $x_1, x_2, \dots, x_8$  represent the stand variables (see Table 6.15b),  $y_1$  - slope (SLP),  $y_2$  - aspect (ASP),  $y_3$  - altitude (ALT),  $y_4$  - topographic positions (TP),  $y_5$  - the soil depth of A and B horizons (AB),  $y_6$  - gravel contents (GC), and  $y_7$  - stand age (AGE).

Table 6.18a Canonical correlation analysis between stand and site variables.

Canonical Correlation					Significance test				
	Canonical Correlations	Eigen Values	Prop. (%)	Cum. (%)	$\Lambda_i$	$\chi^2$	DF	p	Decision
1	0.910	4.806	72.70	72.70	0.0424	161.20	56	0.001	Reject
2	0.701	0.964	14.58	87.28	0.2461	71.50	42	0.003	Reject
3	0.572	0.487	7.36	94.64	0.4833	37.09	30	0.177	Accept
4	0.410	0.202	3.06	97.70	0.7185	16.86	20	0.663	"
	0.292	0.094	1.41	99.11	0.8637	7.47	12	0.825	"
5	0.231	0.056	0.85	99.96	0.9445	2.91	6	0.820	"
6	0.050	0.003	0.04	100.00	0.9975	0.13	2	0.939	"

Table 6.18b Standardised canonical coefficients and correlations between the original variables and the canonical variables of opposite sets of variables.

Stand Variables					Site Variables				
Standardised Canonical Coefficients for stand variables			Corr. Between Stand Vars. & 1st two Cano. Vars. of Site Vars.		Standardised Canonical Coefficients for Site Variables			Corr. Between Site vars. & 1st two Cano. Vars. of Stand Var.	
$x$	$u_1$	$u_2$	$r_{v_1}$	$r_{v_2}$	$y$	$v_1$	$v_2$	$r_{u_1}$	$r_{u_2}$
TH ( $x_1$ )	0.562	-0.654	0.838	0.145	SLP ( $y_1$ )	0.004	-0.181	0.082	-0.279
VOL ( $x_2$ )	0.096	0.863	0.700	0.173	ASP ( $y_2$ )	0.001	0.085	0.107	0.030
MD ( $x_3$ )	-0.065	1.919	0.785	0.269	ALT ( $y_3$ )	-0.303	0.210	-0.549	-0.133
SN ( $x_4$ )	-0.289	1.021	-0.402	-0.059	TP ( $y_4$ )	0.136	0.592	0.261	0.525
BA ( $x_5$ )	0.530	-1.724	0.489	0.088	AB ( $y_5$ )	-0.162	0.585	0.010	0.561
CD ( $x_6$ )	-0.080	-0.046	0.701	0.069	GC ( $y_6$ )	-0.099	-0.088	-0.075	-0.375
UC ( $x_7$ )	0.032	0.202	-0.143	0.094	AGE ( $y_7$ )	0.823	-0.054	0.852	-0.069
CC ( $x_8$ )	-0.399	0.922	-0.269	0.355					

Table 6.18c Canonical redundancy analysis for site and stand variables

Standardised Variance of the Stand Variables Explained by						
Their Own Canonical Variables			The Opposite Canonical Variables			Decisions
Canonical Variables	Proportion (%)	Cumulative Proportion	Canonical R-Squared	Proportion (%)	Cumulative Proportion	
1	42.19	42.19	0.828	34.93	34.93	*
2	6.97	49.16	0.491	3.42	38.35	negligible
3	4.07	53.23	0.327	1.33	39.68	"
4	10.96	64.20	0.168	1.84	41.52	"
5	9.77	73.96	0.086	0.84	42.36	"
6	8.24	82.20	0.053	0.44	42.80	"
7	10.25	92.45	0.003	0.03	42.82	"
Standardised Variances of the Site Variables Explained by						
1	19.33	19.33	0.828	16.00	16.00	*
2	24.21	43.53	0.491	11.88	27.88	*
3	10.77	54.30	0.327	3.53	31.40	negligible
4	10.18	64.48	0.168	1.71	33.11	"
5	12.09	76.58	0.086	1.03	34.15	"
6	14.84	91.42	0.053	0.79	34.94	"
7	8.58	100	0.002	0.02	34.96	"

\* means that the canonical variables are good overall predictor of the opposite set of variables.

As can be seen from Table 6.18a, the first two canonical correlations exceeded 0.7 and were significant at  $p < 0.001$  and  $p < 0.003$  confidence levels respectively. They together explained 87% of the total variance. The first canonical variable (linear combination) for

stand variables was dominated by top height ( $x_1$ ) (0.56) and basal area ( $x_5$ ) (0.53), with more emphasis on top height. The correlation between top height and the first canonical variable of site variables was as high as 0.84. Thus, stand top height can be seen as the best indicator of site quality. Stand age has a large positive canonical coefficient (loading = 0.82) and large positive correlation with the first canonical variable of the stand variable set ( $r = 0.85$ ). This indicates that the first canonical variables are mainly contributed by top height and stand age. Of the other site variables, altitude ( $y_3$ ) showed higher negative canonical coefficients (loading = -0.30) and a large negative correlation with the canonical variable ( $r = -0.55$ ) of stand variables, meaning stand growth decreased with increasing altitude. The other stand and site variables can be considered negligible as they had relatively low loadings and correlations with canonical variables of the opposite variable sets (see Table 6.18b).

The second canonical variable was concentrated on mean diameter (MD,  $x_3$ ) and basal area (BA,  $x_5$ ) in the stand variable set, the canonical coefficients being 1.92 and -1.72 respectively, with the emphasis on mean diameter. In the site variable set, topographic position (TP,  $y_4$ ) and soil depth (AB,  $y_5$ ) had nearly equal loadings (0.592 and 0.585 respectively), more than twice as large as the loadings of the other site variables (Table 6.18b). This indicates that these two variables had most effects on the growth of the radiata pine stands.

The canonical redundancy analysis showed neither of the first pair of canonical variables was a good overall predictor of the opposite sets of variables, the proportions of variance explained being 35% and 16% respectively (Table 6.18c). The other canonical variables added virtually nothing to the total variance of stand variables. The second canonical variable of site variables also made some contribution to the total variance of the site variables (12%). The third and higher canonical variables can be neglected since they added almost nothing to explain the total variance of site variables.

Based on their contributions (i.e. loadings of the canonical correlation coefficients) to the canonical variables, the variables in both sets can be ranked as follows:

Order	1	2	3	4	5	6	7	8
$u_1$ :	TH	⇒ BA	⇒ CC	⇒ SN	⇒ VOL	⇒ CD	⇒ MD	⇒ UC
$v_1$ :	AGE	⇒ ALT	⇒ AB	⇒ TP	⇒ GC	⇒ SLP	⇒ ASP	
$u_2$ :	MD	⇒ BA	⇒ SN	⇒ CC	⇒ VOL	⇒ TH	⇒ UC	⇒ CD
$v_2$ :	TP	⇒ AB	⇒ ALT	⇒ SLP	⇒ ASP	⇒ GC	⇒ AGE	

## **6.5 DISCUSSION**

### **6.5.1 Sensitivity of SPOT and TM Data**

As discussed in the previous chapter, radiometric resolution is an important factor affecting the sensitivity of spectral reflectance to the stand structures. The spectral values for plantation cover are concentrated within a small data range. As shown in Table 6.3, the data ranges for the 60 sample points from age 9 to 42 are 17, 17, 19 for the three XS bands of the SPOT data, 12, 8, 20, 24, 50, 13, 21 for the February-9 TM data, and 7, 3, 6, 17, 22, 7 and 9 for the April-21 TM data. Except for the TM5 band of the February-9 image, all the spectral data ranges were less than the age range of the stands (33 years). As shown in the previous chapters, the spectral response to the radiata pine plantation stands became consistent after 25 years of age, however some of the stand variables continued to increase after 25 years old. This means the radiometric resolution of both TM and SPOT data may not be sensitive enough to differentiate the subtle variations of forest stand structure.

### **6.5.2 The Capability of SPOT and TM Data to Estimate Stand Variables**

As discussed above, decreasing spectral reflectance with increasing stand age resulted in negative correlations with stand variables, most of which are positively correlated with stand age.

Although the correlations were highly significant for some stand variables, the correlation coefficients were still relatively low. This indicates that there was much unexplained variance or non-linearity in using these spectral band data to estimate stand variables. The higher correlation between stand age and the NIR band can be helpful in predicting the stand variables directly related to stand age, such as mean annual increment and site index. This is addressed in the next chapter in estimating site quality by integrating remotely sensed and ancillary data.

### **6.5.3 Comparisons of SPOT and TM DATA**

The results of the correlation analyses presented in this chapter showed the two summer images to be similar in their relations with stand variables. This indicates that under similar data-recording conditions (e.g. same growing season) these two systems can provide similar information on vegetation. Therefore, a wide range of applications in forest monitoring and stand observation may be approached by using multiple sensor data sets which involve TM and SPOT imagery.

However, there may be significant differences in the information provided by either SPOT or TM about stands depending on the time of year in which the imagery data were taken. In this study, the correlations from the autumn image were much poorer than with the summer images. This difference may be due to effects such as changes in the understorey on the reflectance. On the other hand, these differences can also be attributed to the effects of factors such as different sun angles, soil and atmospheric conditions, and even external disturbances (e.g. thinning, pruning and/or fire-burning). The application of corrections for terrain and atmospheric effects may improve the ability of imagery data to detect the changes of stand quality and yield.

Nevertheless, the SPOT HRV sensor has fewer spectral bands than the TM sensor. The two MIR bands (TM5 and TM7) of TM images can provide useful information on stand structure variables. In this study, for example, these two MIR bands were better correlated with basal area, volume and canopy closure than the visible and NIR bands.

#### **6.5.4 Selection of Predictable Stand Variables**

In general, spectral reflectance values in all bands decreased with stand growth. Several stand variables in this work (i.e stand age, top height, mean diameter and canopy cover) showed significant correlations with some spectral band data. This indicates that these stand variables may be predictable from satellite data with some degree of accuracy. However, the accuracies may vary greatly with data type, growing season and data quality. As discussed in Chapter 5, after stands achieve full canopy closure at about 5 to 10 years old, the spectral values showed a gentle decrease with increasing stand age, and became consistent after about 30 years of age. Therefore, the stand variables such as volume, height and diameter may be estimated in the stands between age 5 and 30 years old. It becomes relatively difficult to estimate stand variables after 30 years old due to these consistent or fluctuating reflectance values (see Chapter 5); while stand variables can continue increasing after this age stage, the rate of growth is not as fast as the younger stands. In particular, less canopy depth, density, needle amount and canopy shadow occurring in the mature and over-mature stands lead to higher ground reflectance values and therefore a lower estimate of stand variables.

Tree density normally remains virtually unchanged from say age 3 and the first thinning (if no significant mortality occurred in the first few years). Thus the change of spectral value does not result from tree density but from canopy density and size before thinning. In the older stands, the tree density is usually low because of the removal of trees by thinning, while the spectral value may change little because the canopy density, size and coverage

are still at a high level. This indicates that tree density cannot be predicted from spectral data. This may explain the poor correlation between density and spectral values in all bands in this chapter.

The high correlation between stand age and NIR bands further supports the results obtained in Chapter 5. The age variable is the variable described best by spectral data. It showed a more consistent correlation with spectral data (in NIR band) than any other stand variables which usually showed varied correlations. In addition to stand age, stand top height and stand mean diameter also showed good correlation with some spectral bands, the NIR band in particular.

Previous studies have indicated that stand volume can be estimated with satisfactory accuracy over large areas (region or country level), as stand volume was strongly correlated with spectral data (Franklin 1986; Jaakkola 1986b; Peng 1987; and Poso *et al.* 1987). However, the accuracy of estimation for small areas is relatively low (Jaakkola 1986b). In this study, sample point based (3 x 3 pixel window) volume was statistically significantly related to some spectral bands or band combinations, but the correlation coefficients obtained were relatively low.

### **6.5.5 Principal Component Images**

The results of PCA indicate that the spectral information on stand structure can be extracted by the first two principal components which encompass 90% or more of the total variation in the multi-band data. Their correlations with stand variables were very similar to those obtained for the original spectral band data. In general, the “brightness” (PC1) image was significantly correlated with stand basal area and canopy cover, while the “greenness” (PC2) image was strongly correlated with stand age and top height. This is helpful in addressing the relationships between various forest stand variables and spectral data from multispectral bands, multisensors and multi-temporal images. The analysis can be concentrated on the first two or three principal component images.

The PCA produced different results from correlation and variance-covariance matrices. In this study, the first two principal components produced from the variance-covariance matrices accounted for more of the total variance of the spectral data than they did from the correlation matrices. They also showed higher correlations with stand variables than those from the correlation matrices. The data suggested that when using variables with the same data units such as with satellite data, the variance-covariance matrix approach is better than the correlation matrix approach. This is because variance-covariance allows the variables with higher internal variation to make more variance contribution (Jolliffe 1986). For

instance, NIR and MIR band data usually make higher variances than any other bands and therefore have higher contributions to the total variance. When variable units are different, the correlation matrix approach, the so-called "standardised principal component" (Singh and Harrison 1985), must be used, as the standardised variables in computing the correlation matrix could overcome the effects of variable unit difference on variance contribution (Jolliffe (1986).

### 6.5.6 Canonical Variables

The results of canonical correlation analysis in this work showed the information existing in the multiple spectral data and stand variables could be explained by the first one and/or the first two canonical variables. The first pair of canonical variables were mainly related to age in the stand variable group and NIR band in the spectral variable group. The second canonical variables were mainly contributed by stand top height and the green band (XS1) for SPOT and MIR bands (TM5 and TM7) for TM images. These results showed an agreement with the results obtained in simple correlation and principal component analysis where age was strongly correlated with NIR band; XS1 was better correlated with stand variables than XS2 for SPOT data and the MIR band of the TM data showed higher correlation with stand variables than did the visible and TIR bands.

## 6.6 SUMMARY AND CONCLUSION

Methods for determining the relationships between satellite data and stand variables are reasonably well developed. Analysis was performed by:

1. Using Pearson correlation analysis techniques to evaluate the relationships of the nine stand parameters to the following five data sets:
  - (1) the reflectance values of single bands of raw SPOT and Landsat TM images;
  - (2) the "between-image" band combinations of the multitemporal images, i.e. the difference and mean images of the two dates' Landsat TM data in the corresponding spectral bands;
  - (3) the "within-image" band combinations (vegetation indices);
  - (4) the principal component images; and
  - (5) the site variables (i.e. DTM and soil parameters).

Various bands and their linear combinations were related to stand variables in correlation analysis. The best spectral variables were PC2 produced from PCA. The results obtained from difference and mean images showed they did not improve the correlations with all stand variables, but they did show similar relationships with stand variables to the raw band data (insert between Paragraphs 2 and 3 in Page 169).



2. Using principal component analysis methods to extract information from the multiband, multisensor and multitemporal data sets.
3. Using canonical correlation analysis techniques to detect the relationships of the set of stand variables to the sets of site variables and the three images.

In this chapter, the relationships of several stand variables to spectral responses of SPOT and Landsat TM for a given set of conditions were described. Several of the TM and SPOT XS bands were found to be primarily related to stand age and several other stand variables in the managed coniferous plantations. Except for stand age, the correlation coefficients were not high enough to allow for the development of reliable predictive models of these variables using single waveband data. Because of the extreme heterogeneity of forest stands at the 30x30 m or 20x20 m resolution and the many abiotic and biotic factors acting on a forest ecosystem, a high degree of predictability on small, site-specific areas can not reasonably be expected.

Based upon the results from this study it is concluded that the capability of SPOT and TM data in differentiating and estimating stand variables is limited. The NIR band is the most sensitive single band for detecting the changes of the stand variables, stand age in particular.

Under the same stand and environmental conditions, SPOT and TM showed a nearly equal capability for detecting changes of stand structure. TM data, however, may be more useful in assessing some stand variables which show lower correlation with the NIR band, since the MIR band of TM data provided high correlations with volume and basal area.

In summary, the above conclusions give an indication of the potential of satellite remotely sensed imagery data with higher spatial and radiometric resolution for monitoring, estimating and predicting forest stand growth. The techniques developed and conclusions reached may be applicable to the utilisation of SPOT and Landsat TM data for other tree species and stands.

## **Estimating Forest Site Quality Using Satellite and Biogeographical Data**

### **7.1 INTRODUCTION**

Addressing the relationship between forests and their environments is difficult because of their enormous biogeographical scale in relation to ground-based measures. Satellite imagery is the only source of global, synoptic and timely information on physical and biological features. Not all of the biogeographical features can be directly measured by satellite sensors (see Chapter 2). However, by using the underlying functional relationships between the variable under investigation and a secondary variable that can be measured by a satellite sensor, a model can be developed to predict the desired information on the basis of the satellite sensor data. Such models can be developed using correlation, regression or classification techniques.

As reviewed in Chapter 2, current satellite data can be used for a large number of ecologically meaningful analyses at various scales. These include the assessment of the relationships between satellite data and a variety of forest structure attributes. Forest ecologists have been attempting to use satellite data to estimate forest productivity, usually expressed as biomass (dry-weight per unit area), in terms of all components of the forest ecosystem rather than of the tree boles alone. Some successes have been achieved in estimating forest productivity at regional scales (See Chapter 2). However, the productivity estimate of all components of the forest ecosystem is not of practical

importance for the purpose of forest management and planning which traditionally are based on tree bole volume. Very little work has been reported on estimation of site quality (SQ) of coniferous forest at a local area scale.

The study in Chapter 5 showed that changes in spectral reflectance over time closely matched the changes in the growth of radiata pine plantation stands, and the results obtained in Chapter 6 showed that spectral data were significantly correlated with several stand variables. The purpose of this chapter is to evaluate the potential of satellite data of varying spatial resolution and growing seasons for predicting and mapping forest site quality on a local area scale. This potential may be improved by incorporating topographic and soil information. Specifically, the objectives are fourfold as follows:

- To evaluate the relationships of site quality, expressed by site index and mean annual increment (MAI), with satellite and biogeographical data (with emphasis on topographic variables);
- To develop a multivariate model for site quality estimation using readily available digital satellite images in conjunction with ancillary data generated by computer and hard-to-obtain field measurement variables;
- To test and compare the significance of variables (bands) from multi-spectral bands, multi-temporal and multi-sensors and ancillary data; and
- To classify and map the site quality estimates produced from multiple regression models of different variable combinations.

## **7.2 METHODOLOGY**

### **7.2.1 Data Sources**

Several data sources are used in this chapter. They include imagery data from SPOT and Landsat sensors on three dates and their transformations, and ground ancillary data. The ground ancillary data on sample plots were from field measurements. The topographic data on compartments were generated from DTM. There follows a brief description of the variables used in data analysis. The details have been given in Chapters 3 and 4.

#### **7.2.1.1 Site Variables**

According to Scott (1960), Raupach (1967), Ballard (1971), Jackson and Gifford (1974), Woods (1976), Turvey (1986 and 1987), the site factors most significantly correlated with

radiata pine growth are soil chemical and physical properties. In a small area, however, soil depth of A horizon, slope position, slope steepness and altitude are the most important site factors (Heberle 1968; Kloeden 1969; Byron 1971). Therefore the site variables selected for use here are those which reflect the local (micro landform) variations which are known to affect the growth of radiata pine (Herbele 1969; Byron 1971). In this study, the site variables include topographic and soil physical variables, *i.e.*

- *Topographic variables* on sample plots were from field measurements, and on compartments were computed from digital terrain model (DTM) (see Chapter 4). They include slope in degrees (*SLP*), altitude (*ALT*) in metres, aspect (*ASP*) and topographic position (*TP*) by coding (see Chapter 4).
- *Soil variables* are soil depth of A and B horizons (*AB*) and the content of gravel (*GC*) (> 5 mm). The measurement of these two factors is described in Chapter 4.

#### 7.2.1.2 Satellite Data

The imagery data used in this part of the study are as described in Chapter 6. That is, the mean reflectance value was extracted from a 3 x 3 pixel window surrounding and including the ground sampling point. In addition to the mean original spectral reflectance values of each single band, various within-image (vegetation index) and between-image band combinations (difference and mean images) and transformations (including logarithmic, reciprocal, and principal component transformation) were also used for data analysis.

#### 7.2.1.3 Measure of Site Quality

Several parameters have been used to measure site quality of radiata pine plantation stands in Australia (see Lewis *et al.* 1976). These measures include site index (e.g. Czarnowski *et al.* 1967 and 1971; Turner *et al.* 1977; Ferguson 1979; Turvey 1987; Candy 1989), green index (Lewis *et al.* 1976), volume (Carron 1955), mean annual increment (Lewis *et al.* 1976; and Candy 1989), and indicator species (Ure 1950). Site index (SI) is one of the most widely used measures for estimating site quality in radiata pine plantations. SI, therefore, was considered to be the most important measure of SQ (or productivity) in this study. In addition to SI, several mean annual increment (MAI) indices, named HI, DI, CI, BA<sub>I</sub> and VI respectively, were related to the spectral data. The definitions of these measures (called SQ indices in this study) can be found in Chapter 4.

## 7.2.2 Data Analysis

### 7.2.2.1 Correlation Analysis

Pearson product moment correlation (PPMC) coefficients were computed to test the linear relationships between SQ indices and satellite data as well as each single site variable. The significance of the correlation coefficients was tested with *t*-test methods (Finn 1974).

### 7.2.2.2 Canonical Correlation Analysis

As discussed in Chapter 6, due to the properties of independence (orthogonality) between the canonical variates and non-zero correlation ( $r > 0$ ) between paired canonical variates, one of the most common uses of canonical correlation analysis is for ranking (ordination) of correlations between variables sets. This is because the first few canonical correlation coefficients and their corresponding canonical variables have the largest loading scores of the original variables, and therefore the canonical correlations ( $r_j$ ) of all the canonical variates could be ranked in the order:

$$|r_1| \geq |r_2| \geq \dots \geq |r_p| > 0$$

The relationships between any two single variables can be evaluated by the simple correlation (*i.e.* PPMC), but emphasis of CCA is on the *correlation* between the paired canonical variates extracted from two separated variable sets, and at the same time on the contribution of each individual variable to the *total* correlation. The importance of the individual variable can therefore be ranked on its contribution to the canonical variables. The CCA technique was applied in this work (1) reveal the relationships between the three distinct data attributes: images, physical site variables (topography and Soil) and SQ indices; and (2) to find the most highly correlated variables and spectral bands of the variable pools.

### 7.2.2.3 Principal Component Transformations

In multiple regression (see next section), one of the major difficulties with the usual least squares estimators is the problem of multicollinearity (non-orthogonality), which occurs when there are strong correlations between two or more of the predictor or regressor variables. This is particularly true in using multiple spectral **band** data as there is a strong inter-correlation between the spectral bands. This usually leads to difficulty in interpreting regression coefficients from such data, and other problems also ensue. For instance, *t*-tests can indicate that neither of two highly correlated regressors is significant

when, in fact, both are highly correlated with the dependent variable. This is due to the fact that multicollinearity causes the standard deviations (or standard errors or variance) of the coefficients to be relatively high. This leads to  $t$  tests which are not statistically significant, as well as to unstable coefficients (Gunst 1983; Jolliffe 1986; Ryan 1990). Principal component transformation (PCT) is one of the most widely used techniques to overcome this problem (for example PC regression). As reviewed in Chapter 5, its use in multivariate analysis is of value in that it can often reduce the number of variables to be considered by transforming the original data set onto an identical number of linearly independent (orthogonal) new variables (PCs). The PC images in this study were transformed using variance-covariance matrices of the three single-date and multi-date imagery data sets. The computation procedure can be found in Chapter 5. The analysis was concentrated on the first two or three PCs which explained 90% or more of the total variances.

#### 7.2.2.4 Regression Modelling

The regression analysis was carried out under the hypothesis: the site quality is seen as a function of the spectral reflectance, topographic and/or soil variables, *i.e.*

$$y = f(x_1, x_2, \dots, x_n)$$

where

$y$  is the measure of site quality;

$x_i$  ( $i=1, 2, \dots, n$ ) are the regressors that may contribute to site quality.

The regression model was fitted in the form of:

$$y = \beta_0 + \beta_1 x_1 + \beta_2 x_2 + \dots + \beta_n x_n + \varepsilon_j$$

where

$x_i$  ( $i = 1, 2, \dots, n$ ) are known constants (*i.e.* imagery data and other observed site variables which are controlled by the observer and which are measured with negligible error);

$\beta_i$  ( $i = 1, 2, \dots, n$ ) are unknown regression model parameters to be estimated;

$\varepsilon_j$  are the fluctuation or "error", ( $j = 1, 2, \dots, m$  (sample size)).

The regression parameters  $\beta_i$  were estimated with a least squared algorithm by SAS regression (REG) procedures (SAS Institute 1990). The performances of the regression models were evaluated with the following model parameters:

- *Correlation Coefficient* ( $r$ ) is used to measure the degrees of the dependence of site quality on independent variables. A squared correlation coefficient ( $r^2$ ) (all adjusted squared correlation coefficient ( $r_a^2$ ), also called “coefficient of determination” in some articles, is usually used as a measure of explanatory power of the total variance.
- *Mean Absolute Error* (MAE) and/or *Root Mean Square Error* (RMSE) are used to measure the average differences between observed and model-predicted site quality. MAE and RMSE are similar, but the latter is more sensitive to extreme values than is the MAE (Hardisky *et al.* 1984).
- *F-test* is used to determine the significance of the derived regression models. A regression model can be considered significant if the value of  $F$  is greater than the tabulated  $F$ -value.

Both simple linear (including non-linear) and multiple regression (including stepwise regression) analyses were performed. Simple regression was used to test the effects of a single variable on the site quality and yield. Several non-linear functions defined in Chapter 5 were also used for regression analysis. Multiple regression was used to evaluate the integrated influences of multivariables (multibands) on site quality. The regressors (independent variables) included:

- the original spectral reflectance values of each individual band, i.e. XS1, ..., XS2; TM1, ..., TM7 (not including TM6).
- “between-image” band combination images, *i.e.* the difference and mean images of the two TM images.
- “Within-image” band combinations (including several vegetation indices defined in the previous two chapters).
- Principal component images (Brightness and Greenness).
- DTM data: slope, aspect, altitude and topographic position.
- Soil data, *i.e.* the depth of A and B horizons (AB) and gravel content (GC).

In addition to the simple and multiple regression analyses using the above variables or variable combinations, stepwise regression analysis were performed to determine the “best” variable (band) combinations for site quality estimations. As the three images were acquired from two different sensor’s systems on different dates (growing seasons) (see Chapter 4), the combinations of multi-temporal and multi-sensor images may provide

useful information on vegetation. Due to the differences in sensor systems and recording dates, the images obtained from different growing seasons map compensate each other's inadequacy in the information they provide about vegetation. The selected bands (or band combinations) were then combined with ancillary data.

As qualitative variables (such as topographic positions) can not be used in regression analysis directly, they need to be quantified. This has usually been done by classifying each qualitative variable attribute into several levels, with each level being coded with number 0 or 1. It is coded as "1" if an attribute belongs to a specific level of a certain attribute or "0" otherwise (see Table 7.1). In this study, aspect and topographic positions were treated as qualitative variables. Based on their effects on tree growth, aspect was classified into four levels (named as ASP1, ASP2, ASP3 and ASP4) and topographic positions into five levels (called TP1, TP2, TP3, TP4, and TP5). Each levels of the these two attributes was defined in Table 4.1 in Chapter 4.

Table 7.1 The coding of the qualitative site variables (topographic position and aspect) for qualitative analysis (the definition of the variable attributes is given in Table 4.1).  $n$  - sample number.

Obs.	Aspect				Topographic Positions				
	ASP1	ASP2	ASP3	ASP4	TP1	TP2	TP3	TP4	TP5
1	1	0	0	0	1	0	0	0	0
2	0	1	0	0	0	1	0	0	0
3	0	0	0	1	0	0	1	0	0
⋮	⋮	⋮	⋮	⋮	⋮	⋮	⋮	⋮	⋮
$n$	$n$	$n$	$n$	$n$	$n$	$n$	$n$	$n$	$n$

In quantitative regression analysis (Dong *et al.* 1979), the rank of the coefficient matrix of the normal equation groups,  $X'X$ , is

$$\sum_{j=1}^m k_j - (m - 1)$$

where:

$k_j$  is the number of the levels of  $j$ th attribute,

$m$  is the number of attributes.

This means that one level of each attribute is the linear combination of the rest of the levels. Therefore, one of the variables in each qualitative attribute needs to be deleted and is treated as 0 constant. For convenience, the first level (column) of each attribute is deleted. In this work, ASP1 and TP1 were deleted (*i.e.* seen as 0 regression coefficients).

### 7.2.2.5 Site Quality Classification and Mapping

Site quality classification and mapping are an important and extremely valuable aid to forest planning and management. They should indeed be the final results of any site



quality (productivity) studies. With a certain abstraction (or standard) one can define site classification (or site quality classes) as a means of grouping forest sites according to their capacity for growing trees. In this study, based on the growing conditions in the study site, the model-estimated site quality from various combinations of variables has been grouped into four site quality classes and presented in false colour map format. The accuracy of the SQ classification was evaluated using an error matrix method proposed by Kalensky and Scherk (1975).

## 7.3 RESULTS AND DISCUSSION

### 7.3.1 Correlations

#### 7.3.1.1 Correlations Between Site Quality and Stand Variables

The correlations between the six SQ indices and original stand variables are given in Tables 7.2 and 7.3 respectively. These correlations were computed for the purpose of assessing the relationships between SQ and imagery data detailed in the sub-sections that follow. As shown in Table 7.2, all SQ indices were strongly inter-correlated ( $p = 0.01 - 0.001$ ). The strongest correlation ( $r = 0.97$ ) was found between HI and SI. This is because these two SQ indices were calculated from stand age and top height, both of which were strongly significantly correlated with stand age. DI and CI also showed strong correlation with HI and SI as mean diameter and canopy depth were both highly correlated with stand age and top height (see Tables 7.3 and Table 6.4). In comparison, BAI and VI showed a relatively lower correlation with other SQ indices as they were affected by the density and were less well correlated with stand age.

Table 7.2 Correlations between SQ indices.

Variables	HI	SI	VI	DI	BAI	CI
HI	1					
SI	0.97***	1				
VI	0.39**	0.51***	1			
DI	0.84***	0.81***	0.32*	1		
BAI	0.56***	0.57***	0.80***	0.53***	1	
CI	0.87***	0.84***	0.32*	0.83***	0.56***	1

\* Significant at 95% confidence ( $p < 0.05$ ) level; \*\* 99% ( $p < 0.01$ ) level; and \*\*\* 99.9% ( $p < 0.001$ ) level,  $n = 60$ .

All SQ indices were strongly negatively correlated with stand age. These negative correlations should be attributed to change in growth rate with age, as the mean annual increment (MAI) of the stand parameters (such as top height and basal area) usually significantly increases with age while the trees are young (1-10 years) and then decreases

with increasing with age until about 25 year old. Almost all sample points were observed from 10 years or older stands.

Table 7.3 Correlations between SQ indices and stand variables.

SQ \ Stand Var	AGE	BA	TH	MD	SN	CC	UC	VOL
HI	-0.82***	-0.12	-0.32*	-0.37**	0.23	0.54***	0.01	-0.19
SI	-0.71***	-0.09	-0.21	-0.30*	0.18	0.53***	0.02	-0.12
VI	-0.03	0.80***	0.37**	0.26*	0.31*	0.65***	-0.27*	0.73***
DI	-0.79***	-0.20	-0.38**	-0.19	0.03	0.38**	0.10	-0.26*
BAI	-0.48***	0.57***	-0.21	-0.26*	0.68***	0.69***	-0.11	0.28*
CI	-0.79***	-0.18	-0.40**	-0.40**	0.18	0.46***	0.08	-0.28*

\* Significant at 95% confidence ( $p < 0.05$ ) level; \*\* 99% ( $p < 0.01$ ) level; and \*\*\* 99.9% ( $p < 0.001$ ) level,  $n = 60$ .

### 7.3.1.2 Correlations between Site Quality and Raw Spectral Band Data

#### (1) The correlations between SPOT data and site quality indices

Table 7.4 gives the correlations between SQ indices and raw band data. All six SQ indices were strongly positively correlated with the NIR band (XS3) at 95% to 99.9% significance levels. The two visible bands (XS1 and XS2) showed a poor correlation with HI, SI, DI, BAI, and CI ( $r < 0.18$ ), but significantly correlated with VI ( $r = -0.39$  and  $-0.37$ ;  $p < 0.05$ ). The PS band showed a poor correlation with all site quality indices, with the exception of VI which showed a correlation of 0.3 ( $p < 0.05$ ). HI, SI and DI showed strong and approximately equal correlation coefficients with XS3 ( $r = 0.75 - 0.78$ ,  $p < 0.001$ ).

Table 7.4 Correlations between SQ indices and raw band data.

Images/Dates	Bands	HI	SI	VI	DI	BAI	CI
SPOT Data (24-Jan-87)	XS1	-0.09	-0.05	-0.39**	-0.04	-0.07	-0.05
	XS2	-0.20	-0.14	-0.37**	-0.17	-0.10	-0.16
	XS3	0.78***	0.78***	0.30*	0.75***	0.60***	0.69***
	PS	-0.15	-0.12	-0.26*	-0.07	-0.03	-0.08
2TM Image (9-Feb-88)	2TM1	-0.04	-0.01	-0.38**	0.04	-0.21	0.05
	2TM2	-0.03	-0.02	-0.50***	0.03	-0.29*	0.06
	2TM3	-0.11	-0.06	-0.53***	-0.05	-0.38**	-0.03
	2TM4	0.82***	0.79***	0.15	0.77***	0.49***	0.79***
	2TM5	-0.22	-0.17*	-0.63***	-0.08	-0.46***	-0.10
	2TM6	-0.22	-0.20	-0.30*	-0.10	-0.28*	-0.10
	2TM7	-0.26*	-0.26*	-0.59***	-0.13	-0.45***	-0.14
4TM Image (21-Apr-88)	4TM1	-0.07	-0.06	-0.29*	0.04	-0.15	0.04
	4TM2	-0.03	-0.02	-0.30*	0.04	-0.14	0.08
	4TM3	-0.23	-0.22	-0.30*	-0.14	-0.23	-0.10
	4TM4	0.55***	0.54***	0.14	0.54***	0.39**	0.53***
	4TM5	-0.13	-0.07	-0.38**	-0.03	-0.22	0.01
	4TM6	-0.36**	-0.30*	-0.42***	-0.28*	-0.35**	-0.26*
	4TM7	-0.16	-0.10	-0.36**	-0.10	-0.23	-0.03

\* Significant at 95% confidence ( $p < 0.05$ ) level; \*\* 99% ( $p < 0.01$ ) level; and \*\*\* 99.9% ( $p < 0.001$ ) level,  $n = 60$ .

#### (2) Correlation between TM data and site quality

As with SPOT data, the NIR band (TM4) of the TM data dominated the significantly correlated bands ( $p < 0.01$ ) (Table 7.4); VI showed a very poor correlation with the NIR

band ( $r = 0.15$ ) but was significantly correlated with all other spectral bands (at 95% or higher significance levels). In particular, it was strongly correlated with TM5 ( $r = 0.63$  for 2TM5 and 0.38 for 4TM5) and TM7 ( $r = 0.59$  for 2TM7 and 0.36 for 4TM7). BAI showed correlations of 95% or higher significance levels with TM2, TM5 and TM7 of the February-9 TM image, but did not correlate at the same significance levels with the same bands of the April-21 TM image ( $r < 0.24$ ).

The correlation analysis (Table 7.4) indicated that all spectral bands but NIR had relatively low correlations with SQ indices due to the visible, MIR and TIR bands being poorly correlated with stand age and other stand variables (see Chapter 5 and 6). The SQ indices strongly correlated with stand top height and age were usually significantly correlated with the NIR band due to a strongly negative correlation of NIR with these two variables. The best correlations were obtained between HI and SI and the NIR bands. However, the NIR band was generally poorly correlated with the mean annual increment of stand volume (VI) and stand basal area (BAI). The two MIR bands (TM5 and TM7) provided better information on SQ than the visible bands. The summer images were comparatively better correlated with site quality than the autumn image.

### 7.3.1.3 Correlations between Site Quality and Principal Component Images

All the PC images were related to the SQ indices. Table 7.5 displays only the results from the first two PCs as they explained most of the total variance and also showed higher correlations with SQ indices than those computed from any other PCs. The correlation analysis showed that PC2 (termed *greenness*) was most strongly correlated with SQ indices (excluding VI), with correlation coefficients ( $r$ ) ranging from 0.59 to 0.83 for SPOT PC2, 0.55 to 0.85 for 2TM PC2 and 0.46 to 0.60 for 4TM PC2 ( $p < 0.001$ ). This is because the information of PC2 is mainly contributed by the NIR band which is usually highly correlated with SQ indices (see Table 7.4) as well as stand variables (see Chapter 6).

SPOT PC1 showed no correlations with any SQ indices (Table 7.5). This may be explained by the fewer spectral bands which were significantly correlated with stand variables and SQ indices. PC1 of the TM images showed strong correlation with VI and BAI, but was poorly correlated with other SQ indices. In PCA, using multispectral imagery data, PC1 was usually interpreted as "*brightness*" which indicates the sum of the overall reflectance of the object (Everett and Simonett 1976; and Lodwick 1979b). Therefore it was believed to be the sum of the overall response levels in all bands, the two MIR bands in particular.

Table 7.5 Correlations between site quality and the principal component images.

Site Quality indices	SPOT XS+PS Data		February-9 TM Data		April-21 TM Data		All Three Images (SPOT+2TM+4TM)	
	PC1	PC2	PC1	PC2	PC1	PC2	PC1	PC2
HI	0.09	0.83***	-0.18	0.85***	-0.09	0.60***	-0.16	0.84***
SI	0.11	0.82***	-0.14	0.82***	-0.04	0.58***	-0.11	0.82***
VI	-0.21	0.43***	-0.61***	0.23	-0.36**	0.27*	-0.59***	0.30*
DI	0.16	0.75***	-0.06	0.78***	0.00	0.57***	-0.04	0.78***
BAI	0.13	0.59***	-0.43***	0.55***	-0.19	0.46***	-0.38***	0.61***
CI	0.12	0.71***	-0.07	0.80***	0.04	0.54***	-0.04	0.78***

\* Significant at 95% confidence ( $p < 0.05$ ) level; \*\* 99% ( $p < 0.01$ ) level; and \*\*\* 99.9% ( $p < 0.001$ ) level.

In comparison, the PCs of the two summer images showed approximately equal information contents on SQ, except for the PC1 of 2TM data which showed strong correlations with VI and BAI (Table 7.5). The PC1 and PC2 from the autumn image (April-21 TM data) were strongly correlated with SQ indices, but the correlation coefficients were much lower than those from the two summer images. This may be explained by the low correlations between SQ indices and the raw spectral band data of the April-21 TM data (see Table 7.4).

The PC images calculated from the multi-temporal images (18 bands) showed similar or better correlations with SQ indices than the PCs from the single date images alone (Table 7.5). As shown in the previous chapters, the PC images usually extract the spectral information on vegetation to the first two PCs, while images and/or the bands which have higher correlations with stand variables usually show higher PC loadings. These results further suggest that principal component transformation is the best way to extract maximum information from the multi-temporal images when using the images from different growing seasons and different sensors.

Compared with the results from the raw imagery data, the PC images can improve the relationships with SQ using only the first two PCs. In particular, PC2, the "greenness", provides better spectral information on SQ. The information of the visible and MIR bands on SQ can be extracted in the PC1 image. Thus correlation and/or regression analysis involving multi-bands and multi-temporal images can be concentrated on the first two PC images without losing much information.

#### 7.3.1.4 Correlations between Site Quality and Difference and Mean Images

Correlations of the difference and mean images of the two TM images to SQ indices were presented in Table 7.6. Both the difference and mean images showed a similar correlation pattern to the original data, with the dominant correlation in the combined near-infrared bands. The mean annual increment in volume (VI) was poorly correlated with the

difference and mean images in the NIR band ( $r < 0.15$ ), but was well correlated with all difference and mean images in other bands ( $p < 0.05 - 0.01$ ), in particular with the combinations in TM5 and TM7 ( $r > 0.55$ ,  $p < 0.001$ ).

Table 7.6 Correlations between SQ indices and difference ( $D_1$  to  $D_7$ ) and mean ( $M_1$  to  $M_7$ ) images

<i>SQ</i> <i>CombinedBands</i>	HI	SI	VI	DI	BAI	CI
$D_1$	-0.01	-0.04	-0.28*	0.03	-0.16	0.04
$D_2$	-0.02	-0.03	-0.41**	0.01	-0.26*	0.01
$D_3$	-0.03	-0.03	-0.47***	0.00	-0.33*	0.01
$D_4$	0.72***	0.69***	0.10	0.66***	0.38**	0.69***
$D_5$	-0.20	-0.18	-0.58***	-0.09	-0.46***	-0.14
$D_6$	0.00	-0.02	-0.05	0.09	-0.08	0.08
$D_7$	-0.23	-0.22	-0.53***	-0.10	-0.42***	-0.16
$M_1$	-0.06	-0.01	-0.40**	0.05	-0.21	0.05
$M_2$	-0.03	0.05	-0.47***	0.04	-0.26*	0.07
$M_3$	-0.16	-0.11	-0.51***	-0.08	-0.38**	-0.06
$M_4$	0.77***	0.75***	0.15	0.73***	0.48***	0.74***
$M_5$	-0.20	-0.14	-0.58***	-0.07	-0.40**	-0.06
$M_6$	-0.30*	-0.26*	-0.38**	-0.19	-0.33*	-0.18
$M_7$	-0.25	-0.2	-0.56***	-0.13	-0.41**	-0.11

\* Significant at 95% confidence ( $p < 0.05$ ) level; \*\* 99% ( $p < 0.01$ ) level; and \*\*\* 99.9% ( $p < 0.001$ ) level.  $n = 60$ .

The correlations between the “between-image” combinations and SQ indices fell between the two single date TM images, that is, slightly lower than the results from February-9 TM image and much better than those from the April-21 TM image. In comparison, the mean images showed better correlations with SQ indices than difference images. As discussed in Chapter 5, these differences could be attributed to a number of factors influencing the spectral absorption and reflectance. Some of these are due to actual variation in the target areas being investigated while others are due to variations in external conditions (such as sun angles). There are several ways to minimise these external differences, such as corrections for topography and atmosphere, data standardisation etc. The use of difference and mean images did not improve their correlations with SQ, but they may be helpful to minimise the variation due to temporal changes, with the added advantage that each image contributes equal weight to the analysis.

### 7.3.1.5 Correlations between Site Quality and Vegetation Indices

Strong correlations were observed between the nine forest stand variables and several NIR-related band combinations as reported in the previous chapter. In this chapter, the relationships between SQ and “within-image” band combinations by addition, subtraction and/or ratios were examined. All possible “within-image” band combinations were calculated and related to SQ indices, but their correlations with SQ were only slightly (functionally) different. Table 7.7 lists only the better correlation results.

Table 7.7 Correlations between SQ indices and "within-image" band combinations (*i.e.* vegetation index).

Times	SPOT	HI	SI	VI	DI	BAI	CI
SPOT Data (24-1-87)	AVI	0.83***	0.79***	0.50***	0.78***	0.60***	0.73***
	RVI	0.68***	0.62***	0.54***	0.63***	0.49***	0.60***
	NDVI	0.66***	0.61***	0.50***	0.62***	0.45***	0.58***
	XS3/1	0.76***	0.72***	0.62***	0.68***	0.60***	0.66***
	XS3-1	0.85***	0.81***	0.56***	0.78***	0.65***	0.73***
2TM Image (9-Feb-88)	AVI	0.83***	0.78***	0.43***	0.75***	0.67***	0.76***
	RVI	0.67***	0.61***	0.60***	0.59***	0.71***	0.60***
	NDVI	0.68***	0.62***	0.60***	0.60***	0.71***	0.61***
	TM3/5	0.35**	0.33*	0.58***	0.18	0.48***	0.23
	TM7/5	-0.36**	-0.36**	-0.43***	-0.26*	-0.40**	-0.24
TM4/2	0.82***	0.77***	0.47***	0.74***	0.68***	0.75***	
4TM Image (21-Apr-88)	AVI	0.66***	0.65***	0.27*	0.61***	0.49***	0.58***
	RVI	0.64***	0.62***	0.39**	0.56***	0.55***	0.52***
	NDVI	0.63***	0.61***	0.36**	0.54***	0.50***	0.50***
	TM3/5	0.07	0.01	0.40**	-0.03	0.22	-0.03
	TM7/5	-0.19	-0.17	-0.15	-0.25	-0.22	-0.15
TM4/2	0.60***	0.58***	0.34**	0.55***	0.52***	0.52***	

\* Significant at 95% confidence ( $p < 0.05$ ) level; \*\* 99% ( $p < 0.01$ ) level; and \*\*\* 99.9% ( $p < 0.001$ ) level.  $n = 60$ .

The correlation analyses showed that the use of "within-image" band combinations could improve the correlations with SQ. The NIR-related band combinations were more sensitive to site quality than other band combinations. For the three images the best correlation was obtained from AVI. The highest correlation in the SPOT image was from the differences of NIR and green band differences (*i.e.* XS3-1;  $r = 0.85$ ,  $p < 0.0001$ ), while for TM images, the ratio of these two bands showed an approximately equal correlation to AVI.

Previous studies have shown that the vegetation indices computed from NIR and Red bands (such as NDVI and RVI) could produce better correlations than original band data with biomass (*e.g.* Deering and Haas 1980; Hardisky *et al.* 1984; Kanemasu *et al.* 1990; Sader *et al.* 1989) and LAI (*e.g.* Tucker 1977 and 1979; Holben *et al.* 1980; Spanner *et al.* 1984b; Running *et al.* 1986). In this study, however, the highest correlation was not obtained from NIR/Red ratios but NIR-Red and/or NIR-Green band differences. As discussed in the previous chapters, in general, the spectral reflectance of the visible and NIR bands decreased with stand growth, but the NIR reflectance did not decrease as sharply as the visible bands (see Figure 5.2 and 5.10 and Chapter 5). Therefore the values of the differences and/or ratios of the visible and NIR bands were usually higher in younger stands (5-10 years) and decreased with stand growth. This implies that the band combinations of NIR and visible bands (both difference and ratios) may be able to highlight the variation of stand structure (see Figure 5.10).

### 7.3.1.6 Correlations Between Site Quality and Site Variables

The correlations between SQ and the site variables are given in Table 7.8. Clearly, altitude (ALT), topographic positions (TP) and slope (SLP) had more effects on radiata pine site quality than did the soil depth, aspect and gravel contents. The correlations, although generally poor, were higher for TP and ALT than the other site variables. Similar results were reported in earlier work by Kloeden (1969) in an ACT radiata pine plantation site study. However, the low correlations with soil depth (AB), aspect (ASP) and gravel contents (GC) do not mean that these site variables are not important for indicating site quality. The result might be due to the limited sample numbers in a limited study area. In fact, the importance of any individual site variable can vary greatly from place to place and from species to species. It is in general dependent on the integrated effects of all site features.

The correlation analyses above indicate that spectral data are better correlated with site quality than are individual biogeographical or physical environmental (site) characteristics (e.g. slope, aspect, altitude, and soils). Spectral data are by nature integrators of a large number of factors, many of which (e.g. density, green leaf volume (leaf area index), moisture, green vegetation biomass) could be expected to relate to site quality more than individual site factors (e.g. DTM-derived data). As reviewed in Chapter 2, site quality (or productivity) is the sum of a large number of environmental (site) factors. Nevertheless, this does not mean that all individual site factors have equal influences (contribution) on site quality (productivity). However, the use of site variables (e.g. DTM-derived and soil data), may enhance the performance of the spectral reflectance for site quality and/or yield estimation. This will be further examined below.

Table 7.8 Correlation coefficients between SQ indices and site variables.

Site Variables SQ	SLP	ALT	AB	ASP	GC	TP
HI	-0.23	0.16	0.05	-0.17	-0.12	0.24
SI	-0.22	0.17	0.05	-0.21	-0.12	0.32*
VI	-0.23	-0.38**	0.07	-0.10	-0.11	0.42**
DI	-0.32*	0.05	0.18	-0.17	-0.19	0.26*
BAI	-0.28*	-0.07	0.00	-0.19	-0.07	0.19
CI	-0.26*	0.13	0.02	-0.09	-0.03	0.12

\* Significant at 95% confidence ( $p < 0.05$ ) level; \*\* 99% ( $p < 0.01$ ) level; and \*\*\* 99.9% ( $p < 0.001$ ) level.  $n = 60$ .

### 7.3.2 Canonical Correlations

The relationships between individual variables have been discussed above; the emphasis here is on the relationships between variable groups. Five canonical correlation analyses (CCA) were performed to analyse the relationships of SQ indices to five data sources:

three single date images, three images together, and site variables. As in Chapter 6, the canonical correlations of any two variable groups were evaluated by computing their canonical correlation, performing corresponding significance tests, and calculating eigenvalues and percentage of explained total variance of each pair of canonical variables (variates). Each single variable (band) was further assessed by its canonical coefficients (loadings) and correlations with opposite variables. The results are discussed in the following five sections.

### 7.3.2.1 Canonical Correlations between SPOT Image and Site Quality

The canonical correlation coefficients  $r_k$  ( $k = 1, 2$ , and  $3$ ) from SPOT data (XS+PS) and six SQ indices and their significance test are presented in Table 7.9a. It can be seen that the first two correlations exceeded 0.65 ( $r_1 = 0.89$ ,  $r_2 = 0.67$ ), were significant at the 0.0001 and 0.0003 levels and explained 98% of the total variance. The third canonical correlation,  $r_3 = 0.357$  ( $r^2 = 0.127$ ), was very small and accounted for less than 3% of the total variance. Therefore  $r_1$  and  $r_2$  are certainly suggestive of the existence of two linear relationships between SQ ( $x$ ) and SPOT data ( $y$ ).

Table 7.9a Results of CCA between SQ indices and SPOT data.

Canonical Correlation					Significance test ( $H_0: r = 0$ )				
	Canonical Correlations	Eigen Values	Prop. (%)	Cum. (%)	$\Lambda_i$	$\chi^2$	DF	Significance Levels	Decision
1	0.895	4.003	80.04	80.04	0.0922	127.54	24	0.0001	<i>Reject</i>
2	0.669	0.812	16.23	96.27	0.4633	40.39	15	0.0003	<i>Reject</i>
3	0.357	0.146	02.93	99.20	0.8387	9.06	8	0.3086	<i>Accept</i>
4	0.197	0.040	0.80	100	0.9612	2.00	3	0.5498	<i>Accept</i>

Table 7.9b Standardised canonical coefficients and correlations between the original variables and the canonical variables of opposite sets of variables.

SQ Indices					SPOT Data				
Standardised Canonical coefficients for SQ Indices			Corr. Between SQ & 1st two Cano. Vars. of SPOT Data		Standardised Canonical Coefficients for SPOT Data			Corr. Between SPOT Data & 1st two Cano. Vars. of SQ Indices	
$x$	$u_1$	$u_2$	$r_{v_1}$	$r_{v_2}$	$y$	$v_1$	$v_2$	$r_{u_1}$	$r_{u_2}$
<i>SI</i>	0.280	2.030	0.847	0.059	XS1	-0.607	0.778	-0.114	0.662
<i>HI</i>	0.573	-2.414	0.867	0.014	XS2	0.183	0.145	-0.207	0.614
<i>VI</i>	0.101	-1.618	0.512	-0.324	XS3	1.072	0.157	0.795	0.302
<i>DI</i>	0.224	0.341	0.797	0.061	PS	-0.086	0.046	-0.131	0.400
<i>BAI</i>	0.168	1.599	0.663	0.028					
<i>CI</i>	-0.241	-0.176	0.752	0.040					

Table 7.9b presents the standardised canonical coefficients of the first two canonical variables and their correlations with opposite variables. Like PCA, the canonical variables are the linear combinations of the original data determined by their canonical coefficients. That is, the higher the canonical coefficients (the “loadings”), the more their contributions



to the total variance (canonical variables) of the original data set. From the first pair of canonical variables, HI and XS3 showed the highest loadings (0.57 and 1.07) and highest correlations with opposite canonical variables (0.87 and 0.80) and should be seen as the dominant variables. The second pair of canonical variables were mainly contributed by VI and XS1, as they had the highest loadings and correlations with the second canonical variable of opposite data sets. SI, HI, BAI and XS3 also showed large loadings in the second pair of canonical variables, but their correlations with opposite canonical variables were very weak (Table 7.9b).

### 7.3.2.2 Canonical Correlations between TM Images and Site Quality

The results of CCA between the two TM data sets and the six SQ indices are given in Tables 7.10a-7.10b and 7.11a-7.11b. The two TM images showed a similar correlation pattern, with HI and the NIR band (TM4) being good overall predictors of the opposite set of variables. However, due to the difference in growing seasons, the canonical variables showed some differences in their information content on site quality. As can be seen from Table 7.10a, the first two canonical correlations from the February-9 TM image exceeded 0.73 and were significant at 0.0001 and 0.0008 levels respectively. They explained up to 94% of the total variance. The CCA using the April-21 TM image indicated that only the first pair of canonical variables was significantly correlated ( $r = 0.79$ ,  $p < 0.0002$ ) (Table 7.11a). Nevertheless, it explained only about 69% of the total variance and, together with the second canonical correlation, only 92%, slightly less than 71% and 94% respectively from February-9 TM image (Table 7.10a). These results further indicate that the summer images contain more information than the autumn image on site quality as well as stand structure.

As shown in Tables 7.10b and 7.11b, HI and TM4 had the highest loadings and the highest correlations with the canonical variables of their opposite sets of variables, and therefore they are definitely the dominant variables in the first pair of canonical variables. In the second pair of canonical variables, VI and TM5 can be seen as the dominant variables as they both showed the highest loading and correlations, although the second correlation coefficient ( $r_2$ ) for the April-21 TM image was not significant at the same level as the first correlation coefficient ( $r_1$ ) (Tables 7.10a and 7.11a). SI and HI also showed higher loadings in the second pair of canonical variables; their correlations with the canonical variables of TM data were very poor. In comparison, the MIR (TM5) and TIR (TM7) bands contributed more to the information (canonical variables) on vegetation and site quality than did the visible bands.

Table 7.10a Results of CCA between SQ indices and the February-9 TM Data.

Canonical Correlation					Significance test ( $H_0: r = 0$ )				
	Canonical Correlations	Eigen Values	Prop. (%)	Cum. (%)	$\Lambda_i$	$\chi^2$	DF	Significance Levels	Decision
1	0.895	4.037	70.57	70.57	0.066	145.72	42	0.0001	<i>Reject</i>
2	0.758	1.352	23.63	94.20	0.315	60.62	30	0.0008	<i>Reject</i>
3	0.383	0.171	3.00	97.20	0.732	16.10	20	0.7017	<i>Accept</i>
4	0.299	0.098	1.72	98.92	0.857	7.80	12	0.7832	"
5	0.216	0.049	0.85	99.77	0.941	3.01	6	0.7884	"
6	0.114	0.013	0.23	100	0.987	0.63	2	0.7116	"

Table 7.10b Standardised canonical coefficients and correlations between the original variables and the canonical variables of opposite sets of variables.

SQ Indices					2TM Data				
Standardised Canonical Coefficients for SQ Indices			Corr. Between SQ & 1st two Cano. Vars. of 2TM Data		Standardised Canonical Coefficients for 2TM Data			Corr. Between 2TM Data & 1st two Cano. Vars. of SQ Indices	
$x$	$u_1$	$u_2$	$r_{v_1}$	$r_{v_2}$	$y$	$v_1$	$v_2$	$r_{u_1}$	$r_{u_2}$
SI	-0.001	1.659	0.8263	-0.0492	2TM1	-0.1698	0.1906	0.0268	0.5091
HI	0.890	-2.445	0.8657	-0.1070	2TM2	0.1058	0.5351	0.0500	0.5995
VI	-0.419	-1.189	0.2630	-0.6376	2TM3	-0.0932	-0.8571	-0.0523	0.5758
DI	0.014	0.613	0.7852	0.0151	2TM4	1.0164	-0.0176	0.8583	0.1391
BAI	0.451	0.485	0.5778	-0.3831	2TM5	-0.2774	2.0484	-0.1290	0.6913
CI	-0.042	0.369	0.8046	-0.0082	2TM6	-0.1894	-0.3542	-0.1905	0.3222
					2TM7	0.3030	-0.7498	-0.1804	0.6210

Table 7.11a Results of CCA between SQ indices and the April-9 TM Data.

Canonical Correlation					Significance test ( $H_0: r = 0$ )				
	Canonical Correlations	Eigen Values	Prop. (%)	Cum. (%)	$\Lambda_i$	$\chi^2$	DF	Significance Levels	Decision
1	0.789	1.649	69.03	69.03	0.203	82.99	42	0.0002	<i>Reject</i>
2	0.596	0.551	23.06	92.09	0.537	32.33	30	0.3554	<i>Accept</i>
3	0.292	0.093	3.89	95.98	0.833	9.51	20	0.9765	"
4	0.242	0.062	2.61	98.60	0.911	4.82	12	0.9622	"
5	0.162	0.027	1.12	99.72	0.967	1.73	6	0.9431	"
6	0.082	0.007	0.28	100.00	0.993	0.35	2	0.8409	"

Table 7.11b Standardised canonical coefficients and correlations between the original variables and the canonical variables of opposite sets of variables.

SQ Indices					4TM Data				
Standardised Canonical Coefficients for SQ Indices			Corr. Between SQ & 1st two Cano. Var. of 4TM Data		Standardised Canonical Coefficients for 4TM Data			Corr. Between 4TM Data & 1st two Cano. Var. of SQ Indices	
$x$	$u_1$	$u_2$	$r_{v_1}$	$r_{v_2}$	$y$	$v_1$	$v_2$	$r_{u_1}$	$r_{u_2}$
SI	0.158	1.990	0.743	0.008	4TM1	0.136	0.330	-0.041	0.413
HI	0.568	-3.677	0.772	-0.036	4TM2	0.108	0.129	-0.013	0.394
VI	-0.190	-1.004	0.342	-0.377	4TM3	-0.500	-0.237	-0.212	0.348
DI	0.210	0.903	0.721	0.087	4TM4	0.823	-0.053	0.581	0.172
BAI	0.363	0.615	0.563	-0.173	4TM5	0.418	1.688	-0.097	0.555
CI	-0.082	1.002	0.705	0.096	4TM6	-0.788	-0.159	-0.332	0.418
					4TM7	0.064	-0.744	-0.144	0.497

### 7.3.2.3 Comparisons of the Multi-temporal and Multi-sensor Images

As indicated previously, the SQ information contents of individual spectral bands could be detected by the percentage of the total variance explained or by their scores (loadings) using PCA and/or CCA (including factor analysis) techniques. In this section, CCA was undertaken to compare the spectral information differences of the multi-temporal and multi-sensor's images. The results are presented in Tables 7.12a and 7.12b. Three of the correlations exceed 0.64 (i.e.  $r_1 = 0.95$ ,  $r_2 = 0.88$ , and  $r_3 = 0.64$ ), explaining 65.8%, 22.9% and 4.8% of the total variance, and the three together, 93.5%. However, the significance test showed only the first two canonical correlations were significant ( $p < 0.0001$  and 0.002 respectively).

As can be seen from Table 12b, in the SQ variable set ( $x$ ), HI dominated the canonical coefficients (1.25) in the first pair of canonical variables ( $u_1$ ). The six SQ indices showed a close positive correlation with the canonical variables of the three images, with HI being the highest ( $r = 0.88$ ). In fact, other SQ indices (SI, CI, DI, BAI) can be partially explained by HI as they showed a high correlation with other SQ indices (see Table 7.2). Similarly XS3 of SPOT data dominated the canonical correlation coefficients (0.93) for the three images together, and also showed the highest correlation (0.74) with the canonical variable of the SQ indices variable set. 2TM5 also showed the highest loading for the first canonical variables (0.84), but its correlations ( $r = -0.42$ ) with the canonical variables of the SQ indices were much less than that with the NIR bands (Table 7.12b). 2TM4 and 4TM4 showed higher correlations with the canonical variables of SQ indices, but their canonical correlation coefficients were relatively lower than that of XS3. These two variables were not therefore seen as major variables. These results suggest that XS3 shows the best information on site quality.

Table 7.12a Results of CCA between SQ indices and all three data sets together (XS+PS+2TM+4TM).

Canonical Correlation					Significance test ( $H_0: r = 0$ )				
	Canonical Correlations	Eigen Values	Prop. (%)	Cum. (%)	$\Lambda_i$	$\chi^2$	DF	Significance Levels	Decision
1	0.951	9.453	65.80	65.80	0.0059	238.72	108	0.0001	Reject
2	0.876	3.286	22.87	88.67	0.0617	129.56	85	0.0020	Reject
3	0.640	0.695	4.84	93.51	0.2651	61.74	64	0.5774	Accept
4	0.564	0.467	3.25	96.76	0.4489	37.24	45	0.7980	"
5	0.455	0.261	1.81	98.58	0.6584	19.44	28	0.8890	"
6	0.412	0.204	1.42	100.00	0.8303	8.65	13	0.8026	"

As with the single date images, VI also had the highest canonical correlation coefficients (-1.46) as well as the highest correlation with the second canonical variables of the three images. VI is therefore the dominant variable for the second canonical variable of the SQ

indices. 2TM4 and 2TM5 showed approximately equal loadings (0.93 and 0.94) in the second canonical variables of images, but the correlation (0.53) of 2TM5 with the second canonical variable of the opposite set of variables (SQ indices) was slightly higher than that of 2TM4. 2TM5 was therefore seen as the dominant variable for the second pair of canonical variables (Table 7.12b).

Table 7.12b Standardised canonical coefficients and correlations between the original variables and the canonical variables of opposite sets of variables.

SQ Indices					All Images (XS+PS+2TM+4TM: 18 bands)				
Standardised Canonical Coefficients for SQ			Corr. Between SQ & 1st two Cano. Var. of 4TM Data		Standardised Canonical Coefficients for All Three Data Sets (18 Channels)			Corr. Between Images & 1st two Cano. Var. of SQ Indices	
$x$	$u_1$	$u_2$	$r_{v_1}$	$r_{v_2}$	$y$	$v_1$	$v_2$	$r_{u_1}$	$r_{u_2}$
SI	-0.241	1.3126	0.8363	0.2702	XS1	-0.6280	0.6040	-0.1829	0.5637
HI	1.254	-1.4244	0.8821	0.2380	XS2	0.3285	-0.0025	-0.2585	0.4696
VI	0.204	-1.4586	0.6481	-0.5439	XS3	0.9285	-0.5245	0.7432	0.3871
DI	0.0006	0.2246	0.7726	0.2799	PS	0.0923	-0.1084	-0.1647	0.3108
BAI	0.209	0.9424	0.7794	-0.0840	2TM1	-0.2324	-0.1073	-0.1925	0.4497
CI	-0.334	0.2632	0.7451	0.3147	2TM2	-0.0024	0.4376	-0.2253	0.5459
					2TM3	0.1712	-0.6915	-0.3050	0.4714
					2TM4	0.2108	0.9411	0.7016	0.4986
					2TM5	-0.8407	0.9346	-0.4209	0.5344
					2TM6	-0.0255	-0.3576	-0.3107	0.1736
					2TM7	0.5836	-0.1296	-0.4414	0.4539
					4TM1	0.0390	0.0753	-0.1750	0.3259
					4TM2	-0.0226	0.1783	-0.1479	0.3425
					4TM3	-0.0443	-0.2348	-0.3111	0.2048
					4TM4	-0.1363	-0.1048	0.4907	0.3492
					4TM5	-0.0465	-0.0420	-0.2676	0.4315
					4TM6	-0.1677	0.0793	-0.4471	0.2726
					4TM7	0.1023	0.1513	-0.2923	0.3715

2TM1, ..., 7 are bands 1 to 7 of the February-9 TM data  
 4TM1, ..., 7 are bands 1 to 7 of the April TM data  
 XS1, 2, 3 are channel 1 to 3 of SPOT data  
 PS is the panchromatic mode of SPOT data.  
 $n = 60$

By comparison, XS3 showed the best information on HI (or SI), while 2TM5 contributed the most information to VI. The autumn imagery contained negligible information on SQ since its canonical coefficients (loading) were very small (Table 7.12b). The data suggests that the combinations of SPOT and TM data may compensate each other for inadequacy in their information content on stand structure. In the same spectral bands, SPOT data provided better information on stand variables than TM data, while the two MIR bands of TM data, which SPOT image does not have, could provide useful information on SQ. Different growing seasons may significantly influence the correlations of imagery data with stand variables and SQ.

#### 7.3.2.4 Canonical Correlations between Site Quality Indices and Site Variables

The canonical correlation analysis was performed to determine the correlations between the six SQ indices and six site variables (four topographic variables and two soil variables). As shown in Table 7.13a, the first two canonical correlations were significant at 0.02 or smaller significance levels, respectively explaining 49.7% and 31.8% of the

total variance and 81.5% together. Although the third pair of canonical variables explained about 11% of the total variance, their correlation was not significant ( $p < 0.37$ ). The remaining three canonical correlations together explained only 7% or less of the total variance and therefore were negligible.

Table 7.13a Results of CCA between SQ indices and site variables.

Canonical Correlation					Significance test ( $H_0: r = 0$ )				
	Canonical Correlations	Eigen Values	Prop. (%)	Cum. (%)	$\Lambda_i$	$\chi^2$	DF	Significance Levels	Decision
1	0.6976	0.9481	49.72	49.72	0.2301	77.15	36	0.0001	Reject
2	0.6143	0.6062	31.79	81.50	0.4482	41.33	25	0.0177	Reject
3	0.4177	0.2113	11.08	92.58	0.7198	16.60	16	0.3700	Accept
4	0.2814	0.0860	4.51	97.09	0.8720	6.78	9	0.6173	"
5	0.1982	0.0409	2.14	99.24	0.9469	2.64	4	0.5812	"
6	0.1198	0.0146	0.76	100	0.9856	0.69	1	0.3836	"

Table 7.13b Standardised canonical coefficients and correlations between the original variables and the canonical variables of opposite sets of variables.

SQ Indices					Site Variables				
Standardised Canonical Coefficients for SQ Indices			Corr. Between SQ & 1st two Cano. Var. of Site Var.		Standardised Canonical Coefficients for Site Variables			Corr. Between Site Var. & 1st two Cano. Var. of SQ Indices	
$x$	$u_1$	$u_2$	$r_{v_1}$	$r_{v_2}$	$y$	$v_1$	$v_2$	$r_{u_1}$	$r_{u_2}$
SI	1.1394	-1.9843	0.1692	-0.3850	SLP	-0.0841	-0.3437	-0.2001	-0.0219
HI	-1.6898	-0.0969	0.1228	-0.3141	ALT	-0.5243	-0.7886	-0.5138	-0.3634
VI	1.3761	0.6636	0.5137	0.0399	ASP	-0.1260	0.4044	-0.0855	0.2846
DI	0.9641	0.1074	0.1902	-0.2354	TP	0.6653	-0.5880	0.6036	-0.2304
BAI	-0.8032	-0.3785	0.2115	-0.0684	AB	-0.0249	0.0776	0.2449	-0.0077
CI	-0.1822	1.5061	0.0441	-0.1375	GC	-0.0245	0.4945	-0.2092	0.1420

HI, SI and VI showed large loadings ( $> 1$  in absolute term) for the first canonical variable of the SQ indices, with more emphasis on HI (Table 7.13b). VI showed a slightly lower canonical coefficients (1.38) than HI for the first canonical variable, but it had the highest correlation (0.51) with the canonical variable of the site variables. This means that VI is more sensitive to the first canonical variable contributed mainly by TP (0.67) and ALT (-0.52). This is because volume (VOL) and VI was most correlated with ALT and TP (see Tables 6.5 and 7.8). HI had the highest loading (-1.69) for the first canonical variable of SQ indices, but its correlation with the first canonical variable of SQ indices was relatively small. Therefore VI and TP should be seen as the dominant variables for the first pair of canonical variables.

In the second pair of canonical variables, SI showed the highest loading (-1.98) and also the highest correlation (-0.39) with the second canonical variable of the opposite set of variables. ALT did the same in the site variable set, with the canonical coefficient (loading) and correlation with the canonical variable of SQ indices being -0.79 and -0.36

respectively (Table 7.13b). Therefore SI and ALT can be seen as the dominant variables for the second pair of the canonical variables.

The canonical correlation analysis above showed that both SI and VI are the best two indicators of SQ in the study area. This agrees with the idea that SI is the best indicator of SQ in most studies. The site variables most influencing SQ are altitude (ALT) and topographic positions (TP). The soil variables showed the smallest contributions to SQ and can be considered of negligible importance in this study.

### 7.3.3 Estimation of Site Quality

#### 7.3.3.1 Introduction

The relationships between SQ and imagery data have been comprehensively investigated with correlation analysis, PCA and CCA techniques in the above sections. Some of the spectral bands and/or combinations have shown strong correlations with SQ indices. These results demonstrated that there is some potential for estimating SQ with the bands highly correlated with SQ indices. These high correlations lead to the development of the following two hypotheses:

- (1) SQ can be estimated using SPOT and TM data and their combinations;
- (2) the estimation accuracy of SQ may be improved by incorporating ground ancillary data.

These two hypothesis will be examined in the following sections and subsections using regression analysis techniques, including simple linear and non-linear regression, multiple and stepwise regression. The study serves two major purposes: (1) to determine the predictor variables (spectral bands) for site quality estimation; and (2) to derive prediction models to estimate the site quality from imagery data and ground ancillary data. The investigations in the earlier sections demonstrated that the highest correlations were associated with HI and SI measures of site quality and infrared bands, thus the emphasis of regression analysis will be on the combinations of these two variables. HI and SI are, therefore, used as the major indicators (dependent variables) of site quality in the regression analysis. Table 7.14 summarises the basic statistics of HI and SI. All variables and their combinations (or transformations) used in correlation and canonical correlation analysis were entered into the pool of variables to be regressed against SQ. The performances of each regression model were evaluated by the model correlations ( $r$  and  $r^2$ ) and errors (MAE and RMSE) in the following subsections.

Table 7.14 The basic statistics of SQ indices HI (m/yr) and SI (m).

<i>SQ Measures</i> \ <i>Statistics</i>	<i>Mean</i>	<i>SD</i>	<i>SE</i>	<i>CV</i>	<i>Min</i>	<i>Max</i>	<i>Range</i>
SI	19.12	3.35	0.44	17.53	13.88	26.68	12.80
HI	0.89	0.20	0.03	21.99	0.57	1.32	0.75

### 7.3.3.2 Scatter Plots

The relationships between SQ (HI and SI) and the spectral values of the sixty sample points are shown in Figures 7.1 to 7.3. It can be seen that only the NIR bands (XS3 and TM4) showed a regular (approximately linear) change with SI and HI. The regular change also occurred between the HI and SI and NIR-related band linear combinations (such as PC images and vegetation indices) (Figures 7.4 and 7.5). The plots indicate that the relationships between SQ and spectral reflectance, the NIR band in particular, can be described by linear regression models (see below).

### 7.3.3.3 Simple Regression

The regression modelling began with simple regression analysis between SQ (HI and SI) and NIR and NIR-related band combinations (mainly PC2, AVI, RVI, NIR-Green or NIR/Green). In addition to simple regression analysis, several non-linear functions used in Chapter 5 were also tried in regression analysis, but the results were not as good as those from linear models. The reason is that most of the sample plots were located in the stands between 9 to 32 years of age, in which period the spectral reflectance values decreased (see Chapter 5 and 6). Therefore the regression analysis was concentrated on the linear model. In addition, various band transformations were also regressed against SQ indices. The results presented below are those with better performances (i.e. higher correlations and lower errors).

As shown in Table 7.15, all models were strongly significant at the 0.001 level. All  $F$ -values were 4 times larger than the critical value. The coefficients of determination ( $r^2$ ) ranged from 0.62 to 0.77 for the summer images and 0.32 to 0.49 for the autumn image. The summer images also showed lower estimate errors (MAE and RMSE). NIR and/or NIR related band combinations and principal component transformation could improve the fitting. The best model (with the highest correlations and the lowest RMSE and MAE) was obtained using the PC2 (greenness). This may be attributable to the better information content of PC2 which is believed to be associated with the quality and quantity of vegetation (Lodwick 1979; and Kauth and Thomas 1976) (see Chapter 5).

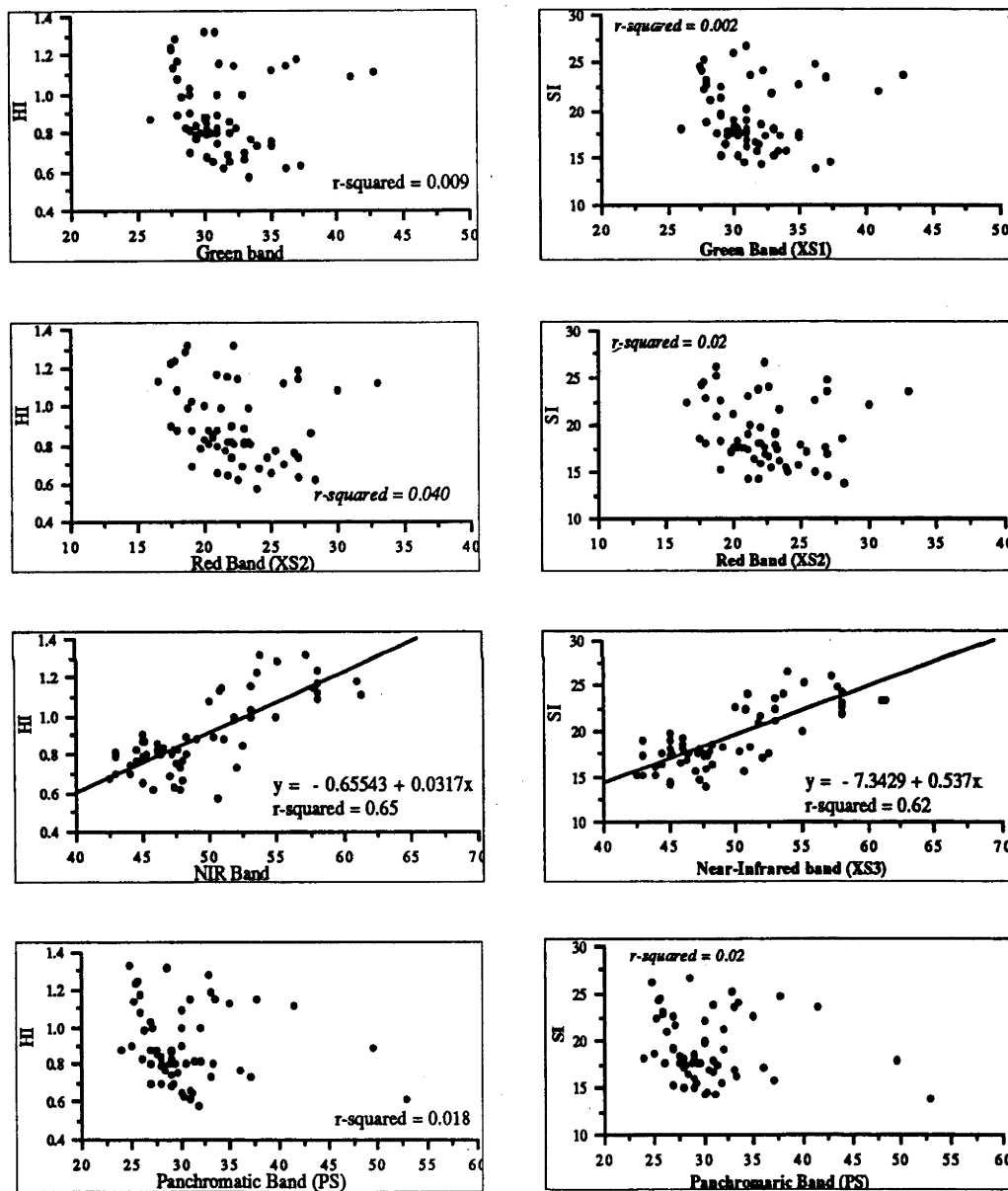


Figure 7.1 Relationships between SQ indices (SI (m) and HI (m/yr)) and SPOT band data.



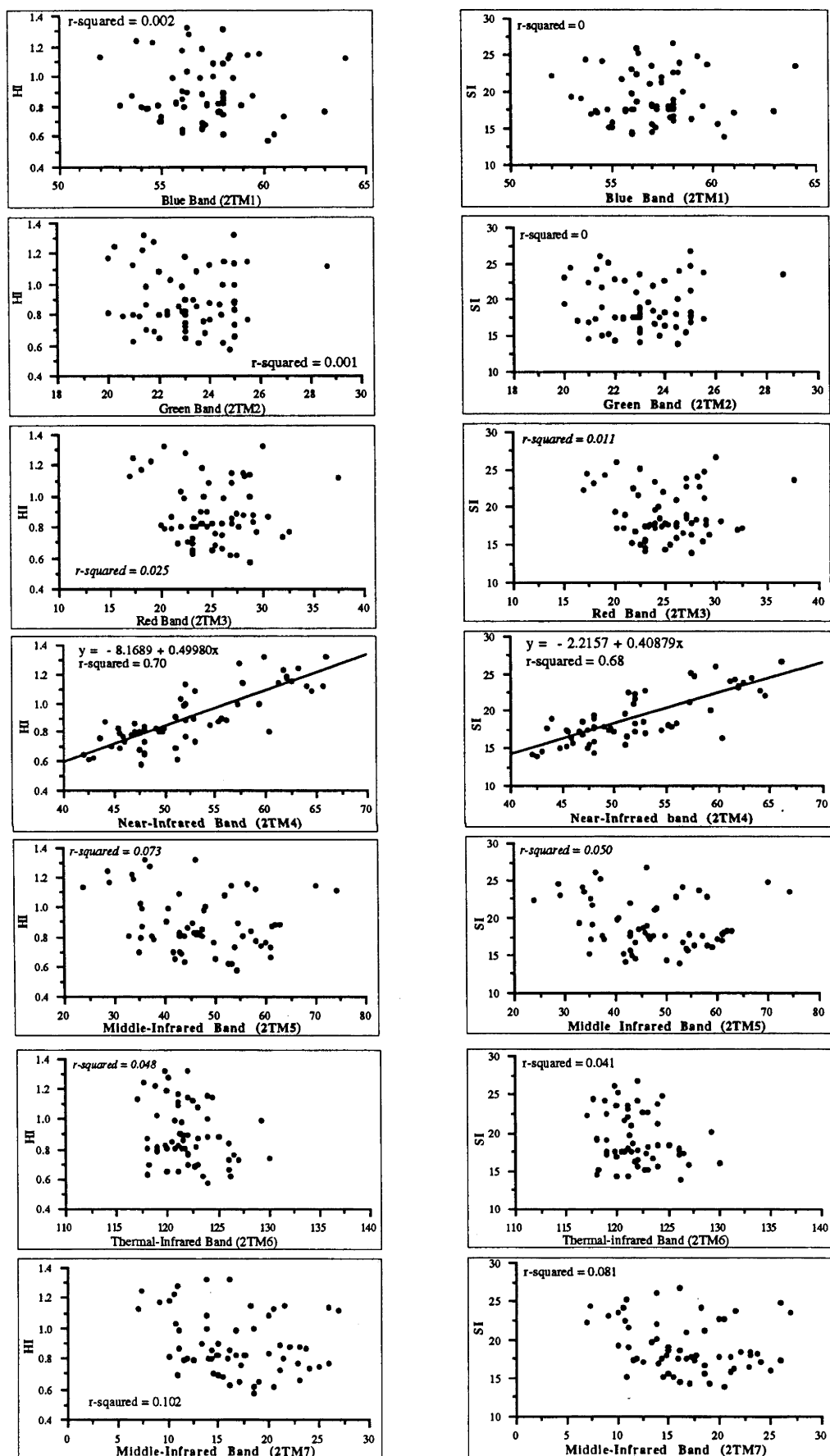


Figure 7.2 The relationships between SQ indices (SI (m) and HI (m/yr)) and the February-9 TM band data.

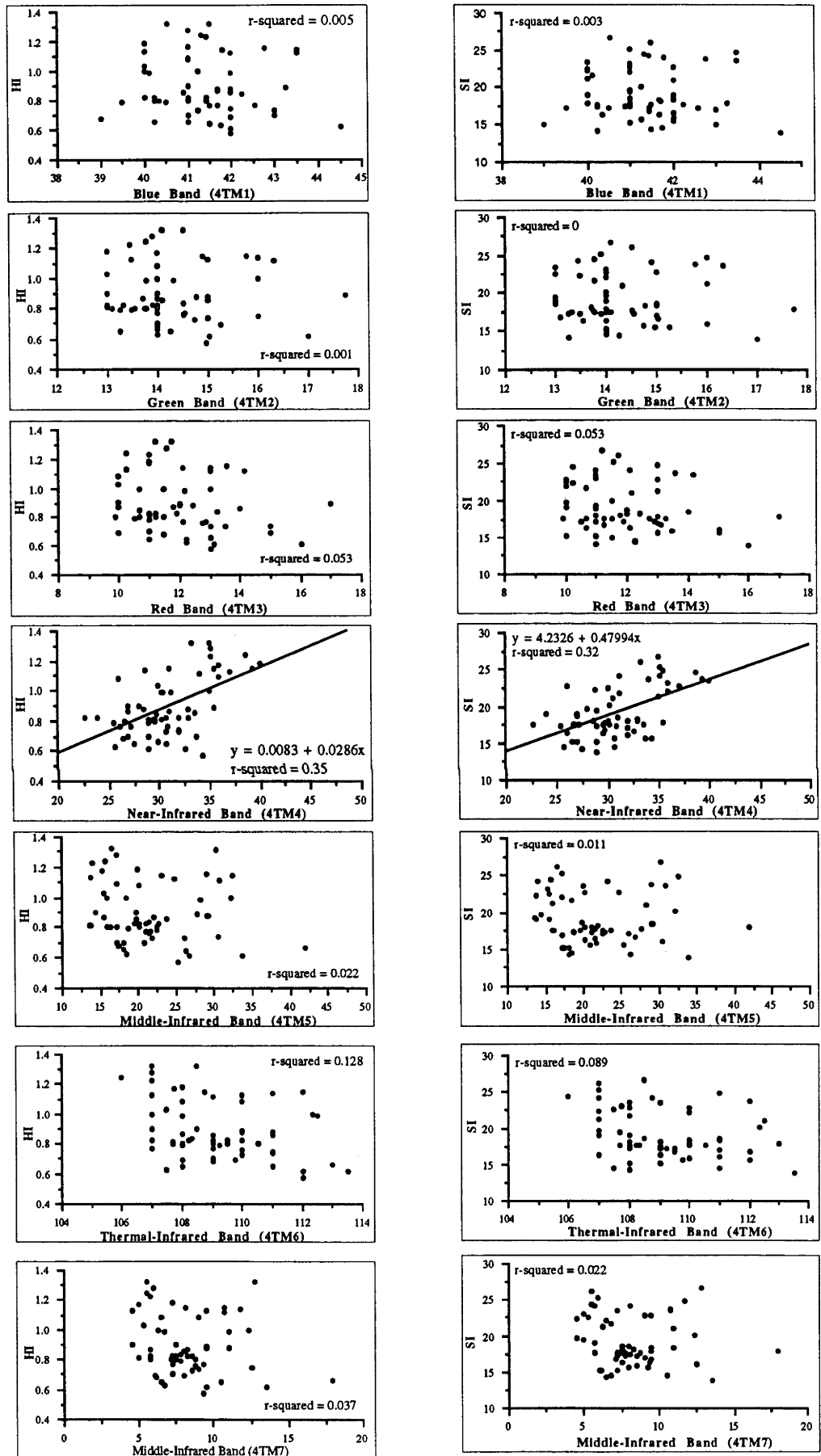


Figure 7.3 Relationships between SQ indices (SI (m) and HI (m/yr)) and the April-21 TM band data.

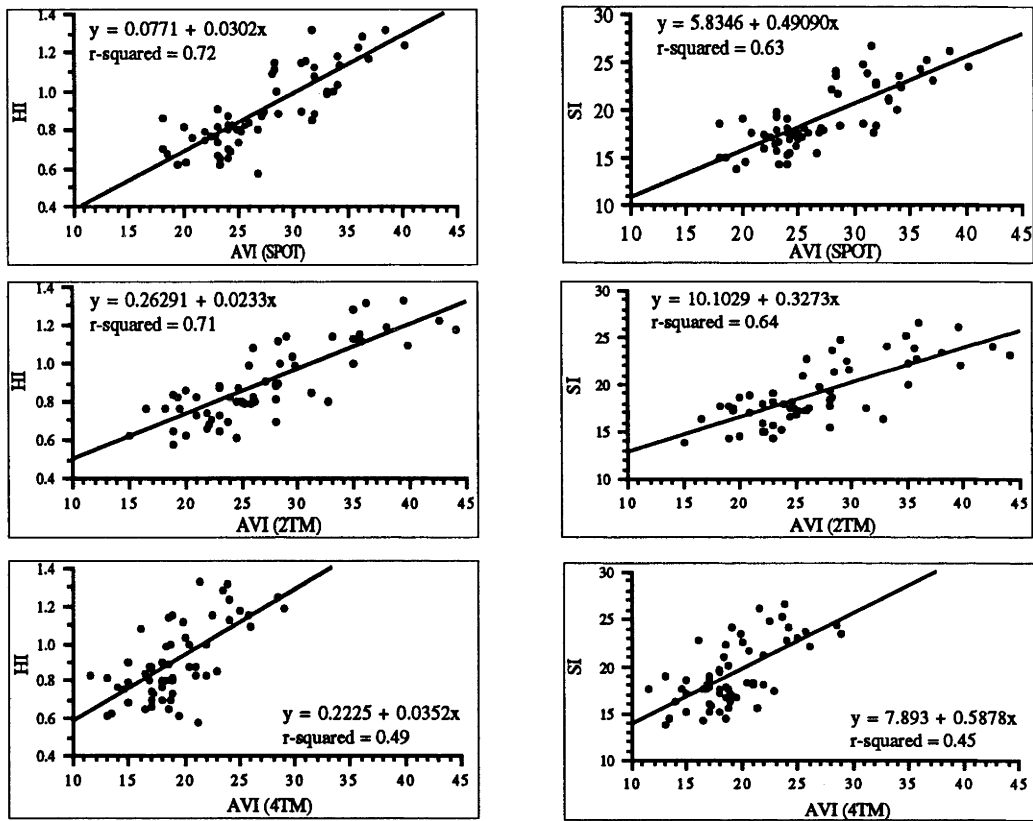


Figure 7.4 Relationships between AVIs and SQ indices (SI (m) and HI (m/yr)).

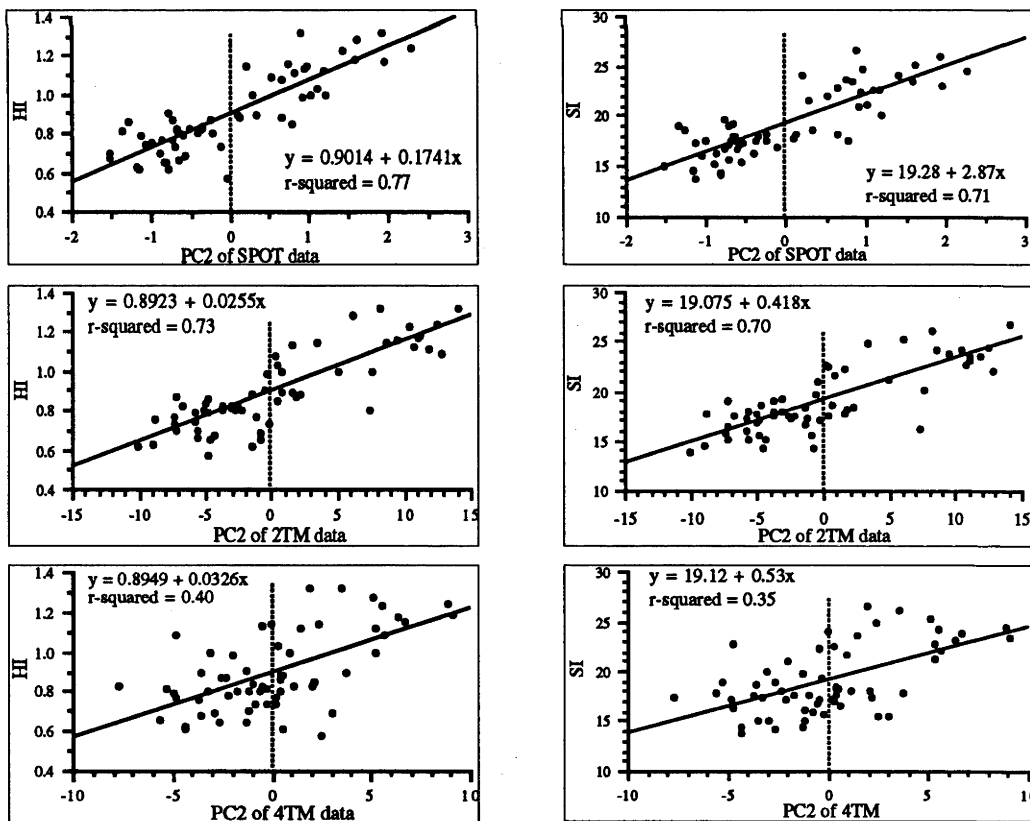


Figure 7.5 Relationships between PC2 (greenness) and SQ indices (SI (m) and HI (m/yr)).

Table 7.15 Evaluation of simple regression model performance for predicting radiata pine plantation site quality (HI and SI) using single band data<sup>1</sup>.  $n = 60$ .

Dependent Variables	Independent Variables	$a$	$b$	MAE	RMSE	$r^2$	$r_a^2$	F-values
The January-24 SPOT Image								
HI	XS3	-0.6643	0.0317	±0.0867	0.1163	0.6466	0.6404	104.270***
	AVI	0.0843	0.0302	±0.0883	0.1043	0.7159	0.7109	143.606***
	XS3-1	0.2840	0.0341	±0.0780	0.0996	0.7406	0.7361	162.774***
	PC2	0.9068	0.1741	±0.0724	0.0936	0.7711	0.7671	192.070***
SI	XS3	-7.3429	0.5370	±1.6176	2.0732	0.6232	0.6166	94.26***
	AVI	5.9123	0.4901	±1.3308	2.0416	0.6346	0.6282	98.98***
	XS3-1	9.0641	0.5598	±1.2504	1.9431	0.6690	0.6632	115.20***
	PC2	19.2845	2.8695	±1.2199	1.8414	0.7027	0.6975	134.74***
The February-9 TM Data								
HI	TM4	-0.4236	0.0253	±0.0827	0.1091	0.7023	0.6971	134.45***
	AVI	0.2548	0.0237	±0.0873	0.1080	0.7081	0.7030	138.26***
	PC2	0.8970	0.0263	±0.0763	0.1034	0.7315	0.7268	155.31***
SI	TM4	-2.87826	0.4232	±1.5277	1.9130	0.6814	0.6760	121.90***
	AVI	8.8467	0.3816	±1.4799	2.0423	0.6369	0.6305	99.96***
	PC2	19.1746	0.4354	±1.3499	1.8715	0.6951	0.6897	129.92***
The April-21 TM data								
HI	TM4	-0.0113	0.0293	±0.1225	0.1451	0.3540	0.3425	30.69***
	AVI	0.2222	0.0353	±0.1086	0.1347	0.4919	0.4825	54.14***
	PC2	0.8964	0.0324	±0.1157	0.1457	0.4049	0.3943	38.11***
SI	TM4	4.0852	0.4843	±2.0038	2.6983	0.3223	0.3102	26.64**
	AVI	7.9468	11.59	±1.8240	2.6117	0.4480	0.4381	45.45***
	PC2	19.1119	0.5204	±2.0038	2.6504	0.3461	0.3345	38.11***

<sup>1</sup> The results listed in this table are only those with better correlations ( $r^2$ ) with HI and SI. RMSE - Root mean square error; MAE - mean absolute error;  $r_a^2$  - Adjusted  $r^2$ , \*\*\* means that the models are significant at 0.001 significance levels.  $a$  - intercept;  $b$  - slope (regression coefficient)

The differences between the NIR and visible bands (i.e. NIR-Red (AVI) and NIR-Green) provided better SQ estimates than the original reflectance values. As discussed in Chapter 5, the spectral values in the visible bands (green and red) exhibited a non-linear inverse (inverse-J shape) change with stand age, while the NIR band showed a linear relationship with stand growth. Due to this difference, the differences between the NIR and visible bands may be able to highlight the subtle variations of the stands in different growth conditions (site quality). Better site quality usually leads a larger canopy and more needles, and therefore higher spectral absorption as well as lower spectral reflectance as the reflectance in the red and green waveband regions is inversely proportional to the amount of chlorophyll present in the tree canopy (Colwell 1974; Tucker 1977 and 1979; and Gausman *et al.* 1976).

Various "between-image" combinations were regressed against the SQ indices. Table 7.16 presents the results of simple regression analysis with the better model performances from the "between-image" combinations -  $D_4$  (2TM4-4TM4),  $M_4$  ((2TM4+4TM4)/2), MAVI ( $M_4$ - $M_2$ ) and the second principal component image of the two seasons' TM data together (14 bands). All these "between-image" combined images showed lower correlations, lower accuracy of estimate and larger estimate errors (MAE and RMSE) than those from the original band data. In comparison, the difference images showed

slightly better results than the mean images. Because the difference and mean images were computed from only two growing seasons in this work, it can not be concluded that the combination of multi-date (growing seasons) images can not improve the ability to detect change of stand structure and site quality.

Table 7.16 Results of simple regression analysis between SQ indices (HI and SI) and “between-image” combinations. The model parameters are the same as in Table 7.15.

Dependent Variables	Independent Variables	<i>a</i>	<i>b</i>	MAE	RMSE	$r^2$	$r_a^2$	F-values
HI	D4	0.1793	0.0338	±0.1003	0.1251	0.6001	0.5929	84.02***
	M4	-0.4189	0.0316	±0.0917	0.1269	0.5885	0.5812	80.09***
	MAVI	0.1604	0.0319	±0.0928	0.1161	0.6555	0.6493	106.54***
	PC2	0.8993	0.0233	±0.0866	0.1086	0.6985	0.6931	129.74***
SI	D4	7.1896	0.5657	±1.6692	2.1884	0.5780	0.5704	76.70***
	M4	-2.9483	0.5323	±1.7716	2.1982	0.5742	0.5666	75.51***
	MAVI	7.1439	0.5268	±1.5774	2.1205	0.6038	0.5967	85.34***
	PC2	19.2234	0.3878	±1.4875	1.9356	0.6698	0.6639	113.62***

\*\*\* means that the models are significant at 0.001 significance levels. MAVI - AVI of mean and difference images

### 7.3.3.4 Multiple Regression with Spectral Data Alone

Simple regression analyses undertaken in the previous sections showed that NIR and/or NIR-related band combinations produced the best estimate of SQ with a single spectral variable, explaining about 35% to 77% of the total variances. Further study focussed on examining how much greater a contribution to SQ estimation could be obtained when more bands and site variables were introduced, and which variables (or band combinations) were best for SQ estimation. These questions were addressed in the following by using multiple and stepwise regression analysis techniques.

All bands of each single date image were first used in the multiple regression analysis to evaluate their multiple contributions to SQ (Table 7.17). For SPOT data, the three bands together provided an estimate of  $0.90 \pm 0.07$  (MAE) m/year for HI (RMSE = 0.093,  $r^2 = 0.78$ ), and  $19.12 \pm 1.2$  m for SI (RMSE = 1.9 m,  $r^2 = 0.73$ ). Elimination of the red band (XS2) by stepwise regression analysis did not change the correlations and the error of estimates (MAE and RMSE). This indicates that the green and NIR bands provided almost all information on SQ.

An approximately equal correlation and estimate were also obtained from the February-9 TM image (Table 7.17). By stepwise regression analysis significance level, only 2TM4 and 2TM5 entered into the model, but the results were almost the same as those from all seven bands. This showed that the NIR and MIR bands of the TM data provided the most information on SQ, while the other five bands provided very little information and their elimination could not significantly reduce the estimate of site quality.

Table 7.17 Results of multiple and stepwise regression analyses between SQ indices (HI and SI) and the original band data. The significant level ( $p$ ) selected for entering variables in stepwise regression was 0.15.

Dependent Variables	Data	Bands	DF	MAE	RMSE	$r^2$	$r_a^2$
HI	SPOT	XS1, XS2, XS3	(3, 57)	$\pm 0.0711$	0.0929	0.7823	0.7704
		XS1, XS3 ( $p=0.15$ )	(2, 58)	$\pm 0.0713$	0.0921	0.7823	0.7745
	2TM	All 2TM bands	(7, 53)	$\pm 0.0697$	0.0960	0.7893	0.7650
		2TM4, 2TM5 ( $p=0.15$ )	(2, 58)	$\pm 0.0711$	0.0954	0.7763	0.7684
		2TM2, 2TM3, 2TM4	(3, 57)	$\pm 0.0760$	0.0975	0.7704	0.7578
	4TM	All 4TM bands	(7, 53)	$\pm 0.0963$	0.1374	0.5181	0.4614
4TM4, 4TM5 ( $p=0.15$ )		(2, 58)	$\pm 0.1086$	0.1341	0.5052	0.4872	
2TM2, 2TM3, 2TM4		(3, 57)	$\pm 0.1072$	0.1342	0.5136	0.4866	
SI	SPOT	XS1, XS2, XS3	(3, 57)	$\pm 1.3821$	1.8005	0.7258	0.7108
		XS1, XS3 ( $P=0.15$ )	(2, 58)	$\pm 1.3808$	1.7895	0.7242	0.7143
	2TM	All 2TM bands	(7, 53)	$\pm 1.3297$	1.8242	0.7357	0.7052
		2TM4, 2TM7 ( $p=0.15$ )	(2, 58)	$\pm 1.4016$	1.7773	0.7298	0.7202
		2TM2, 2TM3, 2TM4	(3, 57)	$\pm 1.4741$	1.8211	0.7214	0.7062
	4TM	All 4TM bands	(7, 53)	$\pm 1.8061$	2.4854	0.4764	0.4148
4TM4, 4TM5 ( $p=0.15$ )		(2, 58)	$\pm 1.9565$	2.4292	0.4606	0.4410	
2TM2, 2TM3, 2TM4		(3, 57)	$\pm 1.9444$	2.4296	0.4702	0.4407	

For the autumn image, all seven bands together explained only about 51% or less of the site quality variation. The errors of the estimate were also much larger than those from summer images. The best bands entered into the model in stepwise regression were the red (4TM3) and the NIR bands (4TM4).

Compared with the results of the simple regression analysis using the NIR band alone (Table 7.15), the introduction of the visible and/or middle and thermal bands (for TM images) increased the correlations ( $r^2$ ) by about 4 to 14%. In particular, the addition of the green band for SPOT data and the MIR band for TM data can significantly improve the correlation and model estimate of SQ. Comparing the equivalent spectral bands (i.e. XS1, XS2, XS3, TM2, TM3, TM4), SPOT data provided a better estimate of SQ (Table 7.17).

### 7.3.3.5 Regression Modelling with Spectral and Site Variables

Topographic variables (i.e. altitude (ALT), slope (SLP), and coded aspect (ASP) and topographic positions (TP)) were used in multiple regression analysis for determining their contributions to site quality (see Table 7.18). The multiple correlation was relatively low ( $r^2 = 0.24$  for HI, and 0.29 for SI). The introduction of soil variables (the depth of A and B horizons-AB, and gravel content-GC) did not improve the fitting. In comparison, the topographic variables showed more contributions to SI than to HI. This confirmed the results obtained in correlation analysis (Tables 7.8; Section 7.3.1.6) and canonical correlation analysis between SQ and site variables (Table 7.13a-b; Section 7.3.2.4) in which SI was more sensitive to site variables, especially ALT and TP, than HI.

Table 7.18 The results of multiple regression analyses by integrating spectral bands with topographic variables (i.e. ALT, SLP, ASP and TP defined in Chapter 4).

Dependent Variables	Variables entering the regression models	DF	MAE	RMSE	$r^2$	$r_a^2$
HI	ALT, SLP, ASP, and TP	(4, 56)	±0.1300	0.1815	0.2446	0.1238
	ALT, SLP, ASP, TP, AB, and GC	(6, 54)	±0.1299	0.1852	0.2450	0.0877
	XS1, XS3, Topographic variables	(10, 50)	±0.0655	0.0908	0.8186	0.7809
	2TM4, 2TM5, topographic variables	(10, 50)	±0.0583	0.0853	0.8468	0.8158
	4TM4, 4TM5, topographic variables	(10, 50)	±0.0882	0.1295	0.6055	0.5216
SI	ALT, SLP, ASP, and TP	(4, 56)	±2.2386	3.0300	0.2939	0.1810
	ALT, SLP, ASP, TP, AB, and GC	(6, 54)	±2.2326	3.0915	0.2944	0.1474
	XS1, XS3, Topographic variables	(10, 50)	±1.1733	1.6691	0.7943	0.7515
	2TM4, 2TM5, topographic variables	(10, 50)	±1.1054	1.5410	0.8259	0.7896
	4TM4, 4TM5, topographic variables	(10, 50)	±1.4765	2.2148	0.6168	0.5353

Further analyses were made to examine the contributions of topographic variables to the estimate of SQ when integrating them with the spectral bands. The multiple regression analyses were undertaken by adding the topographic variables to the spectral bands with better contributions to the SQ estimation (see Table 7.17). As shown in Table 7.18, the integration of the topographic variables with XS1 and XS3 of the SPOT image did not improve their correlations with HI. This can be explained by the low correlations between HI and site variables. However, the errors of the estimates (RMSE) were smaller than that from XS1 and XS3 alone. The introduction of topographic variables could significantly improve the regression model fitting for SI, with correlations ( $r_a^2$ ) increasing from 0.71 to 0.79. The errors of estimate (MAE) were also much smaller, reducing from ±1.38 m to ±1.17 m.

When applying the topographic variables to the TM-derived regression models, the estimate of SQ was significantly improved (Table 7.18). For example, the topographic variables increased the correlations with HI from 0.77 to 0.82, and with SI from 0.72 to 0.79 for the February-9 TM image. The same was true for the April-21 TM image. The integration of topographic variables with the 4TM3 and 4TM4 increased the explanation of the variance ( $r_a^2$ ) from 48.72% to 52.16% for HI and 44.10% to 53.43% for SI (Table 7.17 and 18). The addition of topographic variables to the TM data also gave a greater reduction of the error of the estimates than to SPOT data.

As reviewed in the previous chapters, spectral radiance measurements of canopies are influenced by live biomass, dead biomass, moisture content, canopy geometry, soil background, sun angle and many other factors (Hardisky *et al.* 1984, Häme 1991). The introduction of ground ancillary data, topographic variables in particular, may compensate for the effects of physical characteristics such as aspect and slope on spectral reflectance.

The differences in variance contributions and errors of the estimates (MAE and RMSE) suggest that topographic variables have more effect on the spectral reflectance of the TM image than the SPOT image. The ancillary data may not be very important when using SPOT images, but may be very helpful in improving estimates of site quality and yield when using TM images.

### 7.3.3.6 Regression Modelling with Multi-temporal and Multi-sensor Data and Site Variables

Studies reported in this thesis have shown that the information content of spectral bands of imagery data changes over time (e.g. growing seasons). A further assumption is that the combined images from multi-temporal data may provide better information on SQ and therefore may be able to improve the estimate of SQ. This assumption was tested by stepwise regression using all raw spectral bands and various band combinations. The best bands and/or band combinations entering the regression models and the results of their inclusion are summarised in Table 7.19.

Table 7.19 Performance of several best regression models (a-h) relating SQ indices (HI and SI) to the multi-temporal and multi-sensor data and site variables.

Dependent Variables	Models	Variables entering the regression models	MAE	RMSE	$r^2$	$r_a^2$	$r_{op}^2$
HI	a	XS1, XS3, 2TM4, 2TM5, 4TM4	±0.0630	0.0823	0.8356	0.8201	0.8105
	b	XS1, XS3, 2TM4, 2TM5, 4TM4 and Topographic Variables	±0.0536	0.0756	0.8820	0.8479	0.8820
	c	XS1, XS3-1, 2TM4-2, 2TM3/5 4TM4/2	±0.0631	0.0806	0.8420	0.8270	0.8420
	d	XS1, XS3-1, 2TM4-2, 2TM3/5 4TM4/2, & Topographic Variables	±0.0532	0.0740	0.8871	0.8545	0.8871
SI	e	XS1, XS3, 2TM4, 2TM5, 4TM4	±1.1343	1.4983	0.8123	0.7943	0.8123
	f	XS1, XS3, 2TM4, 2TM5, 4TM4 and Topographic Variables	±0.9914	1.4047	0.8904	0.8192	0.8604
	g	XS3-1, 2TM4/2, 2TM4-2, 2TM3/5 4TM4-2	±1.1322	1.4859	0.8154	0.7977	0.8154
	h	XS3-1, 2TM4/2, 2TM4-2, 2TM3/5 4TM4-2, & Topographic Variables	±0.9551	1.3649	0.8682	0.8293	0.8682

$r_{op}^2$  is the correlation between observed and model-predicted values.

Compared with the results from the single date images (Tables 7.15-7.17), the bands selected from multi-temporal images provided better estimates. The correlations increased by about 5% from summer images and about 30% for the autumn image. The errors of the estimates (MAE and RMSE) were also lower than those from the single date images. Figure 7.6 shows the relationships between the observed and model-estimated SQ (HI and SI). All estimates of SQ showed 81% or higher agreements with the actual values (Table 7.19).



## Mean Annual Increment in Height (HI, m/yr)

## Site Index (SI, m)

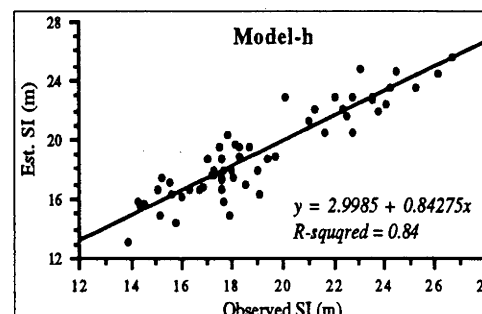
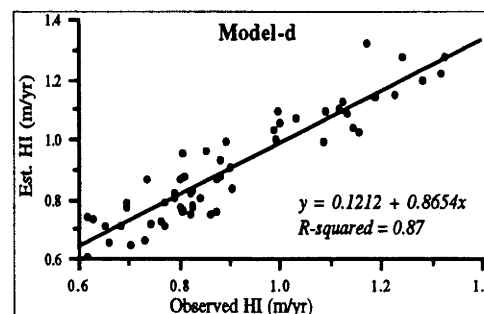
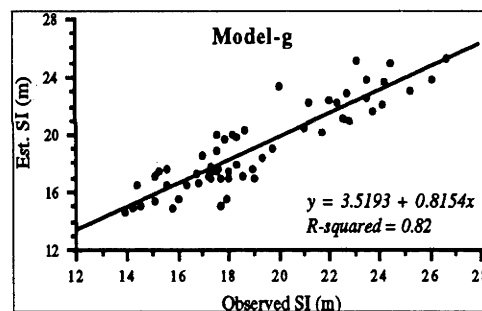
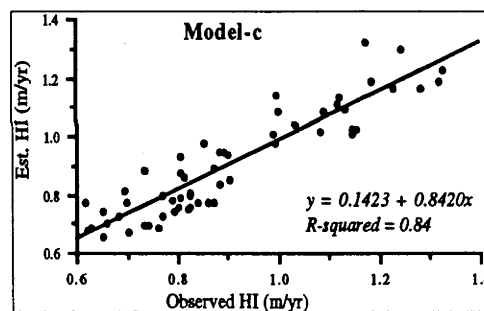
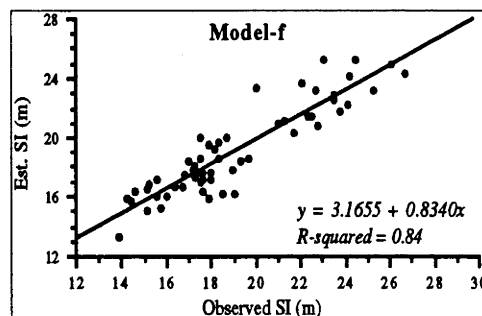
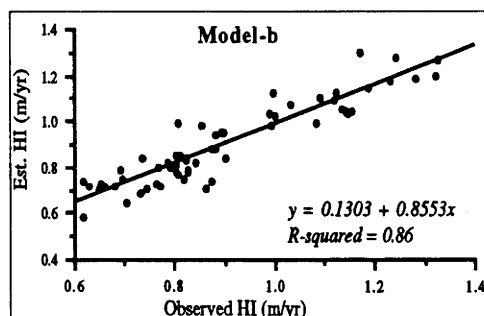
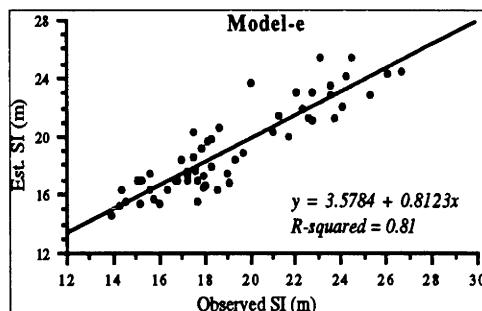
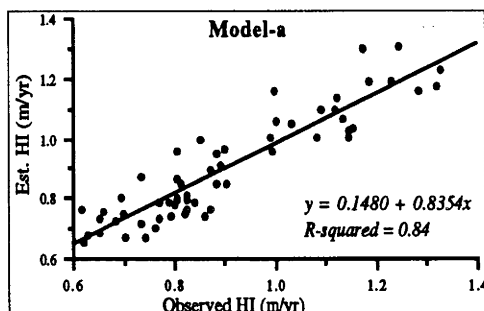


Figure 7.6 Relationships between Observed and model-derived SQ Indices (SI (m) and HI (m/yr)). Model-a to Model-h were defined in Table 7.19.

The following two regression models were used for predicting MAI in height ( $\hat{H}I$ ) and  $\hat{S}I$  (i.e. Model-*d* and Model-*h* in Table 7.19) and SQ mapping (inserted in Page 202).

Model-*d*

$$\hat{H}I = -0.430826 + 0.007596 \cdot XS1 + 0.022023 \cdot (XS3 - XS1) + 0.015383 \cdot (2TM4 - 2TM2) + 0.610794 \cdot \frac{2TM3}{2TM5} - 0.146646 \cdot \frac{4TM4}{4TM2} + 0.000299 \cdot ALT - 0.001192 \cdot SLP + 0.05731 \cdot ASP2 + 0.004319 \cdot ASP2$$

Model-*h*

$$\hat{S}I = 0.514259 + 0.253049 \cdot (XS3 - XS1) - 4.965601 \cdot \frac{2TM4}{2TM2} + 0.553111 \cdot (2TM4 - 2TM2) + 12.324635 \cdot \frac{2TM3}{2TM5} + 0.188073 \cdot (4TM4 - 4TM2) + 0.006883 \cdot ALT - 0.009478 \cdot SLP + 1.19971 \cdot ASP2 + 0.300923 \cdot ASP2$$

### 7.3.4 Site Quality Mapping and Assessment of Accuracy

The two SQ indices, HI and SI, which were best related to the independent variables, were selected for site classification and mapping. The pixel-based SQ was computed using the models listed in Table 7.19 with or without the site variables. The SQ classes were then grouped according to the SQ class standard set by Lewis *et al.* (1976) (see Table 3.2). Figure 7.7 shows the pixel (area) distribution (percentage frequency) of the model-estimated SQ over the study area (Model-*d* for HI and Model-*h* for SI). It can be seen that the site quality of most of the study area was poorer than SQ class V (cf VI: SI = 27; and VII: SI = 24). In order to reflect the differences of the site quality in the study area, the model-estimated SQ was grouped into four site quality classes K1 to K4 (Table 7.20). These four site quality classes were displayed as a classification map showing the classes in blue, green, red and yellow respectively (see Figures 7.8-15).

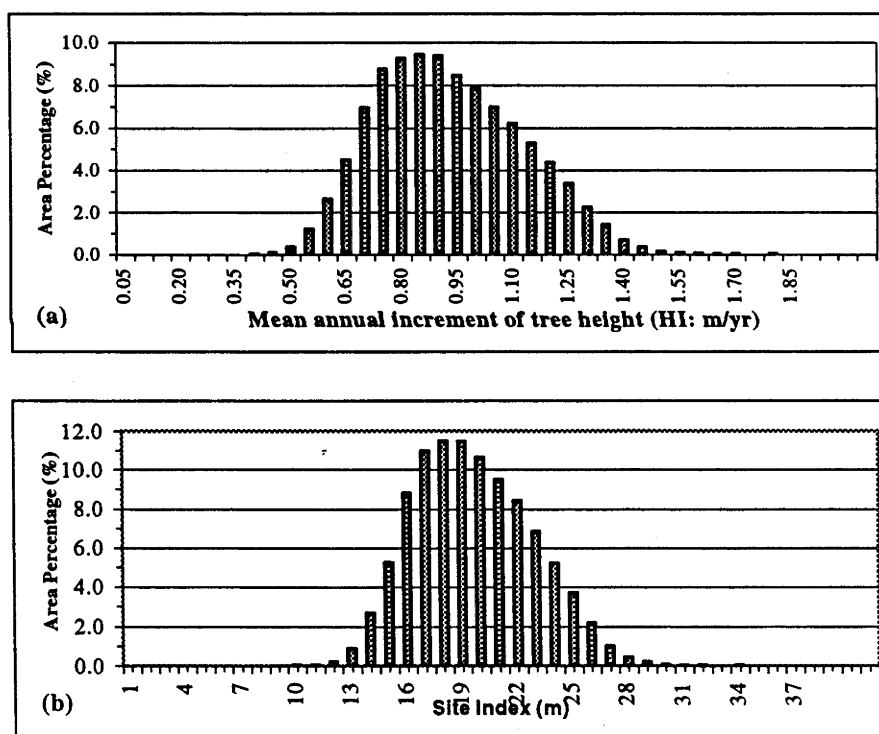


Figure 7.7 Distribution of site quality of the radiata pine plantation sites in the study area: Mean annual increment in height (HI) (b) and site index (SI) (a).

Table 7.20 Site quality classes of the radiata pine plantation sites.

Site Classes	Site Index Limits (m)	Mean Annual Increment Limits (m/yr)	Colours in the SQ maps (Figure 7.10-17)
K-1	25: $\geq 24$	1.30: $\geq 1.10$	Yellow
K-2	22: 21 - 23	1.10: 0.90 - 1.10	Red
K-3	19: 18 - 20	0.90: 0.75 - 0.90	Green
K-4	16: $\leq 17$	0.70: $\leq 0.75$	Blue

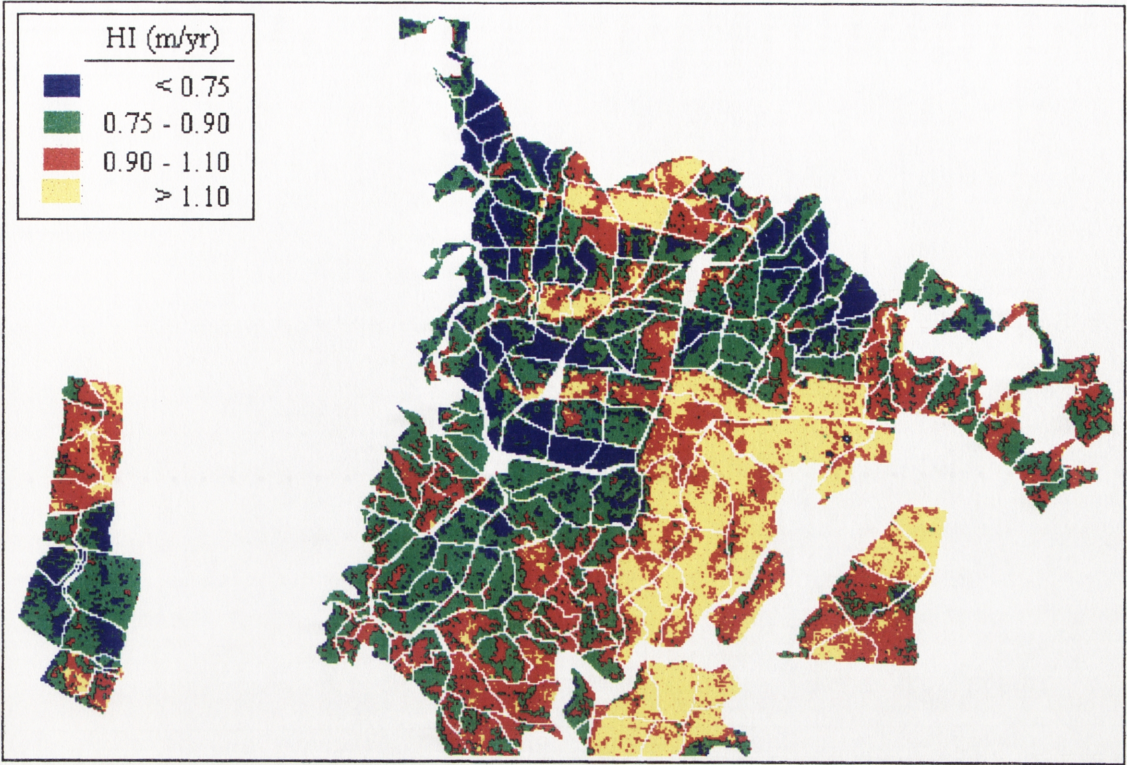


Figure 7.8 Site quality classes based on HI (m/yr) estimated from model-*a* (see Table 7.19 for details).

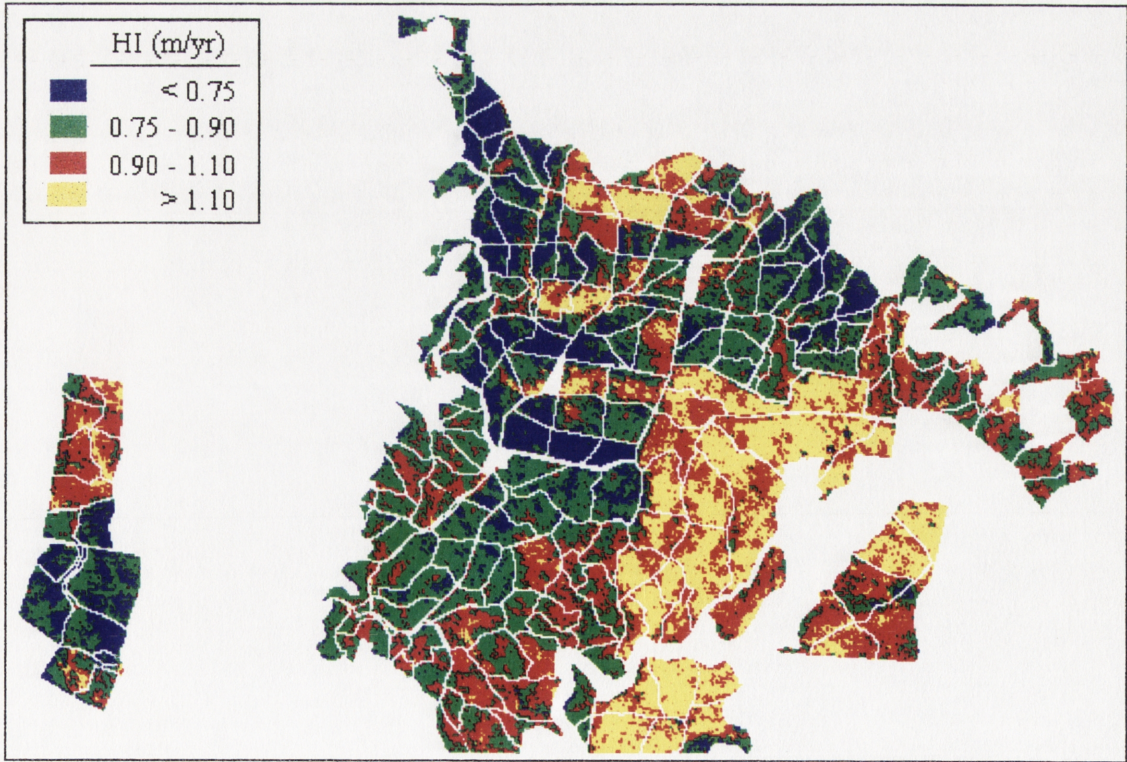


Figure 7.9 Site quality classes based on HI (m/yr) estimated from model-*b* (see Table 7.19 for details).

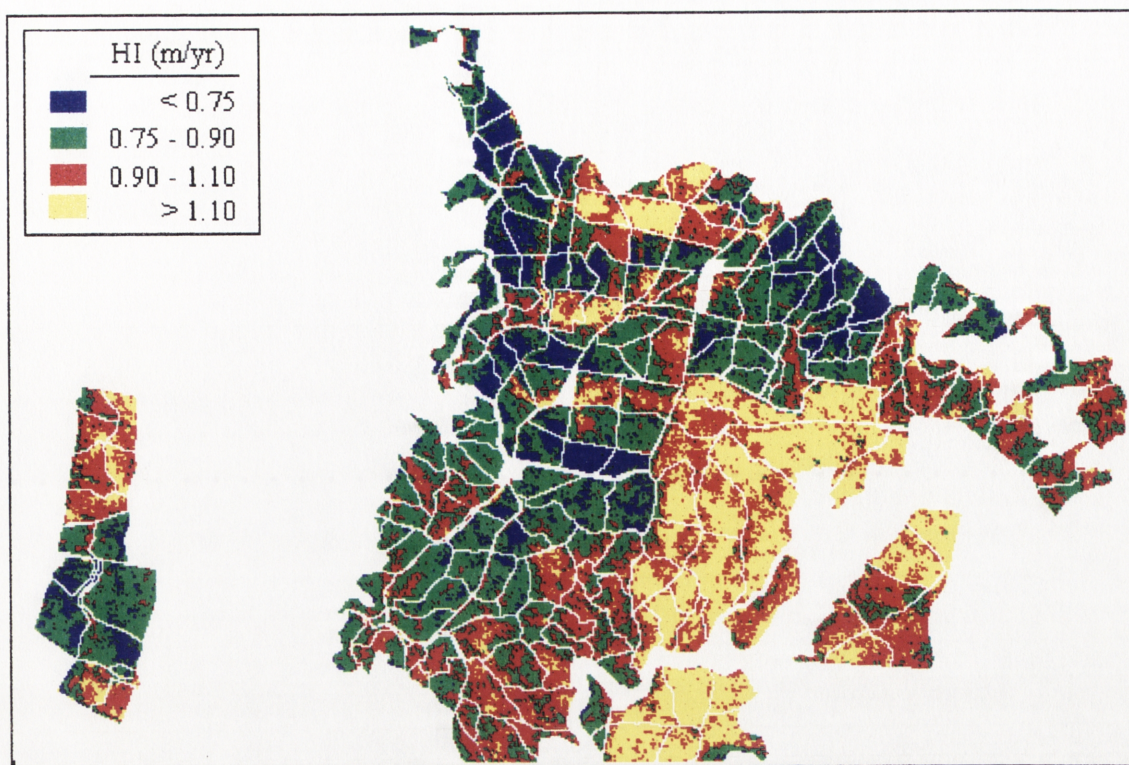


Figure 7.10 Site quality classes based on HI (m/yr) estimated from model-c (see Table 7.19 for details).

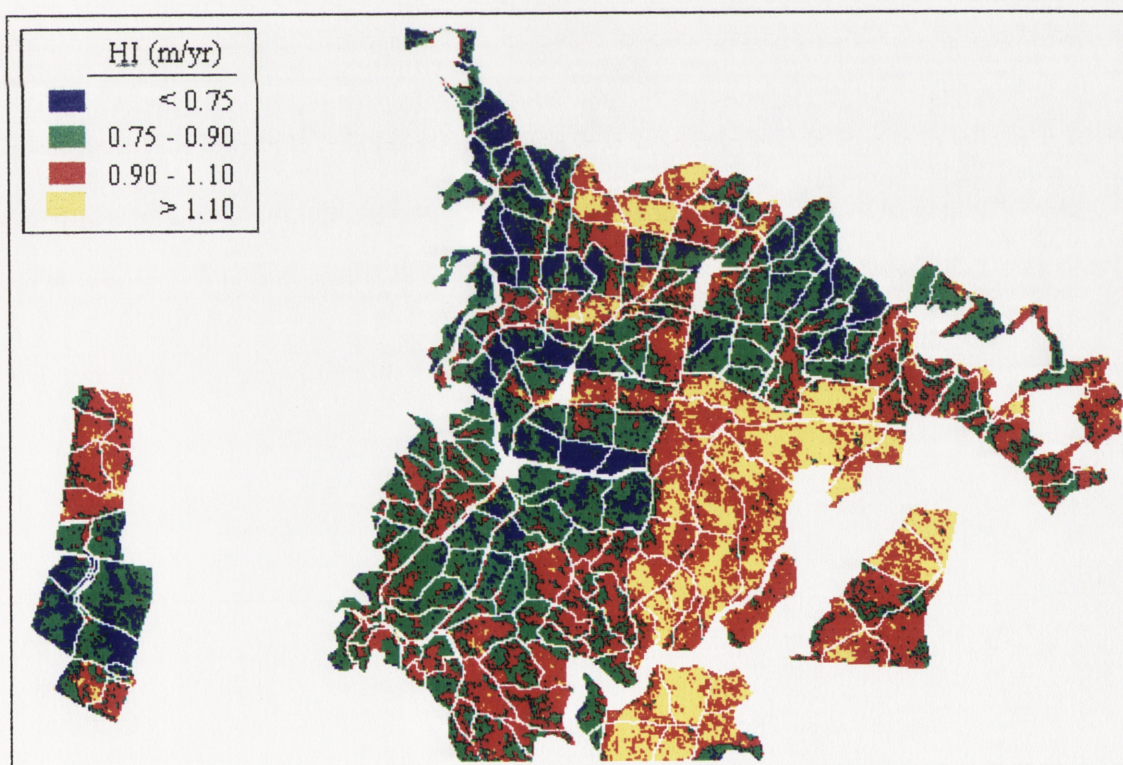


Figure 7.11 Site quality classes based on HI (m/yr) estimated from model-d (see Table 7.19 for details).

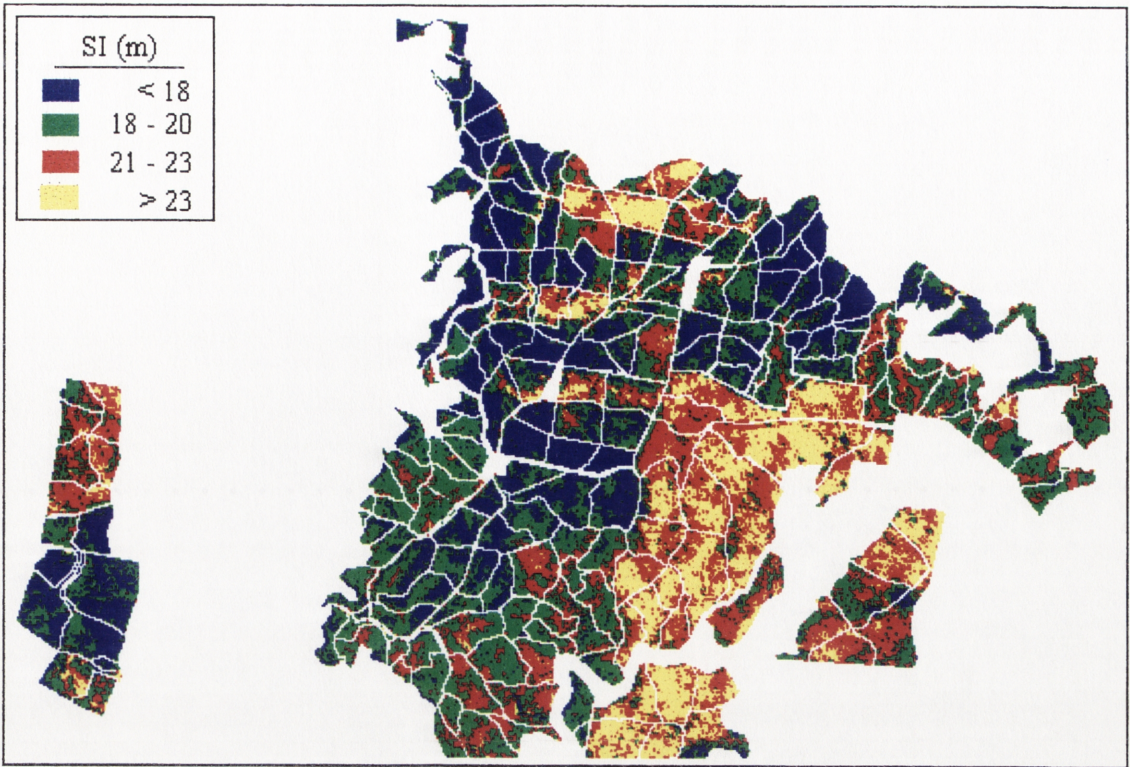


Figure 7.12 Site quality classes based on SI (m) estimated from model-*e* (see Table 7.19 for details).

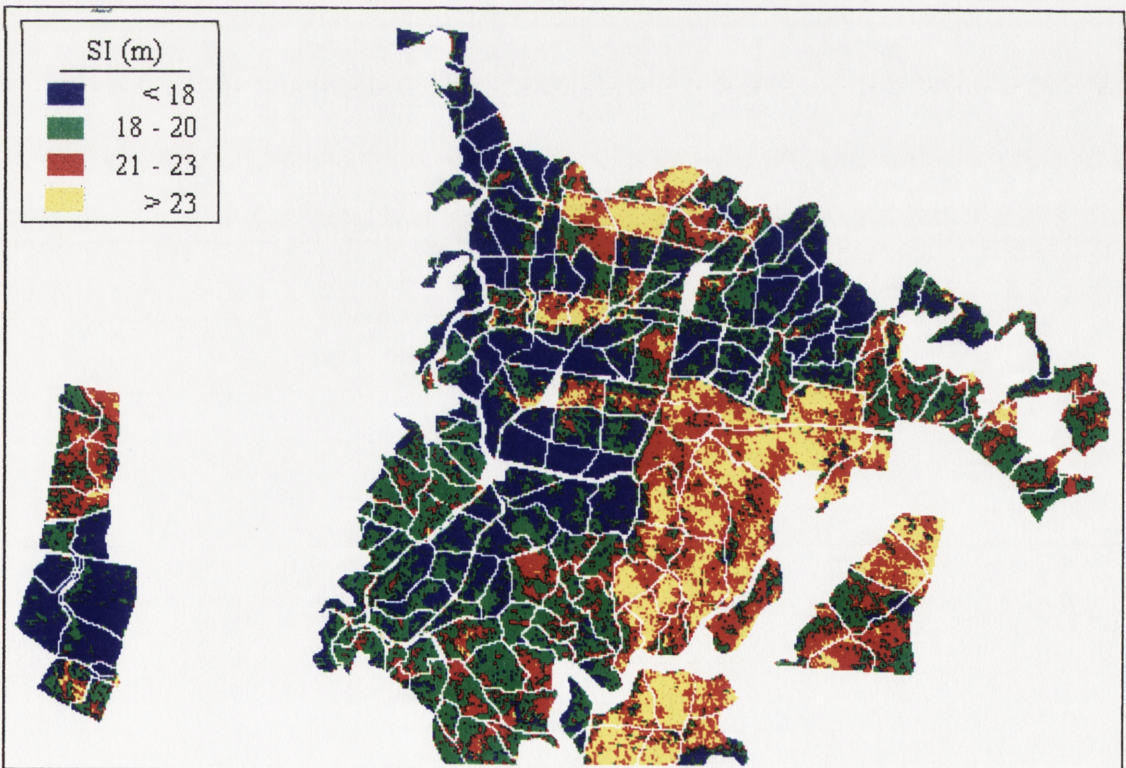


Figure 7.13 Site quality classes based on SI (m) estimated from model-*f* (see Table 7.19 for details).

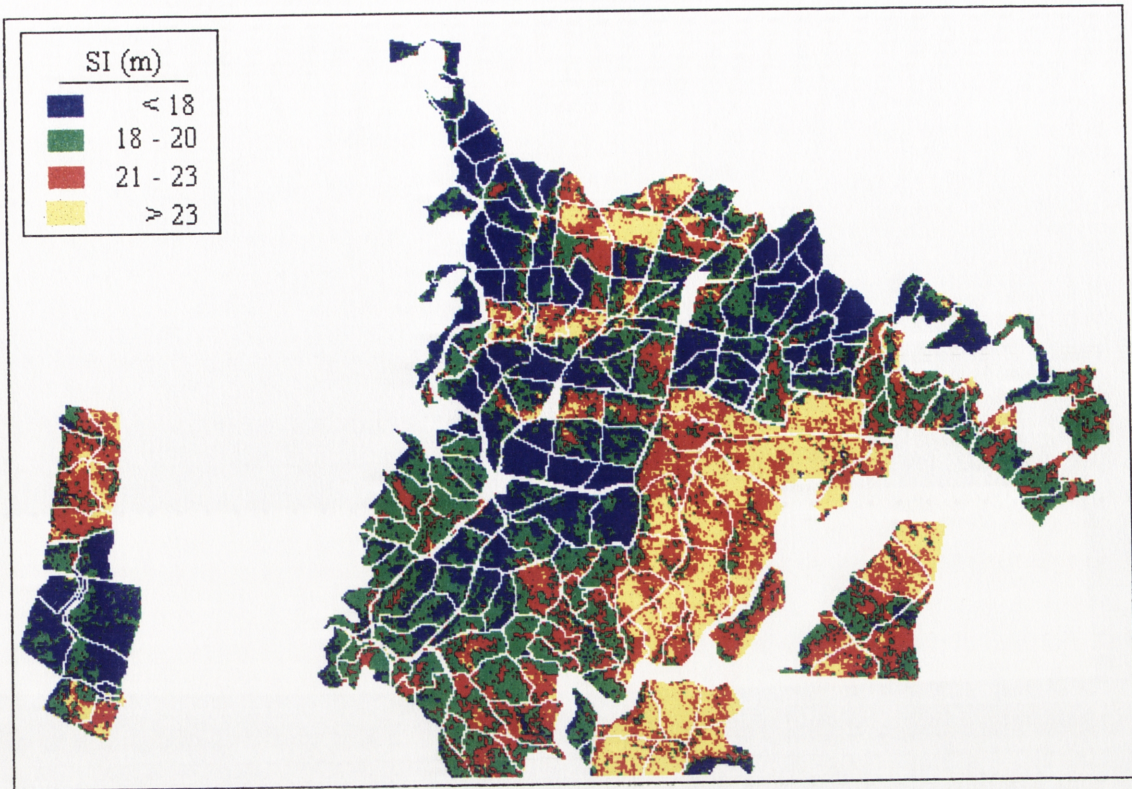


Figure 7.14 Site quality classes based on SI (m) estimated from model-g (see Table 7.19 for details).

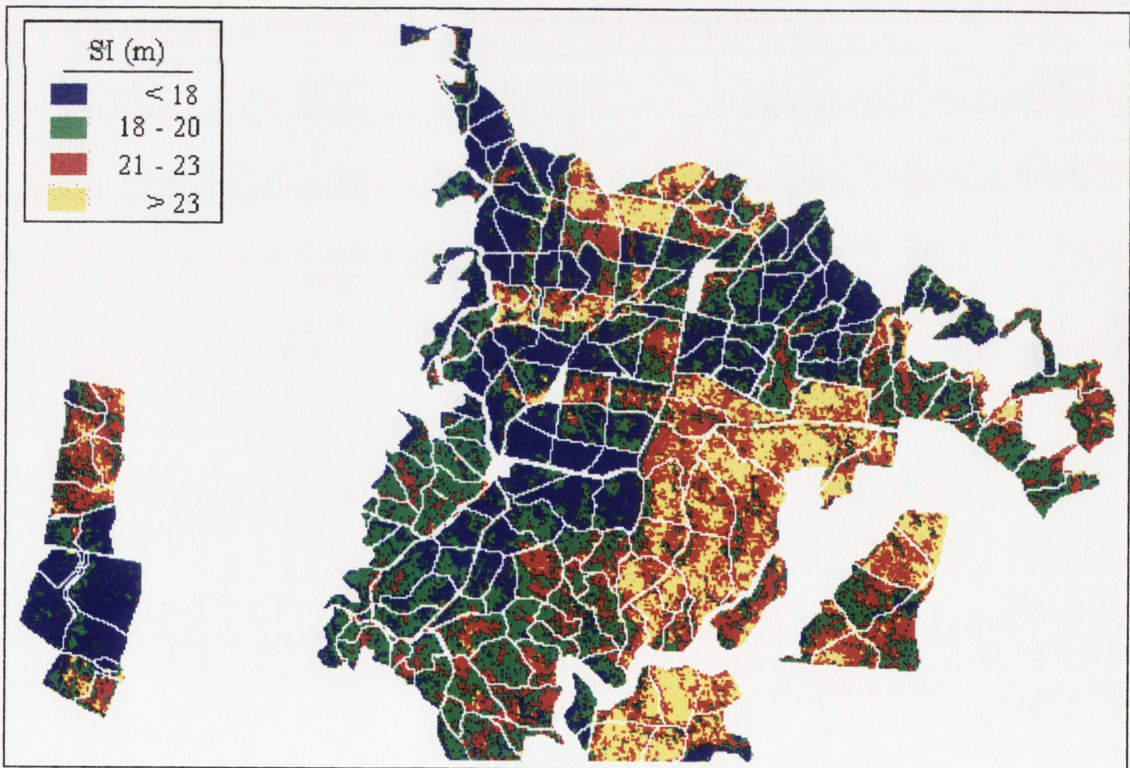


Figure 7.15 Site quality classes based on SI (m) estimated from model-h (see Table 7.19 for details).

The SQ data predicted from Model  $h$  in Table 7.19 were used for accuracy assessment because it had the highest  $r^2$  and lowest estimation errors (MAE and RMSE) (attached to the first sentence of Paragraph 2 in Page 207).



The false colour maps of SQ classes (Figures 7.8-15) visually show that, in general, the pixels with better SQ (i.e. K-1 in yellow and K-2 in red) were usually located at the lower altitude and topographic positions. The areas at lower altitudes (Figure 4.4) and with southeasterly aspects (see Figure 4.6) tend to show the better site quality. The area located on down-slopes (TP3), gully and/or drainage line positions (TP5) (see Table 4.1 in Chapter 4) tend to show the better site quality, consistent with indications that topographic position and altitude generally have more effect on the growth of radiata pine over the study area than other site variables (see Section 7.3.2.4).

The accuracy of the model-estimated SQ classes were further evaluated by comparing them with the SQ classes calculated from recently-measured (1993 and 1994) stand top height of ninety-eight plots in some compartments<sup>1</sup>. This was done by entering the model-estimated (i.e. Model-*h*) and actual SQ classes into a confusion table (error matrix) for the four SQ classes considered (see Table 7.21). The overall plot-based mapping accuracy for the four SQ classes was 68%. In general, areas with the stands of 15 years or older showed better estimates, while the SQ in younger stands (<10 years of age in particular) were usually under-estimated. For instance, the SQ class K4 (in blue colour of Figures 10 to 17) was usually located in the recently-planted stands (< 10 years of age). This does not mean that SQ of these stands (compartments) are poor.

Table 7.21 Error matrix for actual and model-derived (Model-*h*) SQ classes.

SQ Classes		No. of Plots (Predicted SQ Classes)				Total	Omissions	
		K1	K2	K3	K4		No.	%
No. of Plots (Actual SQ Classes)	K1	1				1	0	0
	K2		10	8		18	8	44
	K3		10	47	4	61	14	23
	K4		1	8	9	18	9	50
Total No. of Plots		1	21	63	13	98	31	32

Overall mapping accuracy: 68.37%

### 7.3.5 Selection of Variables for Site Quality Estimation

The correlation and regression analyses between SQ and spectral data in this chapter further indicate that, under similar data-recording conditions (such as in the same growing seasons), SPOT and TM data have a similar capability in SQ estimation. Using the NIR band and/or the NIR-related band combinations alone, the simple regression models could explain about 62% to 77% of total variation in site quality (Table 7.15). The NIR is therefore the first choice for SQ evaluation. For SPOT data, XS2 (red) and PS bands contributed almost nothing to the SQ estimate and can be considered negligible. For TM

<sup>1</sup> The stand top height data were provided by Mr D. Johnston, the Stromlo Forests, ACT.

This study achieved an accuracy of 68% for the four subclasses of SQ and 82% when combined into two actual SQ classes (SQ VI and SQ VII). Although these accuracies are under the 85% standard of Anderson level II, they should be acceptable for SQ class mapping on such a small scale and covering a very restricted range of SQ classes (mainly SQ VI and VII). Anderson's standard itself is also very arbitrary. More accurate results may be expected from this methodology if it were applied to large areas covering a wide range of SQ classes (attached to Page 208, Paragraph 1).

data, in addition to the NIR band, the MIR bands can provide good information on stand variables and can be considered as the second band choice. In addition, the green and red bands can be useful in improving SQ estimates as their combinations with the NIR band (such as various vegetation indices) can usually improve correlations with stand variables and SQ indices. The Blue (TM1) and TIR (TM6) bands of TM data can be considered of negligible value as they did not show any significant correlation with SQ.

## 7.4 SUMMARY AND CONCLUSION

This chapter has focused on deriving numerous models for combining the satellite remotely sensed images acquired from different sensor systems in different growth seasons with ground ancillary data to estimate site quality. The relationships of the site quality and spectral data have also been evaluated. The investigations served (1) to clarify the empirical relationships between the images and site quality through the analysis techniques of correlation, canonical correlation, principal component transformations and regression; (2) to verify the best variable combinations for estimating site quality and yield expressed by site index and/or mean annual increment by these analysis techniques; and (3) to develop a methodology for evaluating forest productivity on a local forest area scale. The methodology and procedures developed in this chapter may be appropriate for other forest ecological studies. The results obtained in this study suggest that forest site quality can be predicted by means of geographic information systems because site variables can be generated by computer or from satellite remote sensors.

The major conclusions are summarised as follows:

- Localised site quality can be estimated with reasonable accuracy with both SPOT and TM data. The accuracy can be significantly improved when integrating spectral bands with site variables.
- The second principal component (greenness) provides better information on site quality than the raw single band data, while the first principal component (brightness) is better correlated with mean annual increment of volume (VI).
- The “between-image” band combinations do not necessarily improve the information content of site quality, but the “within-image” band combinations do provide better estimates of site quality than the raw individual bands. In particular, the difference images between NIR and Red or Green bands are superior to other linear combinations for estimating site quality.

- The time images are recorded significantly affects the amount of information about SQ. Images obtained in the summer growth season may be better predictors of site quality. When recording in the same growing seasons, both SPOT and Landsat TM systems provide similar accuracy of SQ estimate.
- The integration of multi-temporal and/or multi-sensor images provides better information on forest stand structure and SQ than the data from single date or single sensor system.

As stated in Chapter 6, because of the extreme heterogeneity of forest stands at the 30x30 m or 20x20 m resolution and the many abiotic and biotic factors acting on a forest ecosystem, a high degree of predictability for a single pixel probably can not be expected. In addition, low data ranges also limit the sensitivity of spectral data to the subtle variations of SQ in the complex terrain. Higher resolution data (such as AVIRIS) may be helpful to improve the accuracy of SQ estimate for future localised SQ studies.

## Chapter 8

# Summary and Conclusion

The basic objectives of this study were to determine whether remotely-sensed imagery, either directly or indirectly by modelling, can give meaningful site quality information, and to develop ways of using satellite remotely-sensed imagery and ancillary data to estimate forest growth and site quality at a local scale. The study was concerned with the methodology and precision of integrating satellite imagery from different growing seasons and remote sensors with ground-collected and computer-generated biogeographical data for a localised pine plantation forest site.

The study has extensively explored relationships between satellite data and stand variables and SQ with several statistical analysis techniques including correlation, clustering, PCA, CCA and regression modelling. To evaluate the sensitivity of spectral data to stand growth, the study tested the relationships between spectral characteristics and stand ages using statistical tests, correlation and regression analyses (Chapter 5). The information content of spectral bands on forest stands was determined by PCA. The ability of the spectral data to differentiate variation in stand characteristics due to differences in stand age was evaluated using cluster analysis. The capability of spectral data in differentiating stand age classes was determined by clustering analysis. The information content of spectral data on stand variables and SQ transformed to the first two PCs by PCA. CCA was successfully used to examine the relationships between variable sets. Like PCA, it could reduce the redundancy within a set of

variables by a linear combination of within-set variables and determine the most correlated variables. CCA could be seen as <sup>a</sup>useful technique in understanding the overlap of information content in two or more variable groups. For example, by this procedure, TH and Age were found to be most correlated with <sup>the</sup>NIR band, while stand volume and BA were found to be most correlated with MIR bands. In practice, CCA could be used directly for determining the most important variables or spectral bands. The several SQ prediction models could then be built with the variables determined by CCA. Finally, the SQ prediction models were developed with regression analysis (simple, multiple and stepwise regression analysis) by combining spectral and ancillary data.

The main conclusions drawn from the thesis can be summarised as follows:

1. The change of spectral reflectance values of radiata pine plantation stands over age in all bands followed an approximate reverse J-shaped data distribution. For the visible and MIR bands, the general change trend was: a sharp decrease between ages 3 and 5 years; a gentle decrease from ages 5 to 20 years; constant between ages 20 and 30 years; and a slightly increase after age 30 years. For the NIR band, the spectral values increased from age 3 to about 10 years, and then showed an approximately linear decrease from age 10 to about 32 years and became constant or slightly increased after about age 32 years (see Chapter 5). This means that NIR showed a higher correlation with stand age than other bands because it could detect the variation of stands in a wider age range.
2. Cluster analysis showed that the spectral values for different ages could be grouped into 5-year (or larger) age classes (see Chapter 5).
3. Several bands of TM and SPOT data were found to be statistically significantly correlated with stand variables, but the degree of significance of correlation coefficients varied from band to band. Due to highly significant correlations between spectral data and stand age and top height, based on  $r^2$  (see Chapter 6), SI derived from a height-age relation could be seen as an appropriate measure to express SQ with satellite data, while both SPOT and TM data can be used to develop models for estimating SQ (see Chapter 7).
4. The SQ at a local scale cannot be confidently predicted either from topographic and soil variables or satellite data alone (adjusted  $r^2 < 15\%$  in Tables 7.18). However the correlations ( $r^2$ ) can be considerably improved to about 85% by incorporating

satellite data with the site variables (Table 7.19). This result suggests that in areas with highly variable terrain and/or soil conditions, the integration of satellite data with site variables is essential for the improvement of estimation accuracy of SQ.

5. Based on the results of correlation analysis, the NIR and/or the NIR related band combinations were the best predictors of top height and site quality, while the MIR bands were better predictors of stand volume than of other stand variables. The best band combinations for estimating radiata pine site quality were the NIR and green bands for SPOT data, and the NIR and the MIR bands for TM data. The panchromatic (PS) band of SPOT data and the blue (TM1) and the TIR (TM6) bands of TM data were less useful for estimating stand variables.
6. Based on correlation coefficients ( $r$ ),  $r^2$ ,  $MAE$  and/or  $RMSE$  (see Tables 6.6, 7.4, 7.17), for the same stand and environmental conditions as well as similar data recording conditions (for instance, recorded in the same growing season), SPOT and TM data showed nearly equal capability of estimating stand variables and SQ. TM data, however, may be more useful in assessing some stand variables which show lower correlation with the NIR band, since the MIR bands of TM data provided useful information on volume and basal area. The spectral data taken from different growing seasons showed very different accuracy of estimates of stand variables and site quality. For radiata pine, the summer images showed better results than the autumn image because they were more correlated with stand variables and SQ.
7. When multi-images are available, the band combinations from the multi-images can improve the correlations ( $r^2$ ) between spectral values and site quality (see Table 7.19).
8. The information on stand structure and site quality of all spectral bands can be extracted by the first two PCs (see Chapter 5). The PC2 (greenness) was found to be a better predictor of stand variables and SQ than the raw band data.

The narrow range of the reflectance values of satellite data over the forest stands limited the sensitivity of the data to the subtle differences in stand data. Because there is a high heterogeneity of forest stands at the 30×30m or 20×20m pixel size, higher spatial and radiometric resolution data may be necessary to improve the accuracy of the estimate. In addition, when available, the introduction of more site variables such as geological, climatic,

and vegetation factors to estimating models of site quality may be worthy of further investigation.

No attempts were made to normalise the image because it was not considered that this would significantly improve the results since the data analyses in this study were mainly on a single date image basis. Further study, especially in a regional scale, may be needed to confirm whether or not the normalisation of multiple images can improve the results.

The techniques applied and conclusions reached are applicable to the utilisation of both SPOT and TM data, especially for forest ecological studies. In using the methodology developed in this study to evaluate forest site productivity, the bands in Red, NIR and MIR bands of TM or SPOT images could be the optimal option of spectral bands as they contain most information on vegetation. CCA can be directly used to determine their association with stand variables, while regression analysis can be used to develop models for SQ estimate. By incorporating some ancillary data such as topography, the accuracy of estimate can be improved.

The investigation was conducted at a local scale; no attempt was made to separate the tree height or SQ into classes in data analysis. The reason is that the study area covered only a small range of SQ classes (i.e. SQ VI - VII). For future study in a regional scale, it might be better to develop SQ models by separating height or SQ into classes to improve the accuracy of the SQ estimate.



## References

- Ahern, F.J., and D.G. Leckie, 1987. Digital remote sensing for forestry: requirements and capabilities, today and tomorrow. *Geocarto Int.* 2(3):43-52.
- Ahern, F.J., and W.J. Bennett, 1985. Landsat MSS enhancements for forestry applications. *User's Manual 85-1*, Canada Centre for Remote Sensing, Ottawa.
- Ajai, D.S.K., G.S. Chaturvedi, A.K. Sigh, and S.K. Sinha, 1983. Spectral assessment of leaf area index, chlorophyll content, and biomass of Chickpea. *Photogramm. Eng. Rem. Sens.* 49:1721-1727.
- Alban, D.H., 1972. An improved growth intercept method for estimating site index of red pine. USDA For. Serv. North Cent. For. Stn., *Res. Note* 80. 7 pp.
- Aldrich, R.C., 1979. Remote sensing of wildland resources: a state-of-the-art review. *Gen. Tech. Rep.* RM-71, Rocky Mountain Forest and Range Experimental Station, 56p.
- Allee, W.C., O. Park, A.E. Emerson, T. Park, and K.P. Schmidt. 1949. *Principles of Animal Ecology*. Saunders. Philadelphia, Pa. 837 pp.
- Andel, S., M. Bol, C.P. Van Goor, P. Laban, E.M. Iammerts Van Bueren, and A. Van Maaren. (1981). Land utilisation types for forestry. In: Laban P. (ed.), *Proc. Workshop on Land Evaluation for Forestry*, Int. Workshop IUFRO/ISSS, Wageningen, The Netherlands, 10-14 November, 1980, ILRI Publication No. 28, pp. 203-218.
- Anderson, J.R., E.E. Hardy, J.T. Roach and R.E. Witmer, 1976. A land use and land cover classification system for use with remote sensor data. *USGS Prof. Pap.* 964, Washington DC, USGS, 28 pp.
- Anuta, P., L. Bartolucci, E. Dean, F. Lozano, E. Malaret, C. McGillem, J. Valdes, and C. Valenzuela, 1983. Landsat-4 data quality analysis. *Satellite Land Remote Sensing Advancements for the Eighties*, Proc. PECORA VIII Symp., Sioux Falls, South Dakota, October 4-7, 1983. pp. 96-119.
- Anuta, P.E., L.A. Bartolucci, M.E. Dean, D.F. Lozano, E. Malaret, C.D. McGillem, J.A. Valdes, and C.R. Valenzuela, 1984. Landsat-4 MSS and Thematic Mapper data quality and information content analysis. *IEEE Trans. GeoSci. Rem. Sens.* GE-22:222-235.
- Arai, K., 1992. TM classification using local spectral variability. *Geocarto Int.* 7(4):37-45.
- Ardö, J., 1991. Landsat TM based volume estimation of coniferous forest compartments in southern Sweden. *Proc. 24th Int. Symp. Rem. Sens. Environ.*, ERIM, Vol. 1, pp. 813-823.
- Ardö, J., 1992. Volume quantification of coniferous forest compartments using spectral radiance recorded by Landsat Thematic Mapper. *Int. J. Rem. Sens.* 13(9):1779-1786.
- Arnaud, M., and M. Leroy, 1991. SPOT 4: a new generation of SPOT satellites. *ISPRS J. Photogramm. Rem. Sens.* 46:205-215.
- Avery, T.E., 1967. *Forest Mensuration*. McGraw-Hill, New York, 290 pp.
- Avery, T.E., and H.E. Burkhardt, 1983. *Forest Mensuration*. McGraw-Hill, New York, 312 pp.
- Badhwar, G.D., R.B. MacDonald, F.G. Hall, 1986. Spectral characteristics of biophysical characteristics in a boreal forest: relationships between Thematic Mapper band reflectance and leaf area index for aspen. *IEEE Trans. GeoSci. Rem. Sens.* GE-24:322-326.
- Bailey, R.G. 1981. Integrated approaches to classifying land as ecosystems. In: P. Laban (ed.), *Proc. Workshop on Land Evaluation for Forestry*, Int. Workshop of the IUFRO/ISSS, Wageningen, The Netherlands. pp. 95-108.

- Baker, R.D., 1982. What aerial photos tell about east Texas industrial timberlands. *Increasing Forest Productivity*, Proc. the 1981 Convention of the Society of American Foresters, pp. 156-159.
- Baker, J.R., S.A. Briggs, V. Gordon, A.R. Jones, J.J. Settle, J.R. Townshend, and B.K. Wyatt, 1991. Advances in classification for land cover mapping using SPOT HRV imagery. *Int. J. Rem. Sens.* 12(5):1071-1085.
- Bakuzis, V.E., 1974. Foundations of Forest Ecosystems. *Lecture and Research Notes*, Chapter 6, College of Forestry, University of Minnesota, St. Paul, Minnesota, pp. 807-1127.
- Ballard, R., 1971. Interrelationships between site factors and productivity of radiata pine at Riverhead Forest, New Zealand. *Plant and Soil*, 35:371-380.
- Barnes, B.V., 1984. The ecological approach to ecosystem classification. In: D.C. Grey, A.P.G. Schonau, and C.J. Schutz (ed.): *Proc. IUFRO Symp. on Site and Productivity of Fast growing Plantations*, Pretoria and Pietermaritzburg, South Africa, 30 April - 11 May 1984, pp. 69-89.
- Barnes, B.V., K.S. Pregitzer, T.S. Spies, and V.H. Spooner, 1982. Ecological forest site classification, *J. For.* 80:493-498.
- Barrett, E.C., and L.F. Curtis. 1992. *Introduction to Environmental Remote Sensing*. 3rd ed. Chapman & Hall, London. 426 pp.
- Barnett, T.C., and D.R. Thompson, 1983. Large area relation of Landsat MSS and NOAA-AVHRR spectral data to wheat yields. *Rem. Sens. Environ.* 13:277-290.
- Bartlett, M.S., 1941. The statistical significance of canonical correlations. *Biometrika*, 32:29-38.
- Bartlett, M.S., 1965. Multivariate statistics. In: T.H. Waterman and H.J. Morowitz (ed.), *Theoretical and Mathematical Biology*, Balled, New York, pp. 201-224.
- Bary, G.A.V., and C.J. Borough, 1978. Tree Volume Tables for *Pinus radiata* in the Australian Capital Territory. *Division of Forest Research Internal Report 11*, CSIRO, Canberra, Australia, 7 pp.
- Beaubien, J., 1979. Forest type mapping from Landsat digital data. *Photogramm. Eng. Rem. Sens.* 45:1135-1144.
- Beaubien, J., 1986. Visual interpretation of vegetation through digitally enhanced Landsat-MSS images. *Rem. Sens. Rev.* 2:111-143.
- Beek, K.J. 1972. The concept of land utilisation types. Approaches to Land Classification. *FAO Soils Bulletin No. 22*, Rome, pp. 103-120.
- Beek, K.J., and P. Laban, 1981. Land evaluation, a systems approach. In: Laban P. (ed.), *Proc. Workshop on Land Evaluation for Forestry*, Int. Workshop of the IUFRO/ISSS, Wageningen, The Netherlands, 10-14 November, 1980, ILRI Publication No. 28, pp. 298-323.
- Benson, A.S., and S.D. DeGloria, 1985. Interpretation of Landsat-4 Thematic Mapper and multispectral scanner data for forest surveys. *Photogramm. Eng. Rem. Sens.* 51:1281-1289.
- Bercha, F.G., D.H. Currie, and J.A. Dechka, 1990. Multi-sensor airborne forest inventory system. *Proc. 23rd Int. Symp. Rem. Sens. ERIM*, Ann Arbor, Vol. II, pp. 603-608.
- Biossard, P., G. Guyot, and R.D. Jackson, 1990. Factors affecting the radiative temperature of a vegetative canopy. In: M.D. Steven and J.A. Clark (ed.), *Applications of Remote Sensing in Agriculture*. Butterworths, London, pp. 45-72.
- Bitterlich, W., 1984. *The Relascope Idea*. Commonwealth Agricultural Bureaux, 242 pp.
- Boissonneau, A.N., and S. Pala, 1978. An ecological classification project for the Ontario portion of the Hudson Bay-James Bay Region. In: C.D.A. Rubec (ed.), *Applications of Ecological*

(*Biological Land Classification in Canada*. Lands Directorate, Environment Canada. Ecological land Classification Series, No. 7, pp. 65-72.

- Bolstad, P.V., and T.M. Lillesand, 1992. Improved classification of forest vegetation in Northern Wisconsin through a rule-based combination of soils, terrain, and Landsat Thematic Mapper data. *For. Sci.* 38(1):5-20.
- Borrey, E.C., B.P. De Roover, R.R. De Wulf, and R.E. Goossens, 1990. Assessing the value of monotemporal SPOT-1 imagery for forestry application under Flemish conditions. *Photogram. Eng. Rem. Sens.* 56:1147-1153.
- Box, E.O., B.N. Holben, and Kalb, 1989. Accuracy of the AVHRR vegetation index as a predictor of biomass, primary productivity and net CO<sub>2</sub> flux. *Vegetatio*, 80:71-89.
- Bradbury, P.A., R.H. Hainess-Young, P.M. Mather, and A. Macdonald, 1985. The use of remotely-sensed data for landscape classification in Wales: the results of woodlands in the landscape. *Advanced Technology for Monitoring and Processing Global Environmental Data*, Remote Sensing Society, Reading, pp. 401-411.
- Brockhaus, J.A., and S. Khorram, 1992. A comparison of SPOT and Landsat-TM data for use in conducting inventories of forest resources. *Int. J. Rem. Sens.* 13:3035-3043.
- Brockhaus, J.A., S. Khorram, R. Bruck, M.V. Campbell, 1993. Characterisation of defoliation conditions within a boreal montane forest ecosystem. *Geocarto Int.* 8(1):35-37.
- Buchman, R.E., 1962. A method of constructing site index curves from measurements of age and height - its application to inland Douglas Fir. *USDA Res. Pap.* INT-47, 23 pp.
- Burger, D., 1976. The concept of ecosystem region in forest site classification. *Proc. XVI IUFRO World Congr.* Norway, Div. I, pp. 213-218.
- Burger, D., and G. Pierpoint, 1990. Trends in forest site and land classification in Canada. *For. Chron.* 66(2):91-96.
- Burton, A.J., C.W. Ramm, K.S. Pregitzer, D.D. Reed, 1991. Use of multivariate methods in forest research site selection. *Can. J. For. Res.* 21:1573-1580.
- Bush, T.F. Ulaby, T. Metzler, and H. Stiles, 1976. Seasonal variations of the microwave scattering properties of the deciduous trees as measured in the 1-18 GHz spectral range, *Rem. Sens. Lab. Tech. Rep.* 177-60, University of Kansas, Kansas (not seen, cf Smith 1983).
- Bush, T., and F. Ulaby, 1978. An evaluation of radar as a crop classifier. *Rem. Sens. Environ.* 7:15-18.
- Butera, M.K., 1986. A correlation and regression analysis of percent canopy closure versus TMS spectral response for selected forest sites in the San Juan National Forest, Colorado. *IEEE Trans. Geosci. Rem. Sens.* GE-24:122-129.
- Butera, M.K., 1986. A correlation and regression analysis of percent canopy closure versus TMS spectral response for selected forest sites in the San Juan National Forest, Colorado. *IEEE Trans. Geosci. Rem. Sens.* GE-24:122-129.
- Büttner, G., and F. Csillag, 1989. Comparative study of crop and soil mapping using multitemporal and multispectral SPOT and Landsat Thematic Mapper data. *Rem. Sens. Environ.* 29:241-249.
- Byrne, G.F., P.F. Crapper, and K.K. Mayo, 1980. Monitoring land-cover change by principal component analysis of multitemporal Landsat data. *Rem. Sens. Environ.* 10:175-184.
- Byron, N., 1971. *The Factors Influencing the Growth of Radiata Pine at Kowen*, ACT. Hon. Thesis to the Australian National University, 169 pp.
- Cajander, A.K., 1909. Über Waldtypen. *Acta For. Finn.* 1:1-175.
- Cajander, A.K. 1926. The theory of forest types. *Acta For. Finn.* 29:1-108.
- Cajander, A.K., 1949. Forest types and their significance. *Acta For. Finn.* 56:1-71.

- Cajander, A.K., and Y. Ilvessalo, 1921. Über Waldtypen II. *Acta For. Finn.* 20:1-77.
- Canas, A.A.D., and M.E. Barnett, 1985. The generation and interpretation of false-colour composite principal component images. *Int. J. Rem. Sens.* 6(6):867-881.
- Candy, S. G., 1989. Growth and yield models for *Pinus radiata* in Tasmania. *N.Z. J. For. Sci.* 19(1):112-133.
- Carleton, T.J., R.K. Jones, and G. Pierpont. 1985. The prediction of understory vegetation by environmental factors for the purpose of site classification in forestry: an example from northern Ontario using residential ordination analysis. *Can. J. For. Res.* 15:1099-1108.
- Carmean, W.H., 1965. Black oak site quality in relation to soil and topography in southeastern Ohio. *Soil Sci. Soc. Proc.* 29:308-312.
- Carmean, W.H., 1975. Forest site quality evaluation in the United States. *Adv. Agron.* 27:209-269.
- Carneiro, C.M.R., and G. Hildebrandt, 1978. Qualitative and quantitative interpretation of Landsat MSS adapt to forest cover mapping in Germany. In *Proceedings of the International Symposium on Remote Sensing for Observation and Inventory of Earth Resources and the Endangered Environment*, G. Hildebrandt, and H.-J. Boehnel ed., July 2-8, 1978, Freiburg, Germany, Vol. III, pp. 1791-1804.
- Carolis, G.De, and P. Amodeo, 1980. Basic problems in the reflectance and emittance properties of vegetation. In: Frayse, G. (ed), *Remote Sensing application in Agriculture and Hydrology*, A. A. Balkema/Rotterdam, pp. 69-79.
- Carron, L. T., 1955. Site classification and volume assessment of a *Pinus radiata* plantation, Kowen, A.C.T. *Aust. For.* 19(2): 141-145.
- Carron, L.T., 1967. A variable-density yield table for a plantation of radiata pine. *Aust. For.* 31(1):11-18.
- Carron, L, 1968. *A volume tariff system for even-aged forests of Pinus radiata* (D. Don). PhD Thesis to Department of Forestry, the Australian National University.
- Chang, D.H.D., and H.G. Gauch. 1986. Multivariate analysis of plant communities and environmental factors in Ngari, Tibet. *Ecology*, 67:1568-1575.
- Charman, P.E.V., 1978. Soils of New South Wales, their characterization, classification and conservation. *NSW Soil Conservation Service Technical Handbook*, No. 1.
- Chapman, H.H., R.T. Fisher, C.D. Howe, D. Bruce, E.N. Munns, and W.N. Sparhawk, 1921. Classification of forest sites. *J. For.* 19:139-147.
- Chappelle, E.W., M.S. Kim, and J.E. McMurtrey III, 1992. Ratio analysis of reflectance spectra (RARS): an algorithm for the remote estimation of the concentrations of chlorophyll a, chlorophyll b, and carotenoids in soybean leaves. *Rem. Sens. Environ.* 39:239-247.
- Chagarlamudi, P., and G. W. Plunkett, 1993. Mapping applications for low-cost remote sensing and geographic information systems. *Int. J. Rem. Sens.* 14:3181-3190.
- Chavez, P.S., and J.A. Howell, 1988. Comparison of the spectral information content of Landsat Thematic Mapper and SPOT for three different sites in the Phoenix, Arizona region. *Photogramm. Eng. Rem. Sens.* 54:1699-1708.
- Chen, J., 1984. The application of DTM in improving classification accuracy of remote sensing imagery. *J. Wuhan Surveying University*, 1984-11, pp. 68-81.
- Choate, G.A., 1961. Estimating douglas-fir site quality from aerial photographs. U. S. Dep. Agr. Forest Serv., Pacific Northwest For. Range Exp. Stn. Portland, Oregon. *Res. Pap.* 45, 26 pp.
- Chong, D.L.S., E. Mougin, J.P. Gastellu-Etchegorry, 1993. Relating the global vegetation index to net primary productivity and actual evapotranspiration over Africa. *Int. J. Rem. Sens.* 14:1517-1546.

- Choudhury, B., and C. Tucker, 1987. Satellite observed seasonal, and inter-annual variation of vegetation over the Kalahari, the Great Victoria, and the Great Sandy Desert: 1979-1984. *Rem. Sens. Environ.* 23:233-241.
- Christian, C.S., G.A. Stewart, and R.A. Ferry, 1960. Land research in northern Australia. *Geography*, 7:217-231.
- Chuvieco, E., and C. Congalton, 1988. Using cluster analysis to improve the selection of training statistics in classifying remotely sensed data. *Photogramm. Eng. Rem. Sens.* 54:1275-1281.
- Cicone, R.C., W.A. Malila, and E.P. Crist, 1977. *Investigation of Techniques for Inventorying Forested Regions*. Volume II: Forestry Information System Requirements and Joint Use of Remotely Sensing and Ancillary Data. ERIM 122700-35-F<sub>2</sub>, Ann Arbor, Michigan, 135p.
- Ciesla, W.M., C.W. Dull, and R. E. Acciavatti, 1989. Interpretation of SPOT-1 color composite for mapping defoliation of hardwood forests by gypsy moth. *Photogramm. Eng. Rem. Sens.* Vol. 55:1465-1470.
- Clark, C.A., R.B. Gate, M.H. Trenchard, J.A. Boatright, and E.M. Bizzell, 1986. Mapping and classifying large ecological units. *BioSci.* 35:476-478.
- Clarke, R.W., 1956. Wind damage and planting stick. *Aust. For.* 20:37-39.
- Clevers, J.G., 1989. The application of a weighted infrared-red vegetation index for estimating leaf area index by correcting for soil moisture. *Rem. Sens. Environ.* 29:25-37.
- Clutter, J.L., J.C. Fortson, L.V. Pienaar, G.H. Brister, and R.L. Bailey, 1983. *Timber Management: a Quantitative Approach*. John Wiley & Sons, New York. 333 pp.
- Cohen, W.B., 1991. Response of vegetation indices to changes in three measures of leaf water stress. *Photogramm. Eng. Rem. Sens.* 57:195-202.
- Cohen, W.B., and T.A. Spies, 1992. Estimating structural attributes of douglas-fir/weston hemlock forest stands from Landsat and SPOT imagery. *Rem. Sens. Environ.* 41:1-17.
- Coile, T.S., 1952. Soil and the growth of forests. *Adv. Agron.* 4:329-398.
- Coile, T.S., 1960. Summary of soil-site evaluation. In P.Y. Burns (ed.): *Southern Forest Soils - Proc. 8th Ann. For. Symp.* Louisiana State University Press, Baton Rouge, LA, pp. 77-85.
- Coleman, T.L., L. Gudapati, and J. Derrington, 1990. Monitoring forest plantation using Landsat Thematic Mapper data. *Rem. Sens. Environ.* 33:211-221.
- Colwell, J.E., 1974. Vegetation canopy reflectance. *Rem. Sens. Environ.* 3:175-183.
- Colwell, R.N., 1970. Applications of remote sensing in agriculture and forestry. In: Committee on Remote Sensing for Agriculture Purposes (ed.), *Remote Sensing with Special Reference to Agriculture and Forestry*. Agricultural Board, National Academy of sciences, Washington, D.C., pp. 164-222.
- Conese, C. G. Maracchi, F. Miglietta, F. Maselli, and V.M. Sacco, 1988. Forest classification by principal component analyses of TM data. *Int. J. Rem. Sens.* 9:1597-1612.
- Conese, C., and F. Maselli, 1991. Use of multitemporal information to improve classification performance of TM scenes in complex terrain. *ISPRS J. Photogramm. Rem. Sens.* 46:187-197.
- Cook, E.A., L.R. Iverson, and R.L. Graham, 1987. The relationship of forest productivity to Landsat Thematic Mapper data and supplemental terrain information. *Proc. PECORA XI Memorial Symp.*, Am. Soc. Photogramm. Rem. Sens. Falls Church, Virginia, pp. 43-52.
- Cook, E.A., L.R. Iverson, and R.L. Graham, 1989. Estimating forest productivity with Thematic Mapper and biogeographical Data. *Rem. Sens. Environ.* 28:131-141.
- Craig, R.D., 1920. An aerial survey of the forests in northern Ontario. *Can. For. Mag.* 16:546-548.

- Crist, E.P., and R.C. Cicone, 1984. Application of the Tasselled cap concept to simulated thematic mapper data. *Photogramm. Eng. Rem. Sens.* 50:343-352.
- CSIRO Division of Water Resource, 1988. *microBRIAN Resource Manual*. Canberra, Australia.
- Curran, P.J. 1980. Multispectral remote sensing of vegetation amount. *Progr. Phys. Geog.* 4:315-341.
- Curran, P.J. 1985. *Principle of Remote Sensing*. Longman, London, 282 pp.
- Curran, P.J., 1987. Remote sensing methodologies and geography. *Int. J. Rem. Sens.* 8:1255-1275.
- Curran, P. J., and E. J. Milton, 1983. The relationships between the chlorophyll concentration, LAI and reflectance of a simple vegetation canopy. *Int. J. Rem. Sens.* 4:247-255.
- Curran, P.J., and H.D. Williamson, 1987. GLAI estimation using estimates of red, near-infrared, and middle infrared radiance. *Photogramm. Eng. Rem. Sens.* 53:181-186.
- Curran, P.J., J.L. Dungan, B.A. Macler, and S.E. Plunner, 1991. The effects of a red leaf pigment on the relationship between red edge and chlorophyll concentration. *Rem. Sens. Environ.* 35:69-76.
- Curran, P.J., J.L. Dungan, and H.L. Gholz, 1992. Seasonal LAI in slash pine estimated with Landsat TM. *Rem. Sens. Environ.* 39:3-13.
- Curtis, J.T., and McIntoch. 1951. An upland forest continuum in the prairie-forest border region of Wisconsin. *Ecology*, 32:476-496.
- Cushnie, J.L., 1987. The interactive effect of spatial resolution and degree of internal variability within land-cover types on classification accuracies. *Int. J. Rem. Sens.* 8:15-29.
- Czarnowski, M.S., 1964. *Productive Capacity of Locality as a Function of Soil and Climate with Particular Reference to Forest Land*. Louisiana State University Press, Bio. Sci. Seri, No. 5, 174 pp.
- Czarnowski, M.S., F.R. Humphreys, and S. W. Gentle, 1967. Site-index as a function of soil and climatic characteristics, a preliminary note based on man-made stands of *Pinus radiata* D. Don in New South Wales, Australia. *Ekologia Polska*, 5:495-504.
- Czarnowski, M.S, F.R. Humphreys, and S.W. Gentle, 1971. Quantitative expression of site-index in terms of certain soil and climate characteristics of *Pinus radiata* D. Don plantations in Australia and New Zealand. *Ekologia Polska*, 19:291-309.
- Dahlberg, R.E., and J.R. Jensen, 1986. Education for cartography and remote sensing in the service of an information society, the U. S. Case. *The American Cartographer*, 13:51-71.
- Damman, A.W.H., 1979. The role of vegetation analysis in land classification. *For. Chron.* 55:175-182.
- Daniel, T.W., J.A. Helms, and F.S. Baker. 1979. *The Principles of Silviculture*. 2nd ed., McGraw-Hill, New York, 500 pp.
- Danson, F.M., 1987. Preliminary evaluation of the relationships between SPOT-1 HRV data and forest stand parameters. *Int. J. Rem. Sens.* 8:1571-1575.
- Danson, F.M., M.D. Steven, T.J. Malthus, and J.A. Clark, 1992. High-spectral resolution data for determining leaf water content. *Int. J. Rem. Sens.* 13:461-470.
- Darlington, R.B., S.L. Weisberg, and H.J. Walberg, 1973. Canonical analysis and related techniques. *Rev. Edu. Res.* 43:433-454.
- Daubenmire, R., 1952. Forest vegetation of Northern Idaho and adjacent Washington and its bearing on concepts of vegetation classification. *Ecological Monographs*, 22:301-330.
- Daubenmire, R., 1966. Vegetation: identification of typical communities. *Science*, 151:291-298.

- Daubermire, R., 1976. The use of vegetation in assessing the productivity of forest lands. *Bot. Rev.* 42:115-143.
- Daubermire, R.F., 1984. Viewpoint: Ecological site/range site/habitat type. *Rangelands*, 6:263-264.
- Davis, K. P., 1966. *Forest Management: Regulation and Valuation*. 2nd ed., McGraw-Hill Book Company, New York, 519 pp.
- Davis, F.W., and J. Dozier, 1990. Information analysis of a spatial database for ecological land classification. *Photogramm. Eng. Rem. Sens.* 56:605-613.
- Deering, D.W., and R.H. Haas, 1980. Using Landsat digital data for estimating green biomass. *NASA Tech. Memo. #80727*, Greenbelt, MD, 21 pp.
- DeGloria, S.D., 1984. Spectral variability of LANDSAT-4 thematic mapper and multispectral scanner data for selected crop and forest cover types. *IEEE Trans. GeoSci. Rem. Sens.* GE-22: 303-311.
- DeGloria, S.D., and A.S. Benson, 1987. Interpretability of advanced SPOT film products for forest and agricultural survey. *Photogramm. Eng. Rem. Sens.* 53:37-44.
- de Gier, A., and D. Stellingwerf, 1992. Two-phase regression estimate in a stratified sampling design for timber volume determination. *ITC J.* 1992-3:69-80.
- Dijk, D.C. van, 1959. Soil features in relation to erosional history in the vicinity of Canberra. *Soil Publication No. 13*, CSIRO, Australia. 41 pp.
- Dodge, A., and E.S. Bryant, 1976. Forest type mapping with satellite data. *J. For.* 74:526-531.
- Dong, W., G. Zhou, and L. Xia, 1979. *Quantitative Theories and Their Applications*. Jilin People's Publishing House, 189 pp.
- Donker, N.H.W., and N.J. Mulders, 1976. Analysis of MSS digital imagery with the aid of principal component transform. *ITC J.* 3:434-465.
- Dottavio, C.L., 1981. Effects of forest canopy closure on income solar radiance, In: *Proc. 1981 Machine Processing of Remote Sensed Data Symp.*, Purdue University, West Lafayette, Indiana, USA, pp. 375-383.
- Dottavio, C.L., and D.L. Williams, 1982. Mapping a southern pine plantation with satellite and aircraft scanner data: a comparison of present and future Landsat sensors. *J. Appl. Photog. Eng.* 8:58-62.
- Dottavio, C.L., and D.L. Williams, 1983. Satellite technologies: an improved means for monitoring forest insect defoliation. *J. For.* 81:30-34.
- Driscoll, R. S., D. R. Betters, and H. D. Parker, 1982. Land classification through remote sensing techniques and tools, *J. For.* 76:1135-1136.
- Duffy, P.J.B., 1968. Forest land capacity in the Queanbeyan-Shoalhaven Area, A.C.T. and New South Wales. *Aust. For.* 33:195-200.
- Duffy, P.J.B., 1969. Land use in the Queanbeyan-Shoalhaven Area. In: *Lands of the Queanbeyan-Shoalhaven Area, A.C.T. and N.S.W.*, CSIRO Land Research Series No. 24, Part VIII, pp. 145-146.
- Duggin, M.J., 1983. The effect of irradiation and reflectance variability on vegetation condition assessment. *Int. J. Rem. Sens.* 4:601-608.
- Dunteman, G.H., 1989. Principal Component Analysis. *Series: Quantitative Applications in the Social Sciences* 69, Sage Publishers, Newbury Park, 95 pp.
- Eastman, J.R. 1990. *IDRISI User's Guide*. Clark University, Graduate School of Geography, Worcester, Massachusetts, 01610, USA. 178 pp.

- Eaton, M.L., 1983. *Multivariate Statistics: a Vector Space Approach*. John Wiley & Sons, New York, 512 pp.
- Elachi, C., 1987. *Introduction to the Physics and Techniques of Remote Sensing*. Wiley, New York, 413 pp.
- Elachi, C. 1988. *Spaceborne Radar Remote Sensing: Applications and Techniques*. IEEE Press, The Institute of Electronics Engineers, Inc., New York, 255 pp.
- Elvidge, C.D., Z. Chen, and D.P. Groeneveld, 1993. Detecting of trace quantities of green vegetation in 1990 AVIRIS data. *Rem. Sens. Environ.* 44:271-279.
- Enchelmaier, R.L., 1973. *A Study of Infiltration in Pine and Eucalyptus Forests at Kowen, A.C.T.* Honours Thesis to the Australian National University, 156 pp.
- Estes, J.E., E.L. Hajic, and L.R. Tinney, 1983. Fundamentals of image analysis: analysis of visible and thermal infrared data. In: Colwell, R.N. (Editor-in-Chief), *Manual of Remote Sensing* (2nd ed.), Am. Soc. Photogramm., The Sherian Press, Virginia, Vol. I, pp. 987-1124.
- Evans, D.L., and J.M. Hill, 1990. Landsat TM versus MSS for forest type identification. *Geocarto Int.* 5:13-20
- Everitt, B., 1980. *Cluster Analysis*. 2nd ed., Gower Publishing Co., Hampshire, 136 pp.
- FAO, 1982. *Proceedings of the training course on application of new remote sensing techniques to forest survey*. Harbin, P.R. China, 164 pp.
- FAO, 1984. *Land Evaluation for Forestry*. Forestry Paper No. 48. FAO, Rome, Italy, 254 pp.
- Ferguson, D.E., P.D. Morgan, and F.D. Johnson (Compilers), 1989. *Proc. Land Classifications Based on Vegetation: Applications for Resource management*. Moscow, ID, November 17-19, 1987, SAF 88-06.
- Ferguson, I.S., 1979. Computer based growth models for A.C.T. forests. Unpublished Consultancy Report to A.C.T. Forest Branch.
- Fernandez, I. J., 1986. Air pollution: synthesis of the role of major air pollutants in determining forest health and productivity. *Stress Physiology and Forest productivity*. T.C. Hennessey, P.M. Dougherty, S.V. Kossuth, and J.D. Johnson Ed. Martinus Nijhoff Publishers. Dordrecht. pp. 217-239.
- Fernow, B.E., 1905. Forest terminology. *J. For.* 3:255-268
- Ferree, M.J., T.D. Shearer, and C.L. Stone, 1958. A method of evaluating site quality in young red pine plantations. *J. For.* 56:328-332.
- Finn, J.D., 1974. *A general model for multivariate analysis*. Holt, Rinehart and Winston, Inc., New York, 423 pp.
- Fiorella, M., and W.J. Ripple. 1993. Analysis of conifer forest regeneration using Landsat Thematic Mapper data. *Photogramm. Eng. Rem. Sens.* 59:1383-1388.
- Fisher, P.F., and S. Pathirana, 1990. The evaluation of fuzzy membership of land cover classes in the suburban zone. *Rem. Sens. Environ.* 34:121-132
- Fleischmann, C.G. and S.J. Walsh, 1990. Multi-temporal AVHRR digital data: an approach for Landcover mapping of heterogeneous landscapes. *Geocarto Int.* 5(2):5-20.
- Florence, R.G. 1981. The biology of the eucalypt forest. In: J.S. Pate, and A.J. McComb (ed), *The Biology of Australian Plants*, pp. 147-180.
- Forristall, F.F., and S.P. Gessel, 1955. Soil properties related to forest cover type and productivity on the Lee Forest, Snohomish County, Washington. *Proc. Soil Sci. Soc. Am.* 19:384-389.
- Fox III, L., J.A. Brockhaus, and N.D. Tosta, 1985. Classification of timberland productivity in northwestern California using Landsat, topographic, and ecological data. *Photogramm. Eng. Rem. Sens.* 51:1745-1752.



- Frank, T.D., 1984. Assessing change in the Surficial character of a semiarid environment with Landsat residual images. *Photogramm. Eng. Rem. Sens.* 50:471-480.
- Frank, T.D., 1988. Mapping dominant vegetation ecosystems in the Colorado Rocky Mountain front range and Landsat TM. *Photogramm. Eng. Rem. Sens.* 54:1727-1734.
- Franklin, J.F. 1980. Ecological site classification activities in Oregon and Washington. *For. Chron.* 56:68-70.
- Franklin, J., 1986. Thematic Mapper analysis of coniferous forest structure and composition. *Int. J. Rem. Sens.* 7:1287-1301.
- Franklin, J., 1993. Discrimination of tropical vegetation types using SPOT multispectral data. *Geocarto Int.* 8:57-63.
- Franklin, J., F.W. Davis, and P. Lefebvre, 1991. Thematic Mapper analysis of tree cover in semiarid woodlands using a model of canopy shadowing. *Rem. Sens. Environ.* 36:189-202.
- Franklin, J., T.L. Logan, C.E. Woodcock, and A.H. Strahler, 1986. Coniferous forest classification and inventory using Landsat and digital terrain data. *IEEE Trans. Geosci. Rem. Sens.* GE-24:139-149.
- Franklin, S.E., 1992. Satellite remote sensing of forest type and landcover in the Subalpine Forest Region, Kananaskis Valley, Alberta. *Geocarto Int.* 7(4):25-35.
- Franklin, J., and A.H. Strahler, 1988. Invertible canopy reflectance modelling of vegetation structure semi-arid woodland. *IEEE Trans. Geosci. Rem. Sens.* GE-26:809-825.
- Frey, T.E.A., 1980. The Finnish School and forest site-types. In: R.H. Whitaker (ed.), *Classification of Plant Communities*. Dr. W. Junk Publishers, the Hague, pp. 81-110.
- Frisina, R., P. Goodson, and P. Woodgate, 1991. Forest cover changes and carbon dioxide: A remote sensing study in Western Victoria 1987-1990. *Victoria Government Publication*, Department of conservation and Environment & Office of the environment. 25 p.
- Frothingham, E.H., 1914. Forest type: a defence of loose usage. *For. Quart.* 12:425-428.
- Frothingham, E.H., 1918. Height growth as a key to site. *J. For.* 16:754-760.
- Frothingham, E.H. 1921. Classifying forest stands by height growth. *J. For.* 19:374-381.
- Fukue, K., H. Shimoda, Y. Matumae, R. Yamaguchi, and T. Sakata, 1988. Evaluation of unsupervised methods for land-cover/use classification of Landsat TM data. *Geocarto Int.* 3(2):37-43.
- Fuller, R.M., and R.J. Parsell, 1990. Classification of TM imagery in the study of land use in lowland Britain: practical considerations of operational use. *Int. J. Rem. Sens.* 11:1901-1917.
- Fung, K.T., and En P. Pan, 1982. *Cluster Analysis*. Geological Publishing House, Beijing, 281 pp.
- Fung, T., 1990. An assessment of TM imagery for land-cover change detection. *IEEE Trans. Geosci. Rem. Sens.* GE-28:681-684.
- Fung, T., and E. LeDrew, 1987. Application of principal components analysis to change detection. *Photogramm. Eng. Rem. Sens.* 53:1649-1658.
- Gaertner, E.E., 1964, Tree growth in relation to the environment. *Bot. Rev.* 30:393-436.
- Gagnon, J.D., MacArthur, J.D. 1959. *Ground Vegetation as an Index of Site Quality in White Spruce Plantations*. Tech. Note For. Res. Div., Forest Branch, Department of Northern Affairs and National Resources, Canada. No. 70, 12 p.
- Galloway, R.W., 1969. Geomorphology of the Queanbeyan-Shoalhaven Area. In: *Lands of the Queanbeyan-Shoalhaven Area, A.C.T. and N.S.W.*, CSIRO Land Research Series No. 24, Part V, pp. 77-91.

- Gardner, R.R., B.L. Blad, D.R. Thompson, and K.E. Herderson, 1985. Evaluation and interpretation of Thematic Mapper ratios in equations for estimating corn growth parameters. *Rem. Sens. Environ.* 18:225-234.
- Gates D.M., 1970. Physical and physiological properties of plants. In: *Remote Sensing - with Special Reference to Agriculture and Forestry*, National Academy of Science, Washington D.C. pp. 224-252.
- Gausman, H.W., 1974. Leaf reflectance of near infrared. *Photogramm. Eng.* 40:56-72.
- Gausman, H.W., and W.A. Allen, 1973. Optical parameters of leaves of 30 plant species. *Plant Physiol.* 52:57-62.
- Gausman, H.W., R.R. Rodriguez, and A.J. Richardson, 1976. Infinite reflectance of dead compared with live vegetation, *Agron. J.* 68:295-296.
- Gausman, H.W., W.A. Allen, R. Cardenas, A.J. Richardson, 1970. Relation of light reflectance to historical and physical evaluation of cotton leaf maturity. *Appl. Optics*, 9:545-552.
- Gausman, H.W., W.A. Allen, D.E. Escobar, R.R. Rodriguez, and R. Cardenas, 1971. Age effect of cotton leaves on light reflectance, transmittance, and absorptance and on water content and thickness. *Agron. J.* 63:465-468.
- Gelens, H.F. 1984. Land evaluation for forestation. In: K.F. Wiersun (ed.), *Strategies and Designs for Afforestation, Reforestation and Tree Planning*, Wageningen, The Netherlands, pp. 219-230.
- Gessel, S. P., 1967. Concepts of forest productivity. *Proc. XIV IUFRO Congr.*, München, Vol. II, pp. 36-48.
- Gervin, J.C., A.G. Kerber, R.G. Witt, Y.C. Lu, and R. Sekhon, 1985. Comparison of level I land cover classification accuracy for MSS and AVHRR data. *Int. J. Rem. Sens.* 6:47-57.
- Getter, J. and C.H. Tom, 1977. Forest site index mapping and yield model inputs to determine potential site productivity, *Resource Inventory Notes*. BLM 7, Bureau of Land Management, Washington, 14 pp.
- Gillispie, A.R., 1980. Digital techniques of image enhancement. In: B.S. Siegal and A.R. Gillispie (eds.), *Remote Sensing in Geology*, Wiley, New York, pp. 139-226.
- Gittins, R., 1985. *Canonical Analysis: A Review with Applications in Ecology*. Springer-Verlag, Berlin, 351p
- Goel, N.S., and N.E. Reynolds, 1989. Bidirectional canopy reflectance and its relationship to vegetation. *Int. J. Rem. Sens.* 11:1439-1450.
- Goillot C.C., 1980. Significance of spectral reflectance for natural surfaces. In: Frayse, G. (ed), *Remote Sensing Application in Agriculture and Hydrology*, A.A. Balkema/Rotterdam, pp. 53-68.
- Goldstein, R.A., and D.F. Grigal, 1972. Definition of vegetation structure by canonical analysis. *J. Ecol.* 60:277-284.
- Gordon, A.D., 1981. *Classification: methods for the exploratory analysis of multivariate data*, Chapman And Hall, London, 193 pp.
- Gray, H.R., 1945. Site classification of coniferous plantations. *Aust. For.* 9:9-17.
- Green, R.N., P.J. Courtin, K. Klinka, R.J. Slaco, and C.A. Ray, 1984. *Site Diagnosis, Tree Species Selection, and Slashburning Guidelines for the Vancouver Forest Region*. Land Management Handbook No. 8, Province of British Columbia, 146 pp.
- Grey, D.C., 1989a. Site Requirement of *Pinus radiata*: A Review. *South African For. J.* 148:23-27.
- Grey, D.C., 1989b. Site Index: A Review. *South African For. J.* 148:28-32.

- Gugan, D.J., and I.J. Dowman, 1988. Topographic mapping from SPOT imagery. *Photogramm. Eng. Rem. Sens.* 54:1409-1414.
- Gunn, R.H., and R. Story, 1969. General description of the Queanbeyan-Shoalhaven Area. In *Lands of the Queanbeyan-Shoalhaven Area, A.C.T. and N.S.W.*, CSIRO Land Research Series No. 24, Part II, pp. 16-21.
- Gunn, R.H., R. Story, R.W. Galloway, P.J.B. Duffy, and G.A. Yapp, 1969a. Land systems of the Queenbeyan-shoalhaven area. In: *Lands of the Queanbeyan-Shoalhaven Area, A.C.T. and N.S.W.*, CSIRO Land Research Series No. 24, Part III, pp. 22-56.
- Gunn, R.H., R. Story, R.W. Galloway, P.J.B. Duffy, G.A. Yapp, and J.R. McAlpine, 1969b. Lands of the Quenbeyan-Shalhaven Area, A.C.T. and N.S.W. *Lands Research Series No. 24*, Commonwealth Scientific and Industrial Research Organization, Australia, 164 p.
- Gunst, R.F., 1983. Regression analysis with multicollinear predictor variables: definition, detection and effects. *Commun. Statist. Theor. Meth.* 12:2217-2260.
- Goyut, G., 1990. Optical properties of vegetation canopies. In: N.D. Steven and J.A. Clark (ed.), *Applications of Remote Sensing in Agriculture*. Butterworths, London, pp. 19-43.
- Guyot, G., D. Guyon, and J. Riom, 1989. Factors affecting the spectral response of forest canopies: a review. *Geocarto Int.* 3(3):3-18.
- Guyot, G., O. Dupont, H. Joannes, C. Prieur, M. Heut, and A. Podaire, 1985. Investigation into the mid-IR spectral band best suited to monitoring vegetation water content. *Proc. 8th Int. ERIM Symp.* Oct. 1984, Paris, France, ERIM, Ann Arbor, Michigan, Vol. 2, pp. 1049-1063.
- Hägglund, B., 1981. Evaluation of forest site productivity. *For. Abstr.* 42:514-527.
- Hairston, A.B., and D.F. Grigal, 1991. Topographic influences on soils and trees within single mapping units and sandy outwash landscape. *For. Ecol. Manage.* 43:35-45.
- Hall-Könyves, K., 1987. The topographic effect on Landsat data in gently undulating terrain in southern Sweden. *Int. J. Rem. Sens.* 8:157-168.
- Hall, R.J., A.R. Kruger, J. Scheffer, S.J. Titus, and W.C. Moore, 1989. A statistical evaluation off Landsat TM and MSS data for mapping forest cutover. *For Chron.* 65:441-449.
- Hall, D.B., D.B. Botkin, D.E. Strelbel, K.D. Woods, and S.J. Goetz, 1991. Large-scale patterns of forest succession as determined by remote sensing. *Ecology*, 72:628-640.
- Hall, R.J., R.V. Dams, and L.N. Lyseng, 1991. Forest cut-over mapping from SPOT satellite data. *Int. J. Rem. Sens.* 12:2193-2204.
- Hallum, C., 1993. A change detection strategy for monitoring vegetative and land-use cover types using remotely-sensed, satellite-based data. *Rem. Sens. Environ.* 43:177-193
- Häme, T. 1984. Landsat-aided forest site type mapping. *Photogramm. Eng. Rem. Sens.* 50:1175-1183.
- Häme, T., 1991. Spectral interrelation of changes in forest using satellite scanner images. *Acta For. Fenn.* 222:1-111.
- Häme, T., and P. Saukkola, 1982. Satellite imagery in forest taxation in northern Finland (in Finnish with English abstract). Technical Research Centre of Finland, *Res. Rep.* 112, Espoo, 89 p.
- Hamilton, M.K., C.O. Davis, W.J. Rhea, S.H. Polirz, and K.L. Carder, 1993. Estimating chlorophyll content and bathymetry of Lake Tahoe using AVIRIS. *Rem. Sens. Environ.* 44:217-230.
- Hanley, D.P., 1976. Tree biomass and productivity estimated for three habitat types of Northern Idaho. *Bull. No. 539*, Forest Wildlife and Range Experiment Station. 15 pp.
- Hardisky, M.A., C.D. Daiber, C.T. Roman, and V. Klemas, 1984. Remote sensing of biomass and annual net aerial primary productivity of a salt marsh. *Rem. Sens. Environ.* 16:91-106.

- Harris, R. 1987. *Satellite Remote Sensing: an Introduction*. Routledge & Kegan Paul, London, 221 pp.
- Harrison, B.A., and D.L.B. Jupp, 1988. *Image Classification in microBRIAN Resource Manual*. CSIRO Division of Water Resources, Canberra, Australia, pp. 3.1-3.90.
- Hart, J.A., D.B. Wherry, and S. Bain, 1987. An operational GIS for flathead National forest. In *Geographic Information Systems for Resource Management: a Compendium*. W.J. Ripple (ed.). American Society for Photogrammetry and remote Sensing and American Congress on Surveying and Mapping. pp. 219-228.
- Hartigan, J.A., 1975. *Clustering Algorithms*. Wiley, New York, 351p.
- Heath, G.R., 1974. earth resource satellites - their potential in forestry. *J. For.* 72(9):573-576.
- Hegy, F., and R.V. Quenet, 1982. Updating the forest inventory data base in British Columbia. In: C.J. Johnnsen and J.L. Sanders (ed.), *Remote Sensing for Resource Management*, Soil Conservation Society of America. Ankenry, Iowa, pp. 512-518.
- Hegy, F., and R.V. Quenet, 1986. Applications of satellite image data for regional resource management: British Columbia experience. *Rem. Sen. Rev.* 2:145-164.
- Heiberg, S.O., 1956. A site evaluation concept. *J. For.* 54:7-10.
- Heinsdijk, D., 1975. *Forest Assessment*. Centre for Agricultural Publishing and Documentation, Pudoc, Wageningen, Netherlands, 359 p.
- Heller, R.C., 1972. Remote sensing in forestry - promises and problems. In: *Proc. 1972 National Convention*. Hot Springs, arkansas October 1-5. Society of American Foresters, pp. 202-216.
- Heller, R.C., 1976. Remote sesing from airborne and spaceborne imagery. *Proc. XVI IUFRO World Congr.*, Norway, Div. 6, pp. 228-253.
- Heller, R.C., and J.J. Ulliman, 1983. Forest Resources Assessment. In Colwell, R.N. (ed.): *Manual of Remote Sensing* (2nd ed.), Am. Soc. Photogramm., the Sherian Press, Virginia, Vol. 2, pp. 2229-2324.
- Heberle, G.W., 1968. Factors affecting the growth of *Pinus radiata* D. Don at Pierces Creek, A.C.T. Hons. MSc Thesis to Department of Forestry, Australian National University.
- Hilborn, W.H., 1978. Application of remote sensing in forestry. In: B.F. Richason (ed.), *Introduction to Remote Sensing of the Environment*. Kenfall/Hunt Publishing Company, Kerper Boulevard, Dubuque, Iowa, pp. 271-286.
- Hildebrandt, G., 1983. Remote sensing from space for forestry purposes, *Remote Sensing: New Satellite Systems and Potential Applications*, ESA SP-205, ESA, Paris, pp. 67-74.
- Hills, G.A., 1952a. *Field Methods for Investigaing Site*. Ontario Dep. Lands For., Res. Man. 4, 119 pp.
- Hills, G.A., 1952b. The classification and evaluation of site for forestry. *Ontario Dept. lands For., Res. Rep.* No. 24, 41 pp.
- Hills, G.A., 1953. The use of site in forest management. *For. Chron.* 29:128-136.
- Hills, G. A., 1959. Comparison of forest ecosystems (vegetation and soil) in different climatic zones. *Silva Fennica*, 105:33-39.
- Hills, G.A., and G. Pierpoint. 1960. Forest site evaluation in Ontario. *Ontario Dep. Lands and For. Res. Rep.* No. 42, 41 pp.
- Hills, G.A., 1961. The Ecological basis for Land Use Planning. Ontario Dep. Lands. For., Res. Rep. No. 46, 204 pp.
- Hill, J., and D. Aifadopoulou, 1990. Comparative analysis of Landsat-5 TM and SPOT HRV-1 data for use in multiple sensor approaches. *Rem. Sens. Environ.* 34:55-70.

- Hill, G.J.R., and G. D. Kelly, 1986. Integrating Landsat and land systems for cover maps in southern inland Queensland. *Aust. Geog. Studies*, 24:235-243.
- Hix, D. M. 1988. Multifactor classification and analysis of upland hardwood forest ecosystems of the Kickapoo River watershed, southwestern Wisconsin. *Can. J. For. Res.* 18:1405-1415.
- Hobbs, R.J. 1990. Remote sensing of spatial and temporal dynamics of vegetation, In: R.J. Hobbs and H.A. Mooney (ed.), *Remote Sensing of Biosphere Functioning*, pp. 203-219.
- Hodgkins, E.J., 1968. Productivity estimation by means of plant indicators in the longleaf pine forests of Alabama. In: C.T. Youngberg and C.B. Davey (eds.), *Tree Growth and Forest Soils*, pp. 461-474.
- Hodgson, M.E., J.R. Jensen, H.E. Mackey, and M.C. Coulter, 1988. Monitoring wood stork foraging habitat using remote sensing and geographic information systems. *Photogramm. Eng. Rem. Sens.* 54:1601-1607
- Hoffer, R.M., 1986. Digital analysis techniques for forestry applications. *Rem. Sens. Rev.* 2:61-110.
- Hoffer, R.M., 1978. Biological and physical considerations in applying computer-aided analysis techniques to remote sensor data, In: P.H. Swain and S.M. Davis (eds.), *Remote Sensing: the Quantitative Approach*, McGraw-Hill, New York. pp. 227-289.
- Holben, B.N., C.J. Tucker, and C.J. Fan, 1980. Assessing leaf area and leaf biomass with spectral data. *Photogramm. Eng. Rem. Sens.* 46:651-656.
- Hollenbaugh, R.D., 1987. Site selection using Bechtel's Geographic Information System. In: *GIS'87 — San Francisco*. Am. Soc. Photogramm. Rem. Sens. Vol. II, pp. 601-610.
- Holmes, M.G., 1981. Spectral Distribution of Radiation Within Plant Canopies. In: H. Smith (ed), *Plants and the Daylight Spectrum*, Academic Press, New York, pp. 147-158.
- Holter, M.R., 1970. Imaging with nonphotographic sensors. In: Committee on Remote Sensing for Agriculture Purposes (ed.), *Remote Sensing with Special Reference to Agriculture and forestry*, Agricultural Board, National Research Council, National Academy of Sciences, Washington D.C., pp. 73-163.
- Hope, A.S., J.S. Kimball, and D.A. Stow, 1993. The relationship between tussock tundra spectral reflectance properties and biomass and vegetation composition. *Int. J. Rem. Sens.* 14:1861-1874.
- Hopkins, P.F., A.L. MacLean, and T.M. Lillesand, 1988. Assessment of the thematic mapper imagery for forestry applications under lake conditions *Photogramm. Eng. Rem. Sens.* 54:61-68.
- Hord, R.M., 1982. *Digital Image Processing of Remotely Sensed Data*. Academic Press, New York, 256 pp.
- Horler, D.N., and F.J. Ahern, 1986. Forestry information content of Thematic Mapper data. *Int. J. Rem. Sens.* 7:405-428.
- Horler, D.N.H., and J. Barber, 1981. Principles of remote sensing of plants. In: H. Smith (ed), *Plants and the Daylight Spectrum*, Academic Press, New York, pp. 43-63.
- Horler, D.N., M. Dockray, and J. Barber, 1983. The red edge of plant leaf reflectance. *Int. J. Rem. Sens.* 4:273-288.
- Horst, P., 1961. Generalised canonical correlations and their applications to experimental data. *J. Clinical. Psycho.* 14:129-150.
- Hotelling, H., 1935. The most predictable criterion. *J. Edu. Psychol.* 26:139-142.
- Hotelling, H., 1936. Relations between two sets of variables. *Biometrika*, 28:321-377.
- Howard, J.A., 1970. *Aerial Photo-Ecology*. Faber and Faber, London, 325 pp.

- Howard, J.A., 1976. Remote sensing of tropical forest with special reference to satellite imagery. *Proc. XVI IUFRO World Congr.*, Norway, Div. 6, pp. 255-270.
- Howard, J.A., 1991. *Remote Sensing of Forest Resources: Theory and application*. Chapman & Hall, London, 419 pp.
- Hudson, W.D., 1987. Evaluating Landsat classification accuracy from forest cover-type maps. *Can. J. Rem. Sens.* 13:39-42.
- Hüggard, E.R., and T.H. Owen, 1960. *Forest Tools and Instruments*. Adam & Charles Black, London, 119 pp.
- Hutchinson, M.F., 1990. *Instruction for the Use of Program ANUDEM*. Centre for Resource and Environmental Studies, Australian National University, GPO Box 4, ACT 2601.
- Ingebritsen, S.E., and R.J.P. Lyon, 1985. Principal component analysis of multitemporal image pairs. *Int. J. Rem. Sens.* 6:687-696.
- Itten, K., and P. Meyer, 1993. Geometric and radiometric correction of TM data of mountainous forested areas. *IEEE Trans. GeoSci. Rem. Sens.* 31:764-770.
- Iverson, L.R., E.A. Cook, R. Graham, J.S. Olson, T.D. Frank, and Y. Ke, 1988. Interpreting forest biome productivity and cover utilising nested scales of image resolution and biogeographical analysis. Final Report to NASA, Champaign, Illinois.
- Jaakkola, S., 1976. An automated approach to remote sensing oriented forest resource surveys. *Proc. XVI IUFRO World Congr.*, Norway, Division 6, pp. 147-156.
- Jaakkola, S., and P. Saukkola, 1978. Timber and soil classification using numerical interpretation of Landsat-2 and aircraft data. In: *Proc. Int. Symp. Rem. Sens. for Observation and Inventory of Earth Resources and the Endangered Environment*, G. Hildebrandt, and H.-J. Boehnel (ed.), July 2-8, 1978, Freiburg, Germany, Vol. III, pp. 1779-1790.
- Jaakkola, S., and P. Saukkola, 1979. Timber volume estimation and cutting opportunity mapping using multispectral remote sensing techniques. *Photogrammetric Journal of Finland*, Vol. 8, No. 1., pp. 1-56.
- Jaakkola, S., 1986a. Possibility for using satellite imagery (including SPOT) in forest inventory and management. In: S. Sohlberg, and V.E. Sokolov (ed.), *Practical application of Remote Sensing in Forestry*, Martinus Nijhoff Publishers, Dordrecht, pp. 67-80.
- Jaakkola, S., 1986b. Use of the Landsat MSS for forest inventory and regional management: the European experience. *Rem. Sens. Rev.* 2:165-213.
- Jackson, R.D., 1986. Remote sensing of biotic and abiotic plant stress. *Ann. Rev. Phytopath.* 24:265-287.
- Jackson, D.S., and H.H. Gifford, 1974. Environmental variables influencing the increment of radiata pine. 1. Periodic volume increment. *N.Z. J. For. Sci.* 4:3-26.
- Jackson, R.D. 1983. Spectral indices in *n*-space. *Rem. Sens. Environ.* 13:409-421.
- Jackson, R.D., P.N. Slater, and P.J. Pinter, 1983. Discrimination of growth and water stress in wheat by various vegetation indices through clear and turbid atmosphere. *Rem. Sens. Environ.* 13:187-208.
- Jacobs, M.R., 1937. The detection of annual stages of growth in the crown of *Pinus radiata*. *Bulletin No. 19*, Commonwealth Forestry Bureau. 16 pp.
- Janssen, L.L.F., M.N. Jaarsma, and E.T.M. van der Linden, 1990. Integrating topographic data with remote sensing for land-cover classification. *Photogramm. Eng. Rem. Sens.* 56:1503-1506.
- Jensen, J.R., H. Lin, X. Yang, E. Ramsey, III.B.A. Davis, and C.W. Theomke, 1991. The measurement of management characteristics in southwest Florida using SPOT multispectral data. *Geocarto Int.* 6(2):13-21.

- Jiang, Y., 1990. Discussion on establishment of the forest site classification system in China. *Scientia Silvae Sinicae*, 26(3):262-273.
- Joffre, R., and B. Lacaze, 1993. Estimating tree density in oak savanna-like 'dehesa' of southern Spain from SPOT data. *Int. J. Rem. Sens.* 14:685-697.
- Johnson, S.C. 1967. Hierarchical clustering schemes. *Psychometrika*, 32:241-254.
- Jolliffe, I.T., 1986. *Principal Component Analysis*. Springer-Verlay, New York, 271 pp.
- Jones, A.D., 1976. Photographic data extraction from Landsat images. *Photogramm. Eng. Rem. Sens.* 42:1423-1426.
- Jones, J.R., 1969. Review and Comparison of site evaluation methods. *USDA For. Serv. Res. Pap.* RM-51, 26 pp.
- Johnston, R. M., and M. M. Barson, 1990. An assessment of the use of remote sensing techniques in land degradation studies. *Bulletin No. 5*, Bureau of Rural Resources, Department of Primary Industries and Energy, Australia. 64 pp.
- Justice, C.O., J.R. Townshend, N.H. Holben, G.J. Tucker, 1985. Analysis of the phenology of global vegetation using meteorological satellite data. *Int. J. Rem. Sens.* 6:1271-1278.
- Justice, C.O., B.L. Markham, J.R.G. Townshend, and R. L. Kennard, 1989. Spatial degradation of satellite data. *Int. J. Rem. Sens.* 10:1539-1561.
- Kalensky, Z.D., W.C. Moore, D.A. Wilson, and A.J. Scott, 1979. Forest statistics by ARIES classification of Landsat multispectral images in Northern Canada. *Proc. 13th Int. Symp. Rem. Sens. Environ.* ERIM, Ann Arbor, Michigan, Vol. 2, pp. 789-811.
- Kalensky, Z.D., and L.R. Scherk, 1975. Accuracy of forest mapping from Landsat CCTs. *Proc. 10th Int. Symp. Rem. Sens. Environ.* ERIM, Ann Arbor, Michigan, Vol. 2, pp. 1159-1163.
- Kan, E.P., and F.P. Weber, 1978. The ten ecosystem study Landsat ADP mapping of forest and rangeland in the United States. *Proc. 12th Int. Symp. Rem. Sens. Environ.* Environmental Research Institute, Michigan, Ann Arbor, Michigan, Vol. 2, pp. 1809-1825.
- Kanellopoulos, I., A. Varfis, G.G. Wilkinson, and J. M egier, 1992. Land-cover discrimination in SPOT HRV imagery using an artificial neural network - a 20-class experiment. *Int. J. Rem. Sens.* 13:917-924.
- Kanemasu, E.T., C.L. Niblett, H. Manges, D. Lenhart, and M.A. Newman, 1974. Wheat: Its growth and disease severity as deduced from ERTS-1. *Rem. Sens. Environ.* 3:255-260.
- Kanemasu, E.T., T.H. Demetriades-Shah, H. Su, and A.R.G. Lang, 1990. Estimating grassland biomass using remotely sensed data. In: M.D. Steven and J.A. Clark (ed.), *Applications of Remote Sensing in Agriculture*. Butterworths, London, pp. 185-199.
- Karteris, M., 1988. Manual interpretation of small forestland on Landsat MSS data. *Photogramm. Eng. Rem. Sens.* 54:751-755
- Kaufmann, H., and B. Pfeiffer, 1988. Image optimisation versus classification - an application oriented comparison of different methods by use of thematic Mapper. *Photogrammetria (PRS)*, 42:311-324.
- Kauth, R.J., and G.S. Thomas, 1976. The Tasseled Cap-a graphic description of spectral-temporal development of agricultural crops as seen by Landsat. In: *Proc. Symposium Machine Processing of Remotely Sensed Data*, Purdue University, West Lafayette, Indiana, pp. 4B-41—4B-51.
- Kawata, Y., S. Ueno, and T. Kusaka, 1988. Radiometric correction for atmospheric and topographic effects on Landsat MSS images. *Int. J. Rem. Sens.* 9:729-748.
- Kazmierczak, M.L. 1991. Forestry variables assessment using Landsat TM data. In: *Proc. 24th Int. Symp. Rem. Sens. Environ.* 27-31 May 1991, Rio De Janeiro, Brazil, pp. 837-847.

- Kdesinkov, B.P., 1960. Natural historical division of forests (on the example of the Urals). *Proc. 5th World For. Congr.*, University of Washington, Seattle, Washington, U.S.A. Vol. 1, pp. 591-594.
- Keil, M., M. Schardt, A. Schurek, and R. Winter, 1990. Forest mapping using satellite imagery. The Regensburg map sheet 1:200,000 as example. *ISPRS J. Photogramm. Rem. Sens.* 45:33-46.
- Kelley, A.P. 1922. Plant indicators of soil types. *Soil Sci.* 13:411-423.
- Kelly, G.D., and G.J.E. Hill, 1987. Updating maps of climax vegetation cover with Landsat MSS data in Queensland, Australia. *Photogramm. Eng. Rem. Sens.* 53:633-637.
- Kharin, N.G., 1973. Spectral Reflectance Characteristics of the U.S.S.R. Main Tree Species. *Proc. IUFRO Symp.*, Freiburg, 20 pp.
- Khorrarn, S., G.P. Catts, J.E. Cloern, and A. W. Knight, 1987. Modelling of estuarine chlorophyll a from an airborne scanner. *IEEE Trans. GeoSci. Rem. Sens.* GE-25:662-669.
- Kilian, W., 1984. Site classification and mapping. *Symp. In: Site and productivity of Fast Growing Plantations* (IUFRO Proceedings), Vol. 1, pp. 51-68.
- Kimes, D.E., P.R. Harrison, P.A. Ratcliffe, 1991. A knowledge-based expert system for inferring vegetation characteristics. *Int. J. Rem. Sens.* 12:1987-2020.
- Kimes, D.S., J.A. Kirchner, 1983. Diurnal variation of vegetation canopy structure. *Int. J. Rem. Sens.* 4:257-271.
- Fox, D.E., P.R. Harrison, P.A. Ratcliffe, 1991. A knowledge-based expert system for inferring vegetation characteristics. *Int. J. Rem. Sens.* 12:1987-2020.
- King, C., and J. Meyer-Roux, 1990. Remote sensing in agriculture: from research to applications. In: M.D. Steven and J.A. Clark (ed), *Applications of Remote Sensing in Agriculture*. Butterworths, London, pp. 377-395.
- Kinloch, D., and G. Page, 1966. Quantitative techniques for relating site condition to the productivity of certain conifers in North Wales. *Proc. 6th World For. Congr.*, Madrid. Vol. II, pp. 1438-1441.
- Kirby, C.L., and P.I. Van Eck, 1977. A basis for multistage forest inventory in the boreal forest region. *Proc. 7th Can. Symp. Rem. Sens.*, Quebec City, Quebec, pp. 71-94.
- Klinka, K.W.D. van der Horst, F.C. Nuszdorfer, and R.G. Harding, 1980. An ecosystematic approach to forest planning. *For. Chron.* 56(2):97-103.
- Klock, G.O. 1989. Use of GIS to map vegetation in eastern Washington. *Proc. Land Classifications based on vegetation: Applications for Resource Management*. Moscow, ID; November 17-19, 1987. USDA For. Serv., *Gen. Tech. Rep.* INT-257. pp. 105-106.
- Kloeden, A.J., 1969. Soil-Site Studies of *Pinus Radiata* D. Don with Particular Emphasis on Soil Moisture Availability. BSc Thesis, Department of Forestry, Australian National University, Canberra, ACT, 86 pp.
- Kneppeck, I.D., and F. J. Ahern, 1987. Evaluation of a multispectral linear array sensor for assessing juvenile stand conditions. *Proc. 21st Int. Symp. Rem. Sens. Environ.* Ann Arbor, Michigan, October 26-30, pp. 955-968.
- Knipling, E.G. 1970. Physical and physiological basis for the reflectance of visible and near-infrared radiation from vegetation. *Rem. Sens. Environ.* 1:155-159.
- Köhl, M., and H. Sutter, 1991. Application of aerial photographs in the estimation of standing volume in the Swiss national forest inventory. In: Köhl, M. and D. R. Pelz (ed.): *Forest Inventories in Europe - with Special Reference to statistical Methods* (IUFRO Proceedings, May 14-16, 1990, Birmensdorf, Switzerland), pp. 176-191
- Korstian, C.F. 1917. The indicator significance of native vegetation in the determination of forest sites. *Plant World*, 20:267-287.



- Kourtz, P., 1990. Artificial intelligence: a new tool for forest management. *Can. J. For. Res.* 20:431-437.
- Kowal, R.R., M.J. Lechowicz, and M.S. Adams, 1976. The use of canonical analysis to compare response curves in physiological ecology. *Flora*, 165:29-46.
- Krebs, P.V., 1982. Multiresource inventory and mapping of Alaska's wildlands: A cost-effective application of remote sensing. In: C.J. Johnsen and J.L. Sanders (ed.), *Remote Sensing for Resource Management*, Soil Conservation Society of America. Ankeny, Iowa, pp. 81-90.
- Kshirsagar, A.M., 1972. *Multivariate Analysis*. Marcel Dekker, Inc. New York. 534 pp.
- LaBau, V.J., and K.C. Wintgerberger, 1988. Use of four-phase sampling design in Alaska Multiresource vegetation inventories. *Proc. IUFRO Congr.*, Division IV Meeting, Finland.
- Lacate, D.S., and M.J. Romaine, 1978. Canada's land capability inventory program. *J. For.* 76:668-671.
- Lachowski, H.M., C.Y. Borden, and B.F. Merembeck, 1982. Canal Program Description. In: B.J. Turner, G.M. Bauser, and W.L. Meyers (eds.), *The ORSER Remote Sensing Analysis Systems: A User Manual*. The Pennsylvania State University.
- Landgrebe, D.A., R. M. Hoffer, and R.C. Heller, 1972. An early analysis of ERTS-1 data. *Proc. NASA Symp. on Preliminary Results of ERTS Data*, Greenbelt, Maryland, pp. 21-38.
- Lundgren, B. 1981. Land quality and growth in the tropics. In: Laban P. (ed.), *Proc. Workshop on Land Evaluation for Forestry*, Int. Workshop of the IUFRO/ISSS, Wageningen, The Netherlands, 10-14 November, 1980, ILRI Publication No. 28, pp. 237-252.
- Larson, H., 1993. Linear regression for canopy cover estimation in acacia woodlands using Landsat-TM, -MSS, and SPOT HRV XS data. *Int. J. Rem. Sens.* 14:2129-2136.
- Latham, R.P., and T.M. McCarty, 1972. Recent development in remote sensing for forestry. *J. For.* 70:398-402.
- Lavery, P.B., 1986. *Plantation Forestry with Pinus radiata - Review Papers*. Paper No. 12, School of Forestry, University of Canterbury, Christchurch, N.Z., 255 pp.
- Leckie, D.G., 1984. Preliminary results of an examination of C-band synthetic aperture radar for forestry applications. *Proc. 8th Can. Symp. Rem. Sens. and 4th Conf. l'Association québécoise de téléd'ection*, Montreal, Quebec, May 3-6, 1983, pp. 151-164.
- Leckie, D.G., 1986. Practical forestry applications of remote sensing in North America: present and future. In: S. Sohlberg, and V.E. Sokolov (ed.), *Practical Application of Remote Sensing in Forestry*, Martinus Nijhoff Publishers, Dordrecht, pp. 51-65.
- Leckie, D.G., 1990. Advances in remote sensing techniques for forest surveys and management. *Can. J. For. Res.* 20:466-483.
- Leckie, D.G., and D.P. Ostaff, 1988. Classification of airborne multispectral scanner data for mapping current defoliation caused by spruce budworm. *For. Sci.* 34:259-275.
- Lee, J.S., and kW. Hoppel, 1992. Principal component transformation of multifrequency polarimetric SAR imagery. *IEEE Trans. Geosci. Rem. Sens.* GE-30:686-696.
- Lee, K.-S., and R.M. Hoffer, 1990. Analysis of combined SIR-B and TM data for assessing forest biomass. *Remote Sensing Science for the Nineties - IGARSS'90, 10th Ann. Int. Geosci. Rem. Sens. Symp.*, The University of Maryland, May 20-24, 1990. Vol. 2, pp. 1227-1230.
- Lees, B.G., and K. Ritman, 1991. Decision tree and rule induction approach to integration of remotely sensed and GIS data in mapping vegetation in disturbed or hilly environment. *Environ. Manage.* 15:823-831.
- Lewis, N.B., 1967, Economic aspect agriculture and afforestation on comparable lands. *Aust. For.* 31:3-9.

- Lewis, N.B., A. Keeves, and J.W. Leech, 1976. Yield regulation in South Australia *Pinus radiata* plantations. South Australia Woods and Forests Department, *Bulletin* No. 23, 173 pp.
- Li, X., and A.H. Strahler, 1981. An invertible coniferous forest canopy reflectance model. *Proc. 25th Int. Symp. Rem. Sens. Environ*, ERIM, Ann Arbor, Michigan, Vol. III, pp. 1237-1244.
- Li, X., and A. Strahler, 1985. Geometric-optical modelling of a coniferous forest canopy. *IEEE Trans. Geosci. Rem. Sens.* GE-23:207-221.
- Li, X., and A.H. Strahler, 1986a. Geometric-optic bidirectional reflectance modelling of a coniferous forest canopy. *IEEE Trans. Geosci. Rem. Sens.* GE-24:906-919.
- Li, X., and A.H. Strahler, 1986b. Modelling gap probability in discontinuous vegetation canopies. *Proc. IGARSS'87 Symp.*, Ann Arbor, 18-21 May, 1987, pp. 1483-1486.
- Li, X., and A.H. Strahler, 1992. Geometric-optical bidirectional reflectance modelling of the discrete crown vegetation canopy: effect of crown shape and mutual shadowing. *IEEE Trans. Geosci. Rem. Sens.* GE-30:271-292.
- Lillesand, T.M., P.F. Hopkins, M.P. Ruchheim, and A.L. McLean, 1985. The potential impact of Thematic Mapper, SPOT and microprocessor technology in forest type mapping under Lake States conditions. *Proc. 10th W.T. PECORA Mem. Symp.*, Am. Soc. Photogramm. Rem. Sens., Falls Church, VA, pp. 43-57.
- Liu, G., and D. Zheng, 1990. Estimating production of winter wheat by remote sensing and unified ground network. 1. System verification. In: M.D. Steven and J.A. Clark (ed.), *Applications of Remote Sensing in Agriculture*. Butterworths, London, pp. 137-147.
- Lo, C.P., 1986. *Applied Remote Sensing*. Melbourne: Longman Cheshire, Melbourne, 393 pp.
- Loetsch, F.G., and K.E. Haller, 1964. *Forest Inventory*. Volume I: Statistical of Forest Inventory and Information from Aerial Photographs. (English by E.F. Brünig), BLV Verlagsgesellschaft München Basel Wien, Munich, 436 pp.
- Lodwick, G.D., 1979a. A computer system for monitoring seasonal vegetation changes in multitemporal Landsat data. *LANDSAT 79 - Proc. 1st Aust. Rem. Sens. Conf.*, Sydney, Australia, pp. 119-129
- Lodwick, G.D., 1979b. Measuring ecological changes in multitemporal Landsat data using principal components. *Proc. 13th Int. Symp. Rem. Sens. Environ*. Arn Arbor, Michigan, USA, Vol. II, pp. 1131-1141.
- Löffler, H., 1981. Land quality and forest operation. In: Laban P. (ed.), *Proc. Workshop on Land Evaluation for Forestry*, Int. Workshop of the IUFRO/ISSS, Wageningen, The Netherlands, 10-14 November, 1980, ILRI Publication No. 28, pp. 253-274.
- Losee, S.T.B., 1942. Air photographs and forest sites. I. mapping methods illustrated on an area of the Petawawa Forest Experiment Station. *Fo. Chron.* 18:129-144.
- Loughlin, W.P., 1991. Principal component analysis for alteration mapping. *Photogramm. Eng. Rem. Sens.* 57:1163-1169.
- Lovén, L., 1986. Remote sensing in Finnish forest taxation. In: S. Sohlberg, and V.E. Sokolov (eds.), *Practical Application of Remote Sensing in Forestry*, Martinus Nijhoff Publishers, Dordrecht, pp. 159-167.
- Lowell, K.E. 1990. Differences between ecological land type maps produced using GIS or manual cartographic methods. *Photogramm. Eng. Rem. Sens.* 56:169-173.
- Lu, J., 1988. Development of principal component analysis applied to multitemporal Landsat TM data. *Int. J. Rem. Sens.* 9:1895-1907.
- Lundgren, B., 1981. Land quality and growth in the tropics. In: Laban P. (ed.), *Proc. Workshop on Land Evaluation for Forestry*, Int. Workshop of the IUFRO/ISSS, Wageningen, The Netherlands, 10-14 November, 1980, ILRI Publication No. 28, pp. 232-252.

- Luney, P.R., and H.W. Dill, 1970. Uses, potentialities, and needs in agricultural and forestry. In: *Remote Sensing with Special Reference to Agriculture and forestry*, National Academy of Sciences, Washington D.C., pp. 1-34.
- Lynn, D.W., 1986. Monotemporal, multitemporal, and multirate thermal infrared data acquisition from satellite for soil and surface-material survey. *Int. J. Rem. Sens.* 7:213-231.
- Mackinnon, A., D. Meidinger, and K. Klinka, 1992. Use of the biogeoclimatic classification system in British Columbia. *For. Chron.* 68:100-119.
- MacMillan, D.C., 1991. Predicting the general yield class of sitka spruce on better quality land in Scotland. *Forestry*, 64:359-372.
- McGwire, K., M. Friedl, and J.E. Estes, 1993. Spatial structure, sampling design and scale in remotely-sensed imagery of a California savanna woodland. *Int. J. Rem. Sens.* 14:2137-2164.
- MacSiurtain, M.P., P.M. Joyce, N.O. Muigheasa, M.J. Hoey, and N. McCormick, 1989. *Use of second generation earth observation satellite data in the implementation of the forest management models within the less favoured areas in the republic of Ireland*. Department of Forestry, University College, Dublin. (Cited in Howard 1991).
- Makkonen, O. 1968. Ancient forestry, Part 1 - Facts and information on Trees. *Acta For. Finn.* 82:1-84.
- Malingreau, J.P., and C.J. Tucker, 1987. The contribution of AVHRR data for measuring and understanding global processes: large-scale deforestation in the Amazon Basin. *Proc. IGARSS'87 Symp.*, Ann, Arbor, ERIM, pp. 443-438.
- Manière, R., and J. Courboulés, 1989. Comparative performance results between Landsat Thematic Mapper and SPOT 1 high resolution visible image for Mediterranean forest inventory. *Adv. Space Res.* 9:125-134.
- Mardia, K.V., J.T. Kent, J.M. Bibby, 1979. *Multivariate Analysis*. Academic Press, London, 521 pp.
- Markham, B.L., and J.R.G. Townshend, 1981. land cover classification accuracy as a function of sensor spatial resolution. *Proc. 15th Int. Symp. Rem. Sens. Environ.*, Ann Arbor, Michigan, ERIM, 11-15 May 1981, Vol. II, pp. 1075-1090.
- Marsh, S.E., J.L. Walsh, C.T. Lee, L.R. Beck, and C.F. Hutchinson, 1992. Comparison of multi-temporal NOAA-AVHRR and SPOT-XS satellite data for mapping land-cover dynamics in the west African Sahel. *Int. J. Rem. Sens.* 13:2997-3016.
- Mather, P.M.. 1987. *Computer Processing of Remotely-Sensed Images: an Introduction*. Wiley, Chichester, 352 pp.
- Maxwell, E.L., 1976. Multivariate systems analysis of multipsectral imagery. *Photogramm. Eng. Rem. Sens.* 42:1173-1180.
- McCormack, R. J. 1967. Land capacity for forestry. Canada Land Inventory, *Rep. No. 4*. Can. Dept. For. Rural Develop., Ottawa.
- McDonald, R.C., R.F. Isbell, J.G. Speight, J. Walker, M.S. Hopkins, 1984a. Soil Profile. In: R.C. McDonald, R.F. Isbell, J.G. Speight, J. walker, and M.S. Hopkins (ed.), *Australian Soil and Land Survey Handbook*. Inkata Press, Melbourne, pp. 83-132.
- McDonald, R.C., R.F. Isbell, and J.G. Speight, 1984b. Land surface. In: R.C. McDonald, R.F. Isbell, J.G. Speight, J. walker, and M.S. Hopkins (ed.), *Australian Soil and Land Survey Handbook*. Inkata Press, Melbourne, pp. 68-82.
- McKeon, J.J., 1962. Canonical analysis: some relations between canonical correlation, factor analysis, discriminant function analysis, and scaling theory. *Psychometric Monograph*, No. 13, 43 p.

- McNab, W.H., 1987. Integrated site classification in the southern Appalachians: geologic variables related to yellow-poplar productivity. *Proc. 4th Bienn. Southern Silvi. Res. Conf.*, Southern For. Exp. Stn., Asheville, North Carolina. pp. 253-258.
- McNab, W.H. 1989. Terrain shape index: quantitative effect of minor landforms on tree height. *For. Sci.* 35:91-104.
- McNab, W.H., C.E. Merschatt, 1990. Geologic variables associated with height of yellow-popular stands in the Bald Mountains of North Carolina. *J. Elisha Mitchell Sc. Soc.* 106:25-32.
- Mead, R., and M. Meyer, 1977. Landsat digital data application to forest vegetation and land use classification in Minnesota. Res. Rep. 77-6, Uni. Minnesota.
- Meads, W.J., and B.A. Roberts, 1992. A review of forest site classification activities in Newfoundland and Labrador. *For. Chron.* 68:25-33.
- Memani, R., L. Pierce, S. Running, and L. Band, 1993. Forest ecosystem processes at the watershed scale: sensitivity to remotely-sensed leaf area index estimates. *Int. J. Rem. Sens.* 14:2519-2534.
- Meyer, H.A. 1953. *Forest Mensuration*. USA Penns Valley Publishers, Inc. 357 pp.
- Milne, A.K., 1983. Renewable resource applications. *Short Course on Introduction to Remote Sensing Technology and Applications*, Sydney.
- Milne, A. 1988. Change detection analysis using Landsat imagery: A review of methodology. *Proc. IGARSS'88 Symp.*, Edinburgh, Scotland, September 13-16, pp. 541-544.
- Milton, N.M., and D.A. Mouat, 1989. Remote sensing of vegetation responses to natural and cultural environmental conditions. *Photogramm. Eng. Rem. Sens.* 55:1167-1173.
- Minckler, L.S., 1941. The right tree in right place. *J. For.* 39:685-688.
- Minor, C.O., 1954. Site index curves for young-growth ponderosa pine in Northern Arizona. *Res. Note No. 37, Rocky Mount. For. Range Exp. Stn, U.S. For. Serv.*, 88 pp.
- Moik, J.G., 1980. *Digital processing of remotely sensed images*. Scientific and Technical Information Branch, NASA, Washington, D.C., 330 pp.
- Moore, M.M., and M.E. Bauer, 1990. Classification of forest vegetation in North-Central Minnesota using Landsat multispectral scanner and Thematic Mapper data. *For. Sci.* 36:330-342.
- Moore, D.M., B.G. Lees, and S.M. Davey, 1991. A new method for predicting vegetation distributions using decision tree analysis in a geographic information system. *Environ. Manage.* 15:59-71.
- Mouat, D.A., G.G. Mahin, and J. Lancaster, 1993. Remote sensing techniques in the analysis of change detection. *Geocarto Int.* 8(2):39-50.
- Moya, I., G. Guyot, and Y. Goulas, 1992. Remotely sensed blue and red fluorescence emission for monitoring vegetation. *ISPRS J. Photogramm. Rem. Sens.* 47:205-231.
- MPA, 1989. *The microBRIAN Users Manual*. MPA Communications Pty. Ltd. Australia.
- Muirhead, R.J. 1982. *Aspects of Multivariate Statistical Theory*. Wiley, New York, 673 pp.
- Mukai, Y.T. Sugimura, H. Watanabe, and K. Wakamori, 1987. Extraction of areas infested by pine bark beetle using Landsat MSS data. *Photogramm. Eng. Rem. Sens.* 53:77-81.
- Mulders, M.A., 1987. *Remote Sensing in Soil Science*. Elsevier, Amsterdam, 379 pp.
- Murtha, P.A., 1982. Detection and analysis of vegetation stress. In C.J. Johannsen and J.L. Sanders (eds.): *Remote Sensing for Resource Management*. pp. 141-158.

- Murtha, G.G., 1988. Soil properties and soil performance. In: R.H. Gunn, J.A. Beattie, R.E. Reid and R.H.M. van de Graaff (ed.), *Australian Soil and Land Survey Handbook - Guidelines for Conducting Surveys*, Inkara Press, Melbourne, pp. 241-257.
- Myneni, R.B., B.D. Ganapol, and G. Asrar, 1992. Remote sensing of vegetation canopy photosynthetic and stomatal conductance efficiencies. *Rem. Sens. Environ.* 42:217-238.
- Nelson, D.O. 1981. Land quality and conservation. In: Laban P. (ed.), *Proc. Workshop on Land Evaluation for Forestry*, Int. Workshop of the IUFRO/ISSS, Wageningen, The Netherlands, 10-14 November, 1980, ILRI Publication No. 28, pp. 275-297.
- Nelson, B.L. 1983. Detecting forest canopy change due to insect activity using Landsat MSS. *Photogramm. Eng. Rem. Sens.* 49:1303-1314.
- Nelson, P.R., 1990. Design and analysis of experiments. In: H.M. Wadsworth (ed.), *Handbook of Statistical Methods for Engineers and Scientists*. McGraw-Hill, Inc. pp. 14.1-14.40.
- Nelson, R.F., B.S. Latty, and G. Mott, 1984b. Classifying northern forests using Thematic Mapper Simulator data. *Photogramm. Eng. Rem. Sens.* 50(5):607-617.
- Nelson, R., Krabill, W., and G. Maclean, 1984b. Determining forest canopy characteristics using airborne laser data. *Rem. Sens. Environ.* 14:155-159.
- Nelson, R., and B. Holben, 1986. Identifying deforestation in Brazil using multiresolution satellite data. *Int. J. Rem. Sens.* 7:219-448.
- Nelson, R., N. Horning, and T.A. Stone, 1987. Determining the rate of forest conversion in Mato Grosso, Brazil, using Landsat MSS and AVHRR data. *J. World For. Res. Manage.* 8:1767-1784.
- Nelson, R.F., D. Case, N. Horning, V. Anderson,, and S. Pillai, 1987. Continental land cover assessment using Landsat MSS data. *Rem. Sens. Environ.* 21: 61-68.
- Nelson, R., V. Anderson, L.J. Cote, and N. Horning, 1989. Large scale forest resources assessment using Landsat and airphotos. *J. World For. Res. Manage.* 4: 21-36.
- Nelson, R., W. Krabill, and G. MacLean, 1984b. Determining forest canopy characteristics using airborne laser data. *Rem. Sens. Environ.* 15:201-212.
- Nelson, R., W. Krabill, and J. Tonelli, 1988. Estimating forest biomass and volume using airborne laser data. *Rem. Sens. Environ.* 24:247-267.
- Nilson, T. and U. Peterson, 1991. A forest canopy reflectance model and a test case. *Rem. Sens. Environ.* 27:131-142.
- Noakes, L.C., 1954. Geology and Geomorphology - The Canberra Region. In: H.L. White (ed), *Canberra - a Nation's Capital*, Halstead Press, Sydney, pp. 115-131.
- Northcote, K.H., 1979. *A Factual key for the Recognition of Australian Soils*. 4th ed., Rellim, Adelaide, 124p.
- Nowacki, G.J., M.D. Abrams, and C.G. Lorimer, 1990. Composition, structure, and historical development of northern red oak stands along an edaphic gradient in north-central Wisconsin. *For. Sci.* 36:276-292.
- Odum, E.P., 1959. *Fundamentals of Ecology* (2nd ed.). W.B. Saunders Company, Philadelphia and London, 546 pp.
- Oliosio, A. M. Méthy, and B. Lacaze, 1992. Simulation of canopy fluorescence as a function of canopy structure and leaf fluorescence. *Rem. Sens. Environ.* 28:239-247.
- Olsson, L., 1987. Approaches to monitoring renewable resources using remote sensing and geographic information system. In: *Proc. Symp. Rem. sens. for Resources Development and Environmental Management*. Enschede, Finland, August 1986, pp. 1041-1050.

- Öpik, A.A., 1954. Geology of the Canberra City District. In: H.L. White (ed.), *Canberra, a Nation's Capital*, Halstead Press, Sydney, pp. 131-148.
- Oschman, J.L., 1961. Theophrastus (370 B.C. - 285 B.C.) (pp. 998-999). In P. Gray (ed.): *The Encyclopedia of the biological sciences*, Reinhold, N. Y. 1119 p.
- Ovington, D.J., 1971. Some aspects of the biology of radiata pine plantations. *Papers Presented to the Pinus Radiata Symposium*, Department of Forestry, Australian National University, Canberra, Australia, 25-28 August, 1970, Vol. 1, pp. 1A.1-7.
- Page, G. 1970. Quantitative site assessment: some practical applications in British forestry. *Forestry*, 43:45-56.
- Paloscia, S., and P. Pampaloni, 1984. Microwave remote sensing of plant water stress. *Rem. Sens. Environ.* 16:249-255.
- Palter, J.P., 1990. Leaf chlorophyll contents. *Rem. Sens. Rev.* 5:207-220.
- Parks, N. F., and G. W. Peterson, 1987. High resolution remote sensing of spatially and spectrally complex coal surface mines of central Pennsylvania: a comparison between simulated SPOT MSS and Landsat-5 Thematic Mapper. *Photogramm. Eng. Rem. Sens.* 53:415-420.
- Peng, S., 1987. On the combination of multitemporal satellite and field data for forest inventories. *Acta For. Fenn.* 200:1-95.
- Peterson, D.L., W.E. Westman, N.J. Stephenson, V.G. Ambrosia, J.A. Brass, and M.A. Spanner, 1986. Analysis of forest structure using Thematic Mapper simulator data. *IEEE Trans. Geosci. Rem. Sens.* GE-24:113-120.
- Peterson, D.L., M.A. Spanner, S.W. Running, and K.B. Teuber, 1987. Relationship of Thematic Mapper Simulator data to leaf area index of temperate coniferous forests. *Rem. Sens. Environ.* 22:323-341.
- Pfister, R.D., 1976. Forest habitat types classification, mapping, and ecoregions in the north Rocky Mountains. *XVI IUFRO World Congr.*, Oslo, Norway. 11 pp.
- Pfister, R.D., and S.F. Arno, 1980. Classifying forest habitat types based on potential climax vegetation. *For. Sci.* 26:52-70.
- Pfister, R. D., 1984. Forest habitat type classification in the Western United States. In D.C. Grey, A.P.G. Schonau, and C. J. Schutz (eds.): *Proc. IUFRO Symp. Site and Productivity of Fast growing Plantations*, Pretoria and Pietermaritzburg, South Africa, 30 April - 11 May 1984, pp. 149-162.
- Philippis, A. D., 1960. Evaluation of forest site quality from ecological factors. *Proc. 5th world For. Congr.*, University of Washington, Seattle, Washington, D.C., Vol. 1, pp. 530-533.
- Phillips, D.R., and J.R. Saucier, 1981. *Cruising Procedures for estimating total stand biomass*, Georgia For. Res. Pap. No. 14, Georgia Forestry Commission, 7 pp.
- Pielou, E.C., 1977. *Mathematical Ecology* (2nd ed.). Wiley-Interscience, New York, 385 pp.
- Pielou, E.C., 1984. *Interpretation of Ecological Data: A Primer on Classification and Ordination*. Wiley, New York, 263 pp.
- Pilon, P.G., and R.J. Wiart, 1990. Operational forest inventory applications using Landsat TM data: the British Columbia experience. *Geocarto Int.* 5:25-30.
- Plochmann, R. 1981. Problems of land suitability classification for forestry in Central Europe. In: Laban P. (ed.), *Proc. Workshop on Land Evaluation for Forestry*, Int. Workshop of the IUFRO/ISSS, Wageningen, The Netherlands, 10-14 November, 1980, ILRI Publication No. 28, pp. 324-339.
- Plumb, G.A., 1993. Knowledge-based digital mapping of vegetation types in Big Bend National Park, Texas. *Geocarto Int.* 8:29-38.

- Pojar, J., K. Klinka, and D.V. Meidinger, 1987. Biogeoclimatic ecosystem classification in British Columbia. *For. Ecol. Manage.* 22:119-154.
- Poso, S., T. Häme, and R. Paananen, 1984. A method of estimating the stand characteristics of a forest compartment using satellite imagery. *Silva Fennica*, 18(3):261-292.
- Poso, S., R. Paananen, and M. Similä, 1987. forest inventory by compartment using satellite imagery. *Silva Fennica*, 21:69-94.
- Pregitzer, K. S., B.V. Barnes, 1984. Classification and comparison of upland hardwood and conifer systems of the Cyprus H. McCormick Experimental Forest, upper Michigan. *Can. J. For. Res.* 14:362-375.
- Prince, S.D., 1990. High temporal frequency remote sensing of primary production using NOAA AVHRR. In: M.D. Steven and J.A. Clark (ed.), *Applications of Remote Sensing in Agriculture*, Butterworths, London, pp. 169-183.
- Pu, R., and J.R. Miller, 1991. Classifying and evaluating a shelter forest site in a coastal area using remote sensing techniques. *Can. J. Rem. Sens.* 17:323-331.
- Radloff, D.L., and D.R. Betters, 1977. Multivariate analysis of physical site data for wildland classification. *For. Sci.* 24:2-10.
- Ralston, C.W., 1964. Evaluation of forest site productivity. *Int. Rev. For. Res.* 1:171-201.
- Ramann, E., 1893. *Forstliche Bodenkunde und Standortslehre*. Julius Springer, Berlin (in German, available in German Library (cited in Jiang 1990)).
- Randuska, D., 1982. Forest typology in Czechoslovakia. In: G. Jahn (ed.), *Application of Vegetation Science to Forestry*, Dr. W. Junk Publishers, The Hague, pp. 147-178.
- Rao, C.R., 1964. The use of interpretation of principal component analysis in applied research. *Sankhya A*, 26:329-358.
- Raupach, M., 1967. Soil and fertiliser requirements for forests of *Pinus radiata*. *Adv. Agron.* 19:307-353.
- Rauscher, H M., J.W. Benzie, and A.A. Alm, 1990. The red pine forest management advisory system: knowledge model and implementation. *AI Applications in Natural Resource Management*, 4:27-43.
- Ray, R.G., 1956. Site-type, growth and yield at the Lake Edward Forest Experimental Area, Quebec. *Tech. Note For. Res. Div.*, Forest Branch, Department of Northern Affairs and National Resources, Canada. No. 27, 53 pp.
- Ready, P.J., and P.A. Wintz, 1973. Information extraction, SNR improvement and data compression in multi-spectral imagery. *IEEE Trans. Geosci. Rem. Sens.* 21:1123-1130.
- Reed, D.D. 1989. Assessing multiple estimates of plantation productivity. *Can. J. For. Res.* 19: 948-953.
- Reich, R.M., and Y.A. Hussin, 1993. Estimating average stand biomass for a regional forest inventory using radar backscatter. *ITC J.* 1993-1:82-87.
- Renezov, N.P., and P.S. Pogrebnyak, 1965. *Forest soil science*. English Ed. Translated by Y. Haver (1969), Israel Program for Scientific Translations (IPST) Press, Jerusalem, 261 pp.
- Rennie, P.J., 1963. Methods of assessing site capacity. *Comm. For. Rev.* 42:306-317.
- Richards, J.A., 1984. Thematic mapping from multitemporal image data using principal component transformation. *Rem. Sens. Environ.* 16:35-46.
- Richards, J.A., 1986. *Remote sensing Digital Image analysis: an Introduction*. Springer-Verlag, Berlin, 281 pp.
- Richards, J.A., 1993. *Remote sensing Digital Image analysis: an Introduction*. Second Edition, Springer-Verlag, Berlin, 340 pp.

- Richards, J.A., Woodgate, P.W., and A.K. Skidmore, 1987. An explanation of enhanced radar backscattering from flooded forests. *Int. J. Rem. Sens.* 8:1093-1100.
- Richason, B.F., 1978. Remote sensing: an overview. In B. F. Richason (ed.): *Introduction to Remote Sensing of the Environment*. Kenfall/Hunt Publishing Company, Kerper Boulevard, Dubuque, Iowa, 496 pp.
- Ritari, A., and P. Saukkola, 1985. Spectral reflectance as an indicator of ground vegetation and soil properties in Northern Finland. *Comm. Ins. For. Fenn.* 132:1-37.
- Ritchie, J.C., C.M. Cooper, and F.R. Schiebe, 1990. The relationship of MSS and TM digital data with suspended sediments, chlorophyll, and temperature in Moon Lake, Mississippi. *Rem. Sens. Environ.* 33:137-148.
- Roberts, M.R., and N.L. Christensen, 1988. Vegetation variation among successional forest stands in northern lower Michigan. *Can. J. Bot.* 66:1080-1090.
- Robinove, C.J., P.S. Chavez, D. Gehring, and R. Holgren, 1981. Arid land monitoring using Landsat Albedo difference images. *Rem. Sens. Environ.* 11:133-156
- Rock, B.N., J.E. Volgelmann, D.L. Williams, A.F. Volelmann, T. Hoshizaki, 1986. Remote sensing of forest damage. *BioSci.* 36:439-445.
- Roller, N.E., and J. E. Colwell, 1986. Coarse-resolution satellite data for ecological surveys. *BioSci.* 36(7):468-474.
- Roth, F., 1916. Concerning site. *J. For.* 14:3-13
- Roth, F., 1918. Another word on site. *J. For.* 16:749-753.
- Rowe, J.S., 1953. Forest sites - a discussion. *For. Chron.* 29:278-289.
- Rowe, J. S., 1971. Why classify forest land? *For. Chron.* 47:144-148.
- Rowe, R.W., 1956. Uses of undergrowth plant species in forestry. *Ecology*, 37:461-473.
- Running, S.W., and R.R. Nemani, 1988. Relating seasonal patterns of the AVHRR vegetation index to simulated photosynthesis and transpiration of forests in different climates. *Rem. Sens. Environ.* 24:347-367.
- Running, S.W., D.L. Peterson, M.A. Spanner, and K.B. Teuber, 1986. Remote sensing of coniferous forest leaf area. *Ecology*, 67:273-276.
- Running, S.W., R.R. Nemani, D.L. Peterson, L.E. Band, D.F. Potts, L.L. Pierce, M.A. Spanner, 1989. Mapping regional forest evapotranspiration and photosynthesis by coupling satellite data with ecosystem simulation. *Ecology*, 70:1090-1101.
- Ryan, T.P., 1989. Linear Regression. In: H.M. Wadsworth (ed), *Handbook of Statistical Methods for Engineers and Scientists*, McGraw-Hill Publishing Company, New York, pp. 13.1-13.37.
- Sabins, F.F., 1987. *Remote Sensing: Principles and Interpretation*. 2nd ed., Freeman, New York. 426 pp.
- Sader, S.A., 1987. Forest biomass, canopy structure, and species composition relationships with multipolarization L-band synthetic aperture radar data. *Photogramm. Eng. Rem. Sens.* 53:193-202.
- Sader, S.A., and A.T. Joyce, 1988. Deforestation rates and trends in Costa Rica, 1940 to 1983. *Biotropica*, 20:11-19.
- Sader, S.A., R.W. Waide and W.T. Lawrence, 1989. Tropical forest biomass and successional age class relationships to a vegetation index derived from Landsat TM data, *Rem. Sens. Environ.* 28:143-156.
- Sader, S. S., and J. C. Winne, 1992. RGB-NDVI colour composite for visualizing forest change dynamics. *Int. J. Rem. Sens.* 13:3055-3067.



- SAF (Society of American Foresters), 1960. *Forest Terminology*. SAF, Washington D.C.
- SAF, 1971. *Terminology of Forest Science, technology Practice and Products*. English-Language Version. F.C. Ford-Roberston (ed.), Washington D.C. 283p.
- Salu, Y., and J. Tilton, 1993. Classification of multispectral image data by the binary diamond neural network and by nonparametric pixel-by-pixel methods. *IEEE Trans. GeoSci. Rem. Sens.* 31:606-617.
- Sampson, A. W., 1939. Plant indicators-concept and status. *Bot. Rev.*, 5:155-206.
- Santisteban, A., and L. Munoz, 1978. Principal components of a image. An application to a geological problem. *IBM J. Res. Dev.* 22: 444-454.
- SAS Institute Inc., 1989. *SAS/STAT User's Guide*, Version 6, Fourth Edition, SAS Institute Inc., Cary, NC, USA, Vol. 2, pp. 1241-1263.
- Satterwhite, M., W. Rice, and J. Shipman, 1984. Using landform and vegetative factors to improve the interpretation of Landsat imagery. *Photogramm. Eng. Rem. Sens.* 50:83-91.
- Sayn-Wittgenstein, L. 1986. Forest information requirements. *Rem. Sens. Rev.* 2:7-26.
- Schowengerdt, R. A. 1983. *Techniques for image processing and classification in remote sensing*. Academic Press, New York, 249 pp.
- Scott, C.W., 1960. *Pinus radiata*. *FAO Forestry and Forest products Studies*, No. 14, 328 pp.
- Scott, L-A., 1972. *Site Index for Radiata Pine: Definition and Models*, Hon. thesis, the Australian National University, 105 pp.
- Scrafini, M.C., 1986. Spectral response on different growing stages and final winter yield in Trenque Lauquen, Argentina. *Proc. 20th Int. Symp. Rem. Sens. Environ.*, Nairobi, Kenya, Vol. III, pp. 1095-1103.
- Seal, H.L., 1964. *Multivariate Statistical Analysis for Biologists*. Wiley, London, 207 pp.
- Seely, H.E., 1960. Aerial photogrammetry in forestry surveys. *Proc. 5th World For. Congr.*, University of Washington, Seattle, Washington, U.S.A. Vol. 1, pp. 287-290.
- Senoo, T., F. Kobayashi, S. Tanaka, and T. Sugimura, 1990. Improvement of forest type classification by SPOT HRV data with 20 m resolution and DTM. *Int. J. Rem. Sens.* 11:1011-1022.
- Shanmugam, K.S., F.T. Ulaby, V. Narayanan, and M.C. Dobson, 1983. Identification of corn fields using multirate radar data. *Rem. Sens. Environ.* 13:251-264.
- Shen, S.S., G.D. Brahwar, and J.G. Carnes, 1985. Separability of boreal tree species. *Photogramm. Eng. Rem. Sens.* 51:1775-1783.
- Shepherd, K.R., 1986. *Plantation Silviculture*. Martinus Nijhoff Publishers, Dordrecht, 322 pp.
- Shoobridge, D.W., 1951. Mechanical cleaning and ground preparation for softwood plantations in the Australian Capital Territory. *Aust. For.* 15:105-109.
- Short, N., 1982. The Landsat Tutorial Work. *NASA Reference Publication 1078*, NASA, Washington D.C.
- Simonett, D.S., 1983. The development and principles of remote sensing. In: Colwell, R.N. (ed.), *Manual of Remote Sensing* (2nd Ed.), American Society of Photogrammetry, The Sherian Press, Virginia, Vol. 1, pp. 1-35.
- Simonett, D.S., and R.E. Davis, 1983. Image analysis-active microwave. In: Colwell, R.N. (editor-in-Chief), *Manual of Remote Sensing*, 2nd ed., Am. Soc. Photogramm., The Sherian Press, Virginia, Vol. 1, pp. 1125-1181.
- Singh, A., and A. Harrison, 1985. Standardised principal components. *Int. J. Rem. Sens.* 6:883-896.

- Singh, A., 1989. Digital change detection techniques using remotely sensed data. *Int. J. Rem. Sens.* 10:989-1003.
- Singh, S.M., and R.J. Saull, 1988. The effects of atmospheric correction on the interpretation of multitemporal AVHRR-derived vegetation index dynamics. *Rem. Sens. Environ.* 25:37-51.
- Skidmore, A.K., 1989. An expert system classifies eucalypt forest using Thematic Mapper data and a digital terrain model. *Photogramm. Eng. Rem. Sens.* 55:1449-1464.
- Skidmore, A.K., P.W. Woodgate, and J.A. Richards, 1986. Classification of the Riverina forests of southeast Australia using co-registered Landsat MSS and SIR-B radar data. In: M.C.J. Damen, G.S. Sicco, and H. Verstappen (ed.), *Remote Sensing for Resources Development and Environment Management* (Proc.), pp. 517-519.
- Skidmore, A.K., and B.J. Turner, 1988. Forest mapping accuracies are improved using a supervised nonparametric classifier with SPOT data. *Photogramm. Eng. Rem. Sens.* 54:1415-1421.
- Skidmore, A.K., and B.J. Turner, 1989. Assessing the accuracy of resource inventory thematic maps. *Proc. IUFRO/FAO Conf. on "Global Resource Monitoring and Assessments: Preparing for the 21st Century"*, Venice, Italy, September 23-30, 1989.
- Skidmore, A.K., 1989. *Extracting forest Resource Information from Remotely Sensed and Ancillary Data: Use of an Expert system*. Ph.D Thesis to the Department of forestry, the Australian National University, 247 pp.
- Slama, C. C. (ed.), 1980. *Manual of Photogrammetry*, 4th ed., Am. Soc. Photogramm., Virginia, 1056 pp.
- Sleeman, J.R., and P.H. Walker, 1979. The Soils of the Canberra District. *Soils and Land Use Series No. 58*. Division of Soils, CSIRO 49 pp.
- Smith, J.A., 1983. Matter-energy interaction in the optical region. In Colwell, R.N. (ed.): *Manual of Remote Sensing*, 2nd ed., Am. Soc. Photogramm., the Sherian Press, Virginia, Vol. 1, pp. 61-164.
- Smithers, L.A., 1959. Assessment of site productivity in dense lodgepole pine stands. *Tech. Note For. Res. Div.*, Forest Branch, Department of Northern Affairs and National Resources, Canada. No. 30, 20 pp.
- Spanner, M.A., J.A. Brass, and D.L. Peterson, 1984a. Feature selection and the information content of Thematic Mapper simulator data for forest structure assessment. *IEEE Trans. Geosci. Rem. Sens.* GE-22:482-489.
- Spanner, M.A., K. Teuber, W. Acevedo, D.L. Peterson, S.W. Running, D.H. Card, and D.A. Mouat, 1984b. Remote sensing of the leaf area index of temperate coniferous forests. In: *Proc. 1984 Machine Processing Remotely Sensed Data Symp.* West Lafayette, IN, June 12-14, 1984, pp. 362-370.
- Spanner, M.A., L.L. Pierce, S.W. Running, and D.L. Peterson, 1990. The seasonality of AVHRR data of temperate coniferous forests: Relationship with leaf area index. *Rem. Sens. Environ.* 33:97- 112.
- Spanner, M.A., L.L. Pierce, D.L. Peterson, and S.W. Running, 1991. Remote sensing of temperate coniferous forest leaf area index: the influence of canopy closure, understory vegetation and background reflectance. *Int. J. Rem. Sens.* 11:95-111.
- Späth, H., 1980. *Cluster Analysis Algorithms for Data Reduction and Classification of Objects*. Ellis Horwood Limited, Wiley, New York, 226 pp.
- Spies, T.A. and Barnes, B.V. 1985. A multifactor ecological classification of the northern hardwood and conifer ecosystems of Sylvania Recreation Area, Upper Peninsula, Michigan. *Can. J. For. Res.* 61:949-960.

- Speight, J. G., 1984. Landform. In: R.C. McDonald, R.F. Isbell, J.G. Speight, J. walker, and M.S. Hopkins (ed.), *Australian Soil and Land Survey Handbook*. Inkata Press, Melbourne, pp. 8-43.
- Speight, J.G., and R.C. McDonald, 1984. The site conception. In: R.C. McDonald, R.F. Isbell, J.G. Speight, J. walker, and M.S. Hopkins (ed.), *Australian Soil and Land Survey Handbook*. Inkata Press, Melbourne, pp. 1-8.
- Spring, S.N., 1917. Site and site classes. *J. For.* 15:102-103.
- Spurr, S.H., 1948. *Aerial Photographs in Forestry*. Ronald Press Company, New York, 340 pp.
- Spurr, S.H., 1952. *Forest Inventory*. Ronald Press, New York, 476 pp.
- Spurr, S.H., 1960. *Photogrammetry and Photointerpretation*. 2nd ed. Ronald Press, New York, 472 pp.
- Spurr, S.H., and B.V. Barnes, 1980. *Forest Ecology*, 3rd ed., Wiley, New York, 686 pp.
- Stenback, J.M., and R.G. Congalton, 1990. Using Thematic Mapper imagery to examine forest understory. *Photogramm. Eng. Rem. Sens.* 56:1285-1290.
- Stoate, T.N., 1945. Use of a volume equation in pine stands. *Aust. For.* 9:35-41.
- Stow, D., B. Burns, and A. Hope, 1989. Mapping arctic tundra vegetation types using digital SPOT/HRV-XS data: a preliminary assessment. *Int. J. Rem. Sens.* 10:1415-1457.
- Strahler, A. H., 1981. Stratification of natural vegetation for forest and rangeland inventory using Landsat digital imagery and collateral data. *Int. J. Rem. Sens.* 2:15-41.
- Strahler, A.H., T.L. Logan, and Bryant, N.A., 1978. Improving forest cover classification accuracy from Landsat by incorporating topographic information. *Proc. 12nd Int. Symp. Rem. Sens. Environ.*, ERIM, Ann Arbor, Vol. II, pp. 927-942.
- Strahler, A.H., Y. Wu, and J. Franklin, 1988. Remote estimation of tree size and density from satellite imagery by inventory of a geometric canopy model. *Proc. 22nd Int. Symp. Rem. Sens. Environ.*, Abidjan, Cote d'Ivoire, Oct. 20-26. pp. 337-348.
- Strahler, A.H., and D.L.B. Jupp, 1990. Bidirectional reflectance modelling of forest canopies using boolean models and geometric optics. *Proc. 23rd Int. Symp. Rem. Sens. Environ.*, ERIM, Ann Arbor, Vol. II, pp. 1165-1172
- Strahler, A.H., and X. Li, 1981a. An invertible coniferous forest canopy reflectance. *Proc. 15th Int. Symp. Rem. Sens. Environ.*, Ann Arbor, Michigan, ERIM, pp. 1237-1244.
- Strahler, A.H., and X. Li, 1981b. Spatial/spectral modelling of conifer forest reflectance. *Proc. 3rd Aust. Rem. Sens. Conf.*, Gold Coast, Queensland, Australia, pp. 88-90.
- Strusz, D.L. 1971. *Canberra, Australian Capital Territory and new South Wales - 1:250,000 geological series*. Bureau of Resources, Australia Explanatory Notes S1/55-16.
- Strusz, D.L., and G.A.M. Henderson, 1971, *Canberra City, A.C.T., 1:50,000 Geological Map and Explanatory Notes*. Department of National Development Bureau of Mineral Resources, Geology and Geophysics, Australian Government Publishing Service, Canberra, pp. 10-13.
- Suchachev, V., 1960. The correlation between the concept of 'forest ecosystem' and 'forest biogeocenose' and their importance for the classification of forests. *Silva Fennica*, 105:94-97.
- Suchachev, V., and N. Dylis, 1964. *Fundamentals of Forest Biogeocoenology* (English Edition translated from Russia by J.M. Machennan), Oliver & Boyd, Edinburgh, 672 pp.
- Swain, P.H., and S.M. Davis (ed.), 1978. *Remote Sensing: the quantitative Approach*. McGraw Hill, New York, 396 pp.
- Tang, D.( 唐德富), 1990. 我国古代的生态学思想和理论(Ecological thought and theory in ancient China) 《农业考古》(Agricultural Archaeology), 8(2):8-17.

- Tansley, A. 1935. The use and misuse of vegetation terms and concepts. *Ecology*, 16:284-307.
- Taylor, A.M., 1972. Evolution-revolution, general systems theory, and society. *Philosophy Forum*, 11:99-139.
- Teillet, P.M., and K. Staenz, 1992. Atmospheric effects to topography on MODIS vegetation index data simulated from AVIRIS imagery over mountainous terrain. *Can. J. Rem. Sens.* 18:283-291
- Thallon, K.P., 1979. Aerial photography in a national tree and forest inventory of Great Britain. In: W. E. Frayer (ed.), *For. Res. Inventory*, 1:372-383.
- Thomas, I.L., 1980. Spatial postprocessing of spectrally classified Landsat data. *Photogramm. Eng. Rem. Sens.* 46:1201-1206.
- Thomas, I.L., I.M. Benning, and N.P. Ching, 1987. *Classification of Remotely Sensed Images*. Hilger, Bristol, 347 pp.
- Thomas, J.R., and H.W. Gausman, 1977. Leaf reflectance vs. leaf chlorophyll and carotenoid concentrations for eight crops. *Agron. J.* 65:276-284.
- Thomas, M.M., and H. Gruner, 1980. Foundation of Photogrammetry. In: C.C. Slama (ed.), *Manual of Photogrammetry*, 4th ed., Am. Soc. Photogramm., Virginia, pp. 1-36.
- Thompson, D.C., G.H. Klassen, and J. Cihlar, 1980. Caribou habitat mapping in the southern district of Keewatin, N. W. T.: an application of digital Landsat data. *J. Appl. Ecol.* 17:125-138.
- Thompson, B., 1984. *Canonical Correlation Analysis: Uses and Interpretation*. Series: Quantitative Applications in the Social Sciences-47, Sage Publications, Beverly Hills London, 69 pp.
- Thomson, A.G., and C. Jones, 1990. Effects of topography on radiance from upland vegetation in North Wales. *Int. J. Rem. Sens.* 11:829-840.
- Thomson, A.G., 1992. A multi-temporal comparison of two similar Landsat Thematic Mapper images of upland North Wales, U.K., *Int. J. Rem. Sens.* 13:947-955.
- Toll, D.L. 1984. An evaluation of simulated Thematic Mapper data and Landsat MSS data for discriminating suburban and regional land use and land cover. *Photogramm. Eng. Rem. Sens.* 50:1713-1723.
- Toll, D.L., 1985. Effect of Landsat Thematic Mapper sensor parameters on land cover classification. *Rem. Sens. Environ.* 17:129-140.
- Tom, C., and L.D. Miller, 1978. Summary to application to: forest site index mapping in northern central Colorado. In: G. Hildebrandt, and H.-J. Boehnel (ed.) *Proc. Int. Symp. Rem. Sens. for Observation and Inventory of Earth Resources and the Endangered Environment*, Freiburg, Germany, July 2-8, 1978, Vol. III, pp. 1747-1751.
- Tom, C.H., and L.D. Miller, 1980. Forest site index mapping and modelling. *Photogramm. Eng. Rem. Sens.* 46:1585-1596.
- Tom, C.H., and L.D. Miller, 1984. An automated land-use mapping comparison of the bayesian maximum likelihood and linear discriminant analysis algorithms. *Photogramm. Eng. Rem. Sens.* 50:193-207.
- Tomppo, E., 1992. satellite image aided forest site fertility estimation for forest income taxation. *Acta For. Fenn.* 229:1-66.
- Torlegård, K., 1992. Sensors for photogrammetric mapping: review and projects. *ISPRS J. Photogramm. Rem. Sens.* 47:241-262.
- Townshend, J.R.G., and C.O. Justice, 1980. Unsupervised classification of MSS Landsat data for mapping spatially complex vegetation. *Int. J. Rem. Sens.* 1:105-120.

- Townshend, J.R.G., and C.O. Justice, 1981. Information extraction from remotely sensed data. *Int. J. Rem. Sens.* 2:313-329.
- Townshend, J.R.G., C.O. Justice, and V. Kalb, 1987. Characteristics and classification of South American land cover types using satellite data. *Int. J. Rem. Sens.* 8:1189-1207.
- Tucker, C.J., 1977. Asymptotic nature of grass canopy spectral reflectance. *Appl. Optics*, 16:1151-1157.
- Tucker, C.J., 1978. A comparison of satellite sensor bands for vegetation monitoring. *Photogramm. Eng. Rem. Sens.* 44:1369-1380.
- Tucker, C.J., 1979. Red and photographic infrared linear combinations for monitoring vegetation. *Rem. Sens. Environ.* 8:127-150.
- Tucker, C.J., 1980. Remote sensing of leaf water content in the near infrared. *Rem. Sens. Environ.* 10:23-32.
- Tucker, C.J., 1986. Cover maximum Normal Difference Vegetation Index images for sub Sahelian Africa for 1983-1985. *Int. J. Rem. Sens.* 7:1383-1384.
- Tucker, C.J., B.N. Hillman, J.H. Legion, and J.E. McMurtrey, 1980. Relationship of spectral data to grain yield variation. *Photogramm. Eng. Rem. Sens.* 46:657-666.
- Tucker, C.J., J R. Townshend, and T.E. Golf, 1985. African land-cover classification using satellite data. *Science*, 227:369-375.
- Tucker, C.J., L. D. Miller, and R.L. Peason, 1975. Shortgrass prairie spectral measurements. *Photogramm. Eng. Rem. Sens.* 41:1157-1162.
- Turner, B.J., D.M. Moore, and A.K. Skidmore, 1987. Forest management applications of SPOT data in Australia. *Proc. SPOT-1 Image Utilisation, Assessments, Results Symposium*, Paris, France.
- Turner, B.J., G.M. Baumers and L Myers, 1982. *The ORSER Remote Sensing Analysis System: A User's Manual*. Research Publication 109/OR, The Pennsylvania State University, 259 pp.
- Turner, B.J., R.W. Bednarz, and J.B. Dargavel, 1977. A model to generate stand strategies for Intensive managed radiata pine plantations. *Aust. For.* 40:255-267.
- Turvey, N.D., 1983. Soil type yield curves for *Pinus radiata* in Gippsland, Victoria. *Aust. For.*, 46:119-124.
- Turvey, N.D., A.B. Rudra, and J. Turner, 1986. Characteristics of soil and productivity of *Pinus radiata* (D. Don) in New South Wales. I. Relative importance of soil physical and chemical parameters. *Aust. J. Soil Res.* 24:95-102.
- Turvey, N.D. (ed.), 1987. A Technical Classification for Soil of *Pinus* Plantations in Australia: Field Manual. *Bulletin* No. 6 of the School of Forestry, the University of Melbourne, 42 pp.
- Udvardy, M.D.F., 1969. *Dynamics Zoogeography: with Special Reference to Land Animals*. Van Nostrand Reinhold. New York, 445 pp.
- Ulaby F.T., C.T. Allen, G. Eger-III, and E. Kanemasu, 1984. Relating the microwave backscattering coefficient to leaf area index. *Rem. Sens. Environ.* 14:113-133.
- Ure, J. 1950. The natural vegetation of Haingaroa plains as an indicator of site quality for exotic conifers. *N. Z. J. For.* 6:112-123.
- van Genderen, J.L., B.F. Lock, and P.A. Vass, 1978. Remote sensing: statistical testing of thematic map accuracy. *Rem. Sens. Environ.* 7:3-14.
- Vanclay, J. K. 1988. Site productivity assessment in rainforests: an objective approach using indicator species. In: *Proc. IUFRO Growth and Yield in Tropic Mixed/Moist Forests Conference*, Kuala Lumpur, Malaysia, June 20-24, 1988. 14 pp.

- Vanclay, K.J., and R.A. Preston. 1990. Utility of Landsat Thematic Mapper data for Mapping site productivity in tropical moist forests. *Photogramm. Eng. Rem. Sens.* 56:1383-1338.
- Vane, G., and A.F.H. Goetz, 1993. Terrestrial imaging spectrometry: Current status, future trends. *Rem. Sens. Environ.* 44:117-126.
- Vane, G., R.O. Green, T.G. Chrien, H.T. Enmark, E.G. Hansen, and W.M. Porter, 1993. The airborne visible/infrared imaging spectrometer (AVIRIS). *Rem. Sens. Environ.* 44:127-143.
- Verbyla, D. L.; R. F. Fisher. 1989. Ponderosa pine habitat types as an indicator of site quality in the Dixie National Forest, Utah. *Western J. App. For.* 4:52-54.
- Vogelmann, J.E., and B.N. Rock, 1986. Assessing forest decline in coniferous forests of Vermont using NS-001 Thematic Mapper simulator data. *Int. J. Rem. Sens.* 7:1303-1321.
- Vogelmann, J. E., and B. N. Rock, 1989. Use of Thematic Mapper data for the detection of forest damage caused by the pear trips. *Rem. Sens. Environ.* 30:217-225.
- Wakeley, P.C. 1954. The growth intercept method of site classification. In: *3rd Ann. For. Symp. Proc.*, La. State Univ. pp. 32-33.
- Walker, J., D.L.B. Jupp, L.K. Penridge, and G. Tian, 1986. Interpretation of vegetation structure in Landsat MSS imagery: a case study in disturbed semi-arid eucalypt woodlands. Part 1. Field data analysis. *J. Environ. Manage.* 23:19-33.
- Walsh, S.J., 1980. Coniferous tree species mapping using Landsat data. *Rem. Sens. Environ.* 9:11-26.
- Walsh, S.J., 1987. Variability of Landsat MSS spectral responses of forests in relation to stand and site characteristics. *Int. J. Rem. Sens.* 8:1289-1299.
- Walsh, S.J., J.W. Cooper, Ian E. Von Essen, and K.R. Gallager, 1990. Image enhancement of Landsat Thematic Mapper data and GIS data integration for evaluation of resource characteristics. *Photogramm. Eng. Rem. Sens.* 56:1135-1141.
- Walter-Shea, E.A., and L.L. Biehl, 1990. Measuring vegetation spectral properties, *Rem. Sens. Rev.* 5(1):179-205.
- Wang, R.-Y., 1986a. An approach to tree classifier design based on hierarchical clustering. *Int. J. Rem. Sens.* 7:75-88.
- Wang, R.-Y., 1986b. An approach to tree classifier design based on splitting algorithm *Int. J. Rem. Sens.* 7:89-104.
- Wanjura, D.F., and J.L. Hatfield, 1988. Vegetative optical characteristics of four row crop canopies. *Int. J. Rem. Sens.* 9:249-258.
- Waring, H.D., [unknown]. *Report on the Soils of the A.C.T. Jervis Bay.* Forestry and Timber Bureau, Canberra, 18 pp.
- Watson, R. 1917. Sie determination, classification, and applicaytion. *J. For.* 15:552-563.
- Welch, R., 1985. Cartographic potential of SPOT image data. *Photogramm. Eng. Rem. Sens.* 51:1085-1091.
- Welch, R., and M. Ehlers, 1987. Merging multiresolution SPOT HRV and Landsat TM data. *Photogramm. Eng. Rem. Sens.* 53:301-303.
- Werte, D., R.J. Brown, and Y.J. Lee, 1986. The use of multispectral and radar remote sensing data for monitoring forest clearcut and regeneration sites on Vancouver Island, In: *Proc. 10th Can. Symp. Rem. Sens.*, Edmonton, Albert, May 5-8, pp. 319-329.
- Wessman, C.A., J.D. Aber, D.L. Peterson, and J.M. Melillo, 1988. Remote sensing of canopy chemistry and nitrogen cycling in temperate forest ecosystem. *Nature* 335:154-156.
- Wessman, C. A., J. D. Aber, and D. L. Peterson, 1989. An evaluation of imaging spectrometry for estimating forest canopy chemistry. *Int. J. Rem. Sens.* 10:1293-1316.

- Wessman, C.A., 1990. Evaluation of canopy biochemistry. In R. J. Hobbs and H. A. Mooney ed.: *Remote Sensing of Biosphere Functioning*, *Ecol. Studies*, 79:135-156.
- West, P.W., S.G. Candy, and T.E. Osborn, 1988. *Developments to a Simulation Model for Prediction of Wood Volume of Forests of Pinus radiata D. Don in the Australian Capital Territory*. Internal Report of ACT Forests, Canberra, 148 pp.
- Westman, W.E., and J.F. Paris, 1987. Detecting forest structure and biomass with C-band multipolarization radar: physical model and field tests. *Rem. Sens. Environ.* 22:249-269.
- Westman, W.E., and C.V. Price, 1988. Spectral changes in coniferous subjected to air pollution and water stress: experimental studies. *IEEE Trans. Geosci. Rem. Sens.* 26:11-21.
- Westman, W.E., L.L. Strong, and B.A. Wilcox, 1989. Tropical deforestation and species endangerment: the role of remote sensing. *Landscape Ecology*, 3:97-109.
- Whittaker, R. H., 1967. Gradient analysis of vegetation. *Biol. Rev.* 42:207-264.
- Wilde, S.A., 1946. *Forest Soils and Forest growth*. the Chronica Botanica Company, 241 pp.
- Wilde, S.A., 1958. *Forest Soils - Their Properties and Relation to Silviculture*. The Ronald Press Company, New York, 537 pp.
- Williams, D.L., 1991. A comparison of spectral reflectance properties at the needle, branch, and canopy level for selected coniferous species. *Rem. Sens. Environ.* 35:79-93.
- Williams, D.L. and R.F. Nelson, 1986. Use of remotely sensed data for assessing forest stand conditions in the eastern United States. *IEEE Trans. Geosci. Rem. Sens.* GE-24:130-138..
- Williams, D.L., J.R. Irons, B.L. Markham, R.F. Nelson, D.L. Toll, R.S. Latty, M.L. Stauffer, 1984. A statistical evaluation of the advantages of Landsat Thematic Mapper data in comparison to multispectral scanner data. *IEEE Trans. Geosci. Rem. Sens.* GE-22:292-302.
- Williams, L., H.W. Fowler, J. Coulsou, and C.T. Onions, 1964. *Shorter Oxford English Dictionary on Historical Principles*. 3rd ed., Vol. II, 1903 pp.
- Williams, V.L., W.R. Phillipson, and W.D. Philpot, 1987. Identifying vegetable crops with Landsat Thematic Mapper data. *Photogramm. Eng. Rem. Sens.* 53:187-191.
- Wittich, W.H.L., 1960. Classification, mapping, and interpretation of soils for forestry purpose. In: *Proc. 5th World For. Cong.* University of Washington, Seattle, Washington, United States of America, August 29-September 10, 1960. Vol. 1, pp. 502-507.
- Worrell, R., and D.C. Malcolm, 1990a. Productivity of Sitka spruce in northern Britain. 1. the effects of elevation and climate. *Forestry*, 63(2):105-118.
- Worrell, R., and D.C. Malcolm, 1990b. Productivity of Sitka spruce in northern Britain. 2. prediction from site factors. *Forestry*, 63(2):118-128.
- Woods, R.V., 1976. Early silviculture for upgrading on marginal *Pinus radiata* sites in the south-east region of South Australia. *Woods and Forests Department Bulletin 24*, 89 pp.
- Woodcock, C.E., and A.H. Schahler, 1987. The factor of scale in remote sensing. *Rem. Sens. Environ.* 21:311-332.
- Woodcock, E.W., A.H. Strahler, Y. Wu, and X. Li, 1990. Estimating forest stand parameters through inversion of a canopy reflectance model. *Remote Sensing Science for the Nineties - IGARSS'90, 10th Ann. Int. GeoSci. Rem. Sens. Symp.*, The University of Maryland, May 20-24, 1990. pp. 1203-1207.
- Woodcock, C.E., V. Jakabhazy, S. Macomber, S. Ryherd, A.H. Strahler, and Y. Wu, 1990. timber inventory using Landsat Thematic Mapper imagery and canopy reflectance models. *Proc. 23rd Int. Symp. Rem. Sens.*, ERIM, Ann Arbor, Vol. II, pp. 937-943.
- Woollons, R.C., and W.J. Hayward, 1985. Revision of a growth and yield model for radiata pine in New Zealand. *For. Ecol. Manage.* 11:191-202.

- Woodwell, G.M., R.A. Houghton, T.A. Stone, R.F. Nelson, and W. Kvalick, 1987. Deforestation in the tropics: new measurement in the Amazon basin using Landsat and NOAA AVHRR imagery. *J. Geophys. Res.* 92(D2):2157-2163.
- Yamada, N., and S. Fujimura, 1988. A mathematical model of reflectance and transmittance of plant leaves as a function of chlorophyll pigment content. *Proc. IGARSS'88 Symp.*, 12-16 September 1988, Edinburgh, Scotland, Vol. II, 833-842.
- Yang, C., and A. Vidal, 1990. Combination of digital elevation models with SPOT-1 HRV multispectral imagery for reflectance factor mapping. *Rem. Sens. Environ.* 32:35-45.
- Yapp, R.H., 1922. The concept of habitat. *J. Ecol.* 10:1-17.
- Yu, T., and B. Chen, 1990. Topographic correction on Landsat TM data for quantitative extraction of vegetation information. *J. Nanjing Uni.* 11:137-145.
- Zhao, X. (赵宪文), 1983. 林业遥感应用研究, *林业科技通讯*, 1983-4:25-27.
- Zonneveld, I.S., 1981. The role of single land attributes in forest evaluation. In: P. Laban (ed.), *Proc. Workshop on land Evaluation for Forestry*, International Workshop of the IUFRO/ISSS, International Institute for Land Reclamation and Improvement (ILRI), Wageningen, Netherlands. pp. 76-94.



## Appendix A

Land Classes for Forestry (Gunn *et al.*, 1969)

Land Classes (Capacity Classes)	I	II	III	IV	V	VII	VII
Site Index (m) <sup>1</sup>	34	30	27	24	21	18	15
MAI (m <sup>3</sup> /ha/yr) <sup>2</sup>	30	27	24	21	17	13	8

<sup>1</sup> Predominant height: Mean height of 75 tallest oer hectare at age of 30.

<sup>2</sup> Cubic metres to 10 cm top per hectare per year: rotation 50 years

Indices used for site quality for assessment *Pinus radiata* stands in South Australia at age 9 ½ (adapted from Lewis *et al.* 1976)

SQ	Volume to 10 cm u.b.: m <sup>3</sup> /ha	Basal Area: M <sup>2</sup> /ha		Predominant height (m)	Green Level: m		Maximum Tree Diameter: cm
		2.5 x 2.5	2.0 x 2.0		2.5 x 2.5 Stands	2.0 x 2.0 stands	
I	> 226	> 42.2	> 43.8	> 17.0	> 6.1	> 6.4	22 cm Few 20 cm Obvious
II	178 - 226	36.7 - 42.2	39.0 - 43.8	15.7 - 17.0	4.9 - 6.1	5.2 - 6.4	22 cm Nil 20 cm Plenty
III	132 - 178	31.0 - 36.7	33.7 - 39.0	14.4 - 15.7	4.0 - 5.2	4.0 - 5.2	20 cm Few
IV	85 - 132	25.3 - 31.0	27.3 - 33.7	13.1 - 14.4	2.7 - 4.0	2.7 - 4.0	20 cm Nil 18 cm Obvious
V	43 - 85	18.6 - 25.3	20.4 - 27.3	11.8 - 13.1	1.7 - 2.7	1.8 - 2.7	18 cm Few
VI	12 - 43	10.3 - 18.6	13.3 - 20.4	10.5 - 11.8	0.9 - 1.8	0.9 - 1.8	18 cm Nil 17 cm Obvious
VII	< 12	< 10.3	< 13.3	< 10.5	< 1.8	< 0.9	16 cm Few

**Appendix B**

**Point Sampling Data Sheet I: Stand variables**

Point No: \_\_\_\_\_ CPT No.: \_\_\_\_\_ Sign. Class: \_\_\_\_\_ Date / / \_\_\_\_\_

Vegetation Type: \_\_\_\_\_ Age: \_\_\_\_\_ Coverage (%): \_\_\_\_\_

Slope : \_\_\_\_\_ Elevation: \_\_\_\_\_

Aspect : \_\_\_\_\_ Microrelief : \_\_\_\_\_

Understory : \_\_\_\_\_ Coverage (%): \_\_\_\_\_

Condition of Top soil : \_\_\_\_\_

Field Assessment of point: \_\_\_\_\_

Point Location: \_\_\_\_\_  
 \_\_\_\_\_  
 \_\_\_\_\_  
 \_\_\_\_\_  
 \_\_\_\_\_  
 \_\_\_\_\_

Band used:

BAF:

No.	Diameter (cm)		No.	Diameter (cm)	
	IN	B/L		IN	B/L
1			13		
2			14		
3			15		
4			16		
5			17		
6			18		
7			19		
8			20		
9			21		
10			22		
11			23		
12			24		

No.	Top Height (m)
1	
2	
3	
4	
5	
6	
<b>Mean</b>	

\* Sign. Class - signature classes from SPOT data classification  
 BAF - Basal Area Factor

**Basal Area / ha:** \_\_\_\_\_

**Dominant Height:** \_\_\_\_\_

**BA Per Tree:** \_\_\_\_\_

**Stem No/ha :** \_\_\_\_\_

**Mean Diameter :** \_\_\_\_\_

**Volume (cu m/ha):** \_\_\_\_\_



**Appendix D**  
**The Mean, standard deviation (SD) and coefficients of variation (CV) of the January-24-1987 SPOT image of the stands aged from 3 to 42 years.**

Stand Age	PN	XS1			XS2			XS3			PS		
		Mean	SD	CV	Mean	SD	CV	Mean	SD	CV	Mean	SD	CV
3	813	48.80	7.80	15.98	42.74	8.61	20.15	56.09	6.49	11.57	52.65	8.96	17.02
4	3397	43.70	7.36	16.84	36.64	8.50	23.20	56.10	5.29	9.43	47.13	9.96	21.13
5	1944	41.72	6.91	16.56	33.90	7.84	23.13	55.37	5.45	9.84	42.89	8.67	20.21
6	694	43.34	6.87	15.85	37.20	8.55	22.98	55.46	4.22	7.61	48.26	10.67	22.11
9	778	36.90	6.39	17.32	28.44	6.84	24.05	57.41	4.29	7.47	35.64	6.16	17.28
11	520	34.35	3.57	10.39	25.38	2.48	9.77	53.96	2.35	4.36	32.65	2.35	7.20
12	4644	36.37	6.97	19.16	27.86	8.12	29.15	59.12	5.69	9.62	37.55	10.67	28.42
13	504	37.09	4.67	12.59	28.88	5.30	18.35	55.65	2.72	4.89	36.76	4.91	13.36
14	9031	33.93	5.36	15.80	25.09	6.09	24.27	58.03	5.37	9.25	33.92	8.25	24.32
15	699	34.52	6.41	18.57	26.54	7.99	30.11	54.84	5.11	9.32	35.15	10.35	29.45
16	3069	31.30	5.63	17.99	21.85	5.71	26.13	57.61	5.20	9.03	29.96	8.49	28.34
18	401	31.40	5.44	17.32	23.13	6.04	26.11	51.40	4.69	9.12	29.98	6.55	21.85
19	246	30.43	4.38	14.39	21.92	5.46	24.91	50.85	3.28	6.45	30.30	10.35	34.16
20	730	32.55	5.36	16.47	24.08	5.88	24.42	49.40	6.31	12.77	30.66	5.76	18.79
21	2899	32.18	4.74	14.73	22.68	5.52	24.34	52.54	4.14	7.88	31.41	7.74	24.64
23	6838	31.20	3.57	11.44	21.89	4.05	18.50	50.67	3.78	7.46	30.35	5.83	19.21
24	3940	31.51	4.64	14.73	22.67	5.05	22.28	50.61	4.31	8.52	30.41	6.42	21.11
25	969	32.46	3.84	11.83	23.67	3.98	16.81	48.67	2.78	5.71	31.25	4.06	12.99
26	2169	31.49	4.32	13.72	22.16	4.51	20.35	48.15	3.84	7.98	29.20	4.96	16.99
27	495	34.80	5.40	15.52	26.83	5.97	22.25	48.26	4.99	10.34	34.16	8.06	23.59
28	2347	31.73	4.30	13.55	22.37	4.41	19.71	47.34	3.99	8.43	29.94	4.60	15.36
29	2694	31.87	4.96	15.56	22.89	5.28	23.07	47.31	4.34	9.17	30.12	4.12	13.68
30	3525	37.63	5.16	13.71	30.32	6.06	19.99	51.93	5.33	10.26	40.39	8.97	22.21
31	947	32.70	2.93	8.96	24.21	3.09	12.76	46.30	3.42	7.39	32.67	5.71	17.48
32	2327	33.19	4.31	12.99	25.15	5.18	20.60	46.40	4.85	10.45	33.43	6.01	17.98
33	857	32.49	4.58	14.10	23.74	4.88	20.56	48.04	5.00	10.41	31.60	3.77	11.93
34	230	33.11	6.94	20.96	24.31	7.20	29.62	48.43	6.71	13.86	28.06	4.26	15.18
35	173	32.75	2.65	8.09	24.03	2.70	11.24	45.32	2.65	5.85	31.90	4.11	12.88
36	400	31.32	2.98	9.51	21.74	3.12	14.35	45.99	3.83	8.33	29.67	3.40	11.46
37	733	32.85	3.43	10.44	23.84	3.52	14.77	46.17	2.97	6.43	32.33	5.65	17.48
38	938	33.68	3.16	9.38	24.89	3.30	13.26	47.53	3.64	7.66	33.18	4.02	12.12
39	614	34.86	3.23	9.27	26.24	3.46	13.19	48.54	4.10	8.45	35.14	4.59	13.06
40	205	33.87	2.98	8.80	25.09	3.24	12.91	49.68	5.07	10.21	33.90	5.05	14.90
41	362	34.57	5.20	15.04	26.65	5.88	22.06	47.51	4.59	9.66	33.01	4.55	13.78
42	257	35.19	6.68	18.98	26.88	7.85	29.20	50.30	5.34	10.62	33.95	7.49	22.06
		Data Ranges of Stand Ages and Spectral Band Data											
39		18.37			21			13.8				24.59	

The symbols in the table are: SD - Standard deviation, PN - pixel numbers at each age level; and CV - Coefficient of variation (%)

**Appendix E**  
**The Mean, standard deviation (SD) and coefficients of variation (CV) of the February-9-1988 TM image of the stands aged from 3 to 42 years.**

age	2TM1		2TM2		2TM3		2TM4		2TM5		2TM6		2TM7										
	PN	Mean	SD	CV	Mean	SD	CV	Mean	SD	CV	Mean	SD	CV	Mean	SD	CV							
3	813	74.58	5.94	7.96	36.18	5.34	14.76	52.42	11.66	22.24	54.29	5.47	10.08	121.46	16.32	13.44	133.95	2.52	1.88	57.71	11.81	20.46	
4	3397	69.76	6.92	9.92	32.52	5.45	16.76	45.08	11.56	25.64	58.22	5.64	9.69	106.03	30.94	29.18	131.75	5.50	4.17	45.88	16.44	35.83	
5	1944	65.24	6.02	9.23	29.10	5.07	17.42	37.01	11.13	30.07	60.53	5.79	9.57	83.40	24.31	29.15	128.29	3.83	2.99	34.67	13.07	37.70	
6	694	71.11	10.16	14.29	34.86	8.97	25.73	50.59	20.31	40.15	58.57	5.64	9.63	93.11	33.89	36.40	130.88	6.80	5.20	43.31	20.58	47.52	
9	778	60.10	3.82	6.36	25.60	3.06	11.95	30.31	6.93	22.86	60.46	4.43	7.33	68.91	17.36	28.88	122.61	2.44	1.99	22.34	8.30	37.15	
11	52	59.62	1.39	2.33	25.35	0.94	3.71	29.02	1.91	6.58	61.94	3.86	6.23	58.94	5.40	9.16	125.23	1.96	1.57	42.35	1.80	4.25	
12	4644	60.96	6.58	10.79	26.29	5.06	19.25	31.25	11.04	35.33	62.78	6.03	9.20	62.24	29.34	47.14	123.62	5.00	4.04	23.78	15.22	64.00	
13	504	60.46	3.60	5.95	25.46	2.78	10.92	30.17	5.99	19.85	59.63	2.87	4.81	63.13	14.11	22.35	125.21	2.72	2.17	23.69	7.76	32.76	
14	9031	58.48	4.69	8.02	24.29	3.69	15.19	27.12	7.85	28.95	61.35	5.66	9.23	52.03	23.14	44.47	122.41	3.31	2.70	18.57	11.33	61.01	
15	699	59.08	6.26	10.60	24.58	4.77	19.41	28.27	10.48	37.07	57.75	4.45	7.71	54.49	29.99	55.04	123.90	5.43	4.38	20.2	14.98	74.16	
16	3069	56.61	4.35	7.68	22.63	2.60	11.49	23.21	7.72	33.26	60.98	5.64	9.25	40.11	19.26	48.02	119.82	2.60	2.17	13.00	8.88	68.31	
18	401	55.75	3.39	6.08	22.03	2.56	11.62	22.81	5.91	25.91	53.23	6.05	11.37	36.47	12.61	34.58	117.77	2.03	1.72	11.81	5.74	48.60	
19	246	56.67	3.66	6.46	23.02	3.00	13.03	24.71	6.71	27.15	53.27	4.47	8.39	38.21	11.13	29.13	119.87	2.44	2.04	12.71	5.41	42.56	
20	730	57.17	3.18	5.56	23.52	2.69	11.44	25.51	5.85	22.93	51.67	7.89	15.27	40.82	10.82	26.51	118.85	2.29	1.93	13.94	5.15	36.94	
21	2899	58.13	3.78	6.50	23.80	3.22	13.53	25.88	6.79	26.24	55.07	6.03	10.95	45.69	16.10	35.24	122.35	3.52	2.88	15.98	8.58	53.69	
23	6838	56.81	3.05	5.37	22.90	2.36	10.31	24.40	4.99	20.45	53.34	5.05	9.47	43.71	13.55	31.00	119.89	2.06	1.72	14.73	6.66	45.21	
24	3940	57.81	2.88	4.98	23.60	2.36	10.00	26.91	4.89	18.17	52.25	4.84	9.26	50.92	10.16	19.95	120.85	2.23	1.85	17.99	5.03	27.96	
25	969	57.69	2.92	4.09	23.35	1.89	8.09	25.90	3.79	14.63	51.10	3.78	7.40	49.13	7.34	14.94	122.23	2.25	1.84	17.56	3.84	21.87	
26	2169	58.65	2.96	4.98	24.08	2.28	9.47	28.50	4.65	16.32	49.09	4.86	9.90	53.73	10.77	20.04	122.91	2.65	2.16	20.11	5.73	28.49	
27	495	60.71	5.05	8.32	25.72	4.07	15.82	31.71	8.74	27.56	48.77	5.31	10.89	60.30	19.27	31.96	124.79	3.06	2.45	24.12	10.46	43.37	
28	2347	56.53	2.51	4.44	22.73	2.03	8.93	24.41	4.07	16.67	48.83	3.58	7.33	43.08	8.16	18.94	120.08	1.13	0.94	14.71	4.67	31.75	
29	2694	56.47	2.27	4.02	22.70	1.77	7.80	24.37	3.70	15.18	49.41	4.08	8.26	45.68	8.57	18.76	120.60	2.03	1.68	15.76	4.31	27.35	
30	3525	63.65	5.34	8.39	27.79	4.58	16.48	35.50	10.16	28.62	52.77	7.79	14.76	74.36	23.47	31.56	128.05	4.57	3.57	29.94	11.55	38.58	
31	947	57.46	2.47	4.30	23.41	1.78	7.60	26.18	3.68	14.06	47.92	4.66	9.72	49.25	9.55	19.39	119.42	1.54	1.29	17.80	4.41	24.78	
32	2327	58.10	3.35	5.77	23.90	2.61	10.92	27.35	5.53	20.22	46.13	4.65	10.08	53.09	15.51	29.21	120.62	3.26	2.70	19.99	7.87	39.37	
33	857	57.28	2.26	3.95	23.11	1.85	8.01	25.59	3.75	14.65	49.21	4.73	9.61	49.14	9.33	18.99	120.91	1.74	1.44	17.58	4.83	27.47	
34	230	55.29	3.65	6.60	21.82	2.71	12.42	22.62	4.74	20.95	49.28	5.79	11.75	39.41	11.77	29.87	117.73	1.41	1.20	12.94	5.83	45.05	
35	173	58.22	2.43	4.17	23.59	1.82	7.72	26.50	3.74	14.11	45.74	3.10	6.78	47.13	6.27	13.30	121.18	1.52	1.25	17.17	3.58	20.85	
36	400	57.05	2.20	3.86	22.45	1.88	8.37	24.11	3.89	16.13	48.65	5.73	11.78	44.76	8.85	19.77	121.09	2.16	1.78	15.55	4.27	27.46	
37	733	59.06	3.17	5.37	24.13	2.57	10.65	28.00	5.70	20.36	48.17	4.75	9.86	55.28	14.15	25.60	123.87	2.82	2.28	21.03	7.64	36.33	
38	938	62.62	6.24	9.96	27.66	5.46	19.74	37.03	14.78	39.91	55.16	11.40	20.67	75.93	31.93	42.05	126.31	5.33	4.22	30.20	14.48	47.95	
39	614	59.25	2.50	4.22	24.75	1.84	7.43	28.94	3.88	13.41	49.71	5.07	10.20	61.00	11.34	18.59	123.37	1.72	1.39	24.04	5.87	24.42	
40	205	57.98	2.61	4.50	23.96	2.03	8.47	26.90	4.20	15.61	49.28	5.11	10.37	53.68	10.49	19.54	120.38	1.48	1.23	19.47	4.71	24.19	
41	362	58.66	3.01	5.13	24.33	2.45	10.07	28.02	5.40	19.27	46.86	4.57	9.75	53.44	11.13	20.83	122.80	2.85	2.32	20.07	5.74	28.60	
42	257	59.64	2.98	5.00	25.29	2.60	10.28	29.69	5.43	18.29	53.36	6.20	11.62	58.31	9.43	16.17	124.84	2.35	1.88	22.10	5.34	24.16	
39		19.29		14.36		29.80		17.04		84.99		16.22		45.9									

Data Ranges of Stand ages and Spectral Band Data

The symbols in the table are: SD - Standard deviation, PN - pixel numbers at each age level; and CV - Coefficient of variation (%)

**Appendix F**  
 The Mean, standard deviation (SD) and coefficients of variation (CV) of the April-21-1988 TM image of the stands aged from 3 to 42 years.

age	PN	2TM1			2TM2			2TM3			2TM4			2TM5			2TM6			2TM7			
		Mean	SD	CV	Mean	SD	CV	Mean	SD	CV	Mean	SD	CV	Mean	SD	CV	Mean	SD	CV	Mean	SD	CV	
3	813	51.07	4.64	9.09	21.36	3.63	16.99	22.97	6.10	26.56	30.50	3.75	12.30	61.68	12.66	20.53	115.80	1.78	1.54	29.50	8.13	27.56	
4	3397	48.40	3.92	8.10	19.37	2.78	14.35	19.70	4.57	23.20	31.55	3.42	10.84	52.38	17.73	33.85	114.23	2.98	2.61	23.08	8.95	38.78	
5	1944	45.72	3.64	7.96	17.55	2.69	15.33	16.49	4.51	27.35	35.23	4.00	11.35	39.50	13.83	35.01	112.46	2.08	1.85	16.48	7.12	43.20	
6	694	49.57	5.77	11.64	20.57	5.05	24.55	22.24	8.87	39.88	32.84	4.54	13.82	45.93	21.64	47.12	112.52	3.74	3.32	21.67	12.24	56.48	
9	778	42.57	2.31	5.43	15.06	1.81	12.02	12.98	2.74	21.11	32.65	3.12	9.56	24.87	8.66	34.82	109.58	1.64	1.50	9.42	3.72	39.49	
11	52	42.35	1.80	4.25	15.40	1.08	7.01	13.25	1.62	12.23	39.81	2.33	5.85	29.23	3.98	13.62	112.77	0.42	0.37	11.19	2.11	18.86	
12	4644	43.62	3.56	8.16	16.06	2.67	16.63	14.26	4.20	29.45	36.31	4.97	13.69	28.91	15.39	53.23	110.14	2.53	2.30	11.44	7.56	66.08	
13	504	43.13	2.77	6.42	16.09	1.92	11.93	14.34	2.94	20.50	35.25	2.69	7.63	29.15	9.90	33.96	111.54	1.99	1.78	10.90	4.65	42.66	
14	9031	42.44	2.30	5.42	14.84	1.78	11.99	12.52	2.52	20.13	36.40	4.20	11.54	23.05	9.90	42.95	109.18	1.89	1.73	8.46	4.33	51.18	
15	699	43.21	2.90	6.71	15.19	2.48	16.33	12.97	3.54	27.29	34.38	3.64	10.59	23.48	13.78	58.69	109.02	2.55	2.34	8.89	6.11	68.73	
16	3069	41.65	2.01	4.83	14.48	1.54	10.64	11.81	2.25	19.05	35.87	4.11	11.46	19.12	7.98	41.74	108.29	1.10	1.02	6.85	3.43	50.07	
18	401	41.96	1.45	3.46	14.47	1.17	8.09	11.83	1.65	13.95	28.59	3.90	13.64	15.52	4.59	29.57	107.33	0.59	0.55	5.83	1.82	31.22	
19	246	41.06	1.54	3.75	14.31	1.30	9.08	11.88	1.80	15.15	31.72	3.37	10.62	18.36	4.61	25.11	109.15	1.19	1.09	6.83	2.12	31.04	
20	730	41.27	1.73	4.19	14.06	1.42	10.10	11.66	2.08	17.84	27.78	5.14	18.50	16.98	5.31	31.27	107.31	1.28	1.19	6.42	2.22	34.58	
21	2899	41.98	1.87	4.45	14.64	1.61	11.00	12.18	2.39	19.62	31.94	5.49	17.19	20.79	7.44	35.79	108.69	2.13	1.96	7.82	3.60	46.04	
23	6838	41.42	1.70	4.10	14.31	1.20	8.39	11.80	1.71	14.49	31.56	4.26	13.50	19.65	6.13	31.20	108.03	1.20	1.11	7.22	2.77	38.37	
24	3940	42.78	1.89	4.42	15.06	1.37	9.10	12.84	1.76	13.71	29.70	3.67	12.36	21.67	5.72	26.40	108.60	1.38	1.27	8.15	2.50	30.67	
25	969	41.63	1.60	3.84	14.25	1.08	7.58	12.14	1.60	13.18	30.10	3.63	12.06	21.43	4.49	20.95	109.08	1.46	1.34	8.12	2.05	25.25	
26	2169	42.00	1.77	4.21	14.76	1.39	9.42	12.88	1.93	14.98	27.80	4.14	14.89	22.48	6.49	28.87	108.81	1.82	1.67	8.78	2.81	32.00	
27	495	43.25	2.61	6.03	15.61	1.92	12.30	14.26	2.81	19.71	28.15	3.86	13.71	27.32	9.50	34.77	109.94	1.72	1.56	11.34	4.50	39.68	
28	2347	41.06	1.49	3.63	14.02	1.04	7.42	11.58	1.51	13.04	29.70	2.63	8.86	19.09	3.88	20.32	108.42	0.84	0.77	7.03	2.04	29.02	
29	2694	41.17	1.64	3.98	14.16	1.04	7.34	11.88	1.56	13.13	30.37	3.14	10.34	20.32	3.98	19.59	108.99	1.21	1.11	7.45	1.97	26.44	
30	3525	44.49	2.98	6.70	16.74	2.25	13.44	15.86	3.81	24.02	29.90	3.89	13.01	33.26	12.46	37.46	111.01	2.26	2.04	13.43	5.87	43.71	
31	947	41.47	1.34	3.23	14.28	0.93	6.51	11.96	1.28	10.70	26.65	3.45	12.95	19.05	4.35	22.83	107.51	0.98	0.91	7.33	1.89	25.78	
32	2327	41.94	1.94	4.63	14.46	1.39	9.61	12.45	2.10	16.87	26.68	3.10	11.62	22.31	7.74	34.69	108.79	1.67	1.54	8.73	3.53	40.44	
33	857	41.42	1.51	3.65	14.49	1.10	7.59	12.43	1.58	12.71	29.20	3.16	10.82	21.37	5.07	23.72	109.04	1.23	1.13	8.04	2.32	28.86	
34	230	41.36	2.07	5.00	14.10	1.62	11.49	11.78	2.39	20.29	29.03	4.06	13.99	19.04	6.58	34.56	108.70	1.37	1.26	6.97	3.06	43.90	
35	173	41.31	1.23	2.98	14.14	0.91	6.44	11.89	1.49	12.53	26.83	2.54	9.47	18.45	3.53	19.13	108.06	0.87	0.81	7.12	1.96	27.53	
36	400	41.66	1.76	4.22	14.63	1.38	9.43	12.58	2.02	16.06	29.71	4.76	16.02	21.55	5.95	27.61	108.39	1.32	1.22	8.02	2.71	33.79	
37	733	44.56	4.00	8.98	17.03	3.05	17.91	17.65	6.35	35.98	30.42	4.19	13.77	36.59	17.17	46.93	112.15	3.36	3.00	15.06	7.91	52.52	
38	938	44.22	3.96	8.96	16.48	3.02	18.33	16.50	5.94	36.00	29.67	4.57	15.40	35.60	18.93	53.17	111.81	3.68	3.29	14.65	8.82	60.20	
39	614	42.11	1.53	3.63	14.67	1.24	8.45	13.03	1.71	13.12	28.12	3.65	12.98	25.73	5.50	21.38	109.76	1.00	0.91	9.92	2.43	24.50	
40	205	46.54	2.51	5.39	18.63	2.16	11.59	20.02	3.73	18.63	34.04	5.59	16.42	47.26	10.28	21.75	111.89	1.93	1.72	19.51	4.54	23.27	
41	362	41.72	2.07	4.96	14.49	1.41	9.73	12.74	2.36	18.52	27.15	3.40	12.52	22.67	6.31	27.83	109.84	1.85	1.68	8.75	2.79	31.89	
42	257	42.49	2.13	5.01	15.38	1.65	10.73	13.83	2.60	18.80	33.88	4.48	13.22	28.00	6.17	22.04	112.54	1.41	1.25	10.76	3.18	29.55	
		Data Ranges of stand ages and spectral variances in each individual band																					
39		10.01		7.34		11.39		13.16		46.16		8.49		13.67									

The symbols in the table are: SD - Standard deviation, PN - pixel numbers at each age level; and CV - Coefficient of variation (%)

**Appendix G**  
 Data characteristics of spectral values over the radiata pine plantations in each 5-year age classes. (a) the January-24-1987 SPOT data; (b) the February-9-1988 TM data; and (c) the April-21-1988 TM data.

(a) The January-24-1987 SPOT HRV data.

Age Classes	Pixel No.	XS1			XS2			XS3			PS		
		Mean	SD	CV	mean	SD	CV	Mean	SD	CV	Mean	SD	CV
5	6154	43.74	7.59	17.35	36.58	8.74	23.89	55.87	5.52	9.88	46.52	9.92	21.32
10	1472	39.93	7.36	18.43	32.57	8.85	27.17	56.49	4.37	7.74	41.59	10.65	25.61
15	14930	34.82	6.06	17.40	26.15	6.99	26.73	58.14	5.47	9.41	35.21	9.24	26.24
20	4446	31.47	5.53	17.57	22.33	5.82	26.06	55.33	6.29	11.37	30.09	8.07	26.82
25	14646	31.56	4.17	13.21	22.37	4.67	20.88	50.89	4.03	7.92	30.64	6.34	20.69
30	11230	33.70	5.52	16.38	25.15	6.39	25.41	48.97	4.96	10.13	33.31	8.07	24.23
35	4534	32.93	4.25	12.91	24.60	4.85	19.72	46.75	4.73	10.12	32.60	5.58	17.12
40	2890	33.41	3.39	10.15	24.49	3.63	14.82	47.34	3.91	8.26	32.95	4.89	14.84
45	619	34.83	5.87	16.85	26.74	6.76	25.28	48.67	5.10	10.48	33.41	5.96	17.84
		12.27			Data Range			11.39			16.43		

(b) The February-9-1988 TM data.

Stand Age	Pixel No.	2TM1			2TM2			2TM3			2TM4			2TM5			2TM6			2TM7		
		Mean	SD	CV	Mean	SD	CV	Mean	SD	CV	Mean	SD	CV	Mean	SD	CV	Mean	SD	CV	Mean	SD	CV
5	6154	68.97	7.16	10.38	31.92	5.78	18.11	43.50	12.49	28.71	58.43	5.97	10.22	100.92	30.28	30.00	130.95	5.05	3.86	43.90	16.61	37.84
10	1472	65.29	9.3	14.24	29.97	8.01	26.73	39.87	17.95	45.02	59.57	5.13	8.61	75.67	31.17	41.19	126.51	6.47	5.11	32.23	18.59	57.68
15	14930	59.35	5.5	9.27	24.97	4.30	17.22	28.57	9.24	32.34	61.57	5.75	9.34	55.71	25.81	46.33	122.95	4.10	3.33	20.45	12.99	63.52
20	4446	56.63	4.08	7.20	22.74	3.37	14.82	23.64	7.30	30.88	58.32	7.25	12.43	39.79	17.25	43.35	119.48	2.56	2.14	13.03	7.98	61.24
25	14646	57.4	3.14	5.47	23.30	2.56	10.99	25.47	5.41	21.24	53.24	5.23	9.82	46.40	13.32	28.71	120.79	2.63	2.18	16.04	6.71	41.83
30	11230	59.35	4.86	8.19	24.70	3.85	15.59	28.99	8.36	28.84	50.25	5.86	11.66	56.34	20.27	35.98	123.46	4.52	3.66	21.20	10.12	47.74
35	4534	57.67	3.06	5.31	23.53	2.36	10.03	26.50	4.97	18.75	47.23	4.87	10.31	50.62	13.35	26.37	120.30	2.66	2.21	18.61	6.75	36.27
40	2890	59.9	4.66	7.78	25.16	4.04	16.06	30.51	10.40	34.09	50.91	8.29	16.28	61.84	23.41	37.86	123.92	4.04	3.26	23.78	10.96	46.09
45	619	59.06	3.06	5.18	24.73	2.55	10.31	28.72	5.47	19.05	49.56	6.20	12.51	55.46	10.72	19.33	123.65	2.84	2.30	20.92	5.67	27.10
		12.34			9.18			19.86			14.34			61.13			11.47			30.87		

(c) The April-21-1988 TM data.

Stand Age	Pixel No.	2TM1			2TM2			2TM3			2TM4			2TM5			2TM6			2TM7		
		Mean	SD	CV	Mean	SD	CV	Mean	SD	CV	Mean	SD	CV	Mean	SD	CV	Mean	SD	CV	Mean	SD	CV
5	6154	47.91	4.29	8.95	19.06	3.13	16.42	19.12	5.22	27.30	32.57	4.09	12.56	49.54	17.63	35.59	113.88	2.75	2.41	21.84	9.31	42.63
10	1472	45.87	5.54	12.08	17.66	4.61	26.10	17.34	7.90	45.56	32.74	3.85	11.76	34.80	19.26	55.34	110.97	3.19	2.87	15.20	10.74	70.66
15	14930	42.87	2.82	6.58	15.28	2.21	14.46	13.14	3.31	25.19	36.24	4.41	12.17	25.10	12.39	49.36	109.55	2.30	2.10	9.49	5.80	61.12
20	4446	41.58	1.91	4.59	14.40	1.49	10.35	11.79	2.16	18.32	33.66	5.44	16.16	18.40	7.29	39.62	108.09	1.15	1.06	6.68	3.09	46.26
25	14646	41.92	1.82	4.34	14.57	1.37	9.40	12.18	1.92	15.76	31.04	4.45	14.34	20.54	6.28	30.57	108.38	1.58	1.46	7.65	2.87	37.52
30	11230	42.44	2.63	6.20	15.12	1.99	13.16	13.36	3.15	23.58	29.49	3.67	12.44	24.85	10.16	40.89	109.51	1.86	1.70	9.66	4.73	48.96
35	4534	41.69	1.75	4.20	14.40	1.26	8.75	12.29	1.87	15.22	27.27	3.39	12.43	21.14	6.66	31.50	108.53	1.47	1.35	8.16	3.04	37.25
40	2890	43.67	3.53	8.08	16.13	2.77	17.17	15.76	5.40	34.26	29.85	4.62	15.48	32.64	16.09	49.30	110.99	3.10	2.79	13.18	7.43	56.37
45	619	42.04	2.13	5.07	14.86	1.57	10.57	13.19	2.51	19.03	29.94	5.11	17.07	24.88	6.78	27.25	110.96	2.14	1.93	9.58	3.12	32.57
		6.33			4.66			7.33			8.97			31.14			5.79			15.16		